Quantitative characterisation and prediction of deep-marine sedimentary architecture and facies heterogeneity through relational databasing

Sophie Cullis

Submitted in accordance with the requirements for the degree of

Doctor of Philosophy

The University of Leeds

School of Earth and Environment

December 2018

The candidate confirms that the work submitted is her own, except where work which has formed part of jointly authored publications has been included. The contribution of the candidate and the other authors to this work has been explicitly indicated below. The candidate confirms that appropriate credit has been given within the thesis where reference has been made to the work of others.

The work in Chapter 3 of the thesis has appeared in publication as follows:

Cullis, S., Colombera, L., Patacci, M. and McCaffrey, W.D., 2018. Hierarchical classifications of the sedimentary architecture of deep-marine depositional systems. Earth-Science Reviews, 179, p.38-71.

Author contributions:

Cullis, S. - Primary author. Responsible for data collection, processing, interpretation and writing of the manuscript.

Colombera, L., Patacci, M. and McCaffrey, W.D. - Discussion of work, along with review and editing of manuscript.

Submitted: 18th March 2017

Re-submitted: 19th January 2018

Accepted: 22nd January 2018

The work in Chapter 4 of the thesis has been accepted for publication as follows:

Cullis, S., Patacci, M., Colombera, L., Bührig, L.H. and McCaffrey, W.D., *accepted*. A database solution for the quantitative characterisation and comparison of deep-marine siliciclastic depositional systems. Marine and Petroleum Geology.

Author contributions:

Cullis, S. – Primary author. Data upload, querying, interpretation and writing of manuscript.

Patacci, M., Colombera, L. and McCaffrey, W.D. – In depth discussion and review of manuscript.

Bührig, L.A. – Additional data upload.

Submitted: 10th July 2018.

Re-submitted: 6th December 2018

Accepted: 10th December 2018

Acknowledgements

None of this work would have been possible without the Turbidites Research Group (TRG) and my supervisors Bill McCaffrey, Marco Patacci and Luca Colombera. My sincerest thanks is given to them for offering me this opportunity to be part of such an innovative project, as well as the chance to present work here and across the pond. Your constant battle to refine my English skills is also much appreciated! I am also grateful for the allowance to take time away from the office and stare at rocks in the field; these times were invaluable, allowing geological batteries to be recharged, new friendships to be forged and survival skills against rogue wildlife to be honed.

The sponsors of the TRG must be thanked for their financial support towards this project (AkerBP, Anadarko, BP, ConocoPhillips, Dana, Equinor, ENI, HESS, Murphy, Nexen, OMV, Petronas, Shell, Tullow and Woodside). I would also like to thank the Editors and Reviewers who have helped further refine the ideas presented in Chapters 3 and 4 that have subsequently been published; A. Miall, D. Chiarella, S. Hubbard, A. Prélat and two anonymous reviewers.

I cannot forget to thank the friends who have kept me sane during this process and fuelled me with caffeine. I am also so blessed to have such a supportive family – you have always encouraged me and helped keep my eyes fixed on the hope which lies before me.

Finally, my dear Matthew, I cannot begin to thank you enough. I am so richly blessed to have you by my side. You truly are a ‘gift from God’. This may mark the end of this first chapter of our lives together but I am eager to see what the next chapters hold.

Abstract

Many deep-marine sedimentological studies have been published, spanning modern, subsurface and outcropping systems. The ability to integrate this growing volume of data would allow new insight into deep-marine system organisation to be developed. Yet to date, comparative analysis of deep-marine studies has been hindered by the wide variety in methods of data collection, scales of observation, resolution, classification approaches and adopted terminology. To address this variety, a relational database approach has been designed and implemented. Known as the Deep-Marine Architecture Knowledge Store (DMAKS), it offers a means to standardise data acquisition, characterising boundary conditions, together with architectural and facies properties, in a spatial, temporal and hierarchical framework.

Three key work elements are presented. The first is a critical review of deep-marine hierarchical classifications, covering the principles that commonly underpin them, their history of development and the degree to which they can be reconciled. The second comprises a series of DMAKS applications, including (i) channel geometry characterisation, (ii) review of hierarchical organisation of channelised and terminal deposits, (iii) assessment of temporal trends in terminal lobe deposition, (iv) development of scaling relationships between adjacent channel and levee architectural elements, (v) quantification of the likely occurrence of elements of different types as a function of the lateral distance away from a known point, (vi) evaluation of proportions and transition statistics of facies in elements and beds, (vii) characterisation of variability in net-to-gross ratios among element types. Thirdly, a comparative study assesses the influence of external controls on the development of lobate terminal deposits at multiple depositional scales.

The DMAKS database approach is shown to represent an advance on previous deep-marine databasing efforts due to the breadth of its scope and its capacity to characterise deep-marine organisational styles. DMAKS has the capability to i) test facies and architectural models against a wider data pool, ii) tailor quantitative outputs to suit a specific environment through filtering on combinations of stored parameters and iii) establish predictive models and statistically-supported synthetic analogues through comparison with analogous datasets; these all may reduce geological uncertainty in reservoir models. The value of such database outputs arguably augments the value of existing deep-marine sedimentary data; the standardised data contained in DMAKS has the potential to yield deeper understanding than that which can be derived from individual studies alone.

Table of Contents

List of tables

List of figures

List of Annexes

Abbreviations and statistical notation

1D	One-dimensional
2D	Two-dimensional
3D	Three-dimensional
DMAKS	Deep-Marine Architecture Knowledge Store
DQI	Data Quality Index
DWAKB	Deep-Water Architecture Knowledge Base
FAKTS	Fluvial Architecture Knowledge Transfer System
HST	Highstand systems tract
km	kilometres
Kyr	Thousands of years
LAP	Lateral accretion package
LST	Lowstand systems tract
m	metres
MTD	Mass transport deposit
Myr	Millions of years
SMAKS	Shallow Marine Architecture Knowledge Store
SQL	Structured Query Language
TST	Transgressive systems tract
UK	United Kingdom
USA	United States of America

N	Population size
n	Sample size
p	2-tailed significance level
r^2	Regression coefficient
r_s	Spearman's rank correlation coefficient
U	Mann-Whitney U test statistic for comparing mean ranks
$\tilde{x}$	Sample median
μ	Population mean
σ	Standard deviation

Chapter 1:

Introduction

1.1 Background

Deep-marine siliciclastic systems host the largest accumulations of sediment upon the earth (Talling et al., 2012). These important sedimentary environments are thus popular areas of research, an interest further encouraged by their hydrocarbon potential (Stow & Mayall, 2000; Pettingill & Weimer, 2002), and by the potential effects upon deep-sea infrastructure of the gravity currents that build them (Prior & Hooper, 1999). A continually-growing catalogue of deep-marine literature describes both modern and ancient deep-marine systems, their environmental complexities, internal architecture and facies, as well as their spatial, temporal and hierarchical organisation (e.g., Reading & Richards, 1994; Posamentier & Kolla, 2003; Haughton et al., 2009; McHargue et al., 2011(a); Picot et al., 2016; Kane et al., 2017; Zhang et al., 2018). The results of these investigations are typically constrained by the data collection methods used and their scales of observation; for example, the quality and extent of visible exposure within outcrop studies are typically restricted, while modern and subsurface investigations are typically of lower resolution and may be limited in their extent by high acquisition costs. As a consequence of such data variability, difficulties have arisen when trying to compare and reconcile data from modern and ancient studies, such as the data form and extent (i.e., whether derived from 1D, 2D planform, 2D cross-section or 3D datasets) and resolution (e.g., from grain-scale to tectonic); Mutti & Normark (1987), Bouma et al. (1985). These difficulties are compounded by the scale, complexity and incompatibilities of the wide array of terminological terms and descriptive classifications that have been used in the deep-marine literature (Shanmugam & Moiola, 1988; Weimer & Slatt, 2007(a); Terlaky et al., 2016). In the inherited state of knowledge, re-interpretation of data would commonly be necessary to facilitate comparisons between differing datasets. Re-interpretation is a time-consuming process, requiring a clear understanding of the differences between each study, its terminology and method of classification, and therefore falls prey to interpretational bias.

An alternative approach, adopted here, is to exploit relational database methodologies. These methodologies can be used to address information complexities through provision of an organisational structure that enables effective integration of big datasets (Soper, 2013). In this case both deep-marine datasets and their complex internal relationships are stored. In

addition, the development of a centralised database storage system would also inherently act as a method of data standardisation. Sedimentary data become more accessible when stored in standardised form and can therefore be more readily analysed, increasing their overall value. Database approaches have already been adopted within sedimentological studies to capture some of the complex architectural relationships within fluvial (e.g., Dreyer et al, 1993; Gibling, 2006; Colombera et al, 2012(a)), paralic and shallow-marine (e.g., Vakarelov & Ainsworth, 2013; Colombera et al., 2016) and deep-marine environments (e.g., Baas et al, 2005; Moscardelli & Wood, 2015; Clare et al., 2018); these database systems have demonstrated the benefits of meta-analysis of integrated datasets in the characterisation of sedimentary environments. This project will build upon and extend the deep-marine database system of Baas et al. (2005) which included both modern and ancient datasets, by incorporating spatial and temporal relationships between architectural building blocks at all hierarchical scales. The immediate aim of this study is to therefore establish an improved database approach for the storage and quantitative investigation of modern and ancient siliciclastic deep-marine systems, their external controls, internal architecture and facies descriptions, including their spatial, temporal and hierarchical relationships. A broader aim is to exploit the database to search for and characterise the organisational principles that appear to underpin the development of deep-marine systems.

1.2 Aims and objectives

The aim of this Thesis is to develop a methodology for the storage of data pertaining to a large (and expandable) number of siliciclastic deep-marine systems in a way that permits data standardisation, allowing comparison between datasets in a reliable and well-founded manner. This database will differ from previous approaches (e.g., Cossey & Associates Inc., 2004; Baas et al., 2005; Moscardelli & Wood, 2015; Clare et al., 2018) due to its applicability to all deep-marine siliciclastic environmental niches, codifying system settings, architectural and facies observations in a hierarchical, temporal and spatial framework for both modern and ancient systems. The introduction of a hierarchical framework will require a close examination of the documented styles of deep-marine organisation found in the literature, due to the variety found between the wide-range of existent hierarchical classifications (e.g., Mutti & Normark, 1987; Prather et al., 2000; Sprague et al., 2005; Prélat et al., 2009; Flint et al., 2011; Pickering & Cantalejo, 2015 *inter alia*), as well as the ongoing debate concerning the reality of hierarchical (i.e., scale-dependent) sedimentary organisation styles (e.g., Schlager, 2010; Straub & Pyles, 2012). The Thesis will also demonstrate the functionality of the deep-marine database as a research tool that can be applied to help better characterise deep-

marine sedimentary system organisation through its comparative analysis and quantitative outputs, applicable to both pure and applied research.

To achieve the aims of this Thesis, the following research objectives have been set:

- To understand the current methods of clastic deep-marine description and organisation, as well as the differences arising from different methods of data collection, in order to devise more effective approaches to characterise deep-marine system environments, architecture and facies in a systematic manner.
- To critically review the diverse methods of deep-marine hierarchical classification and to understand their significance to ensure that the database can effectively capture these spatio-temporal relationships.
- To establish a database standard for the characterisation of both modern and ancient deep-marine system settings, architecture and facies properties within a spatial, temporal and hierarchical framework.
- To demonstrate general potential applications of the database, in both pure and applied research sectors, in facilitating the characterisation of deep-marine systems through meta-analytic outputs.
- To demonstrate the utility of the database for a specific research application, in this case examining the significance of controlling variables upon the geometry of lobate terminal deposits at multiple depositional scales.

1.3 Thesis outline

The project's research objectives can be divided into two key stages of work. The first is to develop an understanding of deep-marine systems and their classifications in order to devise a suitable method of data standardisation (Chapters 2, 3 and 4); the second is to examine the capabilities of such a tool, in both pure and applied research (Chapters 4 and 5). The project workflow is summarised in Fig. 1.1. Chapters 3 and 4 are presented in manuscript form due to their acceptance in peer-reviewed journals.

Chapter 2 provides an overview of the key literature relating to the characterisation of deep-marine systems and their classification methodologies. Particular attention is given to the classification of architectural types and the terminological variances observed. In addition the key sedimentological processes involved in deep-marine system development are reviewed.

Chapter 3 reviews a range of the most popular hierarchical classification schemes and assesses their utility and limitations. The study furthermore evaluates the possible causes of variation between hierarchical approaches, while also asking whether a 'Rosetta-stone' translation between these approaches is possible. This work has been published within the journal *Earth Science Reviews* under the title 'Hierarchical classifications of the sedimentary architecture of deep-marine depositional systems'.

The database approach developed (the Deep-Marine Architecture Knowledge Store, DMAKS) is outlined within **Chapter 4** wherein modern and ancient datasets are codified in a systematic manner. Deep-marine system settings, architectural elements and facies are digitised, along with their spatial, temporal and hierarchical relationships. Potential database applications are presented, demonstrating the database's capabilities in facilitating the characterisation of deep-marine systems; for example, quantitative outputs that can be used to optimise predictive modelling efforts and improve the accuracy of analogue selection are shown. This work has been accepted for publication within the journal *Marine & Petroleum Geology* under the title 'A database solution for the quantitative characterisation and comparison of deep-marine siliciclastic depositional systems'.

Chapter 5 demonstrates the utility of DMAKS as a research tool for a specific research topic, namely to explore the importance of external controls at multiple architectural scales on deposition within a particular deep marine depositional environment. Accordingly, this quantitative comparative study uses DMAKS to analyse the significance of system-scale variables upon the geometry of terminal deposits from a range of deep-marine system settings (e.g., in relation to tectonics, system scale and morphology).

Finally, **Chapter 6** summarises the work presented in this Thesis, in accordance with the aims previously stated in Section 1.2. Suggestions for future work are also proposed, regarding both potential methodological improvements to the database and also ideas for further application.

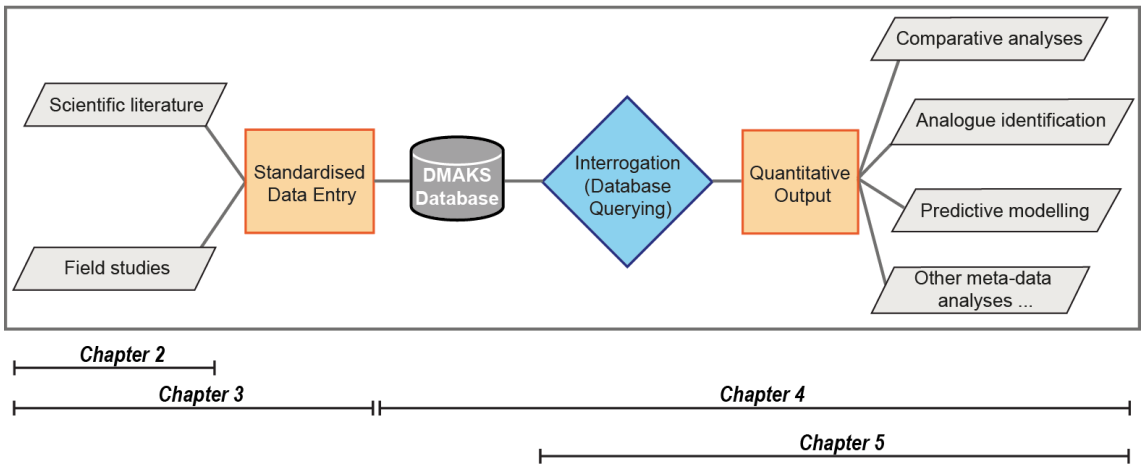

Fig. 1.1. Flowchart illustrating the data-entry-query-analysis workflow of the DMAKS database (modified from Colombera et al., 2012(a)). The standardisation process ensures data output can be consistently interrogated and filtered as desired by the user. The relevant parts of this workflow and the chapters they are explored within are also indicated.

Chapter 2:

Deep-marine systems and their classification

2.1 Introduction

This chapter provides an overview of the key literature concerning approaches to the description of siliciclastic deep-marine systems, and it provides the backdrop for the Thesis requirement to develop a database broad enough to capture facies- to system-scale attributes of deep-marine environments.

"Deep-marine" depositional environments generally lie below 200m sea-level; although they can occur at any water depth, deep-marine processes predominate from the continental slope outwards (Boggs, 1995; Pickering & Hiscott, 2016). Ancient and modern deep-marine systems have been a popular topic of research since the inception of the turbidite paradigm and particularly since the ability to drill deep-water reservoirs was developed (Shanmugam, 2000; Stow & Mayall, 2000). However, the ability to integrate datasets derived from modern and ancient systems, with their differing scales of observation and resolution, remains difficult, e.g., Normark et al. (1979); Mutti & Normark (1987); Weimer (2000); Weimer & Slatt (2007(a)); Bakke et al. (2013). With consideration to the differences observed between datasets describing modern and ancient systems this review will discuss: i) deep-marine sediment distribution processes, ii) the empirical characterisation of architecture along with common interpretations, and iii) the controls upon deep-marine deposition; finally, iv) the available methods of deep-marine characterisation and quantitative analysis are reviewed.

2.2 Sediment transport and deposition

Deep-marine systems are largely the product of sediment gravity flows and their interaction with the substrate. To first order, sediment gravity flow types can be classified into mass movements (i.e., rock fall, creep, slide or slump processes), debris flows and turbidites (Dott, 1963; Middleton & Hampton, 1973; Mulder & Alexander, 2001; Fig. 2.1). Sediment gravity flows are flows characterised by mixtures with varying proportions of fluid and particles driven down-slope by gravity acting upon the density difference between the flow and the surrounding fluid. They comprise a continuum of mechanical end-members, transitioning from elastic and plastic behaviours – with debris flows marking a truly plastic laminar flow, to the fluidal (Newtonian) flows of turbidites (Nardin et al., 1979); Fig. 2.1. Downslope

movement occurs due to a loss of shear strength; this movement can be triggered by the transformation of failed sediments (e.g., from a slide to turbidity current; Heezen & Ewing, 1952), seismically generated slides, instabilities caused by over-steepening of the slope, or through the introduction of suspended sediment via elevated river discharge or hyperpycnal flows (Mulder & Syvitski, 1995; Mulder et al., 2003; Piper & Normark, 2009; Meiburg & Kneller, 2010; Talling et al., 2014). In deep-marine systems, subaqueous material can also be redistributed via bottom-current processes or deposited as a result of suspended-sediment fallout (i.e., pelagic settling); Stow et al. (1996); Rebesco et al. (2014).

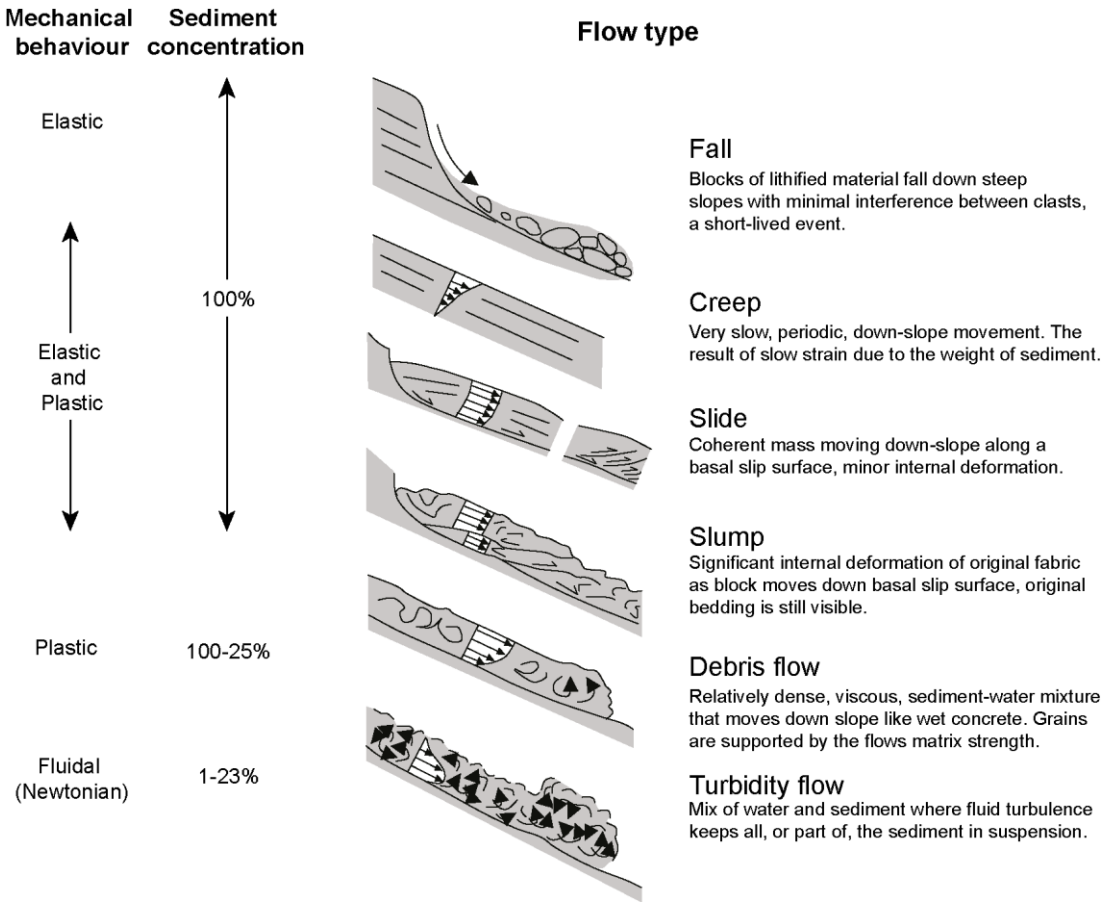

Fig. 2.1. Types of sub-aqueous sediment gravity flows, including brief descriptions. Vertical flow velocity profiles are included in each schematic cross-section. Sediment concentration values (% by volume) are derived from published datasets compiled in Shanmugam (2002). Mechanical behaviour of the gravity-driven downslope processes are based upon Dott (1963). Figure modified from Posamentier & Martinsen, 2011. Descriptions derived from Dott (1963), Middleton & Hampton (1973) and Mulder & Alexander (2001).

Sediment gravity processes have been classified in a number of ways, for instance based upon i) their mechanical (rheological) behaviour, e.g., Dott (1963), Mulder & Cochonat (1996), Shanmugam (2000); ii) particle support mechanisms, e.g., Middleton & Hampton

(1973), Nardin et al. (1979) and Lowe (1979); iii) flow concentrations, Mulder & Alexander (2001); and iv) the type of deposits they leave behind, e.g., Mutti & Ricci Lucchi (1975), Pickering et al. (1989), Ghibaudo (1992). However, all these classifications necessarily entail some uncertainty due to the difficulties in studying deep-marine processes and their associated resultant products first-hand. The linkage between process and product is primarily based upon experimental work (e.g., Kuenen & Migliorini, 1950; van den Berg & van Gelder, 1993; Al Ja'Aida et al., 2004; Sumner et al., 2009; Baas et al., 2011; Cartigny et al., 2014), along with a limited range of direct measurements (e.g., Xu, 2011; Symons et al., 2017). Yet, these experimental outputs are in turn limited in their applicability due to their scaling restrictions and ability to evaluate only a limited number of variables. Understanding sediment gravity deposits is further complicated by a flows ability to transform spatially and temporally in response to changes in sediment concentration via sediment entrainment or deposition (Mulder & Alexander, 2001). An individual deposit may therefore be the product of a number of flow processes, rather than a single dominant process (Shanmugam, 2000; Mulder & Alexander, 2001; Haughton et al., 2009; Talling et al., 2012). Furthermore, a single gravity flow deposit may be the result of a multi-pulsed current, arising in contexts where multiple currents with differing flow concentrations can merge (Ho et al., 2018). Post-depositional deformation processes, such as soft sediment deformation or large-scale injectites, can also mask the original depositional fabric, further adding to the complexities in unravelling process-to-product linkages.

2.2.1 Turbidity to debris flows and their deposits

Turbidity flows are regarded as the most important transportation mechanism for coarse-grained sediment, forming the largest sediment accumulations in the deep-sea (Stow et al., 1996; Talling et al., 2012). Turbidite systems are the focus of significant deep-marine hydrocarbon exploration (Pettingill & Weimer, 2002). The common definition of a turbidity current is a sediment gravity flow characterised by sediment kept in suspension by fluid turbulence (e.g., Middleton & Hampton, 1973; Lowe, 1982). However, diagnosing grain-support mechanics in sediment gravity flow deposits is difficult, therefore this definition has been widened to include deposits that may include evidence of other grain-support mechanisms alongside fluid turbulence (Kneller & Buckee, 2000). Experimental work shows that these non-cohesive flows contain low volumes of suspended particles (<9% volume; Bagnold, 1954); however such conditions are hard to measure in natural flows or infer from ancient deposits. Building upon earlier studies such as Kuenen & Migliorini (1950), Bouma (1962) proposed an idealised model for a continuous turbidite bed sequence (Fig. 2.2), describing a normally graded bed with each facies division sequentially depicting the waning

energy of the single flow. Lowe (1982) extended the Bouma sequence, adding divisions based upon observed sedimentary structures in coarser grained deposits. Lowe proposed that these additional divisions recorded deposition from a relatively more proximal turbidity current, with an increased sediment concentration near the flow base; these flows transition downstream into the lower-density turbidity currents of Bouma (1962).

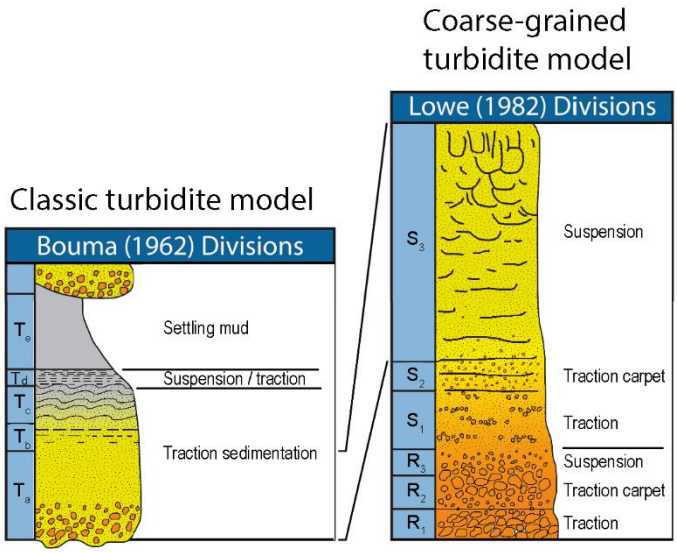

Fig. 2.2. Turbidite facies models for a classical Bouma sequence (1962) and coarse-grained, higher density flows of Lowe (1982). Division interpretations are taken from Lowe (1982). Note the overlap between T_a and S_3 divisions. Figure taken from Johnson et al. (2017).

In contrast, debrite deposits are the result of usually cohesive, laminar flows (Middleton & Hampton, 1973; Lowe, 1982; Mulder & Alexander, 2001). These highly concentrated flows carry sediment via their matrix strength and deposit material by en-masse freezing (Lowe, 1982); this typically results in mounded, tongue-like plan-view geometries, unlike unconfined turbidity flows which spread outwards resulting in lobate or sheet-like geometries (cf. Shanmugam, 2016). Debrite deposits commonly lack significant internal sedimentary structure and instead exhibit poorly sorted chaotic fabrics (Talling et al., 2012). They are typically clast-rich and traces of shear may be identified near the deposits base and margins (Mulder & Alexander, 2001; Posamentier & Martinsen, 2011).

A particular group of deposits have been identified which show a vertical transformation in their flow behaviour in a single event-bed. These deposits transition from being deposited beneath a non-cohesive turbulent flow to a more cohesive turbulence-suppressed flow, sometimes with an inferred return to turbulent conditions (e.g., Haughton et al., 2003, 2009; Talling et al., 2004; Barker et al., 2008; Kane & Ponten, 2012; Fonnesu et al., 2015, 2018). Five internal facies divisions are recognised within these co-genetic deposits termed ‘hybrid event

beds'; Fig. 2.3. These divisions can vary downstream and laterally across deposits (Fonnesu et al., 2015; Kane et al., 2017).

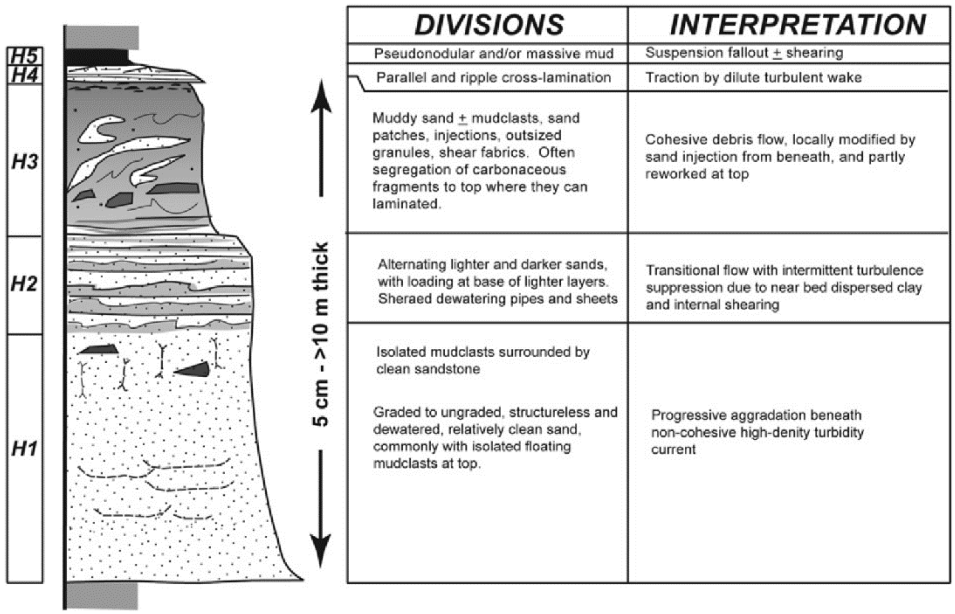

Fig. 2.3. Hybrid event bed facies model showing the five archetypal facies divisions; these divisions need not be present and may vary based upon flow conditions. Figure taken from Haughton et al. (2009).

2.3 Architectural building blocks

Deep-marine sedimentary deposits are commonly categorised into 'architectural elements' based upon the observation of internal facies trends, external geometry and their bounding-surface relationships, e.g., Pickering et al. (1995), Gardner et al. (2003), Sprague et al. (2005) Terlaky et al. (2016). This descriptive methodology was introduced to the classification of deep-marine deposits by Pickering et al. (1995) after its establishment in both aeolian and fluvial sedimentology by Brookfield (1977), Allen (1983) and Miall (1985). Different deep-marine architectural elements form as a result of a suite of deep-marine processes characteristic to the associated sub-environment of deposition (Clark & Pickering, 1996(a); Piper & Normark, 2001; Posamentier & Walker, 2006). The observation of external geometry through bounding surface relationships enables architectural elements and their environmental processes to be considered in relation to their element dimensions, stacking patterns and spatio-temporal arrangements, e.g., Miall (1985; 1989), Pickering et al. (1995), Stow & Mayall (2000) and McHargue et al. (2011(a)). Architectural elements are seen to arrange themselves spatio-temporally and consequently have been hierarchically classified (e.g., Mutti & Normark, 1987; Pickering et al., 1995; Prather et al., 2000; Navarre et al., 2002; Gardner et al., 2003; Sprague et al., 2005; Hadler-Jacobsen et al., 2005; Mayall et al., 2006;

Deptuck et al., 2008; Prélat et al., 2009; Flint et al., 2011; Terlaky et al., 2016). A variety of hierarchical approaches have been formulated, which inhibits the ability to easily compare architectures between hierarchical schemes; this predicament is discussed in detail in Chapter 3; Cullis et al., 2018. In addition, a variety of architectural element terminology is found in the deep-marine literature (cf. Mutti & Normark, 1987; Reading & Richards, 1994; Stow & Mayall, 2000; Posamentier & Walker, 2006; Weimer & Slatt; 2007(a)). This variety is in part associated with the differences observed between different data collection methods and their ability to resolve deep-marine deposits (e.g., limitations in spatial scale and resolution), as well as the continually developing analysis of specific sub-environments and their inferred sedimentary processes (Mutti & Normark, 1987; Stow & Mayall, 2000; Weimer & Slatt, 2007(a)). Architectural elements observable in datasets from both modern and ancient (seismic and outcrop) systems are described below. These element descriptions are both mutually-exclusive and scale-independent and are therefore applicable at multiple hierarchical scales.

2.3.1 Channels

A channel is a long-term conduit for sediment gravity flows; channels can be observed across the complete deep-marine depositional profile, from slope to basin plain. The coarsest sediment deposited in a system is typically found in channel bodies (Mutti & Normark, 1987) and this is commonly mirrored in their high-amplitude seismic reflections (Kolla et al., 2001). These architectural elements can form important hydrocarbon reservoirs (Clark & Pickering, 1996(a); Abreu et al., 2003; Weimer & Slatt, 2007(b)). They display ribbon-like geometries in plan-view and are discerned in cross-section by the concave-up form of their lower boundaries. A planar upper bounding surface is often observed in ancient deposits. Channel deposition typically terminates with a mud-rich cap, often interpreted as a hiatus in sediment gravity flow deposition (Navarre et al., 2002; Mayall et al., 2006). The basal surface may be erosional, aggradational or mixed (depositional-erosional) in character, as originally noted by Normark (1970).

Deep-marine channels share morphological similarities to their fluvial equivalents, e.g., they can display sinuosity, form tributary and distributary networks, and develop point-bars, cut-off loops and flanking levees (Flood & Damuth, 1987; Kolla et al., 2007). However, deep-marine channels exhibit different stratigraphic architectural trends related to the more complicated density and velocity profiles of deep-marine flows; see Peakall & Sumner (2015) and Kolla et al. (2007) for a detailed account of the differences between fluvial and deep-marine processes. For instance, channel bodies preferentially stack vertically, as opposed to the lateral stacking patterns that predominate in fluvial systems (Jobe et al., 2016). The cross-

sectional dimensions of deep-marine channels may exceed those of the largest rivers by an order of magnitude (Konsoer et al., 2013). Contrary to rivers, deep-marine channels decrease in cross-sectional area downstream, (Weimer & Slatt, 2007(b)). This is inferred to be the result of a decrease in flow density and velocity as material is lost through overspilling as the channelized flow moves downstream (Peakall et al., 2000).

Channels may be confined by a larger channel-form, particularly on the slope (Sprague et al., 2005; Janocko et al., 2013; Fig. 2.4). Seismic and outcrop datasets show repeated cycles of cutting, infilling and abandonment expressed over a range of scales which has led to the development of channel hierarchical classifications as part of their analysis, e.g., Pickering et al. (1995), Navarre et al. (2002), Gardner et al. (2003), Sprague et al. (2005), Mayall et al. (2006); see Chapter 3. These cycles commonly show fining-upwards grain-size profiles; elements at each hierarchical scale are proposed to be the product of waxing to waning energy conditions (McHargue et al., 2011(a)). At larger hierarchical orders stacking patterns become relatively more organised, such that individual vertically aggraded channel fills vertically stack and become less amalgamated as the flow behaviour changes from erosional to depositional (McHargue et al., 2011(a); Macauley & Hubbard, 2012). Aggradational channel fills typically show lateral facies changes, i.e., amalgamated sandstones characterise a channel axis, while thin, interbedded siltstones and sandstones dominate the channel margins (Campion et al., 2000; Macauley & Hubbard, 2013).

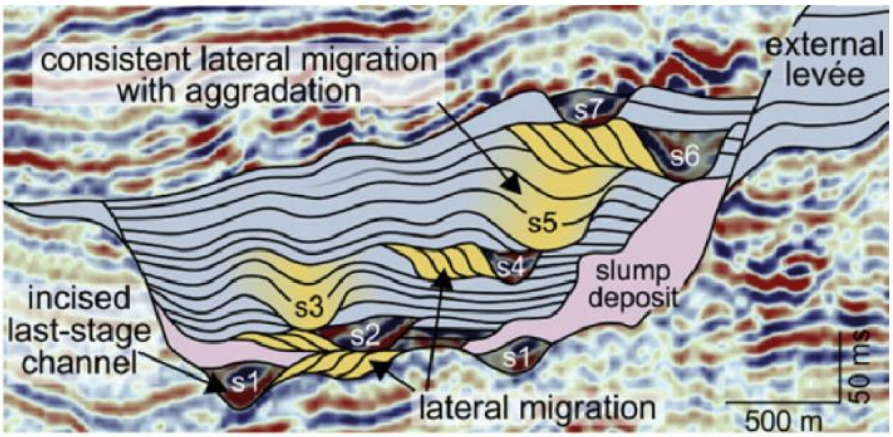

Fig. 2.4. Seismic interpretation of a channel complex and its repeated cycles of cutting and filling. A large confining channel with associated levees constrains the internal organisation of hierarchically smaller vertically aggraded channel bodies (S1-S7) and lateral accretion packages (the yellow clinoforms). Seismic section is taken from Complex III, offshore West Africa, Janocko et al. (2013).

Deep-marine channel systems are commonly sinuous and recently it has been noted that they may be more sinuous in higher latitudes, possibly in association with the increased

effects of Coriolis forces (Menard, 1955; Peakall et al., 2012; Cossu et al., 2015). Within the inner bends of sinuous channels 'lateral accretion packages' (LAPs) can be identified; in a process similar to fluvial point bars these elements are inferred to be the result of continuous lateral migration of the channel thalweg (Abreu et al., 2003; Janocko et al., 2013; Fig. 2.4). However, an alternative method of formation suggests these deposits to be the result of consecutive lateral stacking of cut-and-fill channel deposits (Mayall et al., 2006; Kolla et al., 2007). Shingled, bright seismic amplitude reflections at channel bends typically mark the presence of LAPs (Janocko et al., 2013). These elements show inclined accretion surfaces in cross-section, dipping towards the channel axis. In plan-view these elements are usually crescent shaped when not eroded. LAPs are usually composed of a mix of coarse and fine sandstones, arranged in fining-upwards trends (Abreu et al., 2003; Janocko et al., 2013).

2.3.2 Levees

The term levee defines an aggradational sediment wedge found adjacent to a channel margin. These elements extend laterally away from the genetically-related channel. They are deposited as the result of typically fine-grained sediment (associated with the upper portion of the flow) over-spilling the banks of their confined sediment pathways (Posamentier & Walker, 2006; Kane et al., 2007). Levees typically display planar and largely conformable upper and lower boundary surfaces. They are formed by flows that are generally directed transverse to, and away from the genetically-related channel. Their thickest point, the levee crest, typically lies parallel to the genetically-related channel. As a result of the Coriolis force, one levee is typically thicker than its genetically-related partner on the opposing side of the channel (Menard, 1955); for example, in the northern hemisphere the levee to the right of the channel when looking downstream is typically thickest. These elements have widths and lengths that are proportional to the size of their associated channels. Levee thickness decreases exponentially downstream as well as across the levee crest, Skene et al., (2002) and Nakajima & Kneller, (2013). The decrease in levee thickness across the levee crest (parallel to the elements palaeoflow) is coupled to a reduced variability in bed thickness and a reduced proportion of sand observed away from the channel margin (Beaubouef, 2004; Kane et al., 2007). In seismic datasets levees tend to be characterised by low amplitude continuous to discontinuous reflections (Posamentier & Walker, 2006; Weimer & Slatt, 2007(c)). In comparison to their associated channels, levees are finer-grained and are primarily composed of clays, silts and thinly bedded sands. In proximal regions (close to the channel margin) tractional structures such as parallel laminations, ripple cross-laminations and climbing ripples are identified, associated with high velocity flows and high

sedimentation rates (Kane et al., 2007); as flow velocity decreases away from the channel margin such structures become more scarce.

Levees can be further grouped into 'master levee' and 'overbank terraces', with the latter being distinguished because of their confinement within a larger channel form (Fig. 2.5). Master levees provide lateral confinement to a meandering channel but are generally less sinuous than the active channel (Kane et al., 2007). They have had many guises in the literature such as the 'external levee' of Kane & Hodgson (2011), 'outer levee' of Deptuck et al. (2003) and Hübscher et al. (1997), the 'levees' of von Rad & Tahir (1997), 'master bounding levee' of Posamentier (2003) and the 'high levees' of Piper et al. (1999). Overbank terraces are at least partially confined by a more significant channel or associated master levees. These units can show a range of geometries and multiple palaeoflow directions related to the interaction of the channel flows with the larger confining body (Kane & Hodgson, 2011). Overbank terraces have also been termed 'inner levees' (Hübscher et al., 1997; Deptuck et al., 2003; Posamentier, 2003; Wynn et al., 2007), 'constructional overbank terraces' (von Rad & Tahir, 1997), 'confined levees' (Piper et al., 1999) and 'internal levees' (Kane & Hodgson, 2011).

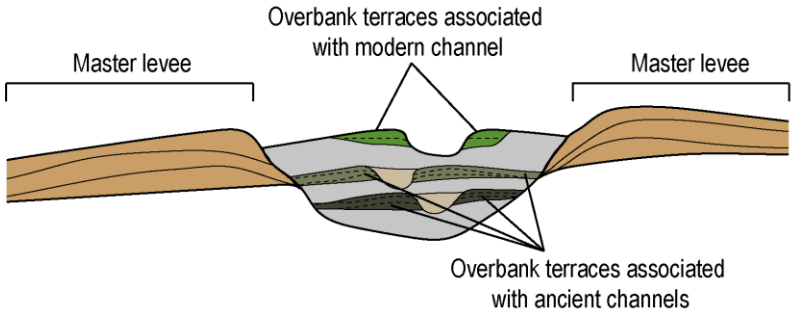

Fig. 2.5. Cross-sectional view showing the relationship between master levees and overbank terraces along with their associated channels.

2.3.3 Lateral splays

A lateral splay is an aggradational element with a lobate or fan-shaped geometry deposited as a result of sediments escaping a channel onto the overbank environment. They can be differentiated further in the literature as 'overbank/spill-over' or 'crevasse' splays based upon whether the sediment-laden flows overtop or breach the banks of their confined sediment pathways (e.g., Posamentier & Kolla, 2003; Gamberi & Marani, 2008; Eschard et al., 2014). For a channelized flow to gain enough energy to break through the adjacent confining walls, it is proposed that the base of the flow, which can carry coarser sediments, must be involved (Posamentier & Walker, 2006). Crevasse splays can also develop distributary channel networks, e.g., the De Soto Canyon, Gulf of Mexico (Posamentier et al., 2003). Lateral splays

can be described as failed channel avulsion attempts as they are thought to represent only a temporary diversion of sediment away from the feeder channel (Posamentier & Walker, 2006).

Lateral splays are commonly found adjacent to outer, rather than inner, channel bends where the flow can reach a higher momentum (Posamentier & Kolla, 2003; Khan & Arnott, 2011). These overbank elements are typically coarser than any associated levees, e.g., Navarro et al. (2007(a)) and Khan & Arnott (2011). The sand-rich deposits are commonly characterised by climbing current ripples and show high levels of amalgamation at their apices (i.e., the point closest to the channel) as rapid sedimentation takes place as the flow transitions from a confined to an unconfined state (Posamentier & Walker, 2006).

2.3.4 Scours

Scour elements are characterised by a negative relief, concave-up, erosive basal surface. These elements show a semi-ellipsoidal ('scoop') geometry which in modern systems may be expressed by an erosive surface that has not yet been infilled. This element can be expressed in plan-view by a variety of shapes (e.g. crescent, elliptical or chevron planforms); however, a headwall is always seen transverse to the main (palaeo-) flow; Wynn et al. (2002), MacDonald et al., 2011(a). Many studies commonly locate scours in channel lobe transition zones (CLTZs), e.g, Mutti & Normark, 1987; Wynn et al., 2002; Hofstra et al., 2015.

Scour elements are often interpreted to be the result of rapid flow expansion or of hydraulic jumps (i.e., the transformation from supercritical to subcritical flow conditions), cf. MacDonald et al., 2011(a), Hofstra et al., 2015. Scours are products of sediment bypass and thus their infill differs from the contemporaneous sediment deposited around the scour depression, Wynn et al., (2002); MacDonald et al., (2011(a)). Scours have been seen to merge with other scour elements and can thus show amalgamated bounding surfaces; multiple stages of cutting and filling have also been identified (MacDonald et al., 2011(a)). Channel and scour elements can often be confused when only cross-sectional views are considered; however, Normark et al. (1979) suggest that a scour infill would contain locally sourced sediment, while a channel infill would be composed of coarser sediment derived from much longer sediment pathways further up-system. Additionally, scour elements are not associated with the synchronous development of lateral splay or levee architectures which can be found alongside some channel elements. Scour elements have also been termed 'flutes' and 'megaflutes' (e.g. Elliott, 2000 and Kane et al., 2009) in some studies. These elements differ from the slump scars left behind by slope failures.

2.3.5 Terminal lobes and sheets

Sediment gravity flows decelerate as they exit the terminus of a channel, resulting in the deposition of terminal deposits. The change in flow behaviour from a confined to unconfined setting typically results in a deposit with a high aspect ratio (width to thickness) geometry. These elements are typically sand-rich as they deposit the sediment bypassed down the channel (Weimer & Slatt, 2007(d)). The high width-to-thickness aspect ratio, good lateral continuity, and limited occurrence of erosional features of terminal deposits make these elements desirable targets for hydrocarbon exploration, (Shanmugam & Moiola, 1988; Posamentier & Kolla, 2003; Weimer & Slatt, 2007(d)). These deposits can show lobate plan-view geometries or can be tabular and sheet-like in form.

Sheet-like deposits display planar upper bounding surfaces and maintain a constant thickness of layered or amalgamated beds (Chapin et al., 1994; Johnson et al., 2001; Weimer & Slatt, 2007(d); Tőkés & Patacci, 2018). Terminal sheets are constrained by topographic relief and are seen to onlap the underlying substrate, e.g., in the Auger basin (Prather et al., 1998) and the Bric la Croce-Castelnuovo turbidite system in the Tertiary Piedmont basin (Felletti, 2016), and many others. The term ‘sheet’ has also been used to describe background deposits of pelagic origin as opposed to the described terminal sediment gravity flows, e.g., Reading & Richards (1994), Stow & Mayall (2000) and Pyles (2007).

Lobate geometries can also be discerned, showing a typically conformable basal surface and convex-up upper surface (Mutti & Normark, 1987; Deptuck et al., 2008). A 2:1 length-to-width ratio has commonly been observed across deep-marine systems, e.g., in the composite studies of Zhang et al. (2017) and Pettinga et al. (2018). Flow energy is thus primarily focused downstream, corroborated by the preferential finding of hybrid event beds at the distal, rather than lateral, fringes (Spychala et al., 2017). Finger-like protrusions along the lobes fringe have been identified in outcrop (e.g., the Tanqua depocentre, Groenenberg et al., 2010) and seismic datasets (e.g., the Nile fan, Migeon et al., 2010). These terminal deposits can be associated with distributary channel networks which have been captured in modern systems using high-resolution seismic techniques, e.g., Dennielou et al. (2017) and Doughty-Jones et al. (2017), and inferred in outcrop studies, e.g., in the Hikuwai sandstone (Burgreen & Graham, 2014).

Hierarchical relationships are identifiable in both modern and ancient datasets and subsequently multiple classification schemes have been developed, e.g., Gervais et al. (2006(a)), Deptuck et al. (2008), Prélat et al., (2009), Flint et al. (2011), MacDonald et al. (2011(b)); see Chapter 3 for an in-depth analysis of these schemes. Background deposition, marking depositional shutdown, is seen to vertically separate hierarchical units (Pyles, 2007;

Prélat et al., 2009; Grundvåg et al., 2014). Bed thickness patterns can be used to infer stacking styles (Prélat & Hodgson, 2013); typically at larger hierarchical orders, compensational stacking patterns are observed between terminal deposits (Mutti & Sonnino, 1981; Straub & Pyles, 2012).

2.3.6 MTDs

Mass transport deposits (MTDs) can constitute well over 50% of the volume of some basin fills; e.g., Basin 4 of the Brazos Trinity system (Beaubouef et al., 2003), offshore Brunei (McGilvery & Cook, 2003) and offshore the Nile (Newton et al., 2004). These elements are the consequence of 'en-masse' movement. MTD is a general term used in the literature to describe a range of mechanical processes related to the remobilisation of sediment following slope failure, including creep, slide, slump and debris flows (Nardin et al., 1979; Moscardelli et al., 2006; Tripsanas et al., 2008; Jenner et al., 2007; Meckel, 2011 and Posamentier & Martinsen, 2011). These elements can show facies evidence for several of these processes to have occurred during transportation and deposition of a single deposit (Tripsanas et al., 2008; Posamentier & Martinsen, 2011). MTDs typically display geometries that are mounded in cross-section and fan-like in plan-view (Moscardelli et al., 2006; Weimer & Slatt, 2007(e); Meckel, 2011). These deposits vary in scale and have been observed in both seismic (e.g., Storegga slide complex, Norway, Solheim et al., 2005; offshore Trinidad and Venezuela, Moscardelli et al., 2006) and outcrop studies (e.g., Tres Pasos Formation, Chile, Armitage et al., 2009; Laingsburg depocentre, South Africa, Brooks et al., 2018) amongst others. Studies in modern systems have suggested that the extent and thickness of MTDs is influenced by sea-floor topography (Moscardelli et al., 2006; Ortiz-Karpf et al., 2017). MTDs can be identified by their erosional basal surfaces, which in modern systems can be traced up-dip to head-wall slope scarps, e.g., Vanneste et al., 2006 and Twichell et al., 2009. MTDs are typically mud-rich and can therefore act as reservoir seals due to their low permeability (Shipp et al., 2004; Meckel, 2011); however, MTD reservoirs and possibly source rocks have been identified (Weimer & Slatt, 2007(e)). MTDs have also been termed 'chaotic mounds' (Reading & Richards, 1994), 'irregular mounds' (Stow & Mayall, 2000) and 'mass transport complexes (MTCs)' (Moscardelli et al., 2006; Pickering & Corregidor, 2005).

2.3.7 Bottom current drifts

Architectural elements of this type consist of sediments deposited or substantially reworked by the persistent action of bottom currents near the seafloor (Stow et al., 2002). They have also been termed 'contourites', although the formation of these deposits is no longer thought to be restricted to contour-parallel thermohaline currents (Stow et al., 2002; Rebesco et al.,

2014). These elements form either sheet-like or mounded geometries, showing (palaeo-) flow directions parallel to the associated bottom currents (Nielsen et al., 2008). Bottom current drifts are often found alongside elongate geomorphic depressions (Rebesco & Stow, 2001; Stow et al., 2008). Cyclicity in the seismic facies of these deposits has been observed and is interpreted to represent fluctuations in the intensity of bottom current processes as a consequence of climate (Stow et al., 2002).

The majority of drifts are strongly bioturbated and thus primary sedimentary structures are not well preserved (Faugeres & Stow, 1993). These deposits can form surficial bedforms at a variety of scales, e.g., erosional lineations to scours, or aggradational ripples to gravel bars (Stow et al., 2009). Bottom current drifts can accumulate at local or regional scales and fine-grained drifts can therefore act as effective hydrocarbon seals, whereas coarse-grained drifts can act as potential reservoirs (Viana et al., 2007). Bottom current drifts are often interbedded with turbidites or other types of sedimentary facies deposited by down-slope flows; however, it remains difficult to differentiate between along-slope bottom current and down-slope sediment gravity flow deposits (Faugeres & Stow, 1993; Stow et al., 2002; Rebesco et al., 2014).

2.3.8 Background deposits

These accretionary elements are characterised by laterally widespread, sheet-like cross-sectional geometries which show little to no facies changes across their extent (cf. the ‘condensed sections’ of Loutit et al., 1988 and ‘mudstone sheets’ of Pyles, 2007). They are composed of very fine grained (clay to silt) sediments which blanket underlying deposits as a result of hemipelagic or pelagic fall-out. These elements are therefore the result of very low sedimentation rates, reflecting the ‘background rate’ of deposition and inferred to be the most pervasive form of sedimentation during periods of regional shoreline transgression (Loutit et al., 1988; Galloway et al., 1989). These elements are characterised by a non-erosive basal bounding surface and near to constant thickness (e.g., Pyles, 2007; Di Celma et al., 2013).

These elements can be used to identify the bounding surfaces of other element architectures, e.g., in lobate or channel architectures, due to their association with the cessation of sediment gravity flows (e.g., Navarre et al., 2002; Hadler-Jacobsen et al., 2005; Gervais et al., 2006(a); Prélat et al., 2009; Flint et al., 2011).

2.4 Controls upon deep-marine systems

Deep-marine systems vary greatly in size and shape (e.g., Barnes & Normark, 1985); for instance, the depositional area of the Navy turbidite system off Southern California, is 560 km^2, in comparison the Zaire turbidite system, offshore Angola, is 290,000 km^2, while the Bengal fan is ten times the size of the Zaire (measurements calculated from Normark et al., 2009, Picot et al., 2016 and Emmel & Curray, 1985, respectively; Fig 2.6). Large deep-marine systems are typically associated with finer grained deposits (e.g., Reading & Richards, 1994; Bouma, 2000); while the proportion of sand-to-mud also influences the type and style of architectural elements deposited, e.g., the formation and down-slope extent of channels with associated levee deposits (Reading & Richards, 1994; Posamentier & Kolla, 2003). The significance of grain-size on deposit geometry, as well as the effects of other flow properties such as concentration, have also been supported through experimental work, e.g., Al Ja'Aidi et al. (2004), Baas et al. (2009), and Fick et al. (2017).

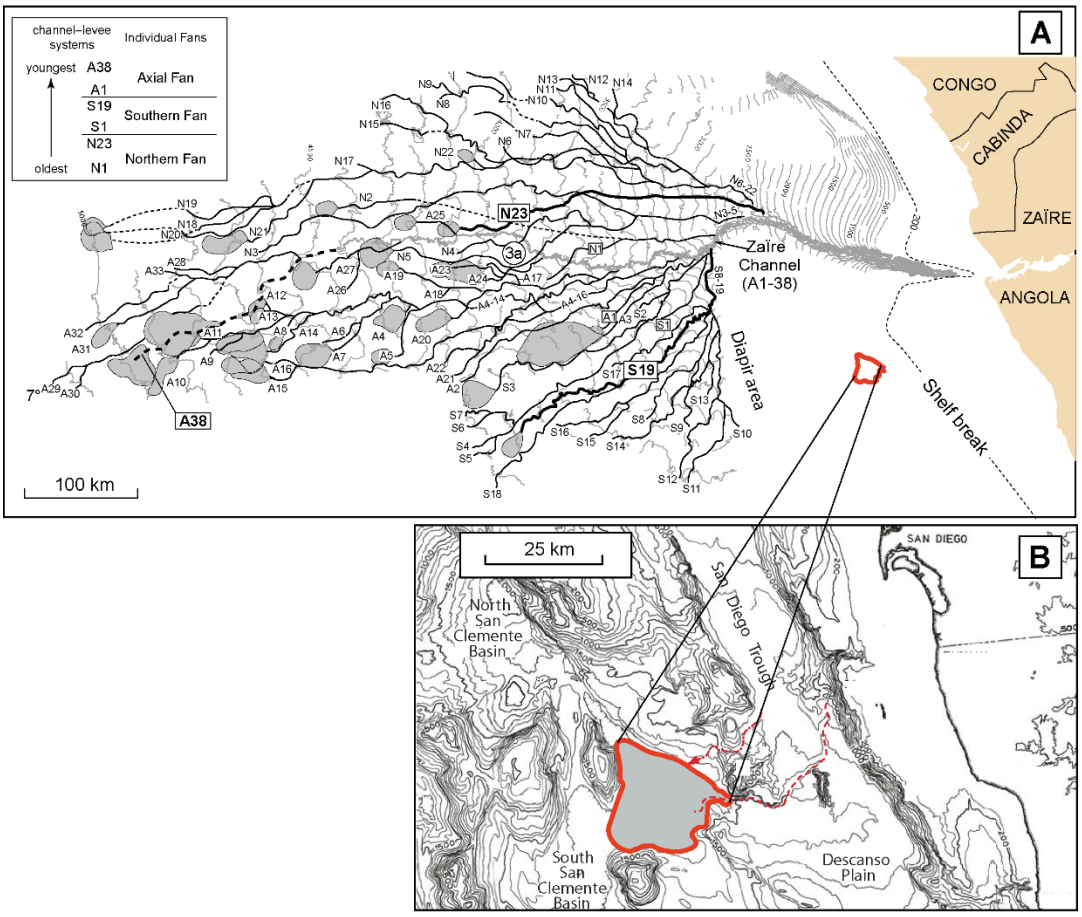

Fig. 2.6. Deep-marine system plan-view images of (A) the Zaire fan and (B) the Navy fan. The systems vary greatly in scale (compare scaled size of the Navy fan area), shelf width, sea-floor topography and architectural characteristics. Images taken from Marsset et al. (2009) and Normark et al. (2009), respectively.

The variety observed between different deep-marine systems is in large measure related to the role of external controls – primarily tectonics, climate, sediment supply and sea-level fluctuations (Reading & Richards, 1994; Stow, 1996; Bouma, 2004; Nelson et al., 2009). A variety of system models have been developed, focusing, to varying degrees, upon the effects of these external characteristics, e.g., Reading & Richards (1994), Shanmugam & Moiola (1988), Bouma (2004) and Gong et al. (2016). It must be noted that these controls - tectonics, climate, sediment supply and sea-level - are all interdependent. For example, regional tectonic regimes characterise the resultant shape and morphology of the depositional system, from the onshore catchment area to offshore depositional sink (c.f., Sømme et al., 2009, 2011; Martinsen, 2011; Bhattacharya et al., 2018; Snedden et al., 2018). In turn, these depositional system configurations modulate sediment supply, as longer sediment pathways, typically associated with passive margins, result in finer deposits downstream (Stow et al., 1985; Bouma, 2004; Michael et al., 2013). Furthermore, the method of sediment transfer from the shelf-edge affects slope morphology (Piper & Normark, 2009; Saller & Dharmasamadhi, 2012), e.g., deltaic systems prevent the formation of large canyons on the slope (Saller & Dharmasamadhi, 2012), as simple open-ended river mouths (i.e., estuaries) transfer sediment more efficiently to the deep-marine environment (Wetzel, 1993). Climatic forcing can influence sediment supply through river floods (Mulder & Syvitski, 1995; Talling et al., 2012; Du et al., 2018), or large-scale sea-level fluctuations (e.g., sub-glacial melts; Covault & Graham, 2010; Gong et al., 2016; Evangelinos et al., 2017). The changes in climate may be the result of astronomically-driven orbital forcings, i.e., Milankovitch cycles, which in turn can align with tectonic events on geological timescales (cf. Pickering & Bayliss, 2009; Payros & Martinez-Braceras, 2014). The effect of external controls can be more easily evaluated in modern systems, where the up-dip portion of the depositional system still exists, allowing comprehension of the mechanisms of sediment delivery to the deep sea. However, the external controls influencing deep-marine deposition may interact in complex manners, rendering it difficult to attribute depositional trends to a specific control. Tectonics, climate, sea-level and sediment supply regimes all vary over multiple time-scales (cf. Miall, 2015) leading to further complications in the assignment of depositional patterns to specific controls. The diversity observed across deep-marine systems can therefore be accredited to the complex interactions between the external controls (Reading & Richards, 1994; Kneller et al., 2009).

Depositional deep-marine systems do not always extend onto the basin plain. Sediment gravity flow processes and their resultant deposits can be affected by the local sea-floor topography, e.g., sea-floor rugosity (Ortiz-Karpf et al., 2017), structural deformation

(Adeogba et al., 2005), salt or mud diapirs (Beaubouef & Friedmann, 2000) or basin confinement (Prather et al., 1998; Lamb et al., 2004; Patacci et al., 2014). Sea-floor topography and local gradient changes influence avulsion profiles in channels (e.g., Heiniö & Davies, 2007), while lateral gradient changes caused by the stacking of elements are proposed to induce lobe switching (e.g., Prélat et al., 2010; MacDonald et al., 2011(b)). The stacking pattern of elements is affected by the frequency and locality of avulsions (Deptuck et al., 2008; Ortiz-Karpf et al., 2015; Picot et al., 2016; Terlaky et al., 2016). Flow velocities decrease over lower gradients, and experimental work has shown how such changes in gradient can influence deposit geometry, e.g., Ouchi et al. (1995), Fernandez et al. (2014). Topographic confinement affects flow direction, velocity, concentration, rheology, and the position of depositional loci (Kneller & McCaffrey, 1999; Mayall et al., 2010). Basin confinement limits the depositional area and overall accommodation space of a system (Prather et al., 1998, 2012; Beaubouef et al., 2003; Covault & Romans, 2009); this can lead to the formation of thicker deposits and eventual overspilling out of the basin if the volume of sediment supplied to the system exceeds the available accommodation space. Facies evidence has shown that the effects of confinement can result in flow transformation, as the flow is deflected by the local topography causing a change in flow velocity (Haughton, 1994; Remacha et al., 2005).

2.5 Quantitative characterisation of sedimentary environments

Deep-marine environments are complex and dynamic. As mentioned in the previous sections, many facies and architectural classifications have been developed in the attempt to better understand these sedimentary systems e.g., Mutti & Normark, 1987; Pickering et al., 1989, 1995; Sprague et al., 2005; Hadler-Jacobsen et al., 2005; Prélat et al., 2009; Flint et al., 2011; Terlaky et al., 2016. Miall (1999) stated that "*at the very least, classifications represent way stations on the road to perfect understanding*". However, communication between such classifications is hampered by the plethora of associated deep-marine terminology. Understanding deep-marine environments is further impeded by the difficulties in confidently assessing process-to-product relationships. These classification systems are grossly oversimplified as they can only consider a limited number of assumed parameters. Modern and ancient analogues have also been used to aid deep-marine interpretations, e.g., Cronin & Kidd (1998), Beaubouef & Friedmann (2000), Moraes et al. (2004), Saller et al. (2004). Analogues are chosen based upon commonalities found between the known properties of a system in question – this method is thus open to bias, as what determines the similarity between systems is left open to the user. Experimental work and numerical

modelling has also been employed to aid deep-marine characterisation, such as the works of Al Ja'Aida et al., 2004; Sumner et al., 2009; Baas et al., 2011; Groenenberg et al., 2010; McHargue et al., 2011; Straub & Pyles, 2012; Cartigny et al., 2014. These methods provide quantitative output but they are again limited by the number of variables they can consider and are also restricted in their applicability because of scaling issues. To overcome the limitations in these methods and for purposes of comparison, relational databases have been developed in all areas of sedimentary geology, e.g., Dreyer et al, 1993; Baas et al, 2005; Gibling, 2006; Richter et al., 2009; Colombera et al, 2012(a); Vakarelov & Ainsworth, 2013; Keogh et al., 2014; Moscardelli & Wood, 2015; Colombera et al., 2016; Clare et al., 2018. A relational database stores data in a standardised manner and enables the organisation of data on a large number of attributes. A database methodology therefore enables the quantitative analysis of big datasets. These empirical outputs can be further used to inform stochastic models and reduce geological uncertainties in reservoir models, e.g., Baas et al., 2005; Colombera et al., 2012(b); Howell et al., 2014. In the field of deep-marine sedimentology a number of deep-marine databases already exist, e.g., Cossey & Associates Inc., 2004; Baas et al., 2005; Moscardeli & Wood, 2015; Clare et al., 2018. However, the scope of these approaches are constrained to either a particular element type (e.g., MTDs; Moscardeli & Wood, 2015, Clare et al., 2018) or data type (e.g., outcrop only deposits; Cossey & Associates Inc., 2004). Deep-marine architecture exhibits a spatio-temporal order; as of yet, no database method exists which takes into account the hierarchical framework of deep-marine deposits from all environmental niches – an omission this project aims to overcome.

Chapter 3:

Hierarchical classifications of the sedimentary architecture of deep-marine depositional systems.

Chapter synopsis

Hierarchical classifications are used in the field of clastic deep-marine sedimentary geology to assign spatial and temporal order to the sedimentary architecture of preserved deep-marine deposits and to genetically-related modern landforms. Although such classifications aim to simplify the description of complex systems, the wide range of developed approaches limits the ease with which deep-marine architectural data derived from different sources can be reconciled and compared. This work systematically reviews and compares a selection of the most significant published hierarchical schemes for the description of deep-marine sedimentary architecture. A detailed account of each scheme is provided, outlining its aims, environmental contexts and methods of data collection, together with the diagnostic criteria used to discern each hierarchical order from observational standpoints (e.g., via facies associations, geometry, scale and bounding-surface relationships) and also on interpretational grounds (e.g., processes and sub-environments of deposition). The inconsistencies and pitfalls in the application of each scheme are also considered.

The immediate goal of this review is to assist sedimentologists in their attempts to apply hierarchical classifications, both in the contexts in which the classifications were originally developed and in alternative settings. An additional goal is to assess the causes of similarities and differences between schemes, which may arise, for example, in relation to their different aims, scales of interest or environmental focus (e.g., channelized or lobate units, or both). Similarities are found between the approaches that commonly underlie the hierarchical classifications. Hierarchies are largely erected on the basis of common types of observations, in particular relating to the lithology and geometries of deposits, in association with analysis of bounding-surface characteristics and relationships. These factors are commonly considered in parallel with their associated genetic interpretations in terms of processes or (sub-) environments of deposition. A final goal of the review is to assess whether a universal standard for the description of deep-marine sedimentary architecture can be devised. Despite the commonalities that exist between classification approaches, a confident reconciliation of the different hierarchical classification schemes does not appear to be achievable in the current state of knowledge.

3.1 Introduction

In the field of deep-marine clastic sedimentology, a wide variety of hierarchical schemes has been proposed to categorise sedimentary deposits, particularly those associated with sediment gravity flows (e.g., Mutti & Normark, 1987; Ghosh & Lowe, 1993; Pickering et al., 1995; Beaubouef et al., 1999; Gardner & Borer, 2000; Prather et al., 2000; Navarre et al., 2002; Gardner et al., 2003; Sprague et al., 2005; Hadler-Jacobsen et al., 2005; Mayall et al., 2006; Gervais et al., 2006(a); Deptuck et al., 2008; Prélat et al., 2009; Campion et al., 2011; Flint et al., 2011; MacDonald et al., 2011(b); Pickering & Cantalejo, 2015; Terlaky et al., 2016). These hierarchies all attempt to classify deep-marine sedimentary architecture by assigning spatial and temporal order or genetic significance to sedimentary packages. Similar hierarchical approaches have also been applied to aeolian (e.g., Brookfield, 1977), fluvial (e.g., Allen, 1983; Miall, 1985), and sequence stratigraphic classifications (e.g., Mitchum & Van Wagoner, 1991; Neal & Abreu, 2009; Catuneanu et al., 2011).

The identification of deep-marine hierarchy has enabled stratigraphic heterogeneities to be better characterised and communicated – an approach which has benefitted hydrocarbon reservoir modelling, resulting for example in more accurate history matching of fluid flow in channel deposits (Stewart et al., 2008) and in improved connectivity models in lobe deposits (Zhang et al., 2009; Hofstra et al., 2016). These largely descriptive hierarchical schemes have also been used to inform models of deep-marine processes (e.g., Gardner et al., 2003; McHargue et al., 2011(a); Macauley & Hubbard, 2013; Terlaky et al., 2016; Hamilton et al., 2017).

However, it can be argued that the wide variety of hierarchical schemes of deep-marine sedimentary architecture no longer simplifies the analysis of deep-marine deposits. Schemes may vary in the number of significant orders, terminology and observational or interpretative criteria used to define significant hierarchical orders. This lack of standardisation significantly hampers comparative studies between different depositional systems and datasets, in turn limiting the effectiveness of predictions or insight derived from the comparison. Terminological variability - a long-standing problem in deep-marine studies (cf. Mutti & Normark, 1987; Shanmugam & Moiola, 1988; Weimer & Slatt, 2007(a); Terlaky et al., 2016) - also calls into question the consistency with which primary sedimentological studies are undertaken.

The aims of this Chapter are as follows:

- To review the variety seen within and between hierarchical classifications of clastic deep-marine deposits. To this end, the most widely adopted and distinctive deep-

marine hierarchy schemes are described in detail. The motivation behind each of these schemes and the scope of each study is assessed. The diagnostic tools used within each hierarchy to identify discrete architectural levels are also evaluated.

- To evaluate the possible causes of variety observed in hierarchical approaches, considering whether the range of observed approaches is a consequence of excessive categorisation or whether it reflects a genuine variability in the organisational styles of deep-marine clastic depositional systems.
- To establish the degree to which hierarchical classifications can be reconciled. Is a 'Rosetta stone' approach, whereby all classifications can be reassigned to a common standard, feasible?

3.2 Approaches to hierarchical classification

A selection of key hierarchical schemes available in the literature are reviewed in this Section, demonstrating the breadth of hierarchical concepts that exist and are used in deep-marine sedimentary geology. These schemes have been chosen due to their importance in the way hierarchical organisation is formalised and/or because of their broad acceptance and usage. The degree and manner in which each scheme has been taken up by fellow scientists are either considered in each summary Section or presented in separate extended subsections. 'Cited by' scores (as of January 2018) are also recorded in Table 3.1; however, caution should be exercised in interpreting these metrics: the citations of an article do not necessarily relate to the popularity of the hierarchical scheme proposed therein, as the same article might be cited for other reasons.

Firstly, a review is undertaken of early studies that popularised the use of hierarchical schemes in deep-marine clastic depositional systems (Mutti & Normark, 1987; Ghosh & Lowe, 1991; Pickering et al., 1995). Secondly, the subsequent schemes that contributed significant concepts to hierarchical classifications are reviewed, based on insights derived from outcrops (Gardner & Borer, 2000; Pickering & Cantalejo, 2015; Terlaky et al., 2016) and reflection-seismic data (Prather et al., 2000; Navarre et al., 2002; Sprague et al., 2005). Thirdly, a series of schemes is reviewed that attempted to assign sequence stratigraphic significance to hierarchical orders (e.g., Sprague et al., 2005; Hadler-Jacobsen et al., 2005; Mayall et al., 2006). Finally, schemes that were specifically developed for depositional lobes, based on both outcrop and seismic data, are reviewed (Gervais et al., 2006(a); Deptuck et al., 2008; Prélat et al., 2009; Flint et al., 2011; MacDonald et al., 2011(b)).

The focus of these hierarchical summaries will be upon understanding the basis on which each hierarchical classification has been formulated, and on explaining how to recognise the discrete hierarchical levels identified in each scheme. This Section will therefore examine the key principles and criteria used by each particular scheme, and describe how these principles for hierarchical division have developed over time. The hierarchies will be reviewed in order of publication; follow-on alterations of the schemes will be considered in sequence with the original study. A summary flowchart (Fig. 3.1) illustrates the influences of earlier hierarchical schemes on subsequent schemes. Table 3.1 lists all the considered hierarchical schemes and highlights their key attributes.

Fig. 3.1. (*overleaf*) Citations flowchart documenting the influences of earlier hierarchical schemes over later schemes. Each box represents a paper detailing a certain hierarchical scheme; the publications are arranged chronologically from top to bottom. Lines represent citations between the various schemes (arrow pointing to younger paper). Orange arrows represent citations to key sequence stratigraphy works or direct reference to sequence stratigraphic units (e.g., systems tracts or depositional sequences) or to timescales derived from either Vail et al. (1977), Mitchum (1977), Van Wagoner et al. (1988), Mitchum & Van Wagoner (1991) or Van der Merwe (2010). Blue arrows represent citations to key publications on architectural element analysis or reference to a given hierarchy of bounding surfaces, e.g., by McKee & Weir (1953), Brookfield (1977), Allen (1983) or Miall (1985, 1987, 1989).

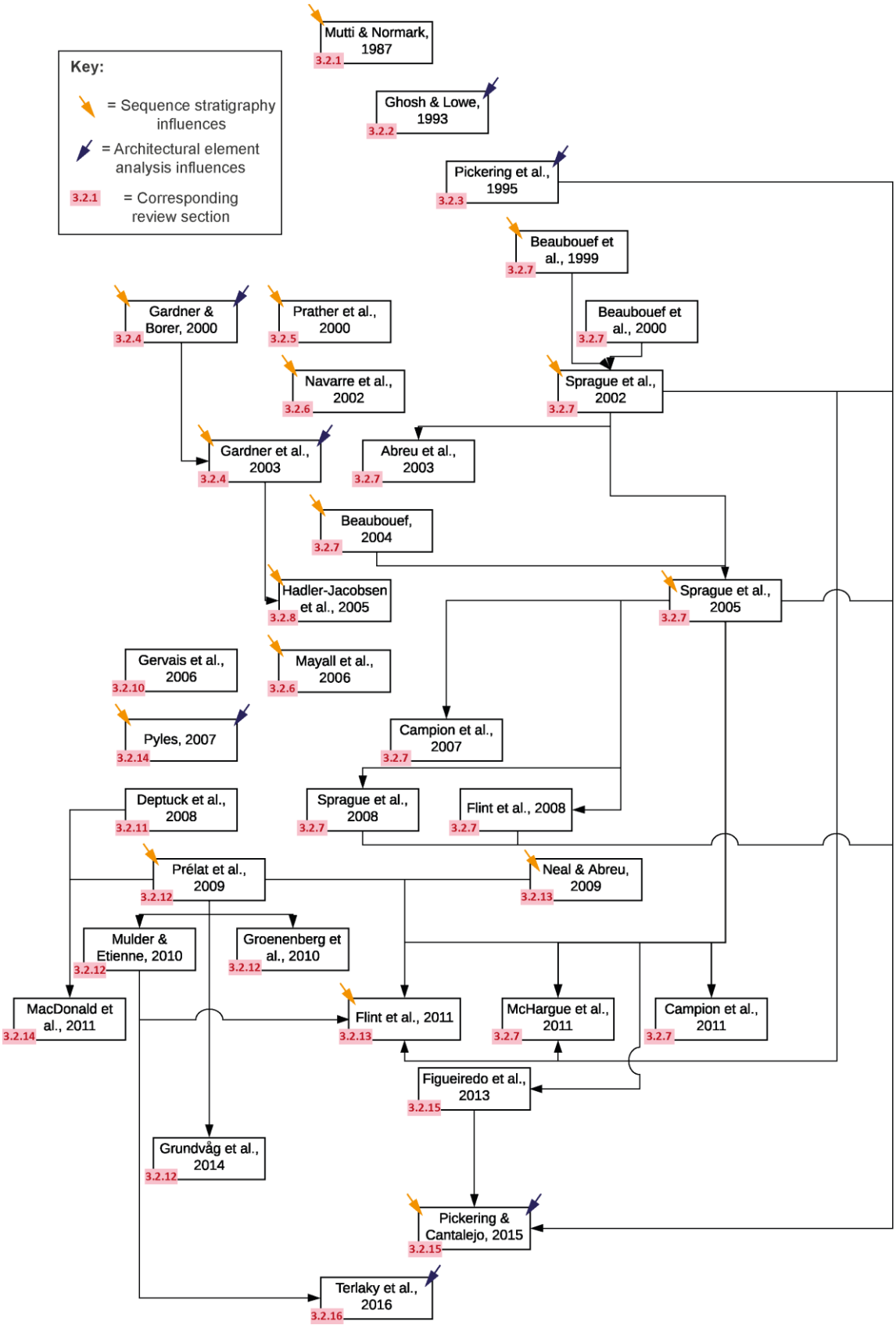
Key:
= Sequence stratigraphy influences
= Architectural element analysis influences
3.2.1 = Corresponding review section
Mutti & Normark, 1987 3.2.1
Ghosh & Lowe, 1993 3.2.2
Pickering et al., 1995 3.2.3
Beaubouef et al., 1999 3.2.7
Gardner & Borer, 2000 3.2.4
Prather et al., 2000 3.2.5
Beaubouef et al., 2000 3.2.7
Navarre et al., 2002 3.2.6
Sprague et al., 2002 3.2.7
Gardner et al., 2003 3.2.4
Abreu et al., 2003 3.2.7
Beaubouef, 2004 3.2.7
Hadler-Jacobsen et al., 2005 3.2.8
Sprague et al., 2005 3.2.7
Gervais et al., 2006 3.2.10
Mayall et al., 2006 3.2.6
Pyles, 2007 3.2.14
Campion et al., 2007 3.2.7
Deptuck et al., 2008 3.2.11
Sprague et al., 2008 3.2.7
Flint et al., 2008 3.2.7
Prélat et al., 2009 3.2.12
Neal & Abreu, 2009 3.2.13
Mulder & Etienne, 2010 3.2.12
Groenenberg et al., 2010 3.2.12
MacDonald et al., 2011 3.2.14
Flint et al., 2011 3.2.13
McHargue et al., 2011 3.2.7
Campion et al., 2011 3.2.7
Figueiredo et al., 2013 3.2.15
Grundvåg et al., 2014 3.2.12
Pickering & Cantalejo, 2015 3.2.15
Terlaky et al., 2016 3.2.16

Study	Hierarchy objective	Number of hierarchical orders	Data type, domain of application	Physiographic setting	Architectural element focus	Case study(ies)	Age of deposits	Additional boundary conditions	Influences	Hydrocarbon industry affiliations	Google scholar citations
Mutti & Normark, 1987	Designed to reconcile studies of modern and ancient turbidite systems, and associated data types	5	Seismic and outcrop datasets	Slope to basin floor	-	-	Applicable to ancient and modern systems	-	Devised as relatable to the sequence stratigraphy framework	-	680
Ghosh & Lowe, 1993	Channel hierarchy by using detailed facies analysis and lateral and vertical facies correlations	5	Outcrop	'mid-fan' (after Normark, 1970; Walker, 1978; Mutti & Ricci Lucchi, 1972) (CLTZ)	Channels	Venado Sandstone Member, California	Applied to Cretaceous	Coarse sand to conglomeratic system	Bounding-surface hierarchy of Allen (1983); architectural-element analysis of Miall (1987, 1989)	-	39
Pickering et al., 1995	Founded on architectural element analysis; hierarchy is emplaced using bounding surfaces	7	Seismic and outcrop datasets	Slope to basin floor	-	-	Applicable to ancient and modern systems	Sand-rich system	Bounding-surface hierarchy of Allen (1983); architectural-element analysis of Miall (1985)	Sponsored by Shell Exploration	84
Beaubouef et al., 1999	Based upon sequence stratigraphy; divisions reflect sequence boundaries	5	Outcrop and well data	Slope to basin floor	Channels	Brushy Canyon Formation, West Texas	Applied to Permian	Tectonically stable shelf with gradually decreasing subsidence rates	Sequence stratigraphy concepts	Workers from Exxon Production Research Company	100
Prather et al., 2000	Largely concerned with seismic scales	7	Seismic, well-log and core data	Slope to basin floor	-	General reference to Central Gulf of Mexico intraslope basins	Applicable to ancient and modern systems	Sand-rich system	-	Workers from Shell International E&P	33
Gardner & Borer, 2000	Specific to channel-lobe transition zone (CLTZ)	4	Outcrop	Slope to basin transition zone (CLTZ)	-	Brushy Canyon Formation, West Texas	Applied to Permian	Sand-rich system	Architectural-element analysis	Sponsored by 13 different research and exploration petroleum companies	130
Navarre et al., 2002	Produced to aid reservoir characterisation through recognition of turbidite stratigraphic architecture	6	Seismic and core and well-log data	Slope to basin floor	-	Gulf of Guinea, West Africa	Applied to Tertiary	-	-	Workers from TotalFinaElf	55
Gardner et al., 2003	Modification of scheme by Gardner and Borer (2000): formative processes now considered	4	Outcrop	Slope to basin transition zone (CLTZ)	-	Brushy Canyon Formation, West Texas	Applied to Permian	Sand-rich system	Architectural-element analysis	Sponsored by 23 research and exploration petroleum companies	129
Abreu et al., 2003	Modification to hierarchy of Sprague et al. (2002); includes LAPs in channel systems	4	Seismic, well data, and outcrop datasets	Slope	Channel lateral accretion packages (LAPs)	Dalia and Grissol fields, offshore Angola	Applied to Miocene	-	Sprague et al. (2002)	Workers from ExxonMobil Upstream Research Company. Seismic data was supplied by 5	294

										petroleum companies	
Sprague et al., 2005	Physical stratigraphic framework developed for hydrocarbon reservoir prediction in slope and basin settings	8	3D seismic, well-log and core data	Slope to basin floor	-	Off-shore west Africa	Applied to Miocene and Pliocene	-	Beaubouef (1999); Campion et al. (2000); sequence stratigraphy concepts	Workers from ExxonMobil & Shell Deep Water Services Company	41
Hadler-Jacobsen et al., 2005	Chronostratigraphic orders assigned based on sequence stratigraphic principles, at seismic scale	5	Seismic and outcrop datasets	Shelf to basin floor	-	Finnmark Platform; Porcupine Basin; Viking Graben; Central Basin in Spitsbergen; Tanqua Karoo Basin; Brushy Canyon Formation	Applicable to ancient systems	Sand-rich system	Sequence stratigraphy concepts	Sponsored by Statoil	51
Gervais et al., 2006	Based upon internal geometry of lobes, observed and interpreted via seismic facies	3	High-resolution seismic	Basin floor	Lobes	Golo basin, East Corsica	Applied to Pleistocene to Holocene	Sand-rich system, ponded basin	-	-	93
Mayall et al., 2006	Based upon recognition of likely stratigraphic setting, and channel element characteristics (sinuosity, facies, cutting and filling, stacking patterns) at each level	3	High-resolution seismic and outcrop datasets	Slope	Erosionally confined channels	Seismic data from a range of studies; outcrop examples from the Brushy Canyon Formation	Applied to Pleistocene and modern systems	-	Sequence stratigraphy concepts	Sponsored by BP, Sonangol, Total, ExxonMobil, Statoil, Norsk Hydro, ENI	243
Deptuck et al., 2008	Applicable to lobes; influenced by recognition of scales of compensational stacking	4	High-resolution seismic, cores	Basin floor	Lobes	Golo basin, East Corsica	Applied to Pleistocene to Holocene	Sand-rich system, ponded basin	-	-	115
Prélat et al., 2009	Based upon characteristics and geometry of fine-grained units between sand-prone lobes	4	Outcrop	Basin floor	Lobes	Tanqua depocentre, Karoo basin, South Africa	Applied to Permian	-	-	Sponsored by Chevron, Maersk, Petrobas, PetroSA, StatoilHydro, Total	138
MacDonald et al., 2011	Based on hierarchy of Deptuck et al. (2008), with modifications in light of process sedimentology	3	Outcrop	Basin floor	Lobes	Ross Formation, Ireland	Applied to Carboniferous	Sand-rich system	Deptuck et al. (2008)	-	33
Flint et al., 2011	Based on regionally mappable hemipelagic claystones; utilises sequence stratigraphy concepts; lobe hierarchy related to sea-level fluctuations	3	Outcrop	Slope to basin floor	Lobes	Lainsburg depocentre, Karoo Basin, South Africa	Applied to Permian	-	Sprague et al. (2002); Neal & Abreu (2009); sequence stratigraphy concepts	Sponsored by ExxonMobil	93
Pickering & Cantalejo, 2015	Used to characterise and correlate stratigraphic surfaces at many scales, allowing identification of bounding surfaces of architectural elements	10	Outcrop, cores	Slope (or basin floor, origin of deposits is debated)	Channels (and MTD/MTC components)	Upper Hecho Group, Ainsa Basin, Spain	Applied to Eocene	Coarse clastic sediment entering from a point source	Flint et al. (2008); Sprague et al. (2008); facies terminology of Pickering et al. (1986; 1989)	Sponsored by CNOOC-Nexen Petroleum UK Ltd	2

Terlaky et al., 2016	Derived from existing schemes; focuses upon recognition of scale and context of channel avulsion	7	Outcrop	Basin floor	-	Windermere Supergroup, British Columbia, Canada	Applied to Neo-proterozoic	Mixed-sediment system	Architectural-element analysis; Mulder & Etienne's (2010) review, itself influenced by Prélat et al. (2009)	Sponsored by 7 research and exploration petroleum companies	8

Table 3.1. Summary table for all works evaluated within this review. The table notes the objectives and deep-marine setting for each study. The case-study examples used within the original studies are also recorded, along with any peer-reviewed literature or sedimentological concepts the study states to have greatly influenced the development of the resultant hierarchy. Citation statistics as of January 2018.

3.2.1 Mutti & Normark, 1987

The hierarchical scheme developed by Mutti & Normark (1987; 1991) is recognised by many as the first attempt to adopt a hierarchical classification that spanned both ancient and modern deep-marine environments (Ghosh & Lowe, 1993; Pickering et al., 1995; Clark & Pickering, 1996(a); Shanmugam, 2000; Weimer & Slatt, 2007(a)). While the application of this particular scheme in following studies has been somewhat limited, many authors have drawn comparisons between hierarchical orders in Mutti & Normak's (1987) scheme and their own orders (e.g., Ghosh & Lowe, 1993; Pickering et al., 1995; Prather et al., 2000; Sprague et al., 2005).

This hierarchy was designed to reconcile the differences between datasets of modern marine environments, acquired by seismic techniques and ancient outcrops of turbidite deposits. Mutti & Normark (1987) recognised that the key difficulty in classifying and thus comparing systems lies in recognising sedimentary bodies that were deposited over similar timescales within the deep-marine realm. Therefore, they aimed to develop a hierarchy that would enable recognisable turbidite bodies ('elements') to be compared over similar temporal as well as spatial scales.

Mutti & Normark (1987) identify five main orders of scale (see Fig. 3.2), which link to the sequence stratigraphic framework of Vail et al. (1977) on the basis of the proposed timescales reflected by each order. Mutti & Normark's estimated timescale ranges are based upon interpretations of the likely cause and extent of the breaks in sedimentation associated with a particular hierarchical order. The smallest recognised hierarchical order is a '**turbidite bed**', which is interpreted by Mutti & Normark (1987; 1991) as being a "normal" small-scale erosional and depositional feature, deposited over "virtually instantaneous", or 1-1000 years, timespans. Genetically related 'turbidite beds' stack laterally and vertically to form facies associations known as '**turbidite sub-stages**' (1-10 metres thick), which equate to individual periods of deposition, bypass or erosion within a specific stage of growth. Mutti & Normark (1987) note that some depositional systems may consist of only one such 'sub-stage' facies character. These 'sub-stage' units are described to be high-frequency deposits, deposited over 1 to 10 kyr timescales. 'Turbidite beds', also described by Mutti & Normark (1987; 1991) as 5th order units, and 'sub-stages' (4th order) are stated to be typically only visible below conventional seismic resolution; thus, the applicability of these elements of Mutti & Normark's (1987) hierarchy to conventional seismic datasets is limited. A '**turbidite stage**' (3rd order) is formed by the stacking of 'turbidite sub-stages' and records what is termed as a specific growth period, consisting of associated facies associations with no significant breaks

in sedimentation (unconformities) within the unit. This 3rd order hierarchical level is stated to be seismically resolvable if the thickness of the unit exceeds several tens of metres.

It is at the 'turbidite stage' or 'turbidite sub-stage' that Mutti & Normark (1987) accredit the formation of recognisable 'elements' in the deep-marine environment. Mutti & Normark (1987; 1991) document five element types that are common to both modern and ancient systems, and that can be differentiated in terms of geometries, resulting from different sets of depositional processes:

- channels, i.e., negative relief pathways for sediment transport;
- major erosional non-channel features, i.e., scours and slope failures;
- depositional lobes, i.e., typically sandy distributary deposits;
- overbank deposits, i.e., laterally extensive fine-grained deposits adjacent to major channels;
- channel-lobe transitions, i.e., a mix of depositional and erosional elements reflecting a transformation of flow, where turbidity currents commonly experience hydraulic jumps.

These elements are described as basic 'mappable' units which can have either erosional or depositional characteristics.

'Turbidite stages' stack to form a '**turbidite system**' (0.1-1 Myr); these deposits are said to be characterised by short-term sea-level change or tectonic activity, whereby no major breaks in sedimentation are seen. Similar sequences in 'turbidite stage' stacking are observed and interpreted to be the product of an overall reduction in flow volume, as relative sea level gradually rises. A 'turbidite system' (2nd order) may contain only a single 'turbidite stage', or it may be a composite unit made of multiple stages of growth. A 'system' is seen by Mutti & Normark (1987) to always terminate with a mudstone interval, interpreted to be the product of a highstand systems tract (HST) in response to short-term sea-level change. A 'turbidite system' is defined by the authors as being a 'part' of a depositional sequence *sensu* Vail et al. (1977) which is defined as a relatively conformable succession of genetically related strata, typically bounded at its top and bottom by unconformities, representing a cycle of sea-level change. The identification of higher orders in the hierarchy (2nd and 1st orders) relies strongly upon the recognition of erosional surfaces that envelope lower-order genetically related units. The largest hierarchical order recognised by Mutti & Normark (1987) is termed a '**turbidite complex**' (1st order). A unit of this order reflects a complete basin-fill succession built through stacking of 'turbidite systems' in the same long-lived depocentre (1 to 10 Myr duration). These sedimentary units are bounded by long-term unconformities, and may be seen to contain multiple 'depositional sequences'. 'Turbidite complex' depositional bodies

may reach volumes over 100 km³ and thus far outreach the scales of investigation of almost all outcrop studies.

Although the scheme aims at being broad, the assignment of hierarchical orders is stated by Mutti & Normark (1987; 1991) to only be effective after an initial categorisation process, whereby studies are categorised into their 'basin types'. Basin types are identified by a number of criteria (e.g., basin size, rate of sediment supply, crustal mobility, syndepositional tectonics), to ensure that potential comparisons are made between relatable basin environments, with the aim of producing more reliable and meaningful comparative analyses.

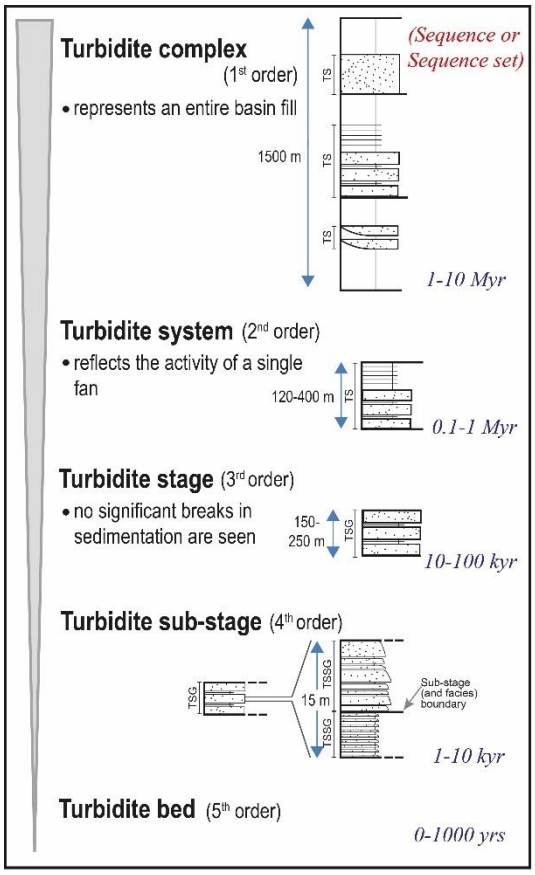

Fig. 3.2. Hierarchical classification of Mutti & Normark (1987), showing the five hierarchical orders, as well as the associated typical thicknesses and durations (blue italic text) proposed for each order. Correspondence with sequence stratigraphic units is also noted (red italic text). Modified after Mutti & Normark (1987).

3.2.2 Ghosh & Lowe, 1993

The hierarchy of Ghosh & Lowe (1993) deals with the nested architecture of channel deposits in the geological record. Until the early '90s, the internal sedimentary architecture of channel units was relatively poorly characterised, due to the limited resolution of seismic datasets and dominantly one-dimensional facies descriptions, as well as the limited lateral extent of most studied outcrops. Ghosh & Lowe (1993) carried out detailed lateral correlations of

closely spaced vertical sections in the Venado Sandstone Member (Great Valley Group, Sacramento Basin, California) and developed a hierarchy focussing upon the internal architecture of channel deposits. Through facies analyses, the study established links between processes of turbidity current erosion and sedimentation, and the resultant channel-deposit architecture.

Ghosh & Lowe (1993) were influenced by Brookfield (1977), Allen (1983) and Miall's (1987; 1989) clastic hierarchical classifications, based upon the recognition of bounding surfaces of different types to distinguish hierarchical orders. Similarly to the approaches taken by these authors, Ghosh & Lowe's (1993) order numbering is from smallest to largest, as opposed to the scheme of Mutti & Normark (1987), which followed sequence stratigraphic convention. Six orders are proposed, although only five were identified in the Venado Sandstone, based upon correlations made between three measured sections over a distance of 475 m, see Fig. 3.3.

Sedimentary gravity flow deposits are typically heterogeneous with regards to sediment texture and structure. Internal variations in grain-size or sedimentary structures define divisions at the smallest and finest scale of this scheme, i.e., '**first-order**' elements. These elements correspond to Bouma divisions (e.g., T_a, T_b or T_c, Bouma 1962) or high-density turbidity current divisions (e.g., S_1, S_2 or R_1 of Lowe, 1982) and represent deposition over minute to hour timescales, by reference to the work of Sadler (1981). These elements are bounded by first-order bounding surfaces, which according to Ghosh & Lowe (1993) record processes of transport and deposition during flow evolution. It is also understood that the arrangement of these first-order divisions within their 'second-order' elements are controlled by the evolution of the flow and its effect upon grain-size distribution. The recognition of these 'first-order' elements is difficult in some cases, especially in massive units such as conglomerates and debris flows, like those found in the basal section of the Venado Sandstone, where the identification of surfaces can be highly uncertain.

The '**second-order**' element is described as a single sedimentation unit based on the terminology of Allen (1983). In the case of heterogeneous deposits, these units comprise a number of 'first-order' elements. Massive deposits, where internal divisions are not easily recognised, will have equivalent 'first-order' and 'second-order' bounding surfaces. These 'second-order' surfaces are recognised as 'inter-flow' surfaces (deposited over day, 10^{-3} yr, timescales) between depositing currents, and are thus stated to be useful indicators of the currents character, e.g., whether flows are depositional, erosional or mixed. Sedimentation units can usually be divided into textural zones representing surges within a single turbidity

current. Twelve 'second-order' units were identified by Ghosh & Lowe (1993) in the Venado Sandstone, with thicknesses in the range of 0.05-8 m and with some inter-channel units extending laterally over the entire 475-m-wide outcrop. The lateral correlation of 'second-order' units can be affected by erosion and scouring of subsequent flows and internal lateral variability can be seen due to the arrangement of internal 'first-order' elements. Grain-size contrasts, internal grading and scoured bases are all facies characters used to determine individual sedimentation units; it can therefore be hard to decipher 'second-order' units within conglomerates, as well as in amalgamated deposits.

'**Third-order**' elements bound groups of 'second-order' sedimentation units. These units are compared to the '5th order' (the 'turbidite-bed') of Mutti & Normark (1987) which Ghosh & Lowe (1993) additionally term a 'macroform'. At least 8 'third-order' elements, between 5-30 m thick, are identified in the Venado Sandstone as 'channel infilling' units, encapsulating deposits of similar flow units. These units are correlated more readily over greater distances than 'second-order' units, as little lateral change can be seen with regards to their internal character. 'Third-order' units are bound by third-order bounding surfaces and are recognised based upon similar internal lithologies and depositional styles. In particular, three types of 'third-order' units are described in this outcrop, respectively made of 1) conglomeratic thick-bedded sandstone, 2) thick-bedded sandstone and 3) thin-bedded mudstone and sandstone interpreted as inter-channel units.

'**Fourth-order**' elements represent individual channel systems and are also termed channel complexes. These units are deposited over 1-10 kyr timescales. Five 'fourth-order' units (50-75 m thick) were recognised in the Venado Sandstone, each showing fining-upwards trends in bed thickness and grain size. These units are made comparable to Mutti & Normark's (1987) '4th order' and '3rd order' ('turbidite sub-stage' and 'stage') elements. Ghosh & Lowe (1993) stated that the genetic significance of 'fourth-order' units still needed to be elucidated. These 'fourth-order' elements separate individual channel units in a multi-channel complex, the '**fifth-order**' hierarchical element. The entire Venado Sandstone Member at Monticello Dam (400-1000 m thick) is recognised as a single 'fifth-order' element. The boundary between the Venado Sandstone and its overlying unit (Yolo shale) can be traced throughout the basin, reflecting the regional scale of this unit. Durations between 0.1-1 Myr are assigned to these 'multi-storey channel stack' units based upon the stratigraphic timescales proposed by Sadler (1981). This order is compared to the '2nd order, depositional system' of Mutti & Normark (1987). A '**sixth-order'** is also made comparable to Mutti & Normark's (1987) '1st order', termed by Ghosh & Lowe (1993) as a 'fan complex'. No such elements are identified in the

Venado Sandstone. Ghosh & Lowe (1993) consider units at this order to develop over 1-10 Myr timescales, based on the work by Sadler (1981).

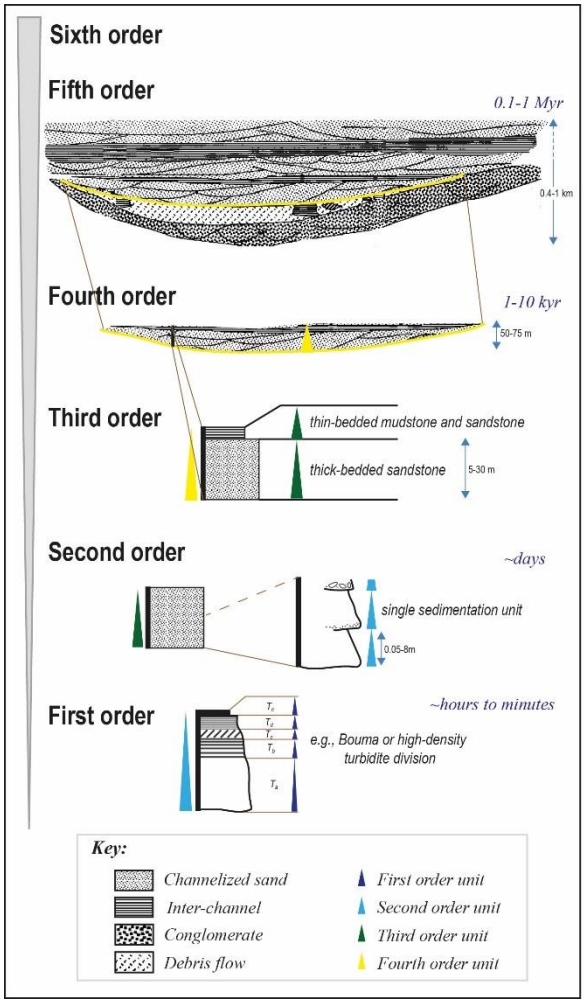

Fig. 3.3. Hierarchical classification developed by Ghosh & Lowe (1993) based upon the coarse channel-fills of the Venado Sandstone. Values of thickness based on field measurements and durations based upon the sedimentation rates of Sadler (1981) are included. Figure modified after Ghosh & Lowe (1993).

The strong reliance on the identification of small-scale facies characters, along with the importance of lateral correlations in defining lithological variations, prevents this hierarchy from being easily applied to seismic datasets. However, this scheme has been used in several studies, and featured in the popular textbook by Reading (1996). The scheme has been used to classify hierarchy in a variety of conglomeratic channel environments, such as the Juniper Ridge Conglomerate (Great Valley Group, California, USA; Hickson & Lowe, 2002), the Cerro Torro Formation (Magallanes Basin, Chile; Hubbard et al., 2008) and the Peri-Adriatic basin (Central Italy; Di Celma et al., 2010; Di Celma 2011), as well as both channel and lobe deposits of the fine-grained Lower Mount Messenger Formation (Taranaki Basin, New Zealand; Masalimova et al., 2016). The study by Hickson & Lowe (2002), which is also focussed on the Great Valley Group, expands upon the original hierarchy of Ghosh & Lowe (1993). For

example, Hickson & Lowe (2002) specify that this scheme is open-ended and thus a variable number of hierarchical orders may be recognised for different case-studies, although only 'third-' and 'fourth-' orders are confidently identified in their study. Hickson & Lowe (2002) also state that each hierarchical order should be assigned based on descriptive features only, and that genetic interpretations of element orders should only be attempted after descriptions have been made.

3.2.3 Pickering et al., 1995

Similarly to Ghosh & Lowe (1993), Pickering et al. (1995) were inspired by the works of Allen (1983) and Miall (1985) and their development of a hierarchy of bounding surfaces. Pickering et al.'s (1995) hierarchy is stated to be directly influenced by the methods of architectural-element analysis, expressed through the diagnosis of characteristic 'building blocks' of sedimentary architecture based on the recognition of facies associations, sedimentary-body geometries and a bounding-surface hierarchy. However, like the scheme of Mutti & Normark (1987), the hierarchy of Pickering et al. (1995) targeted the characterisation of both ancient and modern systems. Thus, a particular focus was placed upon the recognition of surfaces and their 2D and 3D expressions in deep-marine architecture, as opposed to Ghosh & Lowe's (1993) mainly facies-based approach.

Pickering et al. (1995) utilise the three-tiered bounding-surface hierarchy originally employed by Allen (1983). Allen's (1983) hierarchy for fluvial deposits envisaged depositional bodies as being divisible into 'packets' of genetically related strata through the observation of bounding surfaces. This approach was deemed by Pickering et al. (1995) to be transferable to deep-marine systems, as bounding surfaces can be recognised and classified in a similar manner based upon their nature and cross-cut relationships. Four types of bounding surfaces were identified by Allen (1983): 'concordant non-erosional/normal', 'concordant erosional', 'discordant non-erosional' and 'discordant erosional' contacts. This bounding-surface set was applied to deep-marine deposits by Pickering et al. (1995), and the hierarchy was extended through the addition of higher spatial and temporal orders (fourth, fifth, and sixth hierarchical orders), to allow basin-scale deep-marine architectures to also be classified, similarly to Miall's (1985) extension of Allen's (1983) orders for fluvial deposits. The identification of bounding surfaces, their corresponding architectural geometry and internal facies characters are used to generate a sedimentological hierarchical framework, which Pickering et al. (1995) claim ensures a defendable methodical approach to architectural classification in the deep-marine realm (see Fig. 3.4).

In this seven-tiered classification established upon the hierarchy of bounding surfaces, each hierarchical order is associated with both a descriptive name as well as a numerical order referring to a bounding-surface level. '**Bedding contacts**' describe the smallest (zeroth) order (Fig. 3.4a); they are described by Pickering et al. (1995) as normal, concordant bedding contacts found between strata and laminae. These 'bedding contacts' are bound by first-order bounding surfaces, to separate deposits known as '**bedding packages**', i.e., packages of cross-bedding or "concordant beds" (Pickering et al., 1995). Both these zeroth and first order sedimentary packages are comparable to Campbell's (1967) definitions of lamina and beds. Second-order '**sedimentary complexes**' form distinct sedimentary bodies of genetically related facies with a "similar" palaeocurrent direction, though similarity is not defined by Pickering et al. (1995). This hierarchical order was considered comparable to the fluvial 'storey' definition of Friend et al. (1979). Orders zeroth to third are strongly based upon facies descriptors and the associated bounding surfaces are all of limited extent. However, at the third order of the hierarchy, major erosional surfaces are seen to encapsulate multiple 'sedimentary complexes' to form a '**depositional body**'. At this order, distinct architectural-element styles are observed, which reflect different architectural geometries (e.g., channelized, sheet-like, etc.). The fourth order refers to erosional contacts that can be basin-wide, defining groups of third order channels and palaeovalleys, observable at what is described as "mappable stratigraphic scales". Units at this fourth order were termed '**members/sub-members**' by Pickering et al. (1995) and were described as being a hierarchical order that would further subdivide the 'turbidite stage (3rd order)' of Mutti & Normark (1987, 1991). A 'turbidite stage' *sensu* Mutti & Normark (1987) is described as being either a single stage of deposition (hence comparable to the third-order single-channel architectural element of Pickering et al., 1995), or as containing multiple stages of growth, reflecting a composite depositional feature, hence represented by the fourth-order of Pickering et al. (1995). Fifth-order surfaces bound '**individual fan systems**'; these are simply stated by Pickering et al. (1995) to be equivalent to Mutti & Normark's (1987) 'turbidite systems' with no further reasoning. The sixth-order bounding surfaces of Pickering et al., 1995, delineate a whole '**basin-fill sequence**', which is made comparable to Mutti & Normark's 'turbidite complex'.

Pickering et al. (1995) also classify sedimentary units on their cross-sectional and planform geometries (Fig. 3.4b & c). Such geometrical notation is not limited to any particular hierarchical order, however Pickering et al. (1995) note that such classification is limited by the capabilities of the method of data acquisition. The sedimentary units are also characterised by their internal facies associations based on the facies classification scheme of

Pickering et al. (1986). 'Bounding surfaces' are noted as being either erosional or conformable. However, with the exception of facies changes, no criteria are provided by Pickering et al. (1995) as to how significant conformable bounding surfaces would be confidently identified, for example, in lobe settings.

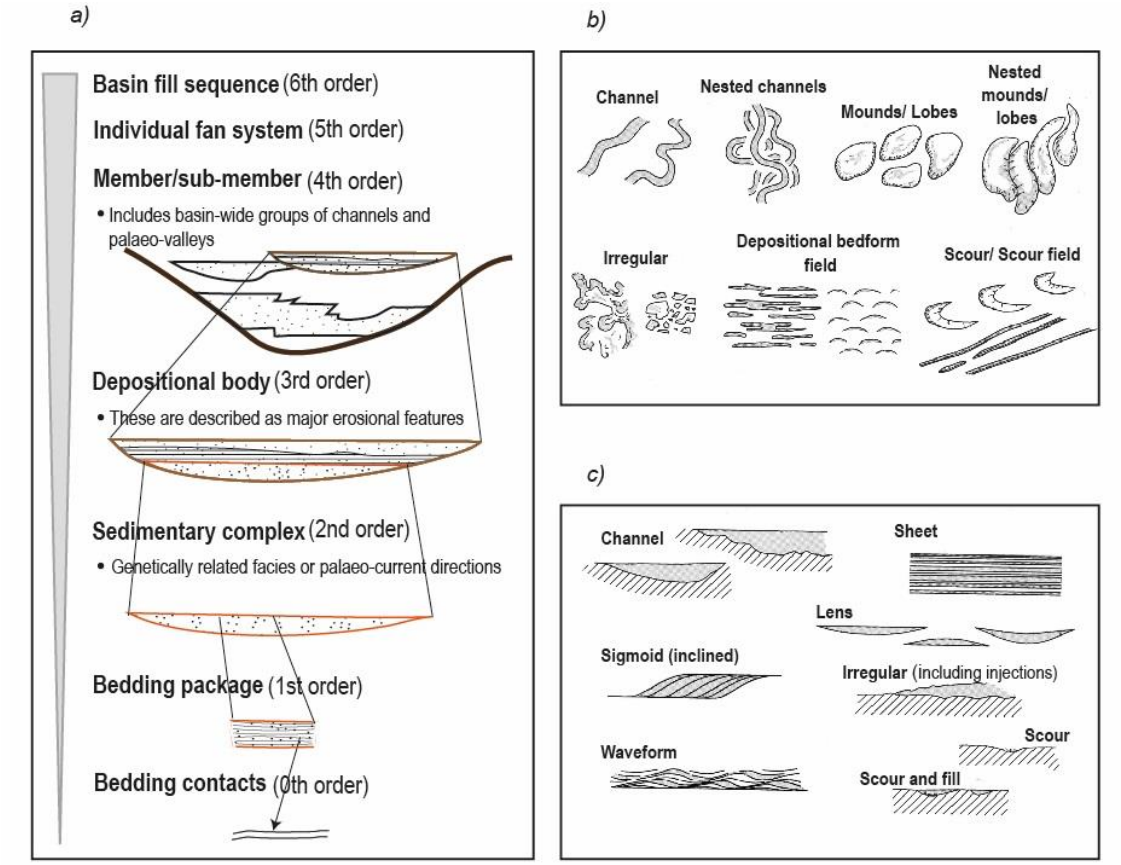

Fig. 3.4. *a)* Hierarchical classification of Pickering et al. (1995), showing the nomenclature and numbering associated to bounding-surface orders. The *b*) planform classification and *c*) cross-sectional classification of deep-water architectural geometries by Pickering et al. (1995) are also shown. These geometrical classifications are applicable over a wide range of scales. Figures modified after Pickering et al. (1995).

Pickering et al. (1995) also stress that not all hierarchical levels may be present in all deep-marine turbiditic systems, as some systems may be more 'punctuated' than others, meaning that hierarchical orders may be missing in some deep-marine systems. The hierarchical divisions are therefore seen to only act as a guide. No dimensional attributes are provided as criteria for the recognition of these hierarchical orders, as bounding-surface levels are seen by Pickering et al. (1995) to be independent of such spatial classifications. Scale is simply implied through the observation of the bounding-surface hierarchy. The concept of scale is therefore expressed in this hierarchy through bounding surfaces being linked on a one-to-one basis to an architectural element; clearly this linkage will fail where an element is bound by a higher-order surface, for example due to punctuation (*sensu* Pickering et al., 1995).

It should be noted that more recent work undertaken by the same group employs a modified hierarchical classification, which includes mass-transport deposit classes and dimensional characteristics for each order; this classification is outlined in detail by Pickering & Cantalejo (2015); see Section 3.2.15.

3.2.4 Gardner & Borer, 2000, and later studies by these authors

A four-fold hierarchy was developed by Gardner & Borer (2000), specifically to characterise the 'channel-lobe transition zone' (CLTZ hereafter) in deep-marine deposits solely based upon outcrop data. As well as developing a hierarchy specific to a single method of data acquisition, this hierarchy was amongst the first to be focused on a specific depositional environment. This hierarchy is stated to be based upon sedimentary, palaeogeographic, stratigraphic and architectural-element analysis concepts, and thus considers bounding surfaces and their cross-cutting relationships. This scheme is based upon four extensive outcrop studies from the Permian Brushy Canyon Formation (Texas, USA) and is largely concerned with the spatial and temporal changes of channel forms in the CLTZ. Significantly, Gardner & Borer (2000) note that in the changing flow regime of the CLTZ, the spatial dimensions of architectural products of corresponding duration will differ as deposition moves downstream; this point establishes the concept that depositional units of similar spatial scales at different positions along-dip may not reflect similar time intervals and thus hierarchical levels. The hierarchical divisions are recognised mainly through the cyclical increases in architectural-element geometry and size, denoted by their bounding surfaces (Fig. 3.5a). Gardner & Borer (2000) refer to the resultant four-tiered hierarchy as a stratigraphic framework of architectural elements.

At the lowest order, a '**single story channel**' (up to 7 m thick and 200 m wide, based upon field measurements) represents a discrete channel fill which may contain multiple sediment bodies with erosional bases termed as 'geobodies'. A geobody is not further defined. The 'single story channel' hierarchical order, through the use of Gardner & Borers' (2000) 'scalar' terminology, is also defined as an 'architectural element'. The next discrete order, the '**channel complex**' (or architectural element set; on average 25 m thick, 800 m wide) is interpreted as reflecting a 5^{th}-order cycle in accordance with the sequence stratigraphic framework (Vail et al., 1977). These units represent "sand bodies with serrated margins" that shingle to form clinoform packages known as '**submarine fan conduits**'. This hierarchical order is said to reflect a 4^{th}-order sequence stratigraphic cycle, forming 1-2 km wide sand fairways. In turn, units at this level stack to form the largest hierarchical order, a '**submarine fan conduit complex**' (or depositional sequence), reflecting the cumulative sediment

pathway that remained active during the depositional lifetime of a fan. This unit was considered comparable to a 3rd-order sequence stratigraphic cycle.

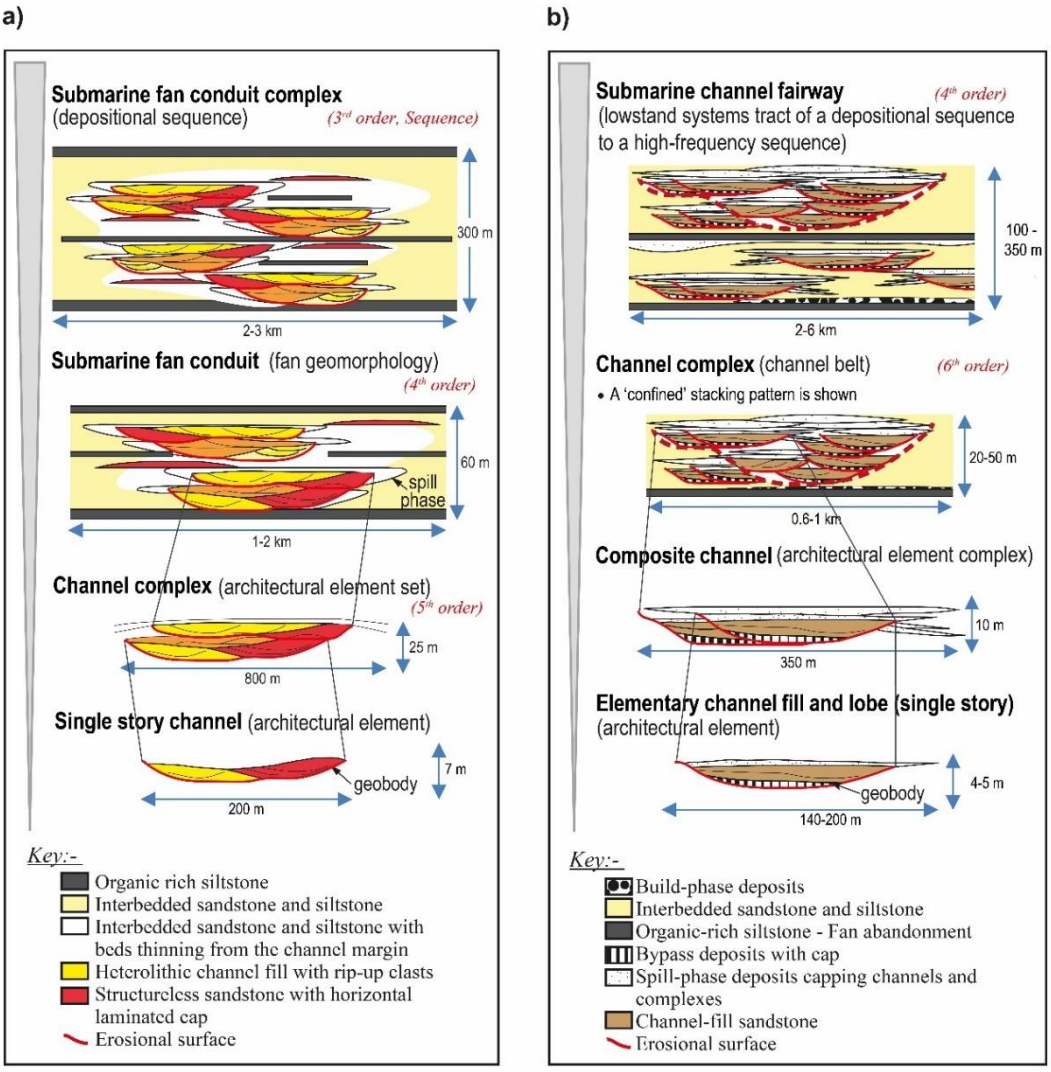

Fig. 3.5. Comparison of the CLTZ hierarchical classifications of *a*) Gardner & Borer (2000) and *b*) Gardner et al. (2003). The dimensions proposed for each hierarchical order are maximum measurements in part *a*) and average ranges in part *b*) calculated based on the studies outcrop investigation of the Brushy Canyon Formation (Texas, USA). Each hierarchical order corresponds to a specific 'scalar term', provided in brackets. The suggested equivalence to sequence stratigraphic orders is also stated (red italics); each key presents classes of deposits provided by each study. Figures modified after Gardner & Borer (2000) and Gardner et al. (2003), for parts *a*) and *b*), respectively.

'Single story channels' and 'channel complexes' are noted by Gardner & Borer (2000) to record recognisable cycles of sediment deposition and bypass, termed 'build-cut-fill-spill' sequences. These build-cut-fill-spill phases record different facies patterns, each of them being a consequence of differing sedimentological processes and energy trends, related to the position of a phase along the slope-to-basin profile. These phases can occur at multiple

temporal and spatial scales. The 'build' component records the depositional phase that precedes channelization, and so it is shown by an erosional surface marking sediment bypass within upper-slope regions.

3.2.4.1 Gardner & Borer's CLTZ hierarchy amendments

The original Gardner & Borer (2000) CLTZ hierarchy was updated by Gardner et al. (2003) to include sedimentary processes and allow each hierarchical division to also be associated with (and thus identified by) the processes controlling the emplacement and geomorphic character of deposits at each level. This update modified the terminology of the scheme (e.g., the definition of a channel complex), its 'scalar' divisions (e.g., the largest order is no longer affiliated with a 'depositional sequence' but only with a lowstand systems tract), and the correspondence with sequence stratigraphic cycles (e.g., the highest hierarchical order is given a 4th-order cycle status, instead of a 3rd-order as in the original hierarchy). This revised scheme was still based upon studies of the Brushy Canyon Formation, but no explicit justification for these alterations was made. The differences between the two versions of the scheme are reported in Figure 3.5 and Table 3.1.

The revised hierarchy remains four-tiered. The lowest hierarchical order defined as an '**elementary channel fill and lobe (single story)**' is still referred to by Gardner et al. (2003) as an 'architectural element' in light of their 'scalar' terminology. An 'elementary channel fill and lobe (single story)' is composed of both unconfined sandbodies (lobes) and erosionally confined channel fills, built up from multiple lower-level cut-and-fill units, or 'geobodies'. Like Gardner & Borer (2000), a 'geobody' is recognised as the smallest sedimentary building block, however yet again it is not defined clearly. The 'elementary channel fills and lobes (single story)' stack to form compound sandstone bodies termed '**composite channels**'. A 'composite channel', also termed an 'architectural complex', records genetically related sandbodies that show a common migration pathway. On average they are 10 m thick and 350 m wide, based upon the examples measured in the study. Multiple genetically related 'composite channels' (including both their lobe and channel-fill architectures) and their associated overbank wedges form a 6th-order-cycle '**channel complex**', otherwise known as a 'channel belt'. This sedimentary unit can be described as showing either a 'migrated' or 'confined' stacking pattern, according to whether the formative channel was laterally mobile or entrenched within an erosional depression, respectively. The build-cut-fill-spill cycles of Gardner & Borer (2000) are still recognised by Gardner et al. (2003), observed at the scales of a 'single story' to 6th order 'channel belts' (see facies patterns in Fig. 3.5b). The largest hierarchical order, the '**submarine channel fairway**' is similar in its definition to Gardner & Borer's (2000)

'submarine fan conduit complex', as it represents a long-lived sediment fairway, encompassing the area where channels reoccupy the same position through repeated cycles of fan growth. Similarity in the scale of submarine channel fairways and conduit complexes is also seen in the overlap of their dimensions (Fig. 3.5). However, Gardner et al. (2003) reinterpret units of this level as the preserved expression of a 4th-order sequence stratigraphic cycle, as opposed to Gardner & Borer's (2000) previous 3rd-order interpretation. In the 2003 scheme, units at this order are suggested to only reflect the lowstand systems tract (LST) of a 3rd-order depositional sequence, as opposed to an entire 'depositional sequence' as previously proposed by Gardner & Borer (2000).

3.2.5 Prather et al., 2000

By the turn of the millennium, Prather et al. (2000) noted that the subdivision of deep-water successions into hierarchical units had become well-established practice. The adoption of different approaches was seen by Prather et al. (2000) to result from the variations in spatial and temporal scales between differing datasets, as well as in relation to the environmental variability of deep-marine systems. Writing from a hydrocarbon-industry perspective, Prather et al. (2000) present a scheme that tries to more readily accommodate the scales of seismically resolvable units in sand-prone deep-water hydrocarbon reservoirs. The hierarchy is produced with consideration of the limits of seismic-data interpretation, and is based upon examples from intraslope basins in the Gulf of Mexico. The hierarchy is structured into four seismic orders and three sub-seismic orders (i.e., orders below conventional seismic resolution), which are applicable to architectural units associated with both channel and lobe environments (see Fig. 3.6). Prather et al. (2000) are able to directly compare their classification against the outcrop and seismic-based hierarchies of Mutti & Normark (1987) and Pickering et al. (1995), as well as Miall's (1985) hierarchy for fluvial deposits, due to common diagnostic characters for the attribution to hierarchical levels, i.e., based on the recognition of external and internal facies geometries, stacking patterns and bounding-surface orders. Prather et al. (2000) concede that significant uncertainty is inherent in the assignment of the sub-seismic orders, because of the inability to easily identify these units using conventional seismic techniques. No reference is made to the role that higher-resolution seismic techniques might play in resolving such uncertainties.

The smallest hierarchical order ('**third order, sub-seismic**') is compared by Prather et al. (2000) to both the 'turbidite bed' and 'bedding package' hierarchical orders of Mutti & Normark (1987) and Pickering et al. (1995), respectively. The largest sub-seismic order, the '**first order, sub-seismic**' level, describes the 'loop morphology' of a sedimentary unit via the

identification of erosional surfaces that bound the products of compensational cycles, classified as either 'channel sands' or 'sheet sands' based upon their sub-environment of deposition. Prather et al. (2000) recognises that modelling channel reservoirs may lead to oversimplification due to their variable sand distributions over shorter bed lengths, as opposed to the sheet sands. Due to this increased challenge, Prather et al. (2000) propose the introduction of a distinctive "building block" order, known as a '**second order, sub-seismic**', whereby the 'first-order' sub-seismic channel-fill sequences can be divided into margin and core blocks, characterised by consistent reservoir properties (e.g., sand fraction) useful for hydrocarbon reservoir modelling. The core and margin block stratal divisions typically cross-cut the 'first order, sub-seismic' stratigraphic boundaries, creating artificial separations within a discrete unit; this in turn allows determination of the connectivity potential of the reservoir under investigation. This style of subdivision of sedimentary architecture, through the segmentation of parent-element packages discordantly to any internal bounding surfaces, is unique to this hierarchical classification.

Units at the smallest seismic-scale order classified by Prather et al. (2000) are termed 'loops'. These '**fourth order, seismic**' loops determine the scale of individual reservoirs and are imaged well through conventional seismic techniques. These loops have characteristic planform shapes (e.g., shoestring, ribbon, sheet, pod-like) and cross-sectional geometries; they can also show locally shingled seismic geometries. This 'loop' hierarchical level is thus the focus of most efforts on the collation of information concerning the geometry of reservoir units, with the scope to constrain reservoir simulations. The '**third order, seismic**' hierarchical level is described as a 'facies unit' or 'loopset', which can be characterised by seismic reflectivity, geometry, lateral continuity and bounding-surface type. However, how these characters help to define this level is not stated by Prather et al. (2000). At this hierarchical scale, geometric characteristics have been used to categorise three primary seismic facies, namely 'draping', 'convergent' and 'chaotic', as previously established by Prather et al. (1998). Prather et al. (2000) state that the consideration of well-log data is useful to reduce some of the uncertainty associated with predictions of lithofacies and sand content in hydrocarbon-reservoir intervals. The degree of wavelet amalgamation has also been used to define the style of stacking in units of this scale, via the non-amalgamated, loosely amalgamated, or highly amalgamated shingling of 'fourth-order, seismic loops'.

Repetitive successions of seismic facies define the '**second order, seismic**' level, also described as a 'facies succession'. 'Second order, seismic' units consist of stacked packages of 'third order, seismic' units and are typically bounded by a condensed zone, formed via waning deposition (Prather et al., 1998). They are interpreted to reflect the filling patterns of

different types of accommodation space and are therefore seen to reflect the external controls upon reservoir architecture, which Prather et al. (2000) state help produce "depositional sequence scale" (or basin scale) stratigraphic models. 'Second order, seismic' facies successions that stack into common packages of seismic facies delineate '**first order, seismic**' bodies or an 'assemblage succession'. The 'first order seismic' level is the largest hierarchical order identified. In the case study from the Gulf of Mexico, these 'assemblage successions' are classified as either ponded or bypass assemblages, and recognising such units enabled Prather et al. (2000) to characterise reservoir-seal architectures. The largest stratigraphic scale is described to record a common assemblage of seismic facies; however, no defining criteria were provided by Prather et al. (2000) to explain what constitutes these 'common assemblages'. Hierarchical-order dimensions based upon the measurements documented within Prather et al. (2000) are shown in Fig. 3.6.

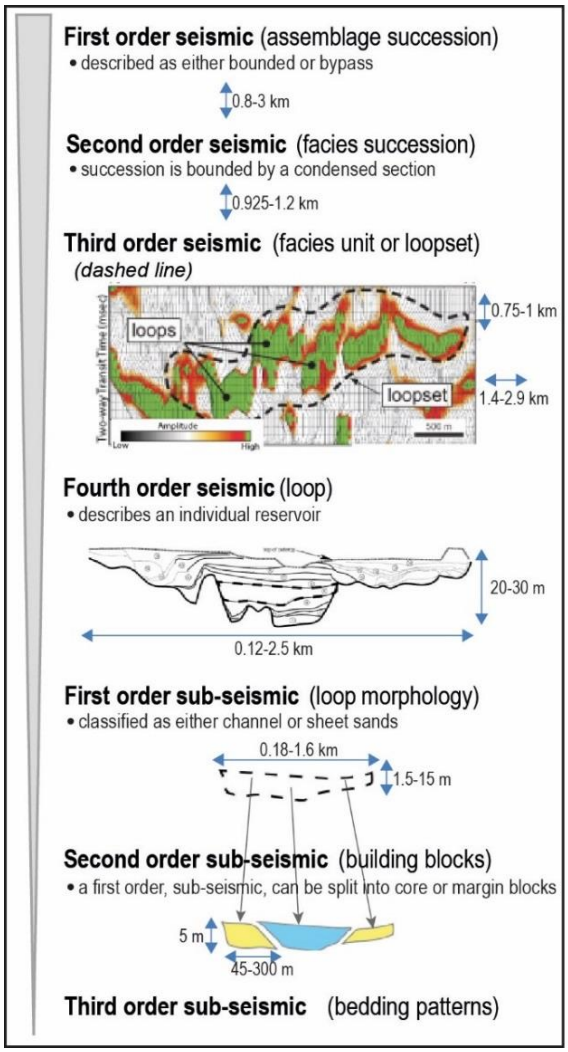

Fig. 3.6. Hierarchical classification of Prather et al. (2000), including thickness and width dimensions taken from summary diagrams and seismic lines from the Central Gulf of Mexico intraslope basins and the Permian Brushy Canyon Formation, USA. Figure modified after Prather et al. (2000).

The seven hierarchical classes (Fig. 3.6) map onto the variable scales of interest at the different stages of reservoir exploration, appraisal, development and production. Prather et al. (2000) state that characterisation at the 'first order' and 'second order' seismic scales is desirable to help determine reservoir potential during the explorative phase; for instance, the initial seismic facies analysis undertaken in the Gulf of Mexico study helped identify sand-prone intervals (Prather et al., 2000). 'Third order' and 'fourth order' seismic scales are useful in the assessment of stacking patterns and architectural classes (e.g., channel or sheet depositional environments), which can facilitate the evaluation of the extent of a reservoir. Sub-seismic levels help to assess heterogeneities at the 'intra-reservoir' scales; they are thus regarded as important scales of analysis for reservoir development, as information relating to units at these orders can be used to make inferences with respect to reservoir connectivity.

3.2.6 Navarre et al., 2002

The hierarchical classification of Navarre et al. (2002) was produced with the aim of aiding the characterisation of hydrocarbon reservoirs through the use of 3D seismic and well-log datasets. The approach aims to honour the stratigraphic architecture of turbidite deposits through the 3D observation of sedimentary units at different spatial and temporal scales, including their lateral continuity. Shaly deposits and erosional bases are recorded as important characteristics, marking the subdivision of units within each hierarchical level. These characteristics are noted as significant because they act as possible barriers to flow in corresponding reservoirs, affecting reservoir connectivity. The hierarchy was tested upon the Gulf of Guinea Tertiary turbidite system, offshore West Africa, and is largely based on 3D seismic data but well-log and core data have also been used to help characterise the smaller hierarchical orders.

The six-tiered hierarchy Navarre et al. (2002) propose is stated to be applicable to both lobate and channelized architectural units and this physiographic distinction is denoted within the hierarchical classification by the use of 'lobe' or 'channel' prefixes in the naming of some of the orders (see Fig. 3.7). However, in practice the hierarchical arrangement described by Navarre et al. (2002) is predominantly focused upon channel architectures.

The smallest recognised hierarchical order corresponds to units termed '**facies associations**'. However, specific criteria for the attribution of sedimentary bodies to this order are not given; these units are solely noted to have limited widths, thicknesses and lateral continuities in comparison to the '**channel or lobe phases**' they stack into. 'Phases' are sub-seismic scale units, which are composed of genetically related facies linked to a common depositional environment. These units typically display an overall vertical facies succession observed

through porosity, permeability and grain size calibrated from well-log data. Both the 'facies association' and 'phase' hierarchical orders are associated with the level of resolution desired for reservoir models; these orders are therefore comparable in scope to Prather et al.'s (2000) sub-seismic orders.

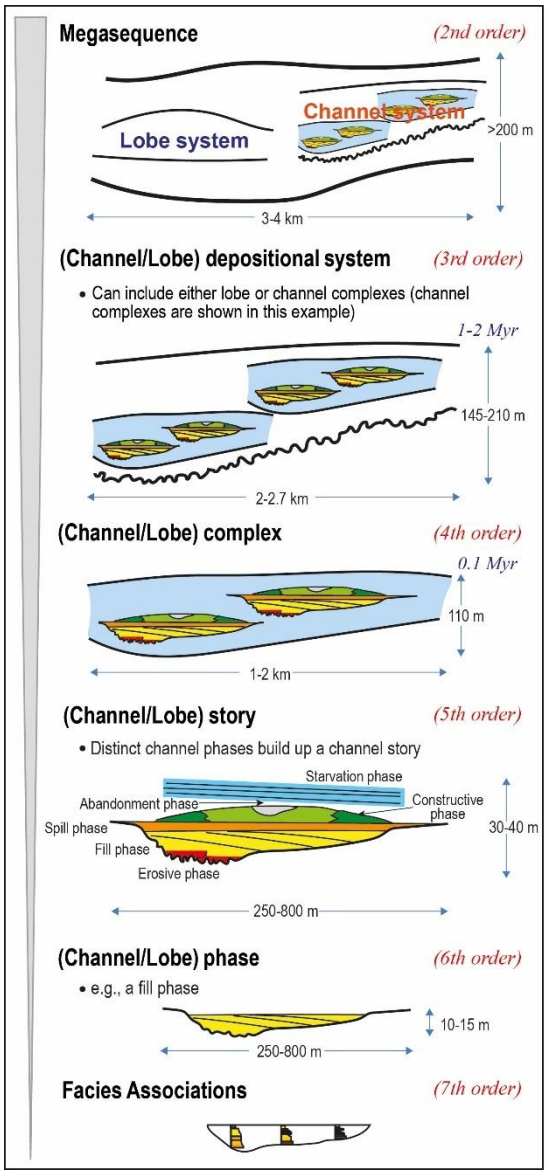

Fig. 3.7. Hierarchical classification developed by Navarre et al. (2002). Dimensions are taken from the seismic dataset analysed in the original paper; durations (blue italic) are provided for those orders that have been temporally defined; numbering related to sequence stratigraphic orders are shown in red italics. The distinct channel phases which build a 'channel story' are also shown (modified after Navarre et al., 2002).

Five distinct phases, reflecting different evolutionary steps within a depositional environment, are typically seen in a predictable succession within the case-study examples investigated by Navarre et al. (2002) – these consist of 'erosive', 'fill', 'plugging', 'spill' and 'constructive' phases. However, other possible phases are acknowledged to exist within the

synthetic channel phase succession model, namely 'abandonment' and 'starvation' phases (see Fig. 3.7). These phases stack progressively, starting with an 'erosive' phase marked by cutting and infill of deposits; typically this basal infill will be related to deposition by a debris flow or slump. A 'fill' phase typically follows, composed of homogenous sandy deposits, indicative of a sandy bar deposition, followed by shaly facies of the 'plugging' phase, which marks the abandonment of a channel form. 'Spill' phases result in sandy channel overspill deposits that indicate unconfined turbidity flows, which later progress to form 'constructive' levee deposits, which are deposited parallel to the channel axis. The possible 'abandonment' and 'starvation' phases are composed predominately of mud-prone internal-levee facies, which in the case of the 'starvation' phase can represent a baffle between 'channel stories'. 'Lobe phases' are also recognised to exist within the hierarchy, but no explicit link is made to the channel-related evolutionary phases, nor is the genetic significance of lobe phases in distributary environments discussed.

Channel phases stack to form a '**channel story**', ranging from around 30 to 40 m thick and 250 to 800 m wide (based on data from the 3 'channel stories' identified in the study; Fig. 3.7). The 'channel story' is analogous in some regards to the build-cut-fill-spill depositional cycle of Gardner & Borer (2000). A 'channel story' may display all types of 'channel phases', but local preservation may be affected by backstepping or progradation; regardless, an erosional base and shaly top are stated to always be observed. Each 'story' fines-upwards. Multiple genetically related 'channel stories' (again, lobe equivalents are not characterised) are seen to vertically stack to form a '**channel complex**' (110 m thick and 1-2 km wide, based on the two examples identified in the study); each component 'channel story' is separated by background muds and limited by stratigraphic surfaces, which in the studied examples are inferred to have developed over a timescale of ~0.1 Myr, based on biostratigraphy.

Hierarchical levels above the 'channel complex' reflect more regional, basin-wide controls. Multiple 'channel complexes' may be bounded by an erosional base and capped by an extensive mud: this composite unit is named a '**depositional system**', for which a duration of 1-2 Myr, corresponding in magnitude to a 3rd-order sequence stratigraphic cycle, is inferred based on biostratigraphy. However, even at this scale, only one dominant architectural element style is envisaged, as sediments are described in this scheme as showing either channelized or lobate forms. The largest order recognised in this hierarchy is the '**megasequence**' (~200 m thick, 3-4 km wide), which represents the complete product of genetically related turbidity flows, and thus is seen to include both lobe and channel architectural units. This hierarchical order is defined by surfaces that embody two major events, interpreted as either maximum flooding surfaces or unconformities of 2nd order

(associated with sequence stratigraphic sequence boundaries). Breaks in sedimentation that bound this 'megasequence' are interpreted to be, for example, the product of long-term relative sea-level change or tectonic salt activity.

3.2.7 Sprague et al., 2005

In the pursuit to better understand and predict hydrocarbon-reservoir properties (reservoir geometries, continuity, net-to-gross, porosity, permeability, etc.) Sprague et al. (2002; 2005) developed a 'deep-water hierarchy' inspired by some of the principles of sequence stratigraphy. This hierarchy was designed to acknowledge spatial and temporal controls on reservoir architecture at multiple scales, for subsurface predictions. The framework was proposed to act as a 'standard' hierarchy, applicable to genetically related deep-marine stratal elements from turbidite settings that include confined and unconfined basin plains and slopes (albeit without mention of channel-lobe transition zones), and has since been applied to a number of case studies (see Section 3.2.7.1). The scheme is based primarily upon interpretations of 3D seismic datasets, but is also supported by well and core analysis. The applied value of this integrated approach was realised through its widespread application within ExxonMobil and Shell, resulting in a reported doubling in accuracy of net-to-gross predictions when well-log data was used along-side seismic to analyse potential reservoirs in West Africa (Sprague et al., 2005). This framework acknowledges earlier works by Beaubouef et al. (1999), which used sequence stratigraphic terminology and concepts to help define the outcrop-based hierarchical arrangement of channel deposits of the Brushy Canyon Formation (Fig. 3.8). Sprague and co-workers originally articulated this 'deep-water hierarchy' through an oral presentation given at the AAPG Annual Conference and Exhibition (ACE) in 2002 (Sprague et al., 2002), whose abstract remains highly cited (although a specific citation statistic cannot be attained). They successively expanded the scheme by widening the temporal framework through the addition of higher orders in a later conference paper (Sprague et al., 2005).

The framework attempts to allow systematic description of, and comparison between, deep-marine systems, and it is founded upon the sequence stratigraphic framework (Vail et al., 1977) in a manner similar to Beaubeouf's (1999) original effort. Hence, strong alignments are evident between the 'deep-water hierarchy' of Sprague et al. (2005) and the sequence stratigraphic framework, in relation to the choice of similar criteria to recognise each hierarchical order, i.e., the physical and genetic relationships of strata, their resultant geometry defined by correlatable major surfaces (unconformities), as well as the vertical and lateral stacking patterns of these resultant architectures. The hierarchy is stated to be

applicable to both channelized and distributary environments (Fig. 3.9). Sprague et al. (2005) therefore state the importance of using a 'prefix modifier', similar to Navarre et al. (2002) to record the level of confinement for an environment (as confined, weakly confined, or lobe/unconfined); these in turn provide a relative physiographic position of the studied section relative to the depositional dip profile. These prefixes are the only variable identifiers used in the scheme to differentiate between the different positions of units in a basin. Differing ranges of dimensions are also recognised for hierarchical orders across these environments (Fig. 3.9). Although sequence stratigraphic terminological equivalents are provided (Fig. 3.9), the resultant hierarchy of nested stratal elements does not utilise sequence stratigraphic terminology directly. Instead, it uses a collection of terms that prevail in the scientific literature.

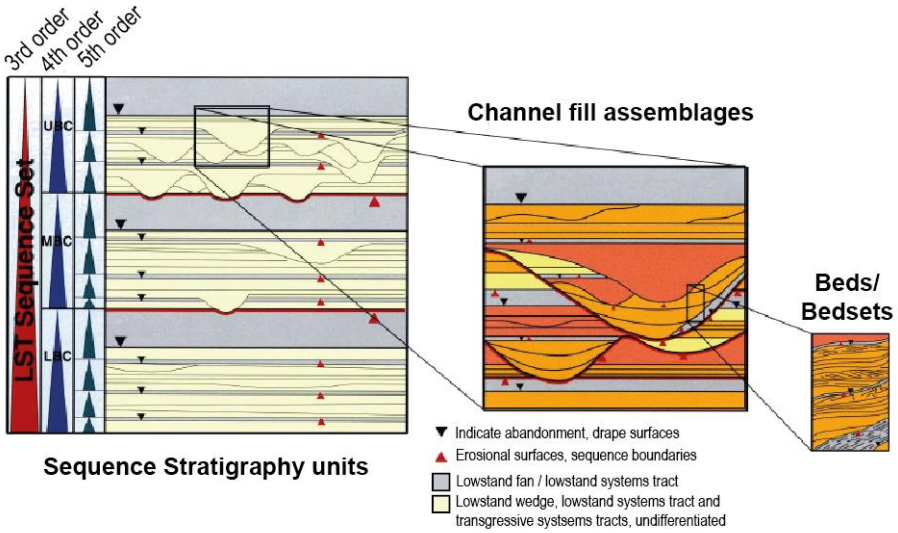

Fig. 3.8. The stratigraphic hierarchy erected by Beaubouef et al., (1999) for their study on the channelized architecture of the Brushy Canyon Formation. The hierarchy recognises sedimentary units through their higher surface orders (e.g., channel fill assemblages and bedsets). It is based on sequence stratigraphic concepts but also incorporates small-scale divisions that are not easily identified at seismic scale. The '4th-order' units are split into 3 units, which correspond to the Lower, Middle and Upper members of the Brushy Canyon Formation. Figure after Beaubouef et al. (1999).

The lowest orders in the scheme by Sprague et al. (2005) are represented by '**beds**', i.e., layers of sedimentary rock bounded above and below by bedding surfaces or unconformities, and '**bedsets**', i.e., the repetition of two or more beds characterised by the same composition, texture and sedimentary structures, based upon definitions of Campbell (1967). The next hierarchical order is a '**storey**', which is based upon the descriptive terminology for fluvial deposits of Friend et al. (1979). A 'storey' is recognised as a scour-based, sub-channel stratal element that shows strong lateral changes in facies organization (i.e., from its 'axis' to

its ‘margin’). However, this facies-based description is not entirely unique to this architectural order, as ‘channel fills’ are also described as expressing lateral facies changes and erosive bases. Sprague et al. (2005) do not provide clear criteria on how to identify ‘lobe storeys’, although these subcomponents of a lobe have been illustrated within the distributary hierarchy as a volume of genetically related facies (Fig. 3.9b). The hierarchical order to which ‘**channel fills**’ and ‘**lobes**’ belong is described as the fundamental building block of deep-water depositional systems. At both this hierarchical level and at the higher-scale ‘**channel/lobe complex**’ order, the sedimentary units are characterised by only one style of architecture. A ‘channel fill’ is interpreted to be the deposit of a single cycle of channel-filling and abandonment, and is described as being generally the smallest seismically resolvable order in the hierarchy. The ‘channel-fill’ units and their sub-component ‘storey’ hierarchical orders are also interpreted by Sprague et al. (2005) as a way of dividing Mutti & Normark’s (1987) ‘turbidite sub-stage’ order into the separate components of deposition, bypass and erosion (components that Mutti & Normark, 1987 did acknowledge to exist), as well as the total product of this evolutionary cycle of deposition. A channel ‘complex’ reflects a group of seismically resolvable, genetically related channel fills (i.e., with similar architectural styles), which show lateral facies changes along strike (orthogonal to flow direction: channel-complex axis to channel-complex margin). Lobe unit equivalents to the ‘fill’ or ‘complex’ hierarchy orders are not specifically defined by Sprague et al. (2005); however, radial planform patterns are noted for these distributary architectures. For the subsequent larger-scale orders, only architectures of confined channelized setting are considered in detail. The ‘**channel complex set**’ order is seen to be directly comparable to a lowstand systems tract (LST) of a depositional sequence. In contrast to the ‘fill’ and ‘complex’ orders, at this level multiple architectural styles (*sensu* Sprague et al., 2005) or element types (*sensu* Mutti & Normark, 1987) might form a unit (e.g., a unit may contain extensive background deposits surrounding channel elements; Fig. 3.9a). The ‘channel complex set’ is a channelized unit composed of two or more genetically related ‘channel complexes’, typically showing a vertical stacking pattern, which is notably capped by a hemipelagic drape, marking a temporary cessation of active channel deposition. A ‘complex set’ is also typically bounded at its base by an unconformity, supporting the comparison made by Sprague et al. (2005) between this hierarchical order and the depositional sequence (i.e., a relatively conformable succession of genetically related strata with chronostratigraphic significance, typically showing no apparent internal unconformities, bounded by unconformable surfaces and their correlative conformities; Vail et al., 1977; Mitchum et al., 1977; Van Wagoner et al., 1988; Mitchum & Van Wagoner, 1991).

'Channel complex sets' stack into '**channel complex systems**', which Sprague et al. (2005) state as being capped by a regional abandonment surface and bounded by a composite sequence boundary below. Sprague et al. (2005) compare these units to a 'stratigraphic sequence set', reflecting long-term effects of relative sea-level change. Multiple cycles of 'channel complex systems' stack to form '**channel complex system sets**' within the basin which Sprague et al. (2005) compare to a 'composite sequence' based upon sequence stratigraphic terminology. This hierarchical order is also stated to directly compare to the 'turbidite system' level of Mutti & Normark (1987). Interestingly, the largest hierarchical order of Mutti & Normark (1987), the 'turbidite complex', originally considered equivalent to a 'composite sequence set' of sequence stratigraphic terminology, is not defined or recognised as significant in the hierarchy of Sprague et al. (2005).

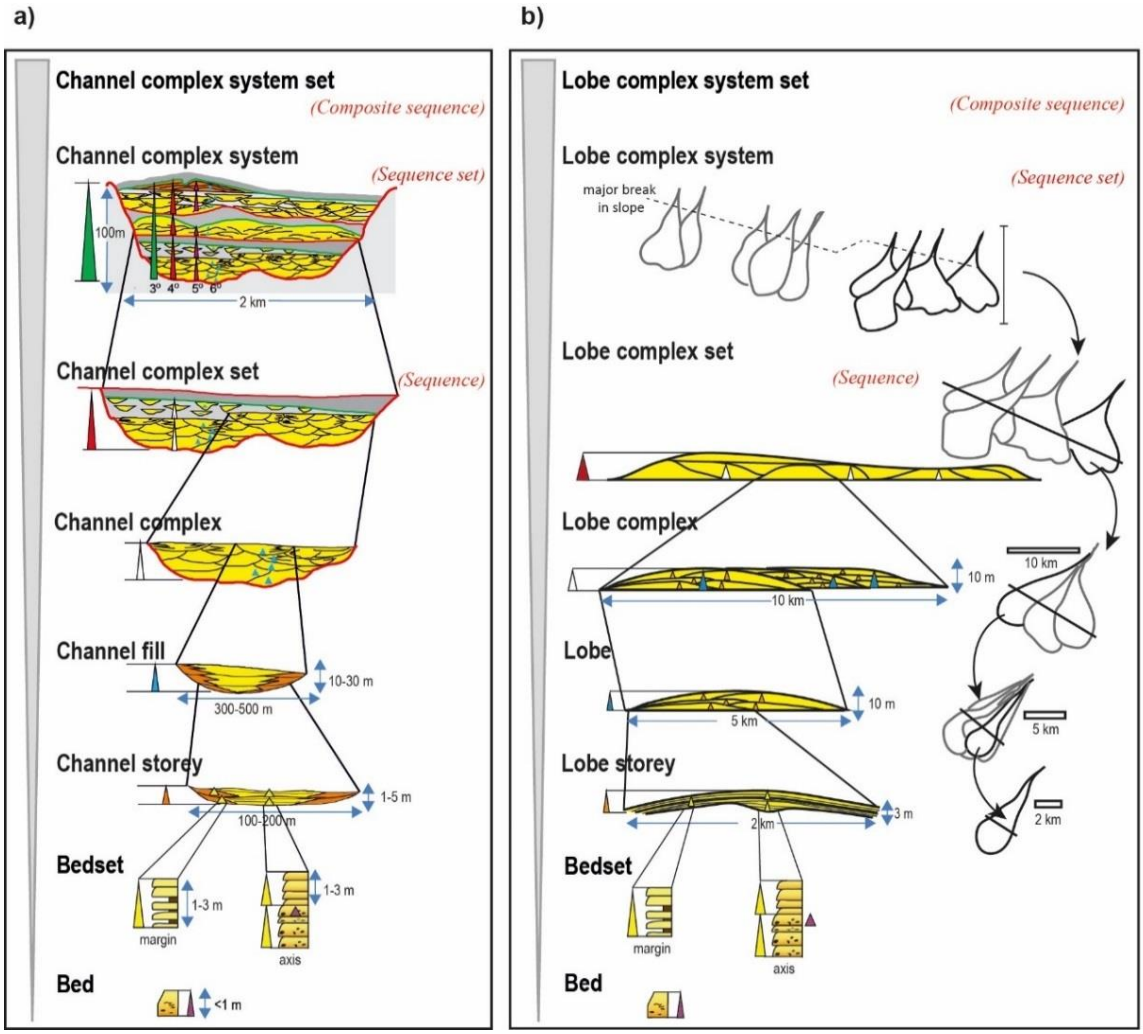

Fig. 3.9. The 'deep-water hierarchy' classification of Sprague et al. (2005) of *a*) channelized units in confined settings and *b*) distributary environments. The proposed dimensions for elements of each hierarchical order are also included and equivalent sequence stratigraphic terminology is shown in red italics, when present in the original work. Modified after Sprague et al. (2005).

3.2.7.1 Application and amendments to the hierarchy by Sprague et al. (2005)

The deep-water hierarchy of Sprague et al. (2002; 2005) was formulated and originally applied to seismic data from Tertiary deep-marine deposits off-shore West Africa (Sprague et al., 2005). Beaubouef (2004) instead applies this classification and its terminology to an outcrop-based study of the Cerro Toro Formation. Sprague et al. (2005) also cites Beaubouef as employing this hierarchical classification in his studies on outcrops of the Brushy Canyon Formation undertaken in 1999 and 2000, though no clear link to this hierarchy is acknowledged in either of these works.

Campion et al. (2007; 2011) also adopt some hierarchical orders from this scheme ('bedset' to 'channel complex set') to categorise an outcrop of the channelized Capistrano Formation. In this context, Campion et al. (2011) also further defines a 'storey' as being a fundamental building block of a channel. 'Storeys' are observed to be confined within the channel-fill elements, as storey bases onlap or coalesce to form the base of channels (lobe storeys are not considered). Each storey contains stacked 'bedsets' that not only show distinct and predictable facies associations that vary laterally (e.g., distinct thickening- and coarsening-upwards packages at the channel axis, as opposed to fining-upwards packages at the channel margins), but also distinct vertical facies changes, whereby the stacked 'bedsets' of a single story reflect a depositional evolution from erosion to bypass and ultimately channel plugging (Campion et al., 2011).

The hierarchy of Sprague et al. (2002; 2005) has also provided a strong foundation for a number of other hierarchical concepts. For example, Abreu et al. (2003) modify the hierarchical structure and terminology of Sprague et al. (2002) to accommodate lateral accretionary packages (LAPs), which embody the preserved product of lateral migration of a channel (Fig. 3.10). This is done through the revision of the definition of a 'channel complex', to allow differing architectural styles, including LAPs, to be included as complex-forming units, as well as units below this hierarchical order. However, despite the initial outward commitment to utilising the deep-water hierarchy of Sprague et al. (2002) differences can be seen in the way a 'channel complex' has been graphically illustrated. Abreu et al.'s (2003) representation of Sprague et al. (2002) hierarchy shows two 'channel complexes' (*sensu* Sprague et al. 2002) to represent a single complex, differing from the original design of Sprague et al. (2002; compare Fig. 3.9a with Fig. 3.10a). This may suggest that a different interpretation of the Sprague et al. (2002) stacking patterns has been made to be able to

incorporate LAPs into the hierarchy; however, no discussion is provided by Abreu et al. (2003) as to why such discrepancies arose.

McHargue et al. (2011(a)) used the hierarchical concepts of Sprague et al. (2002; 2005) to build subsurface models of continental slope channels. McHargue et al. (2011(a)) identified the importance of recognising hierarchical orders in event-based forward modelling in order to produce more realistic model outputs, suitable for quantitative reservoir simulation. Their work focuses on three key scales from the hierarchy of Sprague et al. (2005): the 'channel fill' (denoted as a 'channel element' within McHargue et al., 2011(a), and also stated to be comprised of vertically stacked 'stories'), 'channel complex' and 'channel complex set'. McHargue et al. (2011(a)) state that some terminological modifications have been made, including the separation of temporal and physical scales in the definitions of these elements. McHargue et al. (2011(a)) also state that all three hierarchical scales considered in their model display cycles of waxing and waning flow energy. This cyclicity at the channel complex set scale is highlighted by different stacking patterns as flow behaviour changes from erosional to depositional. Overall a transition is observed from a less to a more 'organised' stacking pattern; the latter being linked to higher rates of aggradation resulting in the younger channel element pathway more closely matching the one of the older channel element.

The original hierarchical concepts of Sprague et al. (2002; 2005) have since been updated and modified by Sprague and other co-workers (Sprague et al., 2008; Flint et al., 2008). In these revised schemes, the definitions of orders have been strengthened to incorporate the scale of well-log and core data and to extend the applicability of the scheme to lobe and overbank/ levee element types. This has been achieved via an extensive outcrop study on the seismic to sub-seismic scale deposits of the Karoo Basin. This has helped to more closely align the original hierarchical orders to sequence stratigraphic concepts, due to an improved focus upon recognising the regional connectivity of sequence boundaries through the assessment of allogenic versus autogenic controls (Flint et al., 2008). 'Channel-fills' are here referred to as 'storey sets' by Sprague et al. (2008) and Flint et al. (2008). This terminology and expanded applicability of Sprague's deep-water hierarchy was subsequently used as the basis for Pickering & Cantalejo's (2015) most recent hierarchical classification approach (see Section 3.2.15). Recent work by Sprague et al. (2014) has concentrated on the characterisation of the main lithofacies forming the 'sequence' (*sensu* Vail et al., 1977) or 'complex set' (*sensu* Sprague et al., 2005) hierarchical orders, in an attempt to improve characterisation of reservoir properties and assess stratigraphic-trap characteristics in basin-floor settings of the Karoo Basin. This work thus expands the applicability of this hierarchy to outcrop-based

distributary environments. The influential relationships shared between these derivative hierarchical schemes and the 'deep-water hierarchy' of Sprague et al. (2002; 2005) are illustrated in Fig. 3.1.

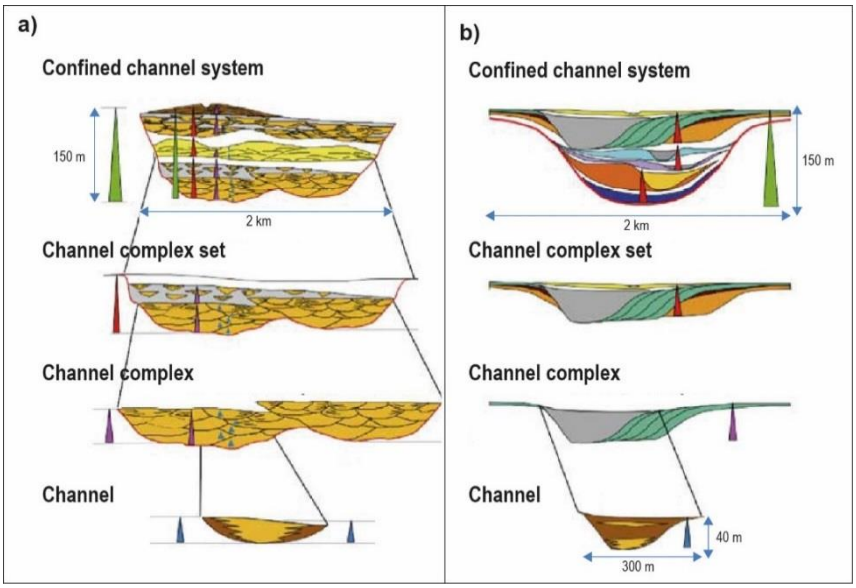

Fig. 3.10. Comparison between *a*) the hierarchical scheme of Sprague et al. (2002; 2005) and *b*) the stratigraphic hierarchy used by Abreu et al. (2003) to classify the channel and LAP architecture in a study based on a seismic dataset of the Dalia M9 Upper Channel System, offshore Angola. Figure taken from Abreu et al. (2003).

3.2.8 Hadler-Jacobsen et al., 2005

With the purpose of providing a more accurate and predictive conceptual model for lithology distribution in submarine fans, Hadler-Jacobsen et al. (2005), of Statoil, conducted an investigation to identify and characterise submarine fans at seismically resolvable scales. The recognition of seismic patterns in sandy distributary deposits was tested upon a number of both seismic datasets (the Triassic Finnmark Platform, the Eocene Porcupine Basin, and the Paleocene/Eocene Viking Graben) and 'analogue' outcrops (the Eocene Central Basin in Spitsbergen, the Permian Karoo Basin and the Permian Brushy Canyon Formation). These datasets were hierarchically classified in terms of the sequence stratigraphic framework (Vail et al., 1977; Mitchum & Van Wagoner, 1991). This link to sequence stratigraphic hierarchies was seen as natural by Hadler-Jacobsen et al. (2005) due to the intimate relationship between subsurface lithological investigations and sequence stratigraphy. However, due to new insights in deep-marine sedimentology resulting from improved seismic acquisition, some of the original concepts of sequence stratigraphy, such as systems-tract nomenclature and depositional-sequence boundaries, were amended by Hadler-Jacobsen et al. (2005). A stratigraphic framework for shelf-slope-basin settings was thus established based upon the

identification of shelf maximum flooding surfaces and their coeval slope and basin condensed sections, a genetic stratigraphic marker previously utilised by Galloway (1989).

The hierarchical orders are called ‘cycles’, as in sequence stratigraphic parlance, and are associated with durations comparable to those of sequence stratigraphic units proposed by Mitchum & Van Wagoner (1991; Fig. 3.11). Second, third, fourth, fifth and sixth orders are noted by Hadler-Jacobsen et al. (2005); however, they do not recognise all these five orders in all the datasets incorporated in their review, and they never identify a ‘first order’ stratigraphic division. The recognition of fourth, fifth and sixth orders is also stated by Hadler-Jacobsen et al. (2005) to be more difficult to achieve due to limited data resolution, and therefore confidence in the assignment of units to these hierarchical orders is low.

Tentative ‘**fifth order**’ cycles are typically observed in seismic datasets as individual seismic reflectors, displayed as a single clinoform geometry, typically capped by a condensed section. These ‘fifth order’ units have been identified by Hadler-Jacobsen et al. (2005) on outcrops of the Brushy Canyon Formation (Gardner et al., 2003); they reach thicknesses of up to 100 m, and have formed over 0.01-0.5 Myr (based upon proposed durations taken from the original case-studies). These ‘fifth order’ fan cycles can be internally divided via facies assemblages into ‘initiation’, ‘growth’ and ‘retreat’ phases, *sensu* Gardner et al. (2003), which represent ‘**sixth order**’ cycles. Hadler-Jacobsen et al. (2005) recognise these ‘sixth order’ cycles in the Delaware Basin and tentatively in the Tanqua Basin and in the Finnmark Platform. These ‘sixth order’ units are typically only identifiable below conventional seismic resolution, and are only generically defined by Hadler-Jacobsen et al. (2005). These ‘sixth order’ cycles, along with ‘fourth order’, ‘third order’ and ‘second order’ cycles can all be divided into initiation, growth and retreat phases of a fan, following the evolutionary sequence of Gardner et al. (2003). A seismically resolvable ‘**fourth order**’ cycle (0.1-1 Myr) is composed of stacked ‘fifth order’ units. They are identified by their bright amplitude in seismic imaging and by a well-defined shelf-break, which may include condensed section intervals and were observed between 30-200 m thick. The ‘fourth’ and ‘fifth’ orders are also interpreted by Hadler-Jacobsen et al. (2005) to represent the main building blocks of a submarine fan. The shelf-to-basin clinoform geometries of the ‘fourth order’ units typically stack into prograding ‘**third order**’ units (e.g., as identified in the study of the Porcupine Basin; Fig. 3.11a). Again, the three distinct phases of initiation, growth, and retreat are recognised. However, according to Hadler-Jacobsen et al. (2005) each phase (1-3 Myr) at this scale can be recognised through seismic-facies assemblages, which can show channel and incised-valley features on the shelf, as well as the presence of onlapping surface geometries at the shelf-edge to slope-break , or distinct downlap across the basin. Examples of ‘third order’ thicknesses range from 155-

400m. The largest order recognised, a '**second order**' cycle (5-13 Myr, 600 m in thickness, based upon the measured Tanqua Karoo example), represents a progradational basin-ward stacked clinoform package, which can record a number of shifts in the shelf-edge position throughout the evolution of the fan.

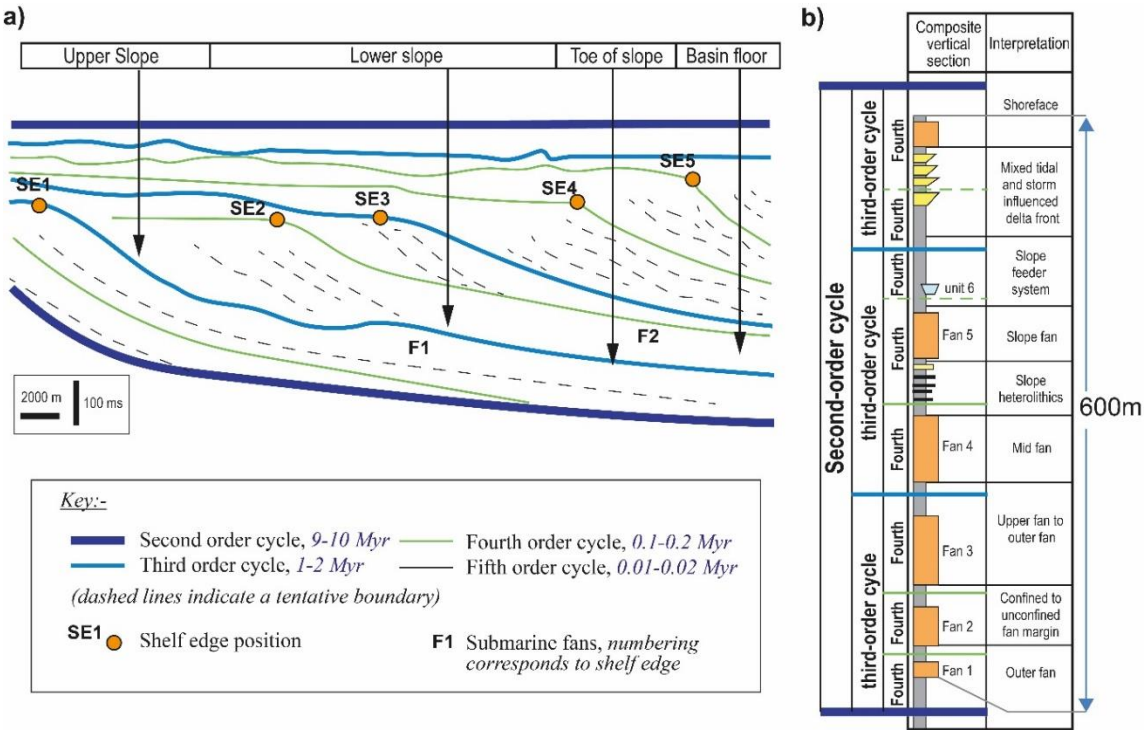

Fig. 3.11. Applications of Hadler-Jacobsen et al.'s (2005) deep-marine hierarchical classification. *a*) Seismic dip section of the Porcupine Basin (Ireland) divided into clinoform packages, termed 'cycles'. SE1-5 notation shows shelf-edge progradation between the fourth-order cycles; F1 and F2 are interpreted by Hadler-Jacobsen et al. (2005) as the fan components of the corresponding SE1 and SE2 shelf-edges. *b*) Shallowing-up vertical succession from the Tanqua Karoo outcrop dataset. Each sandy fan cycle has been interpreted as a fourth-order cycle. Order durations are inferred based upon relationships with sequence boundaries. Modified after Hadler-Jacobsen et al. (2005).

Hadler-Jacobsen et al. (2005) recognise two end-member basin styles: (i) high shelf-to-basin relief, sediment underfilled basins (high SBR/SUB) and (ii) low shelf-to-basin relief, sediment overfilled basins (low SBR/SOB). These two basin styles are observed over 'third' and 'second order' scales and are largely inferred from the stacking patterns detected within the 'fourth' and 'fifth order' building blocks.

Regarding the applicability of their scheme, Hadler-Jacobsen et al. (2005) state that extensive, ideally basin-wide, observations are desirable to apply this hierarchy to outcrop studies in a confident manner. In particular, chronostratigraphic constraints, through

biostratigraphical attributions, are seen as crucial in its application to outcrop studies (see example from the Tanqua depocentre of the Karoo Basin, South Africa in Fig. 3.11b).

3.2.9 Mayall et al., 2006

Mayall et al. (2006) reviewed a number of published studies based on high-resolution seismic and outcrop datasets of turbidite channel architectures (such as Navarre et al., 2002; Campion et al., 2000; Gardner et al., 2003; Abreu et al., 2003; Beaubouef, 2004), in order to establish an effective method of 'sequence stratigraphic' channel reservoir evaluation and classification. In contrast to previous studies, Mayall et al. (2006) highlight the unique nature of every channel and its infill, and acknowledge the difficulty of developing or applying a single, or even multiple, depositional models. Therefore an alternative approach to hierarchical channel classification is proposed, associated with the identification of four recurring characteristics of channel forms (sinuosity, facies, cutting and filling, and stacking patterns), applicable to the characterisation of reservoir facies distribution. However, to be able to compare and classify the channel architectures drawn from multiple literature studies, Mayall et al. (2006) recognise the need to employ a standard set of terminology to describe the variability in channel-form size (Fig. 3.12). The authors avoid using any existing terminologies for hierarchical classification, even those from the hierarchy studies considered in their review (e.g., Gardner & Borer, 2000; Navarre et al., 2002), due to the desire to use "simple terminology" based upon sequence stratigraphic principles (i.e., in relation to sequence stratigraphic boundaries and temporal orders) to describe the channel bodies and their internal architecture in a scalar manner.

The study is focussed on erosionally confined channels, hierarchically bounded by a '3rd-order' sequence boundary. These '**3rd order**' channel bodies are bound at the base by a large erosional surface and they are stated by Mayall et al. (2006) as typically 1-3 km wide and 50-200 m thick. The '3rd-order' sequence boundaries are also identified by their stratigraphic position between '3rd-order' (1-2 Myr) maximum flooding surfaces. These maximum flooding surfaces are often associated with diagnostic biostratigraphic controls, aiding the identification of chronostratigraphic timescales in the basin. According to Mayall et al. (2006), most infill within these channel bodies is associated with periods of 3rd-order eustatic lowstand (and thus embodies lowstand systems tracts; LST), while a thinner overlying mud-prone section is determined to be the product of transgressive and highstand systems tracts (TST/HST). The internal fill of the '3rd-order' channels is complex and smaller erosional cuts within these units reflect '**4th order**' (otherwise termed 'channel systems') and '**5th order**' surfaces. According to Mayall et al. (2006), discrimination between '4th order' and '5th orders'

is hard to achieve with confidence, as periods of abandonment within the '3rd-order' channel may be associated with autogenic channel switching, as opposed to higher-order eustatic controls. Mayall et al. (2006) also state that in the down-dip reaches of a channel element, at the more distal positions, a '3rd order' fill may split into separate '4th order' channels as a result of channel bifurcation; thus, channel bifurcations translate into a downdip reduction of the hierarchical order of the channel forms. The smallest channel elements (10-30 m thick), recognised within a '3rd order' unit are interpreted to represent 'individual channels'. However, these units are not specified by Mayall et al. (2006) to correspond with either a '4th order' or '5th order' and thus their position in the hierarchy is unknown. The stacking patterns of '4th order' and '5th order' channels are recognised by Mayall et al. (2006) to have a critical impact upon facies distribution in turbidite reservoirs.

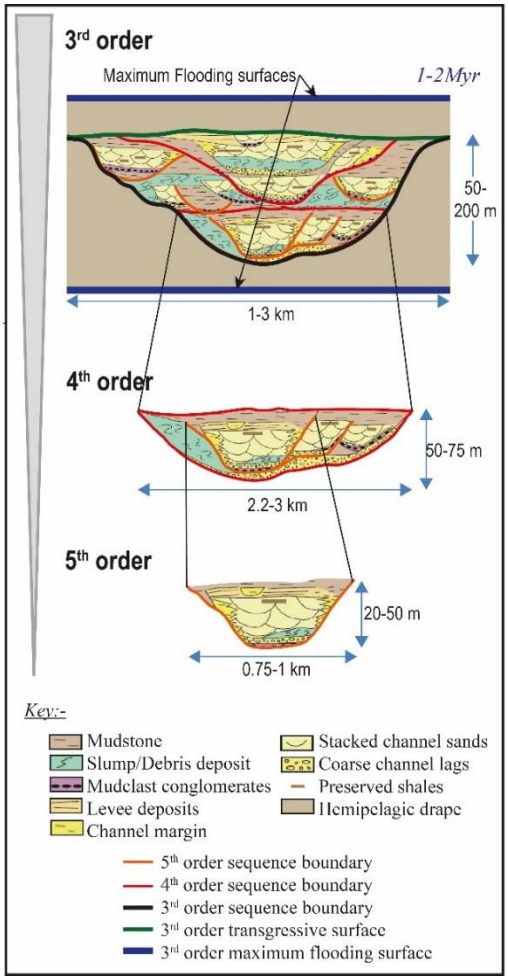

Fig. 3.12. Hierarchical classification for channel deposits by Mayall et al. (2006). Orders are determined by sequence boundaries and order durations are shown in blue italics. Widths and thicknesses ranges for the 4th and 5th order are calculated from the summary diagram presented by the study, while the '3rd order' values are based upon averages explicitly stated by Mayall et al. (2006). Modified after Mayall et al. (2006).

3.2.10 Gervais et al., 2006

The hierarchical scheme of Gervais et al. (2006(a)) was inspired by the improved quality of seismic surveys of submarine fans, revealing details of the geometry and stacking of distal lobe architectures. For example, the sonar-imaging and seismic profiling of Twichell et al. (1992) and Gervais et al. (2004) helped to reveal that lobes in sandy systems were not entirely sheet-like deposits but characterised by channelized geometries, and were equally not the product of a single 'bed'. Building upon these insights Gervais et al. (2006(a)) used high-resolution seismic data to generate a pseudo-3D model of the lobes of the Golo fan (East Corsican margin). This was one of the first models to help illustrate the lithological heterogeneity of sandy lobe deposits and associated hemipelagic drapes, which resulted in a three-fold hierarchy (Fig. 3.13).

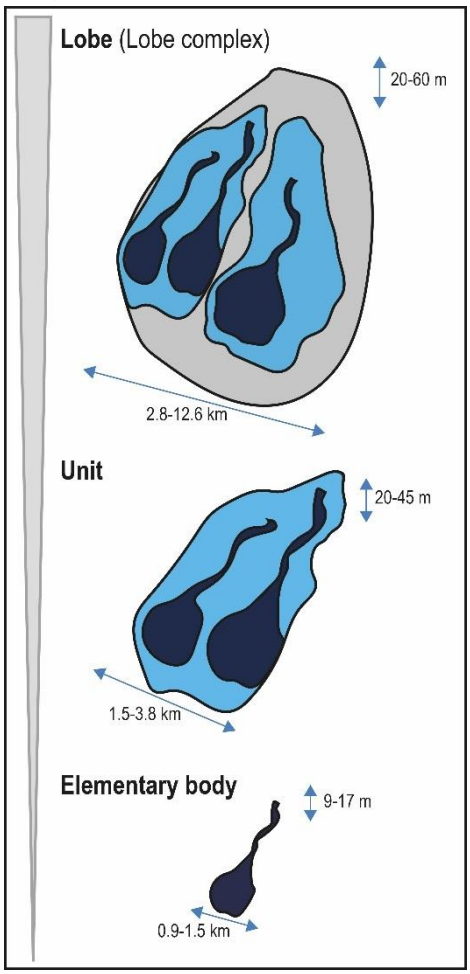

Fig. 3.13. The three-tiered hierarchical scheme used to classify lobe deposits of the Golo fan developed by Gervais et al. (2006(a)). Reported values of thickness and width are measured from the elements identified by Gervais et al. (2006(a)) in the original seismic dataset. Figure modified after Gervais et al. (2006(a)).

Depositional elements at the smallest hierarchical scale, termed '**elementary bodies**', are composed of bedded facies which stack in such a way to produce local gradient changes,

which in turn alter the flow dynamics in the system. These 'elementary bodies' are characterised by two principal geometries: 'sheet' and 'channel'; channels can be associated with levees. Continuous stacking of these 'elementary body' geometries produce higher-scale '**units**'. 'Units' are preferentially deposited with compensational stacking patterns. These depositional bodies are separated by surfaces that may alternate between erosive or concordant character, and breaks in sedimentation can be seen to separate these lobate 'unit' geometries from other 'units'. Numerous successive events, expressed as genetically related 'units', stack to form '**lobe**' deposits' (also known as 'lobe complexes') which are fed by a major channel or channel-levee complex in the turbidite system. A complete 'lobe' deposit is separated from others via a regionally extensive hemipelagic drape, which covers the whole lobe surface. This is recognised by Gervais et al. (2006(a)) by its lateral continuity and bedded, non-chaotic, seismic facies. The degree of lateral and longitudinal confinement is also stated by Gervais et al. (2006(a)) to be an important control on the geometry of a lobe. This, in turn, is believed to greatly influence the stacking patterns of its hierarchical components.

3.2.11 Deptuck et al., 2008

The scheme proposed by Deptuck et al. (2008) is based on the same high-resolution shallow subsurface seismic dataset of the Golo Basin studied by Gervais et al. (2006(a); 2006(b)), and was co-authored by many of the same workers, including B. Gervais and A. Savoye. Similarities between the schemes in the two studies are therefore expected. However, there are notable differences in the interpreted hierarchical organisation of lobe architecture (compare Fig. 3.13 and Fig. 3.14). The study undertaken by Deptuck et al. (2008) focussed upon the investigation of both the cause of geometrical variability and the internally heterogeneous nature of sandy lobes identified by Gervais et al. (2004; 2006(a) and 2006(b)). The observed systematic variability associated with compensational stacking of lobe deposits is seen to highly influence the resultant hierarchy; a four-fold hierarchy is recognised, within which compensational stacking is seen to occur at three different levels (i.e., for the 'lobe element', 'composite lobe' and 'lobe complex' components).

'**Beds or bed-sets**' represent the smallest hierarchical scale and are stated to reflect deposits from a single flow. However, how beds and bed-sets differ to one another is not stated. These 'beds and bed-sets' typically stack in such a way that their respective thickest parts show a systematic lateral offset of up to 500 m; this is referred to by Deptuck et al. (2008) as 'bed compensation'. This level of offset does not result in any lobe-wide discontinuities. The continuous stacking of 'beds and bed-sets' forms a unit termed a '**lobe element**'.

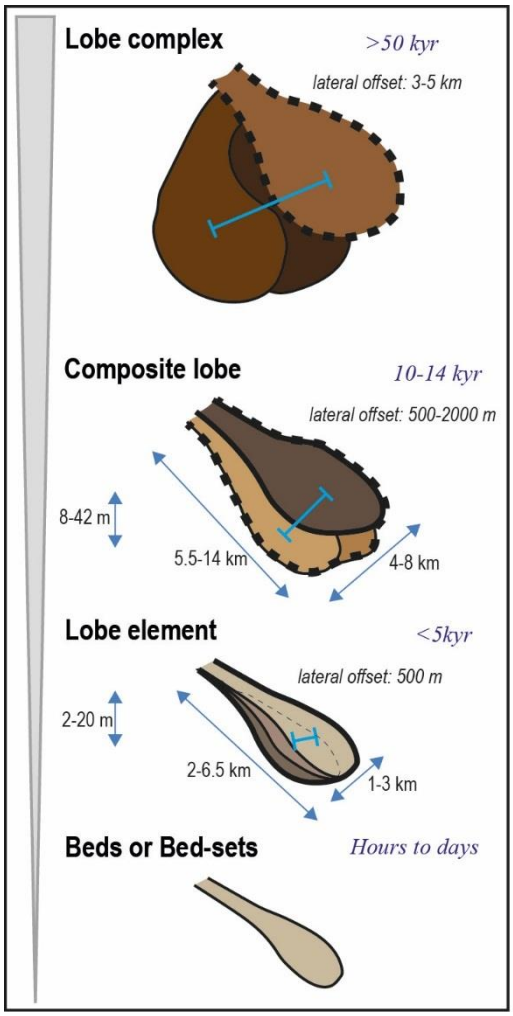

Fig. 3.14. Hierarchical classification employed by Deptuck et al. (2008). Inferred duration for each hierarchical order is shown in blue italics and the magnitude of lateral offset between the thickest parts of each lobate component at a given order is also reported. These lateral offsets also highlight the stacking patterns observed. Modified after Deptuck et al. (2008).

'Lobe elements' are separated by erosive surfaces and represent deposition from a number of similar flows. Deptuck et al. (2008) also note that the 'lobe element' hierarchical order may itself contain two hierarchical levels of stacking, based upon the element's bounding surface. Two or more 'lobe elements' may show compensational stacking (500-2000 m lateral offset) as a result of local channel avulsions, to form a deposit known as a '**composite lobe**'. These units can be separated by disconformable surfaces, abrupt vertical shifts in acoustic facies, or by the presence of thin drapes (the lithological nature of which is not specified). A '**lobe complex**' consists of stacked 'composite lobes' that were fed by the same primary conduit. The lateral shift between the thickest parts of 'composite lobes' (3-5 km) within a 'complex' is interpreted as the result of large-scale channel-mouth avulsions. Abandoned 'composite lobes' can be blanketed by several metres of hemipelagic drape, however this may be eroded

by subsequent events. Temporal scales are provided for this hierarchy based upon previously calculated carbon (^{14}C) dating results for key seismic reflectors (Gervais, 2002), see Fig. 3.14.

3.2.12 Prélat et al., 2009

Prélat et al. (2009) proposed an outcrop-based hierarchy for lobe architectures, which is distinguished from other distributary hierarchical schemes by its critical recognition of fine-grained deposits between sand-rich bodies, otherwise known as 'interlobe' architectural units (Fig. 3.15). A four-fold hierarchy was developed associated with these depositional 'interlobe' elements thanks to good lateral exposure along outcrops of Permian deposits of the Tanqua depocentre of the Karoo Basin, South Africa. This allowed detailed lithological studies that provided the foundation for this hierarchical classification which has since been applied to several other examples (see Section 3.2.12.1).

A unit at the smallest hierarchical order, i.e., a '**bed**', can be 100s of metres wide and up to 0.5 m thick and is interpreted to represent a single depositional event. 'Beds' stack to form a '**lobe element**' that can be up to 2 m thick (Fig. 3.15). The 'lobe element' scale is the lowest order at which inter-sandbody fine-grained units are identified (typically <2 cm thick). Although they may be locally eroded or amalgamated at this scale, '*interlobe elements*' are observed separating vertically stacked, genetically related 'lobe elements'. 'Lobe elements' stack compensationally in topographic lows between previously accumulated depositional bodies to form '**lobe**' deposits, which can be up to 5 m thick and over 20 km wide and also show thicker '*interlobe*' caps up to 2 m thick. 'Lobe' bodies are fed by a single channel upstream and these in turn stack to form '**lobe complexes**' which can be up to 40 km wide and 50 m thick. The '*interlobe complex*' depositional elements are not only thicker than corresponding units at lower scales (they can be in excess of 50 cm), but they are also finer (clay grainsize) than the silty deposits of corresponding units at lower orders. The thick hemipelagic claystones, which mark 'interlobe complexes', are interpreted to be deposited as a result of widespread basin starvation, driven by sea-level change. This allogenically controlled event has also been given a sequence stratigraphic significance by Prélat et al. (2009), who compare the 'interlobe complex' to the transgressive and highstand systems tracts (TST/HST) of a depositional sequence; this is in-line with the interpretation of the Tanqua fan system made by Johnson et al. (2001).

Prélat et al. (2009), also recognise that the 'lobe' hierarchical level is indicative of a transition from autogenic-dominant controls to allogenic-dominant controls. However, Prélat et al. (2009) state that it is difficult to infer the relative importance that autogenic and allogenic

controls play at particular hierarchical levels in outcrop studies, due to the way autogenic and allogenic controls can mutually interact.

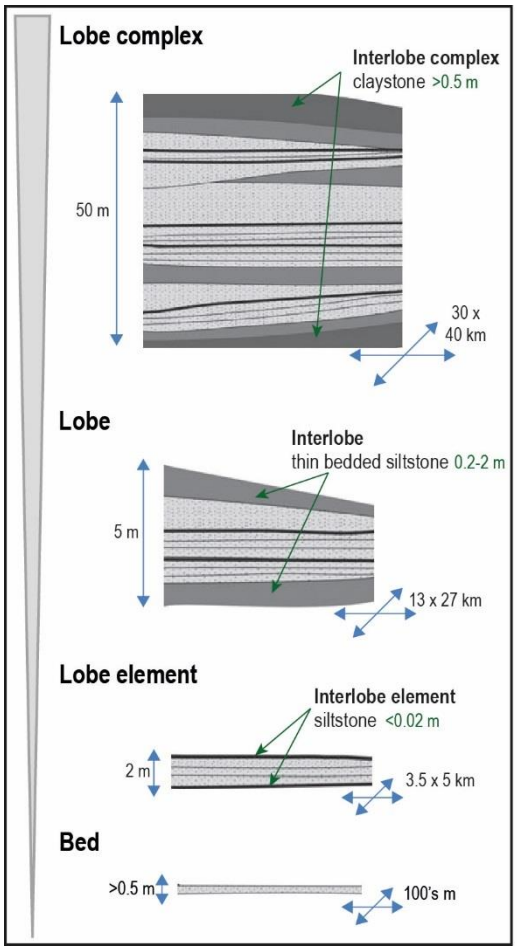

Fig. 3.15. Hierarchical classification of Prélat et al. (2009), showing the four hierarchical orders and their 'interlobe' sedimentary components. Values of sedimentary-body dimensions that are indicated by Prélat et al. (2009) as typical for each order are reported. Modified after Prélat et al. (2009).

3.2.12.1 Use and application of the facies-based lobe hierarchy by Prélat et al. (2009)

This distributary-lobe hierarchical classification developed by Prélat et al. (2009) has been highly regarded by other authors (e.g., Mulder & Etienne, 2010; MacDonald et al., 2011(b)), and has been modified to suit a variety of other studies concerning the architecture of deep-marine lobes (e.g., Macdonald et al. 2011(b), see Section 3.2.14; Grundvåg et al., 2014; Terlaky et al., 2016, see Section 3.2.16). This hierarchy has also been evaluated against a numerical model by Groenenberg et al. (2010). Outputs of the process-based model employed by Groenenberg et al. (2010) supported the hierarchical framework devised by Prélat et al. (2009), with respect to stacking patterns and the digitate geometries of the lobe

architectural units. More recent hierarchical schemes that have links to the scheme and concepts of Prélat et al. (2009) are shown in Fig. 3.1.

Prélat et al. (2010) also applied this hierarchical scheme to a number of other systems, whereby the nomenclature and classifications of previous deep-marine lobe deposits (e.g., the Zaire, Amazon, and Golo systems) from a number of different workers (e.g., Golo data from: Gervais et al., 2006(a); 2006(b); see Section 3.2.10; Deptuck et al., 2008; see Section 3.2.11) were all standardised to the hierarchy of Prélat et al. (2009). Such a process entails uncertainties in the resultant comparison, given the contrast between the nature of the criteria adopted for the facies-based hierarchy devised for the Karoo Basin and the datasets of the other systems which consist predominantly of seismic data (see also the Discussion).

3.2.13 Flint et al., 2011

The authors of this outcrop study on the lobe architecture of the Laingsburg depocentre of the Karoo Basin (South Africa) have not devised their own hierarchical classification but have utilised multiple concepts on hierarchical organisation, in order to establish a classification for slope to basin-floor deep-water architecture that aims to aid sequence stratigraphic interpretations. It therefore focuses upon the recognition of basin-wide sea-level changes through the preservation of predictable stacking patterns (Fig. 3.16).

Flint et al. (2011) state that the terminology used in this three-tiered hierarchical arrangement is based upon: (i) the sequence stratigraphy hierarchical review of Neal & Abreu (2009), whereby each sequence stratigraphic order *sensu* Mitchum et al. (1977) is noted by its varying magnitude and duration of accommodation space creation, as well as (ii) the 'sequence stratigraphic framework' definitions of Sprague et al. (2002). The hierarchy is significantly based upon the recognition of regional hemipelagic claystone units, which Flint et al. (2011) describe as the "most readily identifiable and correlatable 'surfaces' at outcrop". These units are interpreted to be the product of low sediment supply during increased shelf accommodation. They are seen to be contemporaneous to shelfal highstand and transgressive systems tracts (HST and TST), and are thus regarded as 'sequence boundaries' *sensu* Van der Merwe et al. (2010). They can also be paralleled to the maximum flooding surfaces and associated condensed sections of Galloway (1989) and Hadler-Jacobsen et al. (2005). Identifiable increases in the thickness of these hemipelagic claystone boundary units are notably used by these authors to mark the succession of hierarchical orders and are also used, in the absence of age controls, as indicators of relative depositional timescales in a laterally extensive outcrop case study.

A '**sequence**' is the smallest hierarchical order defined by Flint et al. (2011). These depositional bodies exhibit predictable stacking patterns, as sand-prone units (0-150 m thick) overlain by claystone units (1-5 m) are interpreted to reflect LST and TST/HST deposition, respectively. A 'sequence' in the hierarchy of Flint et al. (2011) is therefore comparable to the 3rd-order depositional sequence of the sequence stratigraphic framework (Mitchum & Van Wagoner, 1991). However, Flint et al. (2011) also draw attention to the fact that seismically resolved 'sequences' may have been misinterpreted, in that they may actually reflect larger-scale units at the scale of the 'composite sequence'. 'Sequences' are seen to stack into '**composite sequences**', which are overlain by a thicker hemipelagic claystone unit (10-20 m). These units can exhibit either progradational, aggradational or retrogradational stacking patterns. 'Composite sequences' are capped by an even thicker hemipelagic claystone unit (20-50 m) to form a '**composite sequence set**'. Total thickness estimates for each hierarchical order based on their outcrop data are reported in Fig. 3.16.

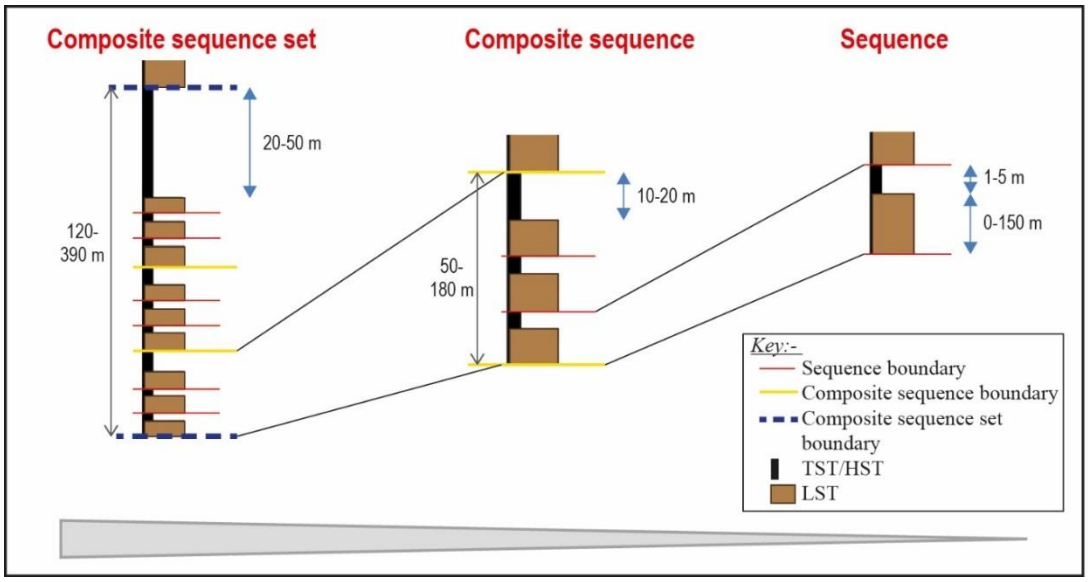

Fig. 3.16. Hierarchical classification developed by Flint et al. (2011) to study lobe architecture from the outcrops of the Karoo Basin. The terminology is related to sequence stratigraphic concepts and thus shown in red. The model is based upon the thicknesses of the hemipelagic transgressive and highstand systems tract; average thicknesses of hemipelagic mudstones, as well as the sand thickness in a 'sequence' as stated by the study are provided. Complete thicknesses for the composite sequence and composite sequence set are also included (calculated from the studies outcrop data). Figure modified from Flint et al. (2011).

The ability to assign sequence stratigraphic classes (sequence boundaries, systems tracts, and systems tract sets, etc.) was achieved by Flint et al. (2011) thanks to the extensive lateral and vertical exposures of outcrops in the Karoo Basin outcrops and to the large body of

knowledge on this basin. This allowed units to be mapped and correlated from the basin plain to shelf-edge deltas, in a manner similar to the work of Hadler-Jacobsen et al. (2005).

3.2.14 MacDonald et al., 2011

MacDonald et al., 2011(b), conducted their outcrop study of the Carboniferous Ross Sandstone Formation (Ireland) with the hope of elucidating the process sedimentology of lobe deposits. MacDonald et al. (2011(b)) state that previous lobe architecture studies have resulted in the production of two similar hierarchical schemes (Deptuck et al., 2008; Prélat et al., 2009), which primarily focused upon the internal architecture of lobe deposits. However, key differences are observed between these two schemes – see Sections 3.2.11 and 3.2.12 – for instance with respect to the terminology they employ, as well as their differing 'lobe-element' definitions, particularly in regard to their consideration of bounding surfaces. MacDonald et al. (2011(b)) derive a hierarchy that is focused on process sedimentology, incorporating process understanding into the hierarchy of Deptuck et al. (2008), based on results from high-resolution facies analysis. Interestingly, MacDonald et al. (2011(b)) discard the possibility of adopting the outcrop-based hierarchy of Prélat et al. (2009; Section 3.2.11), which is also based upon detailed facies analysis; no reason is given as to why this hierarchy is disregarded.

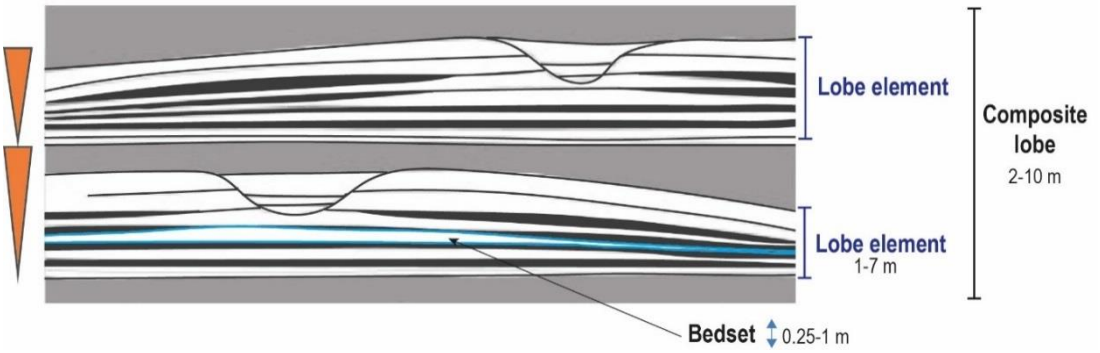

Fig. 3.17. Hierarchical classification used by MacDonald et al. (2011(b)) based upon vertical facies changes. Thickening-upwards trends are seen within the prograding lobe elements. Average unit dimensions are also provided. Modified after MacDonald et al. (2011(b)).

The hierarchy used to classify the architecture of the Ross Formation adopts the same nomenclature of the scheme by Deptuck et al. (2008); however, only three orders are recognised in this study ('bed-set', 'lobe-elements', and 'composite lobes', Fig. 3.17). The smallest hierarchical order, '**Bed-sets**', are stated to include stacked beds and bed-sets, but no information is provided to distinguish between beds and bed-sets. This order is stated to reflect the depositional product of a single flow, and stack into thickening-upwards packages

to form '**lobe-elements**'. MacDonald et al. (2011(b)) state that their use of this term aligns with usage by both Deptuck et al. (2008) and Prélat et al. (2009). 'Lobe-elements' typically contain a mudstone part at the base of each package formed during a depositional 'shutdown' period. The thickness and presence of these basal mudstones is interpreted by MacDonald et al. (2011(b)) to be determined by the lateral distance and duration of avulsion experienced by the subsequent 'lobe-elements'. MacDonald et al. (2011(b)) also propose that a six-stage evolutionary sequence can be observed in the formation of a 'lobe-element'. This sequence includes phases of deposition, amalgamation, bypass and multiple transition events (see MacDonald et al., 2011(b)). This evolutionary model is used to explain why resultant thickening-upwards packages are observed in 'lobe-elements': each depositional body is interpreted as a progradational cycle of distal to proximal deposits, identified through facies changes and an increase in the number of megaflutes. 'Lobe-elements' are subsequently seen to stack compensationally, forming '**composite lobes**'.

Pyles (2007) also studied these deep-marine architectures of the Ross Sandstone. He, in turn, implemented a hierarchical scheme which involved the recognition of 'architectural elements', based on the method of architectural-element analysis of Miall (1985). However, the lobe architecture is identified to be simple, showing no internal hierarchical organisation.

3.2.15 Pickering & Cantalejo, 2015

Pickering & Cantalejo (2015) have recently proposed a deep-marine hierarchical classification based on outcrop studies of the Eocene Ainsa Basin (Spanish Pyrenees). This hierarchy has since been applied by the same research group to additional datasets from the same basin (Bayliss & Pickering, 2015(a; b); Pickering et al., 2015). The devised hierarchy relies on correlation of key stratigraphic surfaces at a variety of scales, allowing bounding surfaces for architectural elements to be defined. The hierarchy is therefore based upon similar criteria to the ones adopted in the original scheme by Pickering et al. (1995): (i) internal facies associations (based upon the facies classification of Pickering et al., 1986), (ii) architectural geometry, and (iii) associated bounding surfaces. However, the way this information is organised and described (Fig. 3.18) differs from the original hierarchy of Pickering et al. (1995; Fig. 3.4a).

The nomenclature used within the hierarchy of Pickering & Cantalejo (2015) is based upon terminology proposed by Flint et al. (2008), Sprague et al. (2002; 2005; 2008; Section 3.2.7), and Figueiredo et al.'s (2013) work on the Karoo Basin. This terminology covers a wide range of scales, from seismic to core or outcrop studies. Compared to Pickering et al., 1995, this nomenclature more closely aligns with current sequence stratigraphic concepts, which in turn

helps to support the aims of Pickering & Cantalejo's (2015) study, i.e., to improve stratigraphic surface correlation through the recognition of sequence boundaries across the basin. However, this focus limits the applicability of this scheme where the scale of observation is limited.

'**Lamina**' and '**laminaset**' define the 1st hierarchical order of the classification, representing the smallest identifiable package of sediments that tend to lack internal layering, having a uniform lithology. One or more 'laminasets' compose a '**bed**', which represents the 2nd-order division and is described as the fundamental building block of stratigraphy. Based on the definition of Campbell (1967), a 'bed', is interpreted as a deposit formed by a single depositional event; it is also considered to be a time stratigraphic unit, a property which Pickering & Cantalejo (2015) state can allow for inter-basinal correlations, *sensu* Van Wagoner (1990). A 3rd-order '**bedset**' is constrained when a bed immediately above or below differs in composition, texture or sedimentary structures. Pickering & Cantalejo (2015) explain that the definition of their 4th-order unit, the '**storey**', was originally used to characterise fluvial deposits (Friend et al., 1979), and has thus been modified to accommodate deep-marine deposits; uniquely, Pickering & Cantalejo (2015) also apply the term to classify mass-transport deposits (MTDs) *sensu stricto* Pickering & Corregidor (2005). Two types of 'storey' are identified, and categorised based upon distinct facies associations: 'sandy storeys' (on average 300 m wide and 3 m thick, based upon 66 examples) and 'mass-transport storeys' (on average 700 m wide and 6 m thick, based upon 32 examples). 5th-order units consisting of multiple 'storeys', are termed '**elements**', and are classified either as channel fill or mass-transport elements. These units typically have an erosional base and commonly show fining-upward trends in their axial domain. 'Channel-fill elements', on average 1000 m wide, 14 m thick (based upon 64 examples) can be divided into distinct regions, i.e., as axis, off-axis, margin and levee regions, but no guidelines on how such regions are recognised are provided. A 6th-order '**complex**', classified as a 'mass-transport complex' (MTC) or 'channel complex' (on average 1400 m wide and 37 m thick, based upon 38 examples) is commonly erosional at the base, and can show either fining- or coarsening-upwards cycles depending on the stacking of its internal elements. A unit composed of multiple 'complexes' is termed a 7th-order '**sandbody**' (on average 2200 m wide and 90 m thick, based upon 19 examples). Pickering & Cantalejo (2015) state that these 7th-order units can also be referred to as 'sequences'; however this term is not favoured by Pickering & Cantalejo (2015) themselves due to the common association of this term with depositional units that are typically larger. In the Ainsa Basin 'sandbodies' are marked by an MTD/MTC at their base and capped by a basin-wide drape, otherwise known as an abandonment facies.

This order signifies a major basin-wide re-organisation, as each 'sandbody' is interpreted to reflect a shift in the depocentre position. Two or more 'sandbodies', typically separated by fine-grained marly sediments in this depositional system, are recognised as 8th-order '**systems**'. Multiple sandy 'systems' are briefly noted by Pickering & Cantalejo (2015) to stack into either fining or coarsening upward packages known as '**system sets**'. In turn these 'system sets' can stack into a 'group', which is the largest hierarchical order of sedimentary unit identified in the Ainsa Basin.

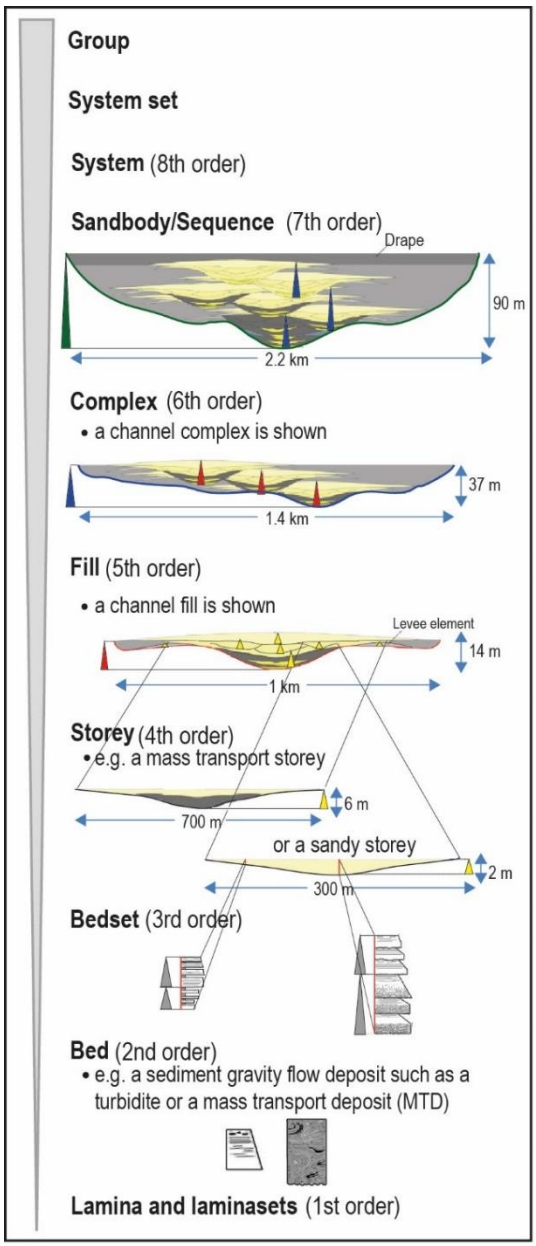

Fig. 3.18. Hierarchical classification developed by Pickering & Cantalejo (2015) and employed in the Ainsa Basin, for channelized environments. Numerical orders and average dimensions of corresponding units are shown, numbering indicates the bounding surface order of the depositional body. Figure modified after Pickering & Cantalejo (2015).

3.2.16 Terlaky et al., 2016

Terlaky et al. (2016) establish their 'avulsion-based' hierarchy building upon existing hierarchical classifications found in the literature. The hierarchy makes reference to architectural-element analysis principles and is based upon the work by Mulder & Etienne (2010), which in turn adopts the hierarchical classification of Prélat et al. (2009). Terlaky et al. (2016) state that differences between their hierarchy and those it is based upon arise in relation to differing types of observations: whereas other hierarchies focus upon the nature of fine-grained inter-sandbody deposits (for instance Gardner & Borer, 2000; Prélat et al., 2009; Grundvåg et al., 2014), Terlaky et al. (2016) develop their hierarchy around the identification of surfaces and the location of avulsion nodes.

Each hierarchical division within the seven-tiered hierarchy is therefore defined by the increasing order of the drainage-pattern hierarchy at which avulsion occurred (Fig. 3.19). This idea is also seen by Terlaky et al. (2016) as a methodology to help bridge the gap between outcrop and modern seismic studies, although the framework is solely developed from outcrop data (Neoproterozoic Windermere Supergroup, British Columbia, Canada).

The smallest hierarchical division recognised by the framework is the '**lamina**'; laminae stack to form '**beds**', which themselves are interpreted to be the deposit of a single flow. 'Beds' stack to form what is known as an '**architectural element**' when a 3D view of the depositional body is known, or a 'stratal element' if the element is expressed only in 2D. Terlaky et al. (2016) define this 'architectural element' hierarchical order by making reference to key characteristics used as criteria for the attribution of corresponding orders in other schemes. For example, Terlaky et al. (2016) describe this order as a mesoscale lithosome (a defining character of Miall's, 1985, fluvial architectural elements) of 'mappable' scale (*sensu* Mutti & Normark, 1987). Terlaky et al. (2016) define architectural elements as the preserved products of deposition taking place between two successive distributary-channel avulsion events. Depositional bodies of this type are characterised by distinctive external shape, bounding surfaces and internal arrangement of sedimentary facies, in agreement with the characteristic properties used by Pickering et al. (1995), Gardner & Borer (2000), Pyles (2007), Prélat et al. (2009), and Grundvåg et al. (2014), in their schemes. Terlaky et al. (2016) use these criteria to define 'architectural elements' as the fundamental building blocks of larger stratigraphic units. This 'stratal/architectural element' order includes units interpreted to have formed under a distinctive set of depositional conditions. Six typical stratal elements recognised in the basin-floor environment of the Kaza Formation are identified by Terlaky et al. (2016) as:

- isolated scours,
- feeder channels,
- distributary channels,
- terminal splays,
- avulsion splays
- (sheet-like) distal and off-axis fine-grained turbidites.

The nomenclature used to describe these geometries is said to be taken from several studies of submarine fans. These 'architectural elements' are also compared by Terlaky et al. (2016) with the 'lobe element' units of Prélat et al. (2009).

Genetically related 'architectural elements', which Terlaky et al. (2016) state can also include debrite, slump and slide bodies, stack to form a '**lobe**'. A lobe is seen to embody the overall active depositional area at any one time on the basin floor, and to form the units deposited between two events of feeder-channel avulsion. 'Lobes' are identified by Terlaky et al. (2016) as the point of transition within the hierarchy, as it is at this level that more basin-wide allogenic controls begin to dominate sedimentary processes (similarly to the 'lobe' order of Prélat et al., 2009). A '**lobe complex**' is produced by the stacking of multiple 'lobes' and may also include genetic debrites, slumps and slide bodies – however, these bodies are not genetically defined by Terlaky et al. (2016). A 'lobe complex' is seen to be the consequence of an episode of channel-levee-system avulsion, which makes this order comparable to the 'lobe complex' of Prélat et al. (2009). A '**fan**' is formed by avulsion of a feeder canyon, an event that Terlaky et al. (2016) state will be reflected in the stacking pattern of the 'lobe complexes'. In turn, multiple 'fans' stack to form '**fan complexes**', the largest recognised hierarchical order. Terlaky et al. (2016) do however state that it will be difficult, especially in outcrop studies, to discern the highest orders of this hierarchical framework.

Other hierarchies based upon distributary 'interlobe' stratigraphic markers (e.g., the hierarchy of Prélat et al., 2009) are not readily applicable to the outcrop studied by Terlaky et al. (2016), due to the limited preservation of fine-grained deposits in the Kaza Formation. Additionally, the scheme by Terlaky et al. (2016) could be applied to datasets with limited facies data, as local evidence of avulsion (marked by lithological boundaries and/or stratal trends) can be combined with basin-wide observations of element position and stacking. However, this scheme can only be applied if extensive, basin-wide correlations can be established, and traced to areas updip of the channel-lobe transition zone.

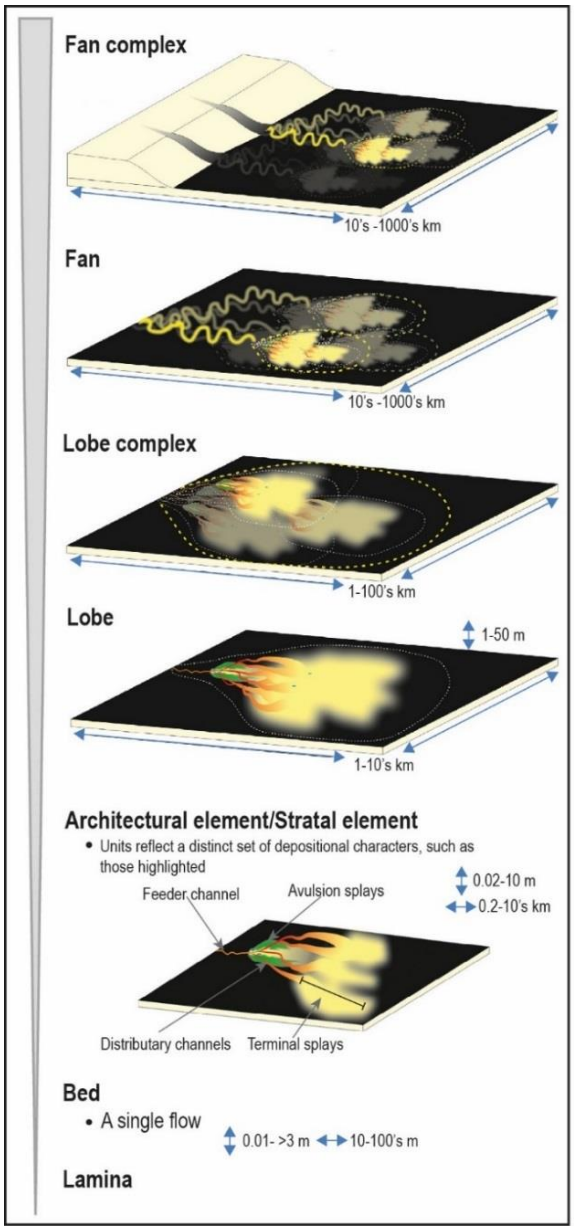

Fig. 3.19. Hierarchical classification for an idealised submarine-fan complex by Terlaky et al. (2016). Dimensions are estimates taken from the study. Figure modified after Terlaky et al. (2016).

3.3 Discussion

Hierarchical classifications attempt to assign order to otherwise complex systems, allowing the spatial and relative temporal evolution of deep-marine systems to be studied. As demonstrated by the schemes reviewed in this Chapter, hierarchical classifications provide a method to better understand this complexity, as they help geologists, both in academia and industry, to:

i) better constrain reservoir models, e.g., by improving the characterisation of hydrocarbon-reservoir properties (such as geometry, facies distribution and

connectivity) – objectives intended by the hierarchical schemes of Prather et al. (2000), Sprague et al. (2005) and Gervais et al. (2006(a));

ii) Establish analogy between outcrop and subsurface data, and enable comparative analyses between both modern and ancient systems – drivers that motivated Mutti & Normark (1987), Hadler-Jacobsen et al. (2005), Mayall et al. (2006) and Prélat et al. (2010) to develop their hierarchical schemes. The hierarchical schemes reviewed in Section 3.2 are summarised in Table 3.1.

However, significant differences exist between hierarchical schemes, casting doubt over their wider utility. The possible causes of these differences, such as differing data-types and environmental controls are evaluated below; in parallel inter-scheme similarities, with respect to both sedimentological observations and common genetic interpretations are reviewed. These analyses can be used to assess whether a common standard for deep-marine architectural hierarchy is possible.

3.3.1 The influence of research aims on the structure of hierarchical schemes

Hierarchical schemes and the number of significant orders they recognise differ in relation to the particular architectural elements, sub-environments or physiographic settings they focus on (see Table 3.1). Because of differences in the aims of the research and types of data underlying each scheme, some hierarchies may be applicable to entire systems, whereas others can be restricted in scope, for example to just 'channelized' or 'lobate' environments, or to the CLTZ setting (Fig. 3.20). Hierarchies that are solely restricted in their application to distributary lobe environments (i.e., Gervais et al., 2006(a); Deptuck et al., 2008; Prélat et al., 2009; MacDonald et al., 2011(b); Flint et al., 2011) commonly recognise only three or four significant orders, starting from a bed or bed-set scale, regardless of whether the underlying dataset is based on seismic or outcrop. Hierarchies developed specifically for channel environments can contain anywhere from three (e.g., Mayall et al., 2006) to ten (e.g., Pickering and Cantalejo, 2015) significant orders, with more complex hierarchies being typical for schemes founded on outcrop datasets due to their higher resolution. Hierarchies that are not restricted in application to a specific sub-environment typically contain five to eight orders; schemes of this type include those of: Mutti & Normark (1987), Pickering et al. (1995), Beaubouef et al. (1999), Prather et al. (2000), Navarre et al. (2002), Hadler-Jacobsen et al. (2005), Sprague et al. (2005) and Terlaky et al. (2016). These schemes display less variability in the number of hierarchical orders than those focussing on channel environments, notwithstanding the wider environmental domain they are applied to. Most of the

publications detailing system-wide hierarchies do not address possible differences in hierarchy between channelized and lobate (or distributary) environments. Only Sprague et al. (2005; Fig. 3.9) and Navarre et al. (2002; Fig. 3.7) distinguish between these settings through the use of environmental prefixes associated with the different architectural geometries. Sprague et al. (2005) also provide distinct ranges of dimensions for the different units associated with these two environments.

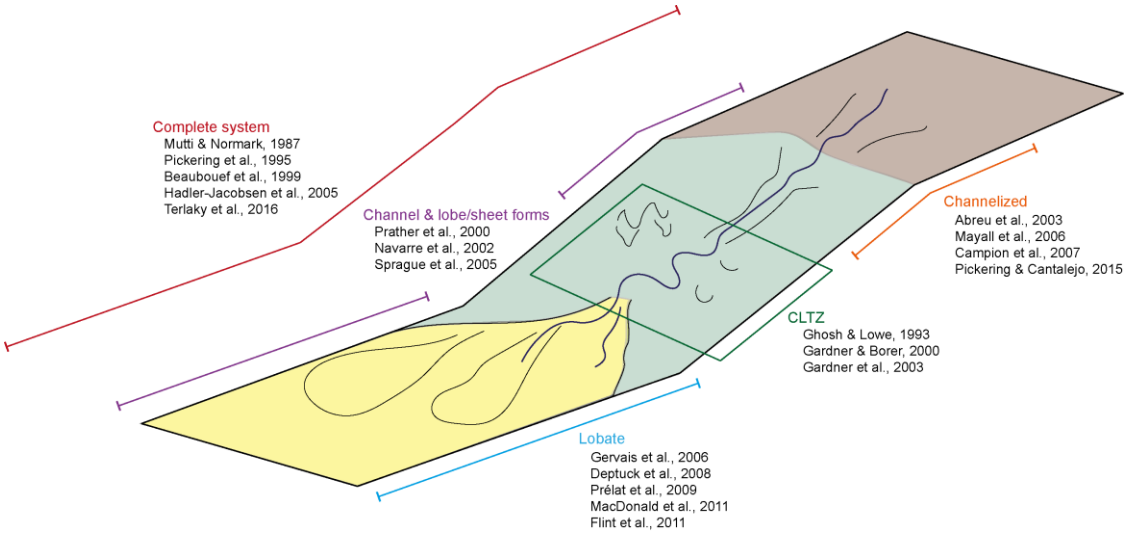

Fig. 3.20. The range of deep-marine sub-environments considered by each hierarchical scheme reviewed in this paper.

The difference in the number of significant orders established for channel and lobe environments suggests that it might not be possible to capture the internal organization of these two environments by using a single hierarchy. It also suggests that the number of hierarchical orders might vary as the system and its architecture evolve downstream. This concept is something Mayall et al. (2006) alluded to in their study, as they proposed that a channel body could display a downstream decrease in hierarchical organization of its deposits, as energy drops and the channel bifurcates becoming simpler in form.

In addition to hierarchical schemes being developed for a specific depositional domain (sub-environment), others have been proposed by studies which focus on partiular architectural elements (e.g., lateral-accretion packages; Abreu et al., 2003), tectonic settings (e.g., confined basins; Mayall et al., 2006), or specific basins (e.g., the Ainsa Basin; Pickering & Cantalejo, 2015). It is therefore reasonable that the variety observed in the way hierarchical approaches are structured reflects different research focuses. Some hierarchical approaches are accompanied by explicit caveats regarding the particular environment each scheme is supposed to be applicable to (e.g., schemes for sand-rich systems by Pickering et al., 1995, Prather et al., 2000 and Gardner et al., 2003). A question arises as to whether the

development of new hierarchical approaches is undertaken without consideration of the available existing schemes, and thus whether enough testing has been done to reject the use of existing ones. On some occasions, new hierarchical schemes are seen to modify existing models based upon new insights or needs. For example, the modification of Gardner & Borer's (2000) CLTZ hierarchy by Gardner et al. (2003) was based upon a process-driven model which was thought to better inform the interpretation of the architecture. Similarly, Abreu et al.'s (2003) adaption of the scheme by Sprague et al. (2002) was designed to accommodate lateral-accretion packages. Typically, the majority of hierarchies presented in this review have only been applied to, or demonstrated through, single case studies (see Table 3.1), raising the question as to whether their broader applicability has been robustly established.

3.3.2 Data types: biases and pitfalls

The method of investigation and the available data can also influence the resultant structure of the hierarchical schemes. For example, outcrop studies are often limited in their scales of observation, because of partial preservation and the quality of exposure. This has brought about the notion that only seismic investigations can capture basin-scale architectures (Prather et al., 2000; Gardner et al., 2003; Posamentier & Kolla, 2003; Prélat et al., 2010; Flint et al., 2011; Terlaky et al., 2016). Most often hierarchical approaches based on seismic datasets include orders that are applicable basin-wide or to the scale of the entire system (e.g., the 'megasequence' of Navarre et al., 2002; the 'turbidite-complex' of Mutti & Normark, 1987). However, the dimensional scales of the largest outcrop-derived architectural orders are comparable to those of the seismic 'basin-wide' architectures; this is evident in the values of lobe thickness reported by Flint et al. (2011), and in the thickness and width measures for the interpreted LST 'submarine channel fairway' depositional body of Gardner et al. (2003), which encompass the scalar ranges of the 'megasequence' basin-fill order of Navarre et al. (2002, see Figs. 3.21 and 3.22, below).

The resolution of the data provided by different methods of acquisition can also affect the resultant hierarchical classification. The poorer resolution of seismic datasets, as opposed to outcrops, results in a diminished ability to recognise lower-order units; thus, 'bed' or individual 'facies' orders are usually not considered in seismic datasets. The resolution of seismic data is known to vary depending on the method used (Posamentier et al., 2000; Weimer & Slatt, 2007(a)); however, even on high-resolution seismic profiles, the smallest order described often correspond to bed packages; these include, for example the 'elementary body' of Gervais et al. (2006(a)) and the 'beds and bed-sets' of Deptuck et al.

(2008). Navarre et al. (2002) state that only their 'channel complex' and 'storey' hierarchical levels were confidently recognised in their study, whereas Mayall et al. (2006) point out that discerning between their '4th order' and '5th order' units might be difficult. The uncertainties caused by poor data resolution in identifying architectures at particular scales hinders the quality and integrity of the hierarchical approaches underpinned by such datasets. This affects the confidence with which hierarchical classifications based on outcrop and seismic datasets can be reconciled, and any subsequent attempt to develop a common hierarchical standard. However, research on large outcrop exposures, at 'seismic' scales, is being undertaken that can help reconcile hierarchies developed using different data types; works of this type include, for example, those on the Karoo Basin (South Africa; Prélat et al., 2009; Flint et al., 2011), the Magallanes Basin (Chile; Romans et al., 2011; Pemberton et al., 2016) and the Brushy Canyon Formation (USA; Gardner & Borer, 2000; Gardner et al., 2003, Pyles et al., 2010).

In an attempt to overcome scale limitations in seismic datasets, some studies supplement seismic data with 'sub-seismic' facies-scale observations (e.g., Prather et al., 2000; Navarre et al., 2002; Sprague et al., 2005) or integrate both data types to inform their hierarchical approaches (e.g., Mutti & Normark, 1987; Pickering et al., 1995; Hadler-Jacobsen et al., 2005; Mayall et al., 2006). The integration of core and well-log data with seismic data helps overcome limitations in vertical resolution. Such integration however has not resulted in consistency across the different hierarchical schemes: variation is still seen in the number of significant orders that are recognised (ranging from three to eight orders, see Table 3.1), as well as in the terminology used (see Figs. 3.4, 3.6 and 3.11). However, all the schemes, bar the hierarchy of Mayall et al. (2006), are seen to incorporate 'basin-wide' hierarchical orders as they capture both channel and lobe environments. Hierarchical schemes developed in the hydrocarbon industry have tended to integrate data of different types (e.g., outcrop, core, well logs, seismic, bathymetry, biostratigraphy) to develop more geologically sound schemes; however, the manner and degree of integration cannot be directly assessed due to the proprietary nature of the data (e.g., Navarre et al., 2002; Abreu et al., 2003 and Sprague et al., 2005).

3.3.3 Hierarchical-order nomenclature

Comparison between hierarchical schemes is hindered by variability in hierarchical nomenclature, arising from:

i) redundancy in terminology; for example, the terms 'channel-fill' (Sprague et al., 2005), 'channel story' (Navarre et al., 2002), and 'elementary channel fill'

(Gardner et al., 2003) are all terms used to identify the interpreted products of a single cycle of fill and abandonment of a discrete channel form;

ii) variations in the meaning of like terms; an example of this is the usage of the term ‘storey’ (or ’story’ in US English), cf. the definition of a ‘channel story’ in the hierarchy of Navarre et al. (2002) as opposed to the scour based, sub-channel ‘storey’ of Sprague et al. (2005).

Terminological discrepancies have arisen because some hierarchical approaches have been influenced by, or have used, components of previous hierarchical classifications. Sharing terminology and definitions can be problematic, as often concepts undergo some re-interpretation when applied in a new scheme. For example, MacDonald et al. (2011(b)) state that they use the ‘lobe-element’ definition of Deptuck et al. (2008) and Prélat et al. (2009) but do not reconcile the differences between these definitions. Thus, the lobe-element definition of Deptuck et al. (2008) is recognised to potentially display relationships with more than one order of bounding surfaces, i.e., this order does not share a one-to-one bounding-surface to element-order relationship; on the contrary, Prélat et al. (2009) recognise a lobe element as being encapsulated by bounding surfaces that belong to the same order as the element. Such differences contribute to the potential for misinterpretation when trying to compare approaches.

Nomenclature is also often amended through time to keep terminology up-to-date, as scientific understanding improves. For example, the definition of a ‘storey’ has been amended multiple times. The original meaning, coined by Friend et al. (1979) was used as a basic descriptive term for fluvial deposits. However, Sprague et al. (2005) redefined the term to describe deep-marine channel bodies showing predictable lateral and vertical bedset facies changes. This definition has since been adopted and expanded by Sprague et al. (2008) to include lobe and levee/overbank deposits and further amended by Pickering & Cantalejo (2016) to incorporate mass-transport deposits. As terminology evolves the risk of inconsistent application may arise.

3.3.4 Common criteria used to diagnose hierarchy in architecture

While a wide range of terminology is used in hierarchical schemes, similarities between order definitions can be found, based largely upon the common descriptive characteristics used to diagnose hierarchy. For example, when discernible, internal facies characteristics, the nature of the bounding surfaces, their scale and observable geometries are all used to distinguish similar hierarchical orders in all schemes reviewed in this paper. Additional criteria that are

sometime used to establish hierarchy include sedimentary-unit stacking patterns, dimensions, and absolute or relative durations or timescales.

These diagnostic characteristics – facies associations, geometry, scale and bounding surface relationships – are also the common criteria used in the 'architectural-element analysis' approach applied to categorise both fluvial and aeolian sedimentary successions (e.g., Brookfield, 1977; Allen, 1983; Miall, 1985). Although only some authors of deep-marine hierarchical schemes might have directly acknowledged these influences (e.g., Ghosh & Lowe, 1993, Pickering et al., 1995, Gardner & Borer, 2000, Gardner et al., 2003, Terlaky et al., 2016 and Pickering & Cantalejo, 2015; see Table 3.1 and Fig. 3.1), all the reviewed schemes implicitly recognise architectural hierarchy using the principles of architectural-element analysis to some degree. Such commonalities suggest that reconciliation between hierarchies should be possible (see also Section 3.3.5, below). Nevertheless, difficulties remain in trying to make definitive links between the hierarchical orders of different schemes. This is due in part to the differing significance given to particular types of diagnostic characteristic. For example, the hierarchy of Prélat et al. (2009) specifically focuses upon facies characteristics, while that of Deptuck et al. (2008) largely relies on stacking patterns of 3D architectural geometries. In addition, difficulties in observing key characters, as a result of the intrinsic complexity of sedimentary successions or because of limitations related to available data types (as discussed in Section 3.3.2), limit the confidence with which hierarchical units can be compared. For instance, Ghosh & Lowe (1993) note the difficulty in recognising bounding surfaces in conglomerates and debris-flow deposits, and in recognising architectural geometries within highly scoured, and subsequently amalgamated, 'first order' and 'second order' units.

Miall's (1985) explanation of the 'architectural-element analysis' was also accompanied by a number of cautions for its application to fluvial deposits, which are also applicable to deep-marine systems. Miall (1985) identified potential issues in identifying architecture in relation to differences in scale, interbedding (the interdigitation of background sedimentation being particularly relevant for deep-marine deposits) and intergradation between sub-environments. These problems make it difficult to establish correlations and delineate deep-marine architectures, particularly at the basin scale, directly impeding the development of a common hierarchy for deep-marine deposits.

3.3.5 Common stratigraphic architectures and their inferred formative processes

Sedimentological and stratigraphic observations of deep-marine deposits can be used to develop our understanding of formative depositional and erosional processes, in combination with numerical and physical experiments (e.g., Gardner et al., 2003; Talling et al., 2012). This is due to limitations in observing such processes first-hand in deep-marine systems, although significant insight has been drawn more recently from direct turbidity-flow monitoring and observations of the geomorphic expression of processes acting on the seafloor (e.g., Paull et al., 2010; Maier et al. 2011; Symons et al., 2017). In several cases common interpretations of formative processes are used in association with the recognition of diagnostic sedimentological features, facies associations, geometry, scale and bounding surface relationships to establish tentative links between hierarchical schemes. Such links are outlined below for the channel and lobe architectures reviewed in Section 3.2 in ascending scalar order, along with caveats in the use of the resulting genetic hierarchies.

3.3.5.1 Common channelized hierarchical architectures

A ‘bed’ is typically the most readily recognisable small-scale hierarchical unit included in schemes applicable to channelized deposits (Mutti & Normark, 1987, 1991; Ghosh & Lowe, 1993; Pickering et al., 1995; Beaubouef et al., 1999; Prather et al., 2000; Sprague et al., 2005; Campion et al., 2011; Pickering & Cantalejo, 2016; Terlaky et al., 2016). The description of a bed is widely influenced by the definition set by Campbell (1967), according to whom it is a layer of sedimentary rock bounded above and below by either accretionary or erosional bounding surfaces and that is not defined on its thickness. These units can be heterogeneous, and as such some schemes divide this unit further into facies divisions, recognised by changes in grain-size and sedimentary structures (e.g., the ‘first order’ and ‘second order’ of Ghosh & Lowe, 1993; the ‘zeroth order’ of Pickering et al., 1995; the ‘lamina and laminasets’ of Pickering & Cantalejo, 2015; Terlaky et al., 2016). In the reviewed schemes, a bed is consistently interpreted as representing a single depositional event, whereby any internal divisions relate to changes in sediment-gravity-flow conditions.

At a higher scale, units that are commonly described in channel environments are composed of vertically stacked, genetically related beds. These units are bound by erosive or accretionary bounding surfaces and are themselves contained within a larger channel form. Units of this type are typically noted as being unresolvable by conventional seismic methods due to their limited size (e.g., Mutti & Normark, 1987; Prather et al., 2000; Navarre et al.,

2002; Sprague et al., 2005). These units show distinct lateral and vertical facies changes, categorised by some studies in terms of predictable organisation arising from variations in processes from channel axis to margin regions (e.g., Prather et al., 2000; Campion et al., 2007; Pickering & Cantalejo, 2015). A variety of terms have been coined to refer to deposits that display these characteristics: e.g., the 'turbidite sub-stage' of Mutti & Normark (1987; 1991), the 'sedimentary complex' of Pickering et al. (1995), the '1st order, sub-seismic' of Prather et al. (2000), the 'geobody' of Gardner & Borer (2000) and Gardner et al. (2003), the 'channel phase' of Navarre et al. (2002), and the 'storey' of Sprague et al. (2002; 2005), Campion et al. (2007; 2011), McHargue et al. (2011(a)) and Pickering & Cantalejo (2015). This channel architecture is recurrently recognised in the deep-marine rock record, as noted by these hierarchical schemes, indicating its importance as a building block of channel deposits. These 'storey' deposits are commonly interpreted as the product of sequences of flows that progressively wax then wane in terms of their energy (McHargue et al., 2011(a)). Periods of erosion, bypass and filling are commonly recorded in the facies patterns of these units (Mutti & Normark, 1987; 1991; Campion et al., 2011). These 'stories' are often termed 'sub-channel' elements due to their containment within larger confined channel forms (Sprague et al., 2005; Campion et al., 2007; 2011).

Multiple genetically related 'stories' stack with little lateral offset, to form a recognisable channel form bounded by a typically erosional basal surface. Units showing these characters have been termed as 'turbidite stages', (Mutti & Normark, 1987; 1991), 'fourth-order' units (Ghosh & Lowe, 1993; Prather et al., 2000), 'depositional bodies' (Pickering et al., 1995), 'channel fills' (Beaubouef et al., 1999; Sprague et al., 2002; 2005; Pickering & Cantalejo, 2015), 'channel stories' (Navarre et al., 2002), 'single-story channels' (Gardner & Borer, 2000), 'elementary channel fills' (Gardner et al., 2003), 'channels' (Abreu et al., 2003; Campion et al., 2007; 2011), 'sixth-order' units (deposits of the Delaware Basin; Hadler-Jacobsen et al., 2005;), 'channel elements' (McHargue et al., 2011(a)) and 'architectural elements' (Terlaky et al., 2016). These 'channel' architectures show distinct cross-sectional and planform geometries (Pickering et al., 1995; Prather et al., 2000; Terlaky et al., 2016), discernible in both seismic and outcrop datasets. No significant unconformities are observed within these deposits, and their tops are typically marked by hemipelagic/pelagic background sedimentation (Mutti & Normark, 1987; Navarre et al., 2002). Mutti & Normark (1987) propose that such patterns in sedimentation are the result of short-term sea-level changes or tectonic activity, suggesting that units at this scale might record the effects of allogenic controls. The relative lack of significant background sedimentation internally suggests that these 'channel' units are interpretable as the product of a complete cycle of channel filling

and abandonment (Sprague et al., 2002; 2005), itself recording multiple cycles of waxing and waning flow energy (McHargue et al., 2011(a)). The stacked internal 'stories' are also seen by some to show a predictable evolutionary sequence, again relating to changes in environmental energy as flows vary through the stages of channel initiation (erosion), growth (filling) and retreat (abandonment or bypass), (Navarre et al., 2002; Gardner & Borer, 2000; Gardner et al., 2003; Sprague et al., 2005; Hadler-Jacobsen et al., 2005; McHargue et al., 2011(a)). The recurrence of these facies successions has been used to produce models of flow evolution and energy trends in channels (Hubbard et al., 2014), as well as to map basin-ward changes (Gardner et al., 2003).

Based upon common sedimentological and stratigraphic observations, a larger-scale, 'regional' hierarchical order can be recognised (Ghosh & Lowe, 1993; Pickering et al., 1995). Erosional surfaces are seen to envelope deposits that contain multiple lower-order genetically related 'channel' architectures, as well as other associated element types (e.g., lateral-accretion packages; Abreu et al., 2003); Mutti & Normark, 1987; Navarre et al., 2002; Sprague et al., 2005; McHargue et al., 2011(a). Vertical stacking trends no longer dominate this architecture. Packages of hemipelagic sediments, relatively thicker than those recognised in lower-scale units, are seen to delineate bodies that stack in highly- or non- amalgamated fashions (cf. 'fifth-order' of Ghosh & Lowe, 1993; 'members/sub-members' of Pickering et al., 1995; 'channel complex' of Gardner & Borer, 2000; Navarre et al., 2002; Sprague et al., 2005; Campion et al., 2011; Pickering & Cantalejo, 2015; 'composite channel' of Gardner et al., 2003; 'complex set' of McHargue et al., 2011(a). These units are interpreted as showing common migration pathways, as the successive internal units exhibit similar lateral and/or vertical patterns within the larger confining channel (Gardner et al., 2003; Campion et al., 2011). Again, such architecture is seen to be the product of a cycle of channel initiation, growth and retreat (Gardner et al., 2003; Hadler-Jacobsen et al., 2005; McHargue et al., 2011(a)). With consideration of observations on hierarchy, McHargue et al. (2011(a)) describe the internal stacking of channel 'complex' architectures, through forward modelling, as sequential – moving from amalgamated, low aggradational stacking to highly aggrading, vertically-stacked deposits. This model has since been supported and developed by Macauley & Hubbard (2013) and Jobe et al., (2016).

Broad correspondence is seen between higher scale units linked by their common generic 'basin-fill' interpretation, for example, the 'turbidite complex' of Mutti & Normark (1987; 1991), the 'sixth-order' of Ghosh & Lowe (1993), the basin-fill sequence' of Pickering et al. (1995), the 'megasequence' of Navarre et al. (2002). These units are inferred to encapsulate architecture spanning the lifetime of multiple submarine fans and their deposits, bound by

long-term unconformities influenced by regional tectonics (Mutti & Normark, 1987; 1991; Navarre et al., 2002). The internal character of these deposits is not well-documented, but Mutti & Normark (1987) still infer cycles of initiation, growth and retreat at this scale.

3.3.5.2 Common hierarchical orders for 'lobe' or 'sheet' architectures

In 'depositional-lobe' deposits (*sensu* Mutti & Normark 1987; 1991), a 'bed' is often the smallest hierarchical division observed, although not always seen as a discrete class (Deptuck et al., 2008; MacDonald et al., 2011(b)). A 'bed' is again interpreted as the product of a single depositional event. Genetically related 'bed' units are commonly observed to stack, separated by non-erosional surfaces, into distinctive lobate geometries, identifying a common hierarchical division often termed a 'lobe element' (Deptuck et al., 2008; Prélat et al., 2009; MacDonald et al., 2011(b)), comparable to the 'elementary body' of Gervais et al. (2006(a)) and the 'architectural element' of Terlaky et al. (2016). In outcrop, units of this type predominantly show vertical internal stacking (Prélat et al., 2009; MacDonald et al., 2011(b)), whereas in high-resolution seismic datasets the thickest part of internal bed deposits are seen to show some lateral offset (Gervais et al., 2006(a); Deptuck et al., 2008), this discrepancy may be associated with data type limitations. This lateral offset, or 'bed compensation' (~500m, Deptuck et al., 2008), is seen to reflect local changes in gradient, not associated with basin-wide discontinuities. In deposits of the Karoo basin, Prélat et al. (2009) recognised that 'lobe element' units are bounded by thin (<2 cm thick) siltstone intervals, interpreted as a temporary depositional 'shutdown'. MacDonald et al. (2011(b)) further recognise these 'lobe-elements' as the product of a predictable evolutionary cycle, as phases of deposition, amalgamation, bypass and abandonment are interpreted from the facies trends; such cycles mirror the initiation-growth-retreat cycles observed in channel deposits.

At a larger-scale, compensational stacking of depositional units is recognised as a key diagnostic character in the attribution of units termed 'lobe' by Sprague et al. (2005), Prélat et al. (2009), and Terlaky et al. (2016), 'lobe story' by Navarre et al. (2002), 'unit' by Gervais et al. (2006(a)), and 'composite lobe' by Deptuck et al. (2008) and MacDonald et al. (2011(b)). Genetically related, lower-order architecture (typically the 'lobe elements' as previously described) stack within topographic lows to generate lobate or lenticular geometries. In deposits of the Karoo basin, Prélat et al. (2009) recognised that 'lobe' units are bounded by muddy intervals 0.2-2 m thick. The internal compensational stacking is seen to be a product of local feeder channel avulsion, associated with the upstream single channel that feeds this 'lobe' (Deptuck et al., 2008; Prélat et al., 2009; MacDonald et al., 2011(b); Terlaky et al.,

2016). The understanding of drainage patterns and its avulsion-based hierarchy can thus be used to better inform lobe hierarchy, a property employed by Terlaky et al. (2016). These deposits are also interpreted by Prélat et al. (2009) and Terlaky et al. (2016) to mark the transition from autogenic- to allogenic-dominant depositional controls – although the precise effects of such controls are not specified.

Typically, the largest hierarchical orders identified in distributary environments are characterised by the occurrence of compensational stacking of genetically related 'lobes'. Units of this type are consistently termed as 'lobe complexes' (Gervais et al., 2006(a), Deptuck et al., 2008, Prélat et al., 2009; Terlaky et al., 2016). In deposits of the Karoo basin, Prélat et al. (2009) recognised that these units are separated by basin-wide claystone intervals that are >50 cm thick (Prélat et al., 2009). The 'lobe complex' deposits of these authors are interpreted as being deposited from a single major channel system, whereby internal breaks in sedimentation and compensational stacking styles result from large-scale channel avulsions (Gervais et al., 2006(a); Deptuck et al., 2008; Terlaky et al., 2016). These avulsions are more significant and occur further upstream in channel-levee systems than those experienced at lower hierarchical orders (Terlaky et al., 2016). The more significant clayey intervals or top bounding surfaces that mantle architectures of this scale are seen to be driven by widespread basin starvation, controlled by allogenic forcing, e.g., relative sea-level change (Prélat et al., 2009). As a consequence of the stacking and position of the internal 'lobe' units, Prélat et al. (2009) recognise phases of growth to be expressed in units of this type (lobe complex 'initiation', 'growth', 'building' and 'retreat'; cf. Hodgson et al., 2006).

3.3.5.3 Notes on the application of an observation-based genetic hierarchy

While commonalities can be found between hierarchical schemes based upon sedimentological descriptions and their interpreted genetic processes, caution in exercising such comparison is necessary. As a general rule, architectural complexity is seen to increase as the scale of deposition increases, with associated difficulties in capturing the architecture of larger bodies. In part these difficulties arises because of the increasingly compound and diachronous nature of deposits at larger scales and in part due to the fact that key observations on which hierarchical orders are defined change with scale. For example, at lower scales, facies characteristics, which are more easily described in outcrop, are heavily relied upon to classify the hierarchy of sedimentary bodies (such as for channelized 'beds' and 'storeys'). At larger scales, the recognition of hierarchy becomes more reliant upon the

geometry of deposits (‘channels’ or ‘lobe elements’), and their stacking patterns (‘channel complexes’, ‘lobes’ and ‘lobe complexes’). Such differences explain the difficulties in reconciling hierarchical schemes for seismic and outcrop datasets, compounded by the fact that the recognition of larger hierarchical orders often depends on recognising the nature of lower-scale internal bodies. Where lower orders cannot readily be identified (e.g., in seismic datasets or in coarse amalgamated deposits; cf. Ghosh & Lowe, 1993) uncertainty may cascade upward through the hierarchical classification, affecting the confidence with which larger orders can be recognised and interpreted.

A genetic hierarchy would ideally relate deposits to processes that are exclusive to specific scales. In practice, however, it is not possible to confidently relate observations in the rock record to specific suites of genetic mechanisms, i.e., the possible four-dimensional expressions of all plausible combinations of depositional and erosional mechanisms cannot be reconciled. Application of a genetic hierarchy is also impeded by uncertainty in process interpretations deriving from difficulties in discriminating the effects of autogenic dynamics and allogenic controls. While allogenic controls (e.g., regional basin tectonics, eustatic sea-level changes, rate and calibre of sediment supply) are widely recognised to affect sedimentary architectures (Stow et al., 1996), their expression and degree of interaction cannot be confidently recognised in a way that enables ties to scales of depositional architecture (McHargue et al., 2011(a)). Hence, links between hierarchical orders and allogenic or autogenic controls are often speculative (e.g., short-term and long-term relative sea-level changes; Mutti & Normark, 1987; 1991) or based on considerations on the physical scale at which processes are excepted to occur (e.g., the ‘bed-compensation’ order of Deptuck et al., 2008, which is interpreted as the product of an autogenic mechanism due to the local extent of discontinuities).

Cycles of ‘initiation, growth and retreat’ are commonly identified in all channelized hierarchical orders (excluding ‘beds’). Similar cyclical evolutionary patterns of deposition have also been identified for depositional-lobe deposits (*sensu* Mutti & Normark, 1987; 1991), (e.g., Hodgson et al., 2006; Prélat et al., 2009; MacDonald et al., 2011(b)), as well as for complete depositional systems (cf. ‘fan cycles’ of Hadler-Jacobsen et al., 2005). Such commonalities suggest that some degree of common hierarchical organisation can be recognised within deep-marine systems. However, the fact that these depositional processes occur over a range of scales limits their value as a criterion for proposing a ‘genetic’ hierarchy, or as the basis for confident translations between hierarchical orders in different schemes.

3.3.6 Spatial and temporal scales of hierarchical orders

The temporal and spatial expression of hierarchical scales is often described, at least tentatively, by the authors of the schemes.

Relationships between hierarchical orders and physical scale are proposed for the majority of hierarchical schemes in the form of dimensional parameters that describe the size of the deposits, for sedimentary bodies at all or some of the hierarchical orders in the schemes (see Figs. 3.21 and 3.22). Ranges in width and thickness are presented in Figs. 3.21 and 3.22 respectively. The data have been derived from the publications where the schemes were presented, and represent: (i) values that were stated as representative of the particular hierarchical order, (ii) scales depicted graphically in synthetic summary models, (iii) values relating to case-study examples referred in the original paper. As far as it can be ascertained, width values reflect 'true' measurements (*sensu* Geehan & Underwood, 1993), whereby a width measurement is taken perpendicular to the modal palaeoflow direction of the deposit. Discrepancies exist between some studies regarding the importance of deposit dimensions as a criterion in hierarchical classifications. For instance, Pickering et al. (1995) state that the characterisation of an architectural geometry does not need to be dependent upon scale; rather, in their view, scale is implicit in the ordering of bounding surfaces, which denote 'relative' scalar relationships.

System controls (e.g., tectonic setting, dominant grain size) affect the magnitude of deep-marine depositional processes and thus their architectural expressions (Richards et al., 1998; Weimer & Slatt, 2007(a)). This phenomenon hinders the use of absolute scale as a universal criterion to determine hierarchy in deep-marine systems; indeed, overlaps between hierarchical order dimensions can be found within single system datasets, e.g., most notable in Gardner & Borer (2000); Prather et al. (2000); Gardner et al. (2003) and Gervais et al. (2006(a)). Nonetheless, some general associations between hierarchical orders and dimensions of sedimentary units can be found for selected environmental settings or types of deposits (e.g., channels vs. lobes). For example, in channel environments, sub-channel 'storeys' *sensu* Sprague et al. (2002; 2005) and broadly equivalent deposits (see Section 3.3.5) usually range in thickness from 1 to 15 m fairly consistently across the different schemes. However, further research is warranted to assess the extent to which geological controls influence the geometrical expression of any recognised hierarchy. For example, Prélat et al. (2010; cf. Zhang et al., 2017) test the effects of topographic confinement on the size of lobe deposits across six depositional systems, identifying areally smaller but thicker deposits within topographically confined systems.

Temporal scale can also be used to define hierarchy. Some studies provide timescales for some or all of their hierarchical orders (Fig. 3.23), usually to allow comparison to sequence stratigraphic orders (Mutti & Normark, 1987; Navarre et al., 2002; Hadler-Jacobsen et al., 2005; Mayall et al., 2006). The temporal expression of hierarchical orders in selected schemes is shown in Fig. 3.23. The data have been derived from the publications where the schemes were presented, and represent: i) data ranges based on chronostratigraphic constraints (e.g., Navarre et al., 2002) or radiometric dating (e.g., Deptuck et al., 2008), ii) inferred temporal magnitude, estimated either on the basis of known relationships between sedimentation rates and timescales (Sadler, 1981; cf. Ghosh & Lowe, 1993) or by reference to the presumed temporal significance of sequence-stratigraphic orders (Vail et al., 1977; Mitchum & Van Wagoner, 1991).

Correspondences between hierarchical orders can be seen across the schemes on the basis of their timescales, largely through interpretations of their equivalence to sequence stratigraphic scales. For example, Mitchum & Van Wagoner (1991) suggest that 3rd-order depositional sequences should be recognisable in deep-marine successions through the recognition of bounding surfaces and condensed sections. Units of this type, interpreted to embody a time span of 1-2 Myr, can be compared to the '3rd order' units of Hadler-Jacobsen et al. (2005) and Mayall et al. (2006), and to the 'depositional sequence' of Navarre et al. (2002) (Fig. 3.23). The 'turbidite complex' of Mutti & Normark (1987), and the comparable 'sixth order' unit of Ghosh & Lowe (1993), are interpreted as containing multiple depositional sequences. The ability to link hierarchy in stratigraphic architecture to traditional sequence stratigraphic timescales is, however, a questionable approach for assigning temporal significance to deep-marine deposits. Identification of sequence stratigraphic units in deep-marine successions is challenging (Catuneanu et al., 2011), largely due to difficulties in correlating time-equivalent packages across linked depositional systems and recognising the expression of surfaces with sequence stratigraphic significance. It is notable that significant discrepancies can be found in the study of Hadler-Jacobsen et al. (2005) between the inferred duration of the deposits and the timescale that is expected for the same orders in the scheme based on how units map onto the sequence stratigraphic framework.

The relative scarcity of radiometric ages for deep-marine deposits makes inferences of timescale challenging, particularly since extrapolation of durations to lower scales cannot be attempted based on limited constraints, since the average duration of hiatuses increases with the timescale (Sadler, 1981). Necessarily, the inherent incompleteness of the geological rock record must be taken into account in the classification of hierarchy. Findings in a range of marine and non-marine clastic environments highlight the fractal organisation in which time

is recorded in their preserved stratigraphy, in relation to the dependency on timescale of sedimentation rates and durations of depositional gaps (Sadler, 1981, 1999; cf. Miall 2015, 2016). The identification of common cyclical processes in deep-marine environments, i.e., cycles of initiation, growth and retreat, could be used to suggest that a similar fractal organisation might exist in the stratigraphic architecture of deep-marine systems, at least over a certain range of scales. The idea that fractal modes of organisation might permeate aspects of sedimentary architectures has been probed by several authors (Thorne, 1995; Schlager, 2004; 2010; Catuneanu et al., 2011; Straub & Pyles, 2012; among others). Whether fractal patterns exist in the geometry of certain deep-marine deposits in relation to the scale-invariance of certain processes is a subject that deserves further investigation.

Fig. 3.21. (*Overleaf, page 91*). Element widths for specific hierarchical orders, taken from the original studies. Ranges (lines and bars) or single values (diamonds) have been sourced from the text (black outline), measured from summary figures (no outline) or represent data from examples shown in the paper (lines empty diamonds). Maximum widths, measured orthogonal to the dip or palaeoflow direction of the unit were recorded when possible. Colours denote the type of elements the ranges refer to (blue: lobe deposits; orange: channel deposits; grey: lobe and channel, other or unspecified deposits). Uncertainty on ranges is represented by faded lines and bars.

Fig. 3.22. (*Overleaf, page 92*). Element thicknesses for specific hierarchical orders, taken from the original studies. Ranges (lines and bars) or single values (diamonds) have been sourced from the text (black outline), measured from summary figures (no or white outline) or represent data from examples shown in the paper (lines or empty diamonds). Maximum thicknesses were recorded where possible. Colours denote the type of elements the ranges refer to (blue: lobe deposits; orange: channel deposits; grey: lobe and channel, other or unspecified deposits). Uncertainty on ranges is represented by faded lines and bars. See key in Fig. 3.21.

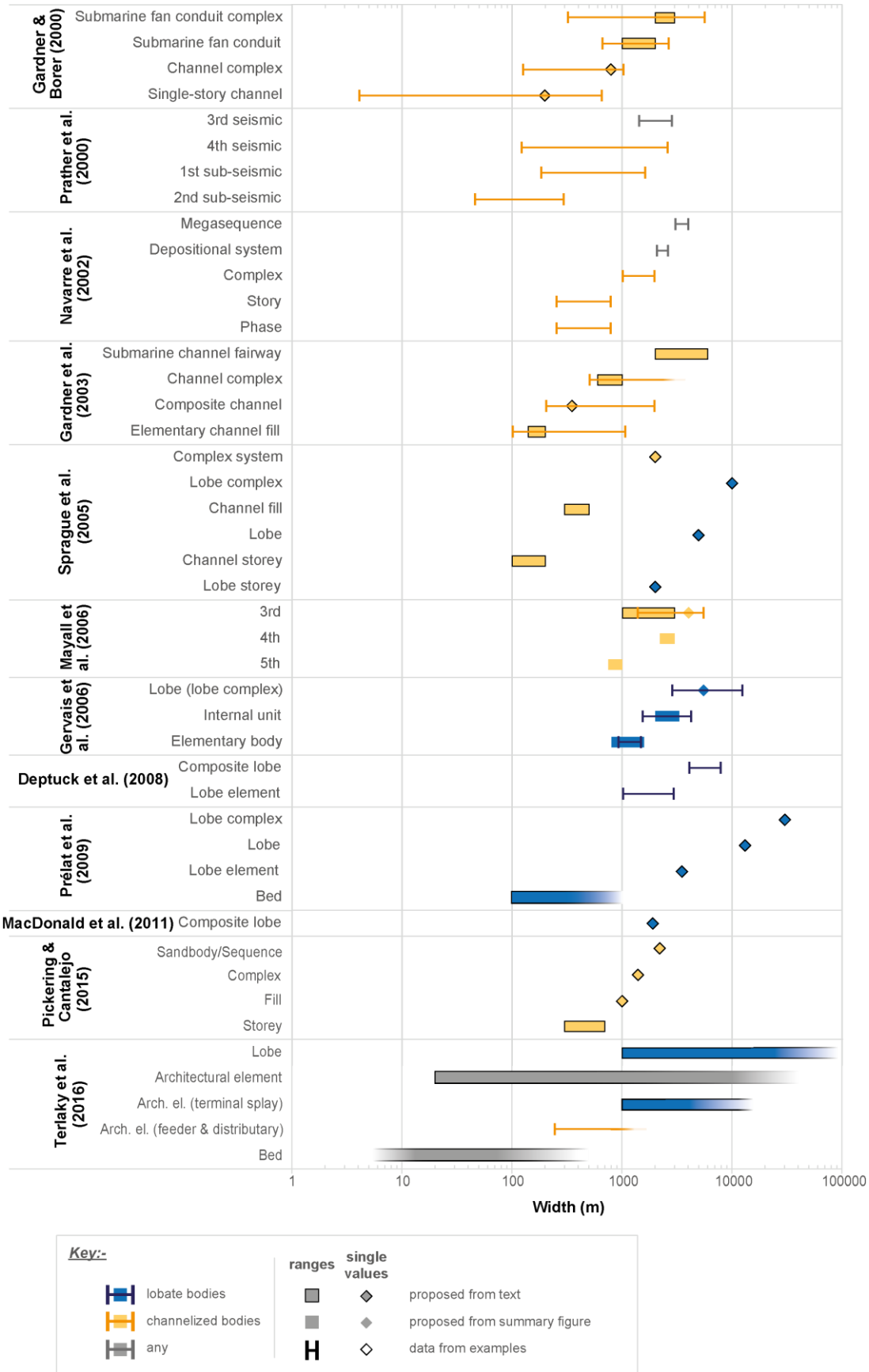
Gardner & Borer (2000)
Submarine fan conduit complex
Submarine fan conduit
Channel complex
Single-story channel
Prather et al. (2000)
3rd seismic
4th seismic
1st sub-seismic
2nd sub-seismic
Navarre et al. (2002)
Megasequence
Depositional system
Complex
Story
Phase
Gardner et al. (2003)
Submarine channel fairway
Channel complex
Composite channel
Elementary channel fill
Sprague et al. (2005)
Complex system
Lobe complex
Channel fill
Lobe
Channel storey
Lobe storey
Mayall et al. (2006)
3rd
4th
5th
Gervais et al. (2006)
Lobe (lobe complex)
Internal unit
Elementary body
Deptuck et al. (2008)
Composite lobe
Lobe element
Prélat et al. (2009)
Lobe complex
Lobe
Lobe element
Bed
MacDonald et al. (2011)
Composite lobe
Pickering & Cantalejo (2015)
Sandbody/Sequence
Complex
Fill
Storey
Terlaky et al. (2016)
Lobe
Architectural element
Arch. el. (terminal splay)
Arch. el. (feeder & distributary)
Bed
1
10
100
1000
10000
100000
Width (m)
Key:-
lobate bodies
channelized bodies
any
ranges
single values
proposed from text
proposed from summary figure
data from examples

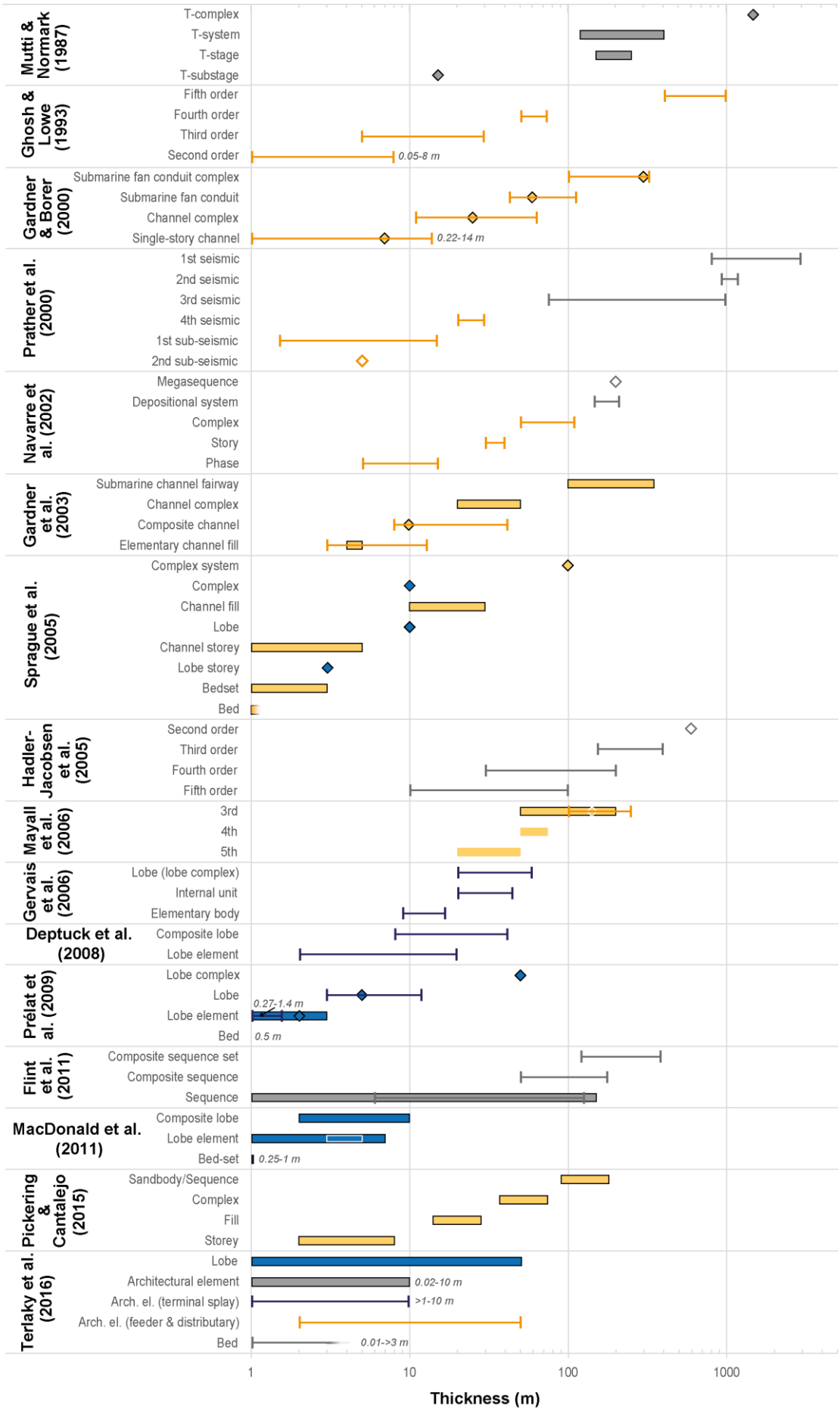
Mutti & Normark (1987)
T-complex
T-system
T-stage
T-substage
Ghosh & Lowe (1993)
Fifth order
Fourth order
Third order
Second order
0.05-8 m
Gardner & Borer (2000)
Submarine fan conduit complex
Submarine fan conduit
Channel complex
Single-story channel
0.22-14 m
Prather et al. (2000)
1st seismic
2nd seismic
3rd seismic
4th seismic
1st sub-seismic
2nd sub-seismic
Navarre et al. (2002)
Megasequence
Depositional system
Complex
Story
Phase
Gardner et al. (2003)
Submarine channel fairway
Channel complex
Composite channel
Elementary channel fill
Sprague et al. (2005)
Complex system
Complex
Channel fill
Lobe
Channel storey
Lobe storey
Bedset
Bed
Hadler-Jacobsen et al. (2005)
Second order
Third order
Fourth order
Fifth order
Mayall et al. (2006)
3rd
4th
5th
Gervais et al. (2006)
Lobe (lobe complex)
Internal unit
Elementary body
Deptuck et al. (2008)
Composite lobe
Lobe element
Prélat et al. (2009)
Lobe complex
Lobe
Lobe element
0.27-1.4 m
Bed
0.5 m
Flint et al. (2011)
Composite sequence set
Composite sequence
Sequence
MacDonald et al. (2011)
Composite lobe
Lobe element
Bed-set
0.25-1 m
Pickering & Cantalejo (2015)
Sandbody/Sequence
Complex
Fill
Storey
Terlaky et al. (2016)
Lobe
Architectural element
0.02-10 m
Arch. el. (terminal splay)
>1-10 m
Arch. el. (feeder & distributary)
Bed
0.01->3 m
1
10
100
1000
Thickness (m)

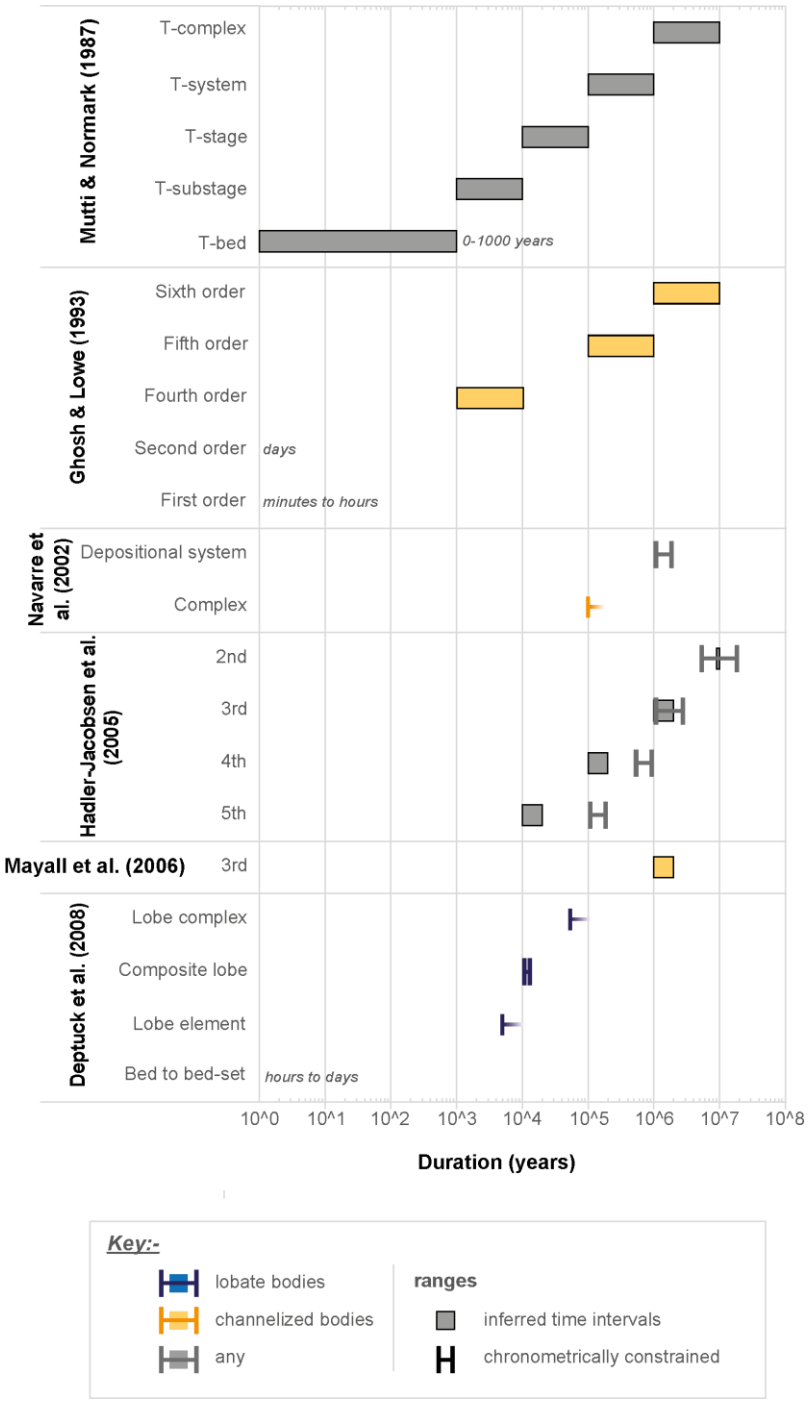

Fig. 3.23. Compilation of documented durations for hierarchical orders, taken from those hierarchical schemes within the review that apply them. Ranges are based on each respective study, as either proposed ranges in inferred durations (bars) or as ranges in estimated durations based on available temporal constraints (lines), both as reported by the authors of the scheme. Uncertainties on minimum and maximum values are shown as fading bars and open-ended lines. Bar colour denotes the type of elements the ranges refer to (blue: lobe deposits; orange: channel deposits; grey: lobe and/or channel deposits, other deep-marine or unspecified deposits).

3.4 Conclusions

The widespread use of hierarchical classifications has helped make the complexity of deep-marine stratigraphy more tractable. However, many different hierarchical classification schemes have been devised to describe deep-marine sedimentary architecture, with new ones often being devised for new case studies, regardless of whether the aims of the study and the types of deposits being examined were comparable to those of previous investigations. This work, for the first time, has systematically reviewed and compared a representative selection of the most widely adopted deep-marine hierarchy schemes. By reviewing the principal characteristics of each hierarchical classification (i.e., the study aims, data types and scope) and the common diagnostic criteria used to attribute deposits to given hierarchical orders, the causes of similarity and variability between different schemes can be assessed. This review can therefore be used to aid sedimentologists who wish to classify a deep-marine system using an existing classification scheme, or who wish to compare their results, fully or partly, to those described using other classifications.

Notwithstanding the observed variety in hierarchical schemes, recurrent sets of observations are seen to underlie all the classification approaches detailed in this Chapter. To define each hierarchical order these approaches commonly entail the recognition of lithological properties (notably facies associations) and architectural geometries, along with the recognition of bounding-surface characteristics and inter-surface relationships. Different classification approaches also apparently share similar genetic interpretations - derived from the sets of common sedimentological features - although this theme deserves further work. Such commonalities of approach may be used as a basis to justify a best-practice methodology for the description of the hierarchy of deep-marine clastic sedimentary architecture. Thus, it is recommended that hierarchical relationships be categorised on the basis of primary sedimentological observations (e.g., facies association, cross-cutting relationships, unconformities, and relative containment of sedimentary units within higher-scale bodies), rather than through predefined schemes developed for particular contexts and whose application entails interpretation.

The recognition of similar criteria for hierarchical classification supports the idea that at least some degree of hierarchical organisation in deep-marine depositional systems does occur. Nonetheless, it remains difficult to reconcile the different hierarchical schemes. Such difficulties arise in part from differences between the underlying studies (e.g., data types, scales of interest, specific environmental settings) and in the significance given to the diagnostic criteria, as well as from the adoption of non-standard terminology. Different numbers of hierarchical orders are commonly recognised for units in different sub-

environments (such as channels *vs.* lobes), and furthermore, it remains unclear whether a particular hierarchal level in one sub-environment necessarily corresponds to the same level in another from a process standpoint. Such inconsistencies reflect an understudied problem in the erection of system-wide hierarchies. In the current state of knowledge, it is therefore concluded that a universal, process-based hierarchy, applicable to all data-types and across all deep-marine clastic systems cannot be established; the Rosetta stone remains elusive.

Chapter 4:

A database solution for the quantitative characterisation and comparison of deep-marine siliciclastic depositional systems

---

Chapter synopsis

Comparative analysis of deep-marine sedimentological studies is hindered by the wide variety in methods of data collection, scales of observation, resolution, classification approaches and terminology. A relational database, the Deep-Marine Architecture Knowledge Store (DMAKS), has been developed to facilitate such analyses, through the integration of deep-marine sedimentological data collated to a common standard. DMAKS hosts data on siliciclastic deep-marine system boundary conditions, and on architectural and facies properties, including spatial, temporal and hierarchical relationships between units at multiple scales. DMAKS has been devised to include original and literature-derived data from studies of the modern sea-floor, and from ancient successions studied in the subsurface and in outcrop.

The database can be used as a research tool in both pure and applied science, allowing the quantitative characterisation of deep-marine systems. The ability to synthesise data from several case studies and to filter outputs on multiple parameters that describe the depositional systems and their controlling factors enables evaluation of the degree to which certain controls affect sedimentary architectures, thereby testing the validity of existing models. In applied contexts, DMAKS aids the selection and application of geological analogues to hydrocarbon reservoirs, and permits the development of predictive models of reservoir characteristics that account for geological uncertainty.

To demonstrate the breadth of research applications, example outputs are presented on: (i) the characterisation of channel geometries, (ii) the hierarchical organisation of channelised and terminal deposits, (iii) temporal trends in the deposition of terminal lobes, (iv) scaling relationships between adjacent channel and levee architectural elements, (v) quantification of the likely occurrence of elements of different types as a function of the lateral distance away from an element of known type, (vi) proportions and transition statistics of facies in elements and beds, (vii) variability in net-to-gross ratios among element types.

4.1 Introduction

Deep-marine siliciclastic systems remain an attractive topic of study, due in large measure to their importance for the hydrocarbon industry (Posamentier & Kolla, 2003; Prather, 2003;

Hadler-Jacobsen et al., 2005; Mayall et al., 2006; Weimer & Slatt, 2007(a); Zhang et al., 2017). In particular, a considerable research effort has been made to better understand the architectural and facies properties of such systems, and especially the role that external controls play in influencing their development (e.g., Shanmugam & Moiola, 1988; Reading & Richards 1994; Stow & Mayall 2000; Prather, 2003 and Picot et al., 2016). System analogue and classification approaches to understanding such controls have been influential (e.g., Reading and Richards, 1994), but are necessarily oversimplified as they can only be undertaken with consideration of a limited number of controlling factors. In principle, comparative analyses exploiting the large number of studies on deep-marine systems should enable better characterisation of system architecture (and associated facies distributions) under a range of combinations of controls, together with an improved understanding of the geological processes they record. However, the synthesis of sedimentological data from deep-marine systems is hindered by the fact that studies differ with regard to aims, methods of data collection (e.g., outcrop versus seismic), scales of observation and resolution, classification approaches (in relation to architecture, facies and unit hierarchy), and nomenclature (cf. Mutti & Normark, 1987; Mulder & Alexander, 2001; Weimer & Slatt, 2007(a); Cullis et al., 2018).

To facilitate comparative analysis a relational database, the Deep-Marine Architecture Knowledge Store (DMAKS), has been developed. This database allows data collation to be carried out in a systematic and standardised manner. It can handle large datasets, allowing meaningful comparisons to be made between the different datasets that it stores. The capacity to integrate different datasets from different deep-marine depositional systems would therefore facilitate subsurface prediction, in part by improving the process of analogue selection via quantitative analysis. The database extends an approach originally proposed by Baas et al. (2005) and is aligned with similar endeavours for fluvial and shallow-marine systems (Colombera et al., 2012(a); 2016). The fluvial and shallow-marine database methodologies have proven the benefits of this approach in sedimentary geology through quantitative outputs (Colombera et al., 2012(a; b); 2015; 2016). The aim of this Chapter is to demonstrate the value of DMAKS as both a fundamental and applied research tool. This will be achieved by:

1- outlining the structure and content of DMAKS, showing how it enables the synthesis and analysis of diverse sedimentological data;
2- demonstrating potential database applications, through showcasing its capabilities in facilitating characterisation of deep-marine systems.

4.2 Database purpose, design and standard

The Deep-Marine Architecture Knowledge Store (DMAKS) is a relational database that hosts data on deep-marine siliciclastic depositional systems, recording their architectural properties and facies characteristics with consideration of spatial and hierarchical organisation. A summary of the geological entities considered in DMAKS, along with the type of data stored in these tables, is presented in Fig. 4.1. DMAKS allows digitisation of both the sedimentary architecture of ancient successions and the geomorphological organisation of modern environments. These data are coded as entries within tables organized in a relational schema implemented in a MySQL database management system. Annex 1 presents an entity-relationship diagram outlining the relationships shared between the database tables, as well as lists the attributes each table contains. These data are derived from peer-reviewed publications and also unpublished sources (theses, original field studies), and are coded in a consistent manner through adoption of a database standard that outlines definitions of database entities and data-entry workflows. The database schema has been developed to try and minimise confusion set by the plethora of terminology that exists in the study of deep-marine clastics. For this reason and to facilitate deep-marine interrogation between empirical based information, the characterisation of geological entities in the database relies where possible upon observation-based attributes (e.g., dimensions, palaeoflow, gradient, sinuosity wavelength etc.). Some commonly used and well-cited descriptive schemes (e.g., Wentworth's sand grain size classification; Reading & Richards, 1994, popular system feeder type scheme; or Ingersoll's 2012 basin type classification) are also included. Where the characterisation of geological units is based on interpretative classes (e.g., in the classification of element type sub-environments; see Section 4.2.1.1) these 'interpretation-based' attributes are quality controlled (see description of 'DQI' in Section 4.2.2). This methodology aims to make data entry a consistent and repeatable process, limiting the opportunity for individual investigation's preferences or an inputter's personal bias.

DMAKS accounts for geological entities at different scales of observation (e.g., from lithofacies to stratigraphic intervals), which are commonly investigated through different approaches (e.g., facies and architectural analysis of outcropping successions or bathymetric surveying of modern sea floors). Annexes 2 to 5 demonstrate how data is extracted from these different data types and input into the DMAKS database via the assignment of unique identifiers for each geological unit. Regardless of the source-works method of data collection, data is systematically input into DMAKS via the recognition of individual geological entities.

Fig. 4.1. *(overleaf)* Conceptual model showing the geological units (systems, basins, elements, beds and facies) stored in DMAKS. The depositional fairway extending from the shelf-break to most distal reaches denotes a System, while the Basin table, characterises a topographic low favourable for deposition; some environmental attributes have been depicted (see Annex 1 for a complete list of System and Basin table attributes). Sedimentary bodies, geomorphic surfaces or mixed architectures at multiple scales are digitised in the Element table. Hypothetical example Element data is shown in parts d) and e) demonstrating how hierarchical organisation can be captured via parent element identifiers (parent_el_ID) and highest hierarchical unit (highest_level) notation. Down-dip (downstream) transitions between adjacent 'channel' elements are digitised in the Channel Networks table, exemplified in part b); other spatial relationships (along strike, and vertical) are digitised in the Element transition table, part c). The Facies table characterises the deep-marine lithofacies (distinguished by changes in texture, grain size, grading, sedimentary structures, palaeoflow and bedding surfaces). Associated bed units are captured in the Facies table, see example Facies table in part g) where correlations between beds are also noted (lb_correlation attribute). Vertical transitions between facies are also tracked in the Facies table via 1D data ordering (1D_data_order). For more information on how entities are digitised see appropriate sections in Section 4.2.1. No scale intended.

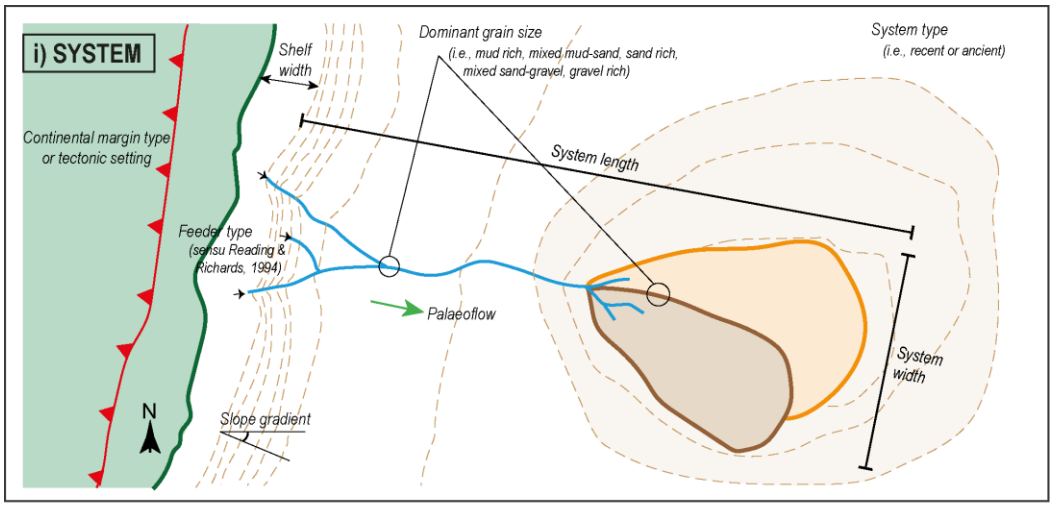

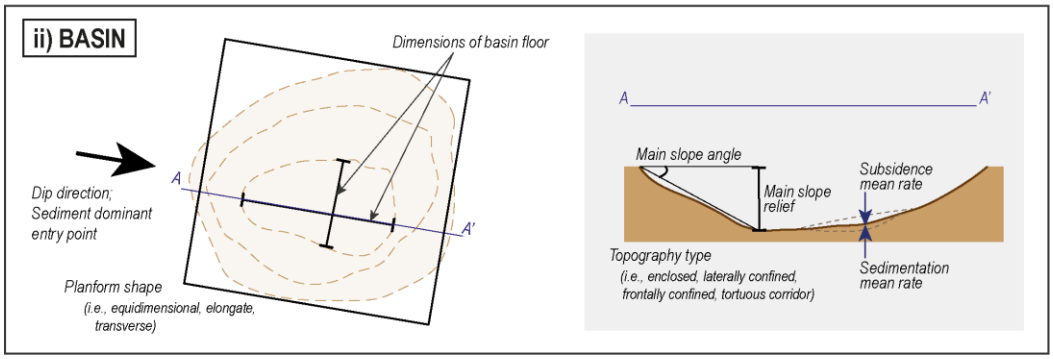

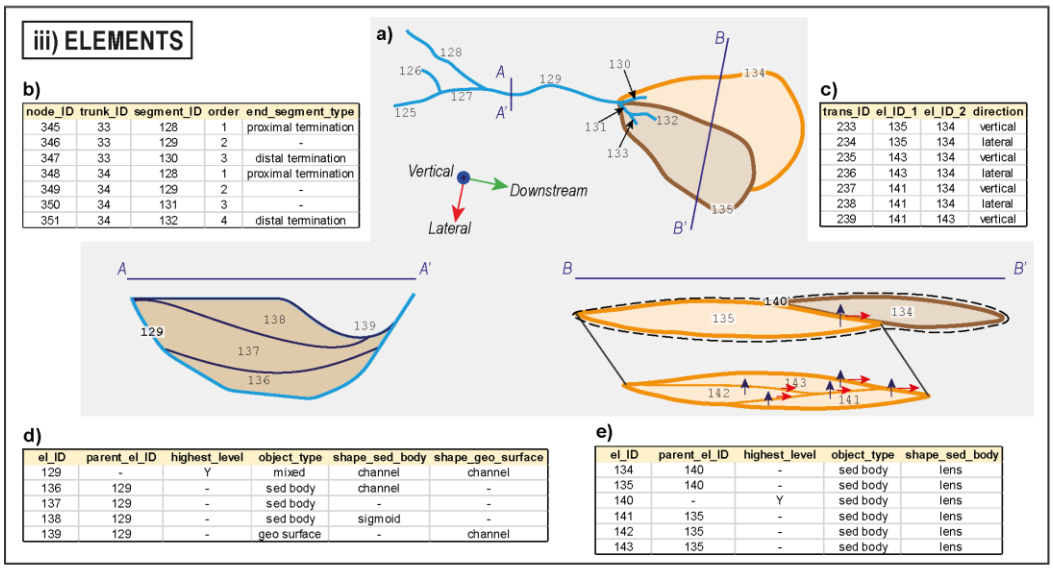

b)

node_ID	trunk_ID	segment_ID	order	end_segment_type
345	33	128	1	proximal termination
346	33	129	2	-
347	33	130	3	distal termination
348	34	128	1	proximal termination
349	34	129	2	-
350	34	131	3	-
351	34	132	4	distal termination

c)

trans_ID	el_ID_1	el_ID_2	direction
233	135	134	vertical
234	135	134	lateral
235	143	134	vertical
236	143	134	lateral
237	141	134	vertical
238	141	134	lateral
239	141	143	vertical

d)

el_ID	parent_el_ID	highest_level	object_type	shape_sed_body	shape_geo_surface
129	-	Y	mixed	channel	channel
136	129	-	sed body	channel	-
137	129	-	sed body	-	-
138	129	-	sed body	sigmoid	-
139	129	-	geo surface	-	channel

e)

el_ID	parent_el_ID	highest_level	object_type	shape_sed_body
134	140	-	sed body	lens
135	140	-	sed body	lens
140	-	Y	sed body	lens
141	135	-	sed body	lens
142	135	-	sed body	lens
143	135	-	sed body	lens

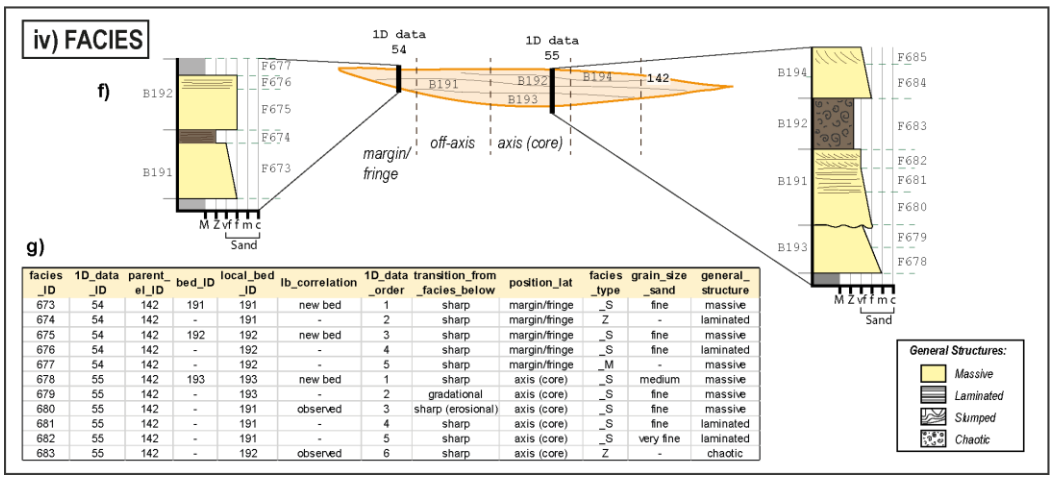

g)

facies_ID	1D_data_ID	parent_el_ID	bed_ID	local_bed_ID	lb_correlation	1D_data_order	transition_from_facies_below	position_lat	facies_type	grain_size_sand	general_structure
673	54	142	191	191	new bed	1	sharp	margin/fringe	_S	fine	massive
674	54	142	-	191	-	2	sharp	margin/fringe	Z	-	laminated
675	54	142	192	192	new bed	3	sharp	margin/fringe	_S	fine	massive
676	54	142	-	192	-	4	sharp	margin/fringe	_S	fine	laminated
677	54	142	-	192	-	5	sharp	margin/fringe	_M	-	massive
678	55	142	193	193	new bed	1	sharp	axis (core)	_S	medium	massive
679	55	142	-	193	-	2	gradational	axis (core)	_S	fine	massive
680	55	142	-	191	observed	3	sharp (erosional)	axis (core)	_S	fine	massive
681	55	142	-	191	-	4	sharp	axis (core)	_S	fine	laminated
682	55	142	-	191	-	5	sharp	axis (core)	_S	very fine	laminated
683	55	142	-	192	observed	6	sharp	axis (core)	Z	-	chaotic

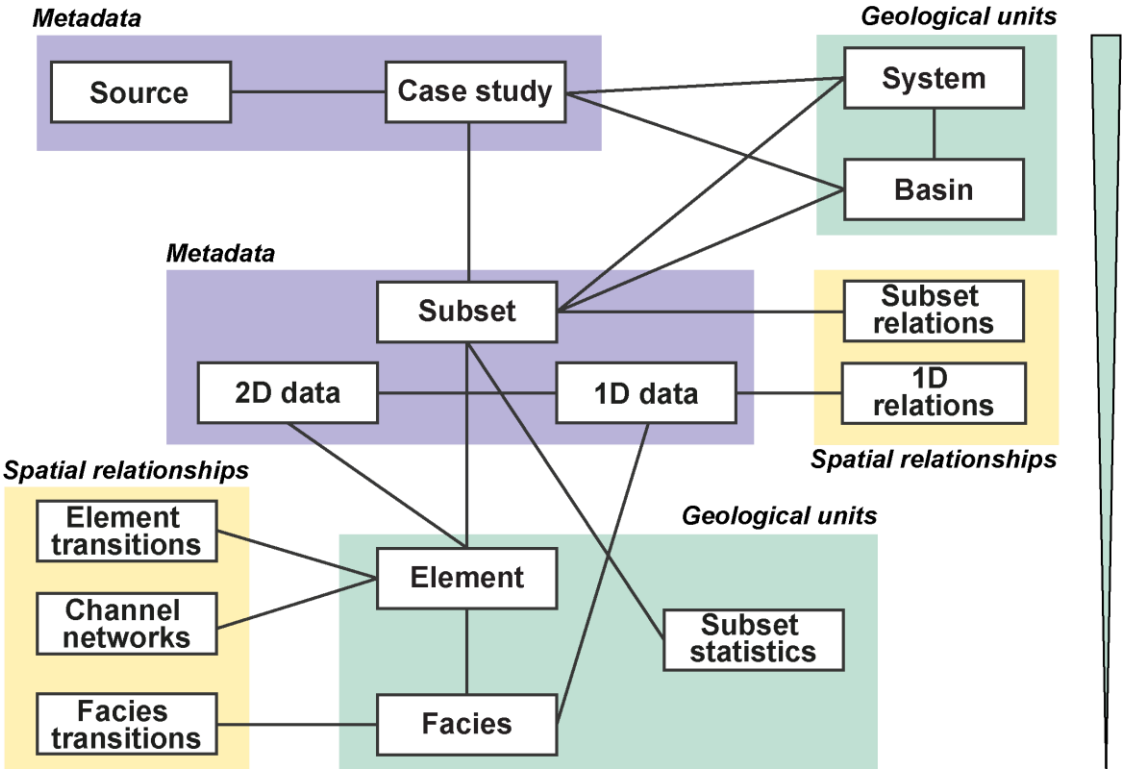

Fig. 4.2. Simplified representation of the relational schema of DMAKS, showing tables (boxes) and their relationships (connecting lines). For simplicity, look-up tables are not included. The type of data these tables characterise (i.e., geological units, spatial relationships or metadata) are labelled in italics and colour coded. Geological units are arranged in order of descending size. See Annex 1 for a comprehensive list of each table's attributes.

4.2.1 Database entities and their relationships

DMAKS currently hosts 18 tables, some of which act as look-up tables for attribute classification. Collectively, these tables store:

i) data on geological units (i.e., sedimentary packages and geomorphological surfaces), see Fig. 4.1;

ii) data on spatial relationships between units, in the form of spatial transitions between geological entities of a given type in three dimensions;

iii) associated metadata (e.g., original data types, descriptors of data quality).

Each table contains entries representing multiple instances of a particular type of entity. For example, the 'Element' table digitises multiple architectural bodies or geomorphic surfaces, characterised by many attributes. Each entry in a table is given a unique numerical identifier, known as a 'primary key', which can be used to link the same entries in other tables as 'foreign keys'. A graphical summary of the tables and their relationships is presented in Fig. 4.2, while Annex 1 provides a comprehensive list of all the tables attributes, including the

primary and foreign key notation. The sample data entry tables presented in the worked examples of Annexes 2 to 5 also demonstrate the value of these unique numerical identifiers in allowing geological entities to be traced, along with their hierarchical and spatial relationships. The database structure facilitates data entry from the largest deep-marine entity to the smallest, as relationships between the database tables allow unique identifiers of the higher geological units to cascade down and be affiliated with the smaller, contained units.

Data are organised in 'Case studies'. A case study can refer to a system, or to a portion thereof, which has been the subject of study by a group of authors, or by more than a group if the studies were intended to be complementary. Alternatively, a case study might include data from multiple deep-marine systems, if such data cannot be unravelled and related to single system entries.

Case studies that include data from one sedimentary system are linked to an entry in the 'System' table. In DMAKS, a deep-marine 'system' is defined so as to span sedimentary fairways extending from the slope-break to the most distal point of gravity-flow deposition (see Fig. 4.1). This definition is applied flexibly, in view of the possible need to capture features for which this definition may not apply (e.g., bottom-current deposits); multiple fairways that terminate in the same receiving basin (i.e., topographic depression) are also classified as a single system, e.g., the Santa Monica basin deposits (Normark et al., 2009). In systems that possess a geomorphological expression on the present-day seafloor, active fairways can be readily recognised (e.g., the Zaire fan, Congo-Angola margin; Babonneau et al., 2002). In ancient successions, because of the difficulty in discerning individual fairways, systems generally reflect lithostratigraphic or informal divisions that are commonly accepted in the published literature. DMAKS stores data on the dimensions of a system, its geographic position (and palaeo-position, if applicable), as well as attributes that describe external controls and the geological context (e.g., tectonic setting, source area, shelf width, dominant grain size, feeder type); see Annex 1 for a detailed list of System attributes.

A case study can be divided into a number of 'Subset' entries. A subset is a set of data that might represent a stratigraphic or planform window or a part of a case study that can be distinguished on the basis of the information it provides. These entries are used to capture the variability in the geological attributes on which a system can be classified and the suitability of the data in a case study. A different subset may be assigned to reflect geographic or stratigraphic subdivisions (e.g., attribution to slope, ramp, or basin-plain settings; see example in Annex 3), variation in attributes that describe external controls,

changes in data type, as well as variability in the suitability of the data for certain types of analyses (e.g., for deriving output on unit dimensions, proportions or transition statistics). Ultimately, subsets aid database interrogation. A subset can be linked to data on geological entities directly, or via additional tables ('2D data' and '1D data' tables) containing specific metadata when the data are sourced from a 2D or 1D dataset (e.g., cross-sections or logs); see example in Annex 5.

Information on sedimentary basins, smaller sub-basins and individual depocentres is also stored in DMAKS. Attributes include tectonic setting, mechanisms of formation, and geological evolution (e.g., subsidence rates, basin type according to the classification of Ingersoll, 2012) and basin physiography (e.g., basin dimensions, slope gradient, topographic confinement), see Annex 1 for an exhaustive list of Basin attributes. Through time, different systems might accumulate into the same sedimentary basin (e.g., the Cerro Toro and Tres Pasos Formations into the Magallanes Basin, Romans et al., 2011). However, each 'Basin' record is created to allow description of the characteristics of the receiving basin during the lifetime of a specific system (see Table 4.1). In DMAKS, a system may be associated with a number of basins, in cases where the system accumulates over sub-basins consisting of multiple coalescing topographic depressions or depocentres (e.g., the Brazos-Trinity in the Gulf of Mexico, Prather et al., 2012). Parent-child relationships between basins, sub-basins and depocentres can be recorded in the 'Basin' table.

Currently, DMAKS stores 40 case studies from 29 systems, and 3 multi-system case studies (Table 4.1, Fig 4.3).

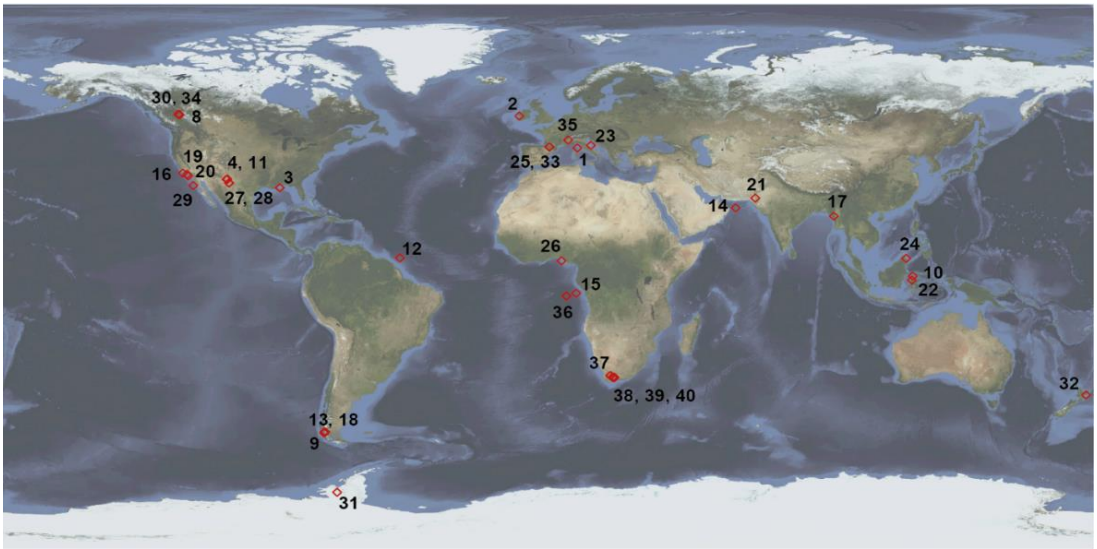

Fig. 4.3. Map showing the locality of the 40 case studies which relate to a single system, currently included in DMAKS. Numbers correspond to identifiers in Table 4.1. Image from Stöckli et al. (2005).

	Case study	System	Basin	Literature
1	Late Pleistocene deposits offshore East Corsica, Golo Turbidite System	Golo Turbidite System	Golo Basin	Pichevin et al., 2003; Gervais et al., 2006(a; b); Deptuck et al., 2008; Prélat et al., 2010; Sømme et al., 2011
2	Ross Sandstone at Loop Head Peninsula and Ballybunnion, Ross Formation	Ross Sandstone Submarine Fan System	Shannon Basin	Pyles 2007; MacDonald et al., 2011(b)
3	Channel-levee system in the DeSoto canyon, NE Gulf of Mexico, Joshua System	Joshua Channel System	-	Posamentier, 2003
4	Channel Complex, Popo Fault Block, Brushy Canyon Formation	Brushy Canyon	Delaware Basin	Beaubouef et al., 1999; Gardner & Borer, 2000; Gardner et al., 2003; Beaubouef et al., 2007; O'Byrne et al., 2007(a)
5	Channel dimensions based upon data type taken from McHargue et al., 2011(a)	-	-	McHargue et al., 2011(a)
6	Channel gradients, continental slope of the Niger Delta taken from McHargue et al., 2011	-	-	McHargue et al., 2011(a); McHargue et al., 2011(b)
7	Channel element thickness based upon gradient taken from McHargue et al., 2011(b)	-	-	McHargue et al., 2011(b)
8	Isaac Unit 5, Castle Creek area, Isaac Formation	Isaac Formation	-	Arnott, 2007(a; b); Arnott & Ross., 2007; Barton et al., 2007(a); Navarro et al., 2007(a; b); O'Byrne et al., 2007(b); Ross & Arnott, 2007; Schwarz & Arnott, 2007; Khan & Arnott, 2011
9	Turbiditic sandstones in the Sierra Contreras, Tres Pasos Formation	Tres Pasos Deep-Water Slope System	Magallanes Basin	Barton et al., 2007(b; c); Armitage et al., 2009; Romans et al., 2011
10	Pleistocene basin-floor offshore E Kalimantan, Kutai Turbidite System	Kutai Pleistocene System	Kutai Basin	Saller et al., 2004; Saller et al., 2008; Sugiaman et al., 2007; Prélat et al., 2010
11	Basin-floor deposits at Willow Mountain, Bell Canyon Formation	Bell Canyon Turbidite System	Delaware Basin	Barton & Dutton, 2007
12	Quaternary Amazon Fan offshore N Brazil, Amazon Turbidite System	Amazon Turbidite System	-	Flood et al., 1991; Piper & Normark, 2001; Jegou et al., 2008

13	Channel-levee deposits Lago Nordenskjold and Laguna Mellizas Sur, Cerro Toro Formation	Cerro Toro Deep-Water System	Magallanes Basin	Bouma, 1982; Barton et al., 2007(b; c)
14	Turbidite lobe architecture from the Oman margin, Al Batha Turbidite System	Al Batha Turbidite System	-	Bourget et al., 2010
15	Modern Deep Sea Fan, offshore Congo-Angola margin, Zaire Turbidite System	Zaire Fan	-	Babonneau et al., 2002; Droz et al., 2003; Marsset et al., 2009; Babonneau et al., 2010
16	Submarine canyons and fans offshore California, Santa Monica Basin	Santa Monica	Santa Monica Basin	Normark et al., 1998; Piper et al., 1999; Piper & Normark, 2001; Normark et al., 2009
17	G-series turbiditic sandstones in the NE Bay of Bengal, Shwe Fan	Bengal Fan	-	Barnes & Normark, 1985; Pickering et al., 1989; Yang & Kim, 2014
18	Condor Channel Belt in the Parque Nacional Torres del Paine, Cerro Toro Formation	Cerro Toro Deep-Water System	Magallanes Basin	Bouma, 1982; Barton et al., 2007(b; c)
19	Black's Beach channel system, La Jolla, California, Scripps & Ardath Formations	Black's Beach	San Diego Basin	May & Warme, 2007; Stright et al., 2014
20	San Clemente slope channel system, California, Capistrano Formation	Capistrano Formation	Capistrano Embayment	Li et al., 2016
21	Channel complexes, Drabber Dhora, Pakistan, Pab Formation	Lower Pab Turbidite System	Pab basin	Eschard et al., 2004; Euzen et al., 2007(a; b); Albuoy et al., 2007
22	Gendalo 1020 Fan, offshore Kalimantan, Miocene System	Gendalo Field	Kutai Basin	Sugiaman et al., 2007; Saller et al., 2008
23	Pleistocene submarine canyon fill, eastern central Italy, Monte Ascensione system	Monte Ascensione system	Peri-Adriatic Basin	Di Celma et al., 2014
24	Outcrop 5 levee-channel turbidites, Papar Highway NW Borneo, West Crocker Formation	West Crocker Fan System	Northwest Sabah Basin	Crevello et al., 2007(a; b; c); Hall, 2013
25	Morillo 1 member channel systems, Ainsa, Morillo Formation	Morillo Turbidite Sub-System	Ainsa Basin	Moody, 2010; Moody et al., 2012; Bayliss & Pickering, 2015(a)
26	Pleistocene canyons, NW Niger Delta, Benin major & Benin minor systems	Continental slope NW Niger Delta	-	Damuth, 1994; Deptuck et al., 2007; Olabode & Adekoya, 2008; Deptuck

				et al., 2012; Hansen et al., 2017(a)
27	Beacon Channel Complex, Delaware Mountains, Brushy Canyon Formation (data from Beaubouef)	Brushy Canyon	Delaware Basin	Beaubouef et al., 1999; Gardner & Borer, 2000; Gardner et al., 2003; O' Byrne et al., 2007(a); Beaubouef et al., 2007
28	Beacon Channel Complex, Delaware Mountains, Brushy Canyon Formation (data from Pyles)			Beaubouef et al., 1999; Gardner & Borer, 2000; Gardner et al., 2003; O' Byrne et al., 2007(a); Pyles et al., 2010
29	Slope channel system, San Fernado, Mexico, Rosario Formation	San Fernando Turbidite System	San Quintin Sub-basin	Morris & Busby Spera, 1988; Morris & Busby Spera, 1990; Dykstra & Kneller, 2007; Kane et al., 2007; Kane et al., 2009; Kane & Hodgson, 2011; Callow et al., 2013(a; b); McArthur et al., 2016; Hansen et al., 2017(b); Li et al., 2018
30	Isaac channel 3, Castle Creek area, Isaac Formation	Isaac Formation	-	Arnott, 2007(a; b); Arnott & Ross., 2007; Barton et al., 2007(a); Navarro et al., 2007(a; b); O'Byrne et al., 2007(b); Ross & Arnott, 2007; Schwarz & Arnott, 2007; Khan & Arnott, 2011
31	Channel-levee complexes, Antarctica, Himalia Ridge Formation	Himalia Ridge Formation Turbidite System	Fossil Bluff Group Basin	Butterworth et al., 1988; MacDonald et al., 1995; Miller & MacDonald, 2004; Butterworth & MacDonald, 2007; Riley et al., 2012
32	Deep-water clastic succession, Taranaki, Urenui Formation	Late Miocene North Taranaki	Taranaki Basin	King & Trasher, 1992; King et al., 1994; King et al., 1996; Arnot et al., 2007(a; b); Browne et al., 2000; Browne et al., 2005; Browne et al., 2007(a; b); King et al., 2007(a; b; c); King et al.,2011; Rotzien et al., 2014; Masalimova et al., 2016
33	Ainsa-1 & Ainsa-2 channel complexes, Huesca, San Vincente Formation	Ainsa Turbidite System	Ainsa Basin	Arbues et al., 2007; Falivene et al., 2010; Pickering & Cantalejo, 2015; Pickering et al., 2015; Scotchman et al., 2015

34	Isaac channel complex 2, S Castle Creek area, Isaac Formation	Isaac Formation	-	Arnott, 2007(a; b); Arnott & Ross., 2007; Barton et al., 2007(a); Navarro et al., 2007(a; b); O'Byrne et al., 2007(b); Ross & Arnott, 2007; Schwarz & Arnott, 2007; Khan & Arnott, 2011
35	Champsaur sandstones, Haute Alpes, Grès du Champsaur Formation	Grès du Champsaur Turbidite System	Western Champsaur Basin	Waibel, 1990; McCaffrey et al., 2002; Brunt, 2003; Brunt & McCaffrey, 2007; Brunt et al., 2007; Vinnels et al., 2010
36	Active channel-mouth lobe complex, Congo-Angola margin, Zaire turbidite system	Zaire Fan	-	Droz et al., 2003; Marsset et al., 2009; Dennielou et al., 2017
37	Tanqua Karoo basin floor fan complex (studied by Prélat et al., 2009)	Tanqua Karoo Turbidite System	Tanqua depocentre	Goldhammer et al., 2000; Hodgson et al., 2006; Bouma et al., 2007; Bouma & Delery, 2007; Prélat et al., 2009; Prélat et al., 2010; Kane et al., 2017
38	Unit A proximal basin floor system, Laingsburg Formation	Laingsburg Karoo Turbidite System	Laingsburg depocentre	Sixsmith et al., 2004; Fildani et al., 2007; King et al., 2009; Flint et al., 2011; Prélat & Hodgson, 2013; Hofstra et al., 2015; Spychala et al., 2017(b); Spychala et al., 2017(c)
39	Unit B & A/B interfan base-of-slope system, Laingsburg Formation			Grecula et al., 2003; Sixsmith et al., 2004; Pringle et al., 2010; Flint et al., 2011; Brunt et al., 2013; Hofstra, 2016
40	Unit C & B/C interfan lower-middle slope system, Fort Brown Formation			Grecula et al., 2003; Sixsmith et al., 2004; Pringle et al., 2010; Di Celma et al., 2011; Flint et al., 2011; Brunt et al., 2013; Morris, 2014; Morris et al., 2016

Table 4.1. Case studies currently stored in DMAKS and the original source works from which the data have been derived. Basin and system records (if applicable) are also shown. Numbering relates to the order of case study input in DMAKS.

4.2.1.1 Elements

An ‘element’ is a geological unit (sedimentary package or geomorphic surface) with a distinct architectural or geomorphological expression, which reflects a particular suite of processes occurring in a specific deep-marine sub-environment. Elements can be nested hierarchically (e.g., see the South Golo lobe shown in Annex 3). They are typically discerned in the original sedimentological studies by a combination of descriptive features: geometry, scale, internal facies (characterised in the ‘Facies’ table, see Section 4.2.1.2) and relationships with bounding surfaces (e.g., Mutti & Normark, 1987; Pickering et al., 1995; Gardner et al., 2003; Posamentier & Walker, 2006; Terlaky et al., 2016) – characteristics that form the basis of the ‘architectural-element analysis’ (cf. Miall, 1985).

Architectural units are commonly organised in a hierarchical manner and a variety of hierarchical classification schemes exist in the literature (see review in Cullis et al., 2018). To permit synthesis of different datasets, hierarchical relationships between elements in DMAKS are recorded either by: i) tracking parent-child element relationships, i.e., the containment of a lower-scale element within a higher-scale parent element, see examples in Fig. 4.1 parts d) and e); ii) tagging the highest-order elements (the largest element unit of a particular ‘general’ type, see below), see example in Fig. 4.1 parts d) and e), and iii) recording the hierarchical assignment made in the source work (see review in Cullis et al., 2018 of the range of approaches that exist); bespoke hierarchical classifications can also be accommodated - Appendix C outlines the current hierarchical classification used in DMAKS, developed based upon the findings of Cullis et al., 2018.

Different element ‘types’ can be categorised on their interpreted sub-environment of formation, with reliance on interpretations by the authors of the original studies. DMAKS categorises element types in a three-tiered hierarchical manner, as demonstrated in Fig. 4.4, based upon the available data and specificity in sub-environment attribution. Element types can be classified according to the following schemes based upon the detail of available information in the source work: -

i) element ‘depositional style’, based upon the unit being either a ‘cut (and fill)’ or ‘accretionary deposit’;
ii) ‘general element type’, an interpretative classification of element sub-environments that largely relies on observational (geometrical and geological) characteristics, applicable over a range of hierarchical scales; all classes are mutually exclusive (Table 4.2);

iii) ‘detailed element type’, a more specific, interpretational classification of depositional sub-environments; these classes are in some cases restricted to a particular hierarchical level; all classes are mutually exclusive (Table 4.3).

Element boundaries might be marked by bounding surfaces, or by gradational facies changes (e.g., as an outer-levee deposit interdigitates into background deposition). Channel elements are defined as segments of a channel network bounded by points of channel avulsion or branching (e.g., tributary or distributary channel bifurcation); additionally, channels can be split into multiple channel elements if a change is observed in the depositional style (e.g., a canyon passing downstream to an accretionary channel). Spatial relationships between elements are stored in the ‘Element transition’ or ‘Channel network’ tables (see Section 4.2.1.4 for detail), the latter is only applicable to dip transitions between channel elements. Elements are stored in DMAKS as ‘sedimentary bodies’, ‘geomorphic surfaces’ or ‘mixed’ units (e.g., a parent unit which contains both sedimentary body and geomorphic surface components), see example in Fig. 4.1 part d). Elements are characterised by many attributes, e.g., their 3D geometry, sinuosity, palaeoflow, gradient, age (absolute and relative), style of stacking of internal units, net-to-gross ratio; Annex 1 contains a comprehensive list of attributes.

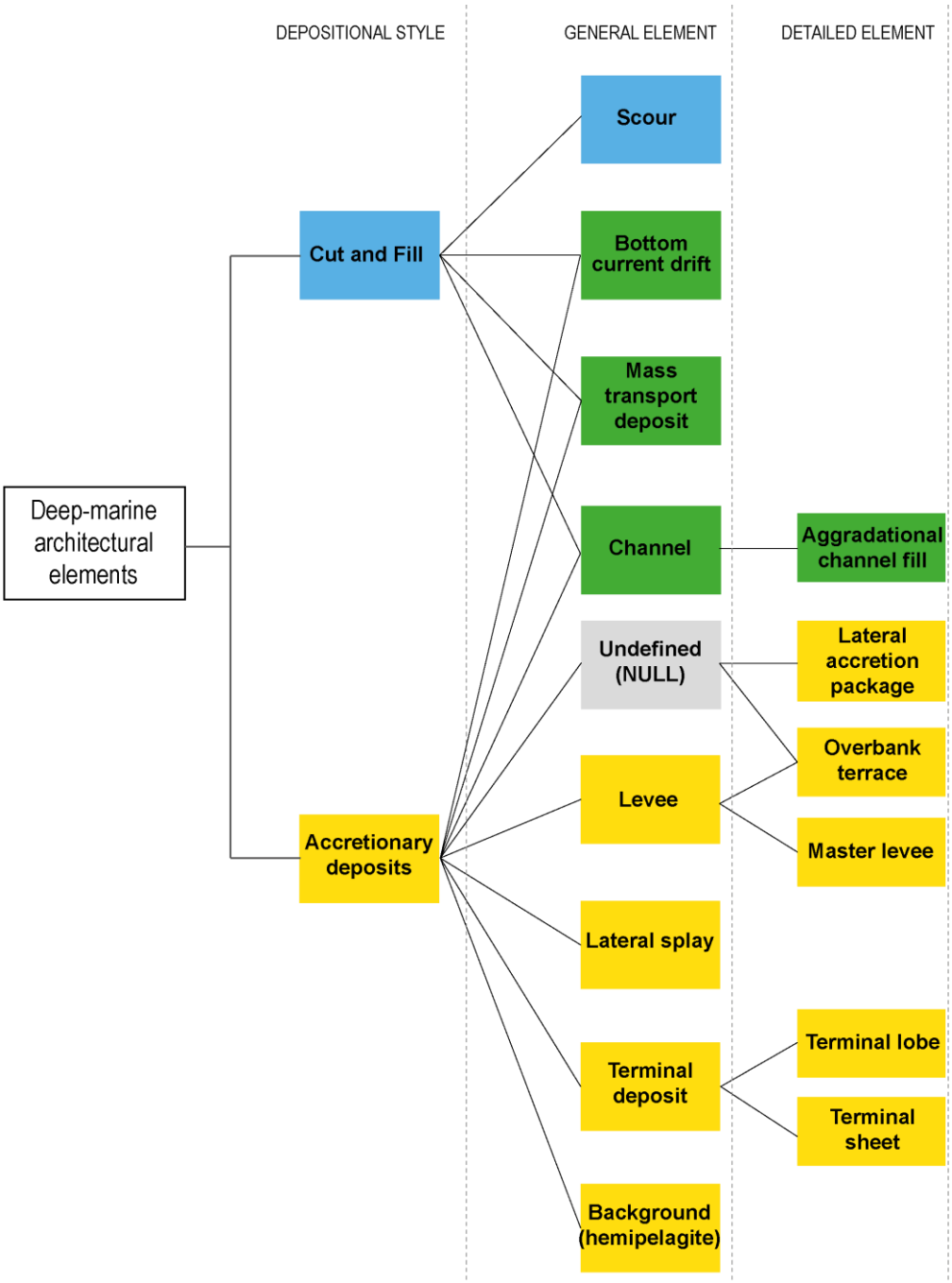

Fig. 4.4. Element type classification tree showing how element type classifications are dependent upon one another, for instance the 'depositional style' attribute constrains the 'general element type' classifier that can be chosen, likewise constraining the 'detailed element type' classifier. This three-tiered naming process therefore acts to quality control element data entry and classification, as element dependency relationships (lines between classifiers) must be obeyed.

General	Description
Channel	An elongate element with negative relief (modern form) or concave-up basal surface (deposit), often observed as the primary pathway of sediment transport in a deep-marine system.
Levee	An aggradational sediment wedge found adjacent to a genetically-related channel. The overbank element forms as sediment-laden flows over-spill their confined sediment pathways.
Scour	Erosional element with negative relief (modern form), or concave-up basal surface (deposit), usually displaying a semi-ellipsoidal ('scoop') cross-section, often interpreted as the result of rapid flow expansion or hydraulic jumps.
Lateral splay	An aggradational element formed as sediment-laden channelised flows overtop or breach their banks. This aggradational element can display a lobate or fan-shaped plan-view geometry, expressing a flow direction transverse to the associated confined flow.
Terminal deposit	A depositional body that can display a lens, mounded or sheet 3D geometry. A terminal deposit is found at the terminus of a genetically-related channel architecture.
Mass-transport deposit	An element bound by unconformable surfaces and constituted by remobilised sediments.
Background	A laterally widespread accretionary element composed of very fine grained (clay to silt) sediments from hemipelagic and pelagic fallout.

Table 4.2. General element type descriptions employed in DMAKS. A scale-independent nomenclature reflecting different sub-environments of deep-marine deposition based upon geometrical and geological (e.g., nature of contacts and facies associations) characteristics. Element types are mutually exclusive; new types can be added to meet available data.

Detailed	Description
Aggradational channel fill	A 'channel' element that records vertical accretion (aggradation), with no significant lateral shift in the 'axial' part of the deposit.
Lateral-accretion package	Sediment organised in packages that dip towards the axis of a genetically related channel. They are interpreted as the depositional product of the finite lateral migration of a channel.
Master levee	A 'levee' element which provides lateral confinement to a channel and is not itself contained within a larger channel.
Overbank terrace	A 'levee' element that is contained within a larger-scale channel-form, in some cases bounded by master levees.
Terminal lobe	A lobate or fan shaped plan-view 'terminal deposit' geometry. They are composed of multiple facies assemblages that display vertical offset in their stacking, typically in a compensational manner.

Table 4.3. Detailed element type descriptions used in DMAKS. All elements are mutually exclusive and the list can be expanded to account for new available data and interpretations. This nomenclature builds upon the 'general element types' (Table 4.2), using process interpretations to inform depositional deep-marine sub-environments.

4.2.1.2 Facies and beds

The ‘Facies’ table records the lithological and textural characters of lithofacies or 'facies', the smallest units characterised in the database; each facies unit is contained in a single element. Facies are distinguished where a change is observed in lithology (texture and grain size), grading style, sedimentary or biological structures, palaeoflow direction, or across hiatal surfaces and element boundaries. Each facies record can be tagged as being part of a bed unit, allowing information on ‘beds’ to also be stored in the Facies table, see example in Fig 4.1 part f) and g) or Annex 5b. A bed is defined as a layer of sedimentary rock bounded below and above by either accretionary or erosional bounding surfaces (*sensu* Campbell, 1967) and deposited by a single flow event, formed by either single- or multi-pulsed flows. The position of a facies within its parent element is recorded via lateral and dip position identifiers, see Section 4.2.2.2.

Facies attributes include the original facies codes, grain size, sorting, roundness and clast support type based upon common field notation (cf. Tucker et al., 2011). Grain-size is classified based upon the textural classes of Folk (1980). A textural class is assigned when measured or estimated grain-size distributions allow it. Percentages of grain-size classes based upon granulometric analyses can also be stored when known. The grain size of a sand/sandstone (‘S’ facies type) can be specified as very coarse to very fine (Wentworth, 1922). The mud, ‘M’, class of Folk’s textural classification (1980) can be further specified into silt/siltstone (‘Z’) or clay/claystone (‘C’) categories if possible. When the level of detail for Folk’s classes is not provided, facies types can be classified as generic sand/sandstones (_S), mud/mudstones (_M), and gravel/conglomerates (_G).

Sedimentary structures are characterised through a number of attributes. For instance, the general structure of a facies can be classified as ‘massive’, ‘laminated’, ‘slumped’ (when original bedding can be identified) or ‘chaotic’. Laminations can be further characterised on their type (planar parallel, non-planar parallel, ripple cross-lamination, cross-stratification, hummocky or wavy), deformation (convoluted, growth structures, flames or unspecified), and clarity (well-developed or faint). In addition, a facies entry can also record information relating to grading, palaeoflow direction, overprinting structures, presence of amalgamation surfaces, trace fossils, clast characteristics (e.g., type, density and orientation), absolute age and more. The dimensions of facies are also recorded. Annex 1 records an exhaustive list of attributes used to classify each Facies record.

Most commonly, facies and their vertical transitions are derived from a measured 1D section (e.g., core, a stratigraphic column or wire-line log). The vertical ordering of facies is thus stored in the Facies table together with information on the facies basal contact (e.g., contact type and geometry).

4.2.1.3 Aggregate data

In some cases, data are available in the form of statistical summaries that cannot be related to an individual element, bed or facies unit. These data, which describe a group of likewise classified genetic units, are stored in the 'Subset statistics' table. The table records descriptive statistics of unit dimensions, net-to-gross ratios, and transition statistics, linked to a specific subset. See Annex 1 for a comprehensive list of attributes digitised in this table.

4.2.1.4 Transitions and relationships

Three-dimensional spatial relationships between adjacent units are stored in DMAKS, as transitions. Transitions between elements are stored in the ‘Element transitions’ table, except channel-to-channel dip relationships which are stored separately in the ‘Channel networks’ table (see example data in Fig. 4.1 part b) and c) and Annex 2). Transitions between facies can be captured in the ‘Facies’ table in the form of vertical ordering or are stored in the ‘Facies transitions’ table (Annex 5b provides example data entry).

Each transition entry contains the unique identifiers for the two units in question (cf. Colombera et al., 2012(a); 2016), see the example data entry in Fig. 4.1 part c) and Fig. 4.5 part b). Transitions can be either vertical (younging), lateral (rightwards when facing downstream) or down-dip (downstream) of the system (Fig. 4.5). The style of contact across which elements and facies transition can also be documented (e.g., as sharp, sharp erosional, or gradational). Transitions stored in the facies table may also be classed as ‘artificial’ or ‘inferred’, the latter used when a transition is deduced instead of seen. An artificial contact is employed when a facies entry needs to be ‘split’ artificially, for example to map its occurrence at multiple lateral or dip positions in the same element. Classifiers are used to indicate the position where elements are seen to transition, based on the way elements are subdivided along dip and strike (e.g., axis to margin, proximal to distal; see Section 4.2.2.2). Transitions are stored between all adjacent objects, regardless of hierarchical significance.

The ‘Element transition’ table also accounts for the stacking style of elements, by recording their degree of vertical incision, as well as vertical and lateral offsets. The dip relationships between channel elements, stored in the ‘Channel network’ table, are used to track channel evolution, by recording avulsion nodes, bifurcation points, or confluences.

Spatial relationships between datasets are also digitised in DMAKS. For instance, the 'Subset relations' table records transitions between subsets of the same case study, whereas the '1D relations' table records the relative position of 1D datasets (see example data entry in Annex 5b).

a)

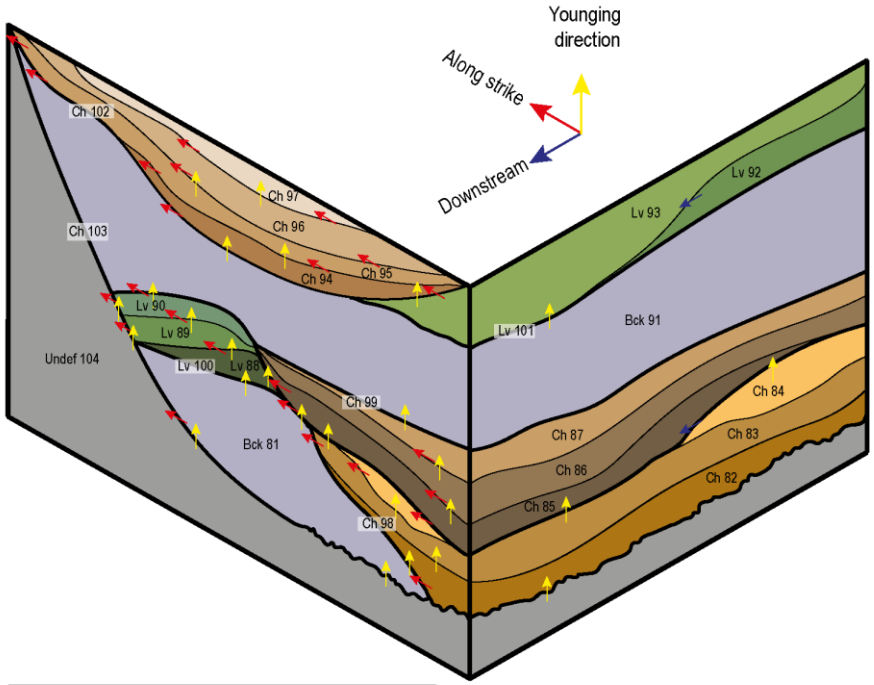

b)

trans_ID	el_ID_1	el_ID_2	direction	type
163	104	98	vertical	sharp (erosional)
164	98	99	dip	sharp
165	84	99	dip	sharp
166	98	85	dip	sharp
167	98	99	vertical	sharp
168	83	99	vertical	sharp
169	84	99	vertical	sharp
170	84	85	vertical	sharp
171	98	85	vertical	sharp
172	85	84	lateral	sharp

Fig. 4.5. Hypothetical example of how spatial relationships between adjacent elements across varying hierarchical boundaries are documented in the Element Transitions table, part b) showing example data entry. Element identifiers are used to reference these spatial relationships and the 'type' of boundaries shared between elements are documented.

4.2.2 Database-wide definitions and common attributes

DMAKS includes both quantitative (e.g., dimensions, sinuosity index) and qualitative data (e.g., basin type, element type). In order to allow comparative analysis, data standardisation is achieved by employing a consistent and repeatable process of data entry. Common attributes across different tables all use the same conventions and units of measure (see Section 4.2.2.1). Original source-work coding or naming conventions are also stored, allowing the data to be traced back to interpretations in the original source. Text-domain "note"

attributes are also included for every active table (excluding look-up tables, see Annex 1) to allow the inclusion of any additional information.

Metadata are employed throughout the database to record the quality of data stored. For instance, a 'data quality index' (DQI) attribute is used to rank the perceived data quality and reliability of interpretations (e.g., element-type classifications), using a three-tiered classification (from A, highest, to C, lowest quality; cf. Baas et al., 2005; Colombera et al., 2012(a); 2016). DQIs are used to rank the confidence with which attributes can be assigned, based on expert judgement. All attributes stored in DMAKS are presented in Annex 1.

4.2.2.1 Dimensions

Length, width and thickness are all taken with respect to a reference system orientated relative to the dominant local (palaeo-) flow direction, except for levee elements, whose dimensions are measured relative to (palaeo-) flow direction in their genetically related channel. Metadata characterising these measurements are also stored. For example, unit dimensions are classified on the type of measurement, as values may not represent the true maximum element width, length or thickness (see Fig. 4.6). Dimensions may be incomplete as a product of erosion or because of the spatial limits of the dataset (e.g., outcrop termination). The completeness of element dimensions can be classified as either true, apparent, partial or unlimited, *sensu* Geehan & Underwood (1993). A 'spatial type' attribute classifies the spatial constraints of the dataset from which the measurements have been taken (e.g., whether a 'true' value has been recorded from observations in 1D, 2D or 3D).

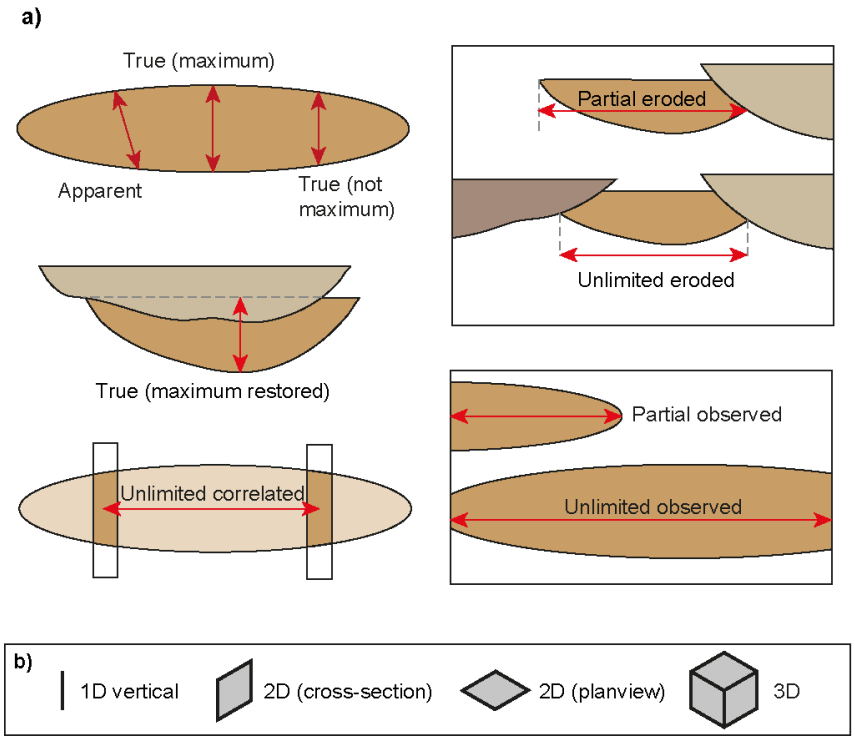

Fig. 4.6. Dimensional parameters used to characterise element dimensions with respect to a) type of measurements and b) spatial coverage offered by a dataset. The 'true restored' measurement type is only applicable to thicknesses, while the 'unlimited correlated' class is only applicable to width and length values.

4.2.2.2 Position classifiers

Position classifiers are used to record i) the position across which an element–to-element transition occurs (see example Element Transition tables and their lateral and dip position classifiers in Annex 2 and 3), and ii) the position of a facies within its parent element to account for lateral variations in facies architecture within elements. Intra-element divisions along strike and dip have therefore been established based upon geometrical rules (Fig. 4.7). An element is divided into 5 equal portions along its strike width, denoting margin/fringe, off-axis and axis(core) regions. Levee elements are divided into 3 portions based upon the position of their crest peak. The dip length of an element is divided into 3 equal portions, denoting proximal, medial and distal regions. Descriptions of the internal partition of elements based on criteria of facies organisation and as adopted in the source work can be additionally recorded in the 'Facies' table.

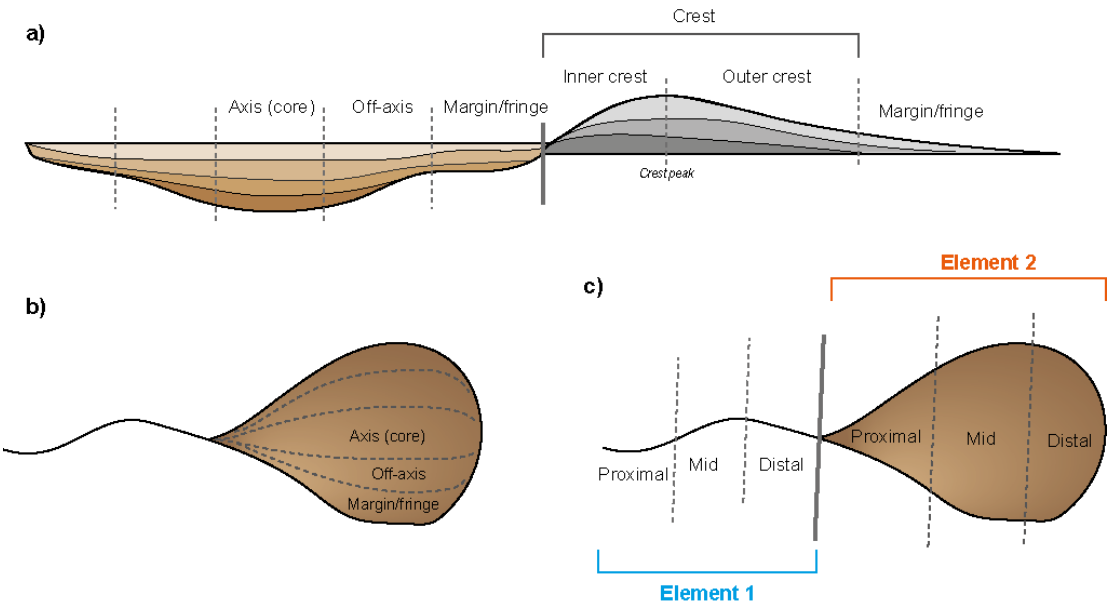

Fig. 4.7. Position classifiers applicable in the 'Facies', 'Facies transition' and 'Element transition' tables. Lateral intra-element divisions for a) channel, levee and b) terminal deposit architectures are shown. A general 'crest' classifier is used when the levee crest peak is unknown or unclear. The outer crest to margin/fringe boundary is defined as the half-distance between the crest peak and the elements outer termination point. Dip positions in a channel and terminal deposit are shown in part c).

4.3 Database applications

DMAKS is interrogated through Structured Query Language (SQL). Seven example applications are presented here, based upon quantitative outputs derived from the current database content (Table 4.1). These examples demonstrate some of the types of analyses that are feasible, and how these can be applied to further our understanding of deep-marine systems. Data upload is ongoing.

4.3.1 Quantification of element geometries

The ability to integrate data from seismic and outcrop enables dimensional data to be considered across multiple orders of magnitude, bridging the gap between studies conducted at different scales of observation and resolution. For example, Figs. 4.8 A and B show discrepancies between channel widths described in outcrop vs. seismic or bathymetric studies, which have mean widths of 746 and 1,120 m, respectively.

DMAKS output can be employed to assess trends between geometrical properties, leveraging a wide data pool. For instance, a 10:1 width-to-thickness aspect ratio (resulting in a constant linear relationship of y = 10x, where y is width and x is depth) is often cited to be typical for

submarine channel-forms and channel bodies, based upon the study conducted by Clark & Pickering (1996(b); Fig. 4.8 C). This result is based upon 50 measurements of channel and scour elements associated with a range of hierarchical scales. Weimer & Slatt (2007(b)) extended upon this proposed trend by suggesting that the channel aspect ratio changes in response to system gradient, resulting in a width-to-thickness ratio of 50:1 down-dip compared to the 10:1 relationship up-dip. Data collected by Konsoer et al. (2013) from 23 modern submarine channels suggests that width-to-depth approximates the 50:1 ratio, whereby channel width (y) varies with depth (x) following a relationship of $y = 47.4x^{0.94}$. However, these channel measurements are a mix taken from both slope and basin-plain environments (Fig. 4.8 C). DMAKS currently enables comparison of data from 196 channels of all hierarchical scales derived from multiple studies (Fig. 4.8 C). Based on DMAKS, a positive relationship between channel width and thickness (or depth, in the case of modern forms) is also identified ($r^2 = 0.50$, Pearson's coefficient = 0.91, p-value <0.001), but with a smaller exponent ($y = 73.7x^{0.61}$) in comparison to the previously proposed trends.

Outputs can be filtered on any boundary conditions, to test relationships between element geometries and possible predictors or controlling factors. For instance, channel elements from sand-rich systems are associated with thinner and narrower channel geometries (Fig. 4.8 C), supporting the role of controlling factors on which depositional models have been categorised by Reading & Richards (1994) and Normark & Piper (1991). Additionally, channel elements from sand-prone systems show a larger aspect ratio, on average, compared to channels from systems dominated by fine-grained deposits, challenging the findings of Delery & Bouma (2003).

Scatter is observed, over an order of magnitude, about the line of best fit (Fig. 4.8 C). The geometric variability of channels has been related to the variability that can be found in turbidite flow properties (Wynn et al., 2007; Konsoer et al., 2013; Jobe et al., 2016 and Qin et al., 2016). For example, high-aspect-ratio channel outliers identified in Fig. 4.8 C are typically associated with weakly confined environments (c.f. spill phases *sensu* Gardner et al., 2003, or distributary channels *sensu* Posamentier & Kolla, 2003). This association supports work by Brunt et al. (2013), suggesting that deep-marine channel geometry can be affected by the degree of flow confinement.

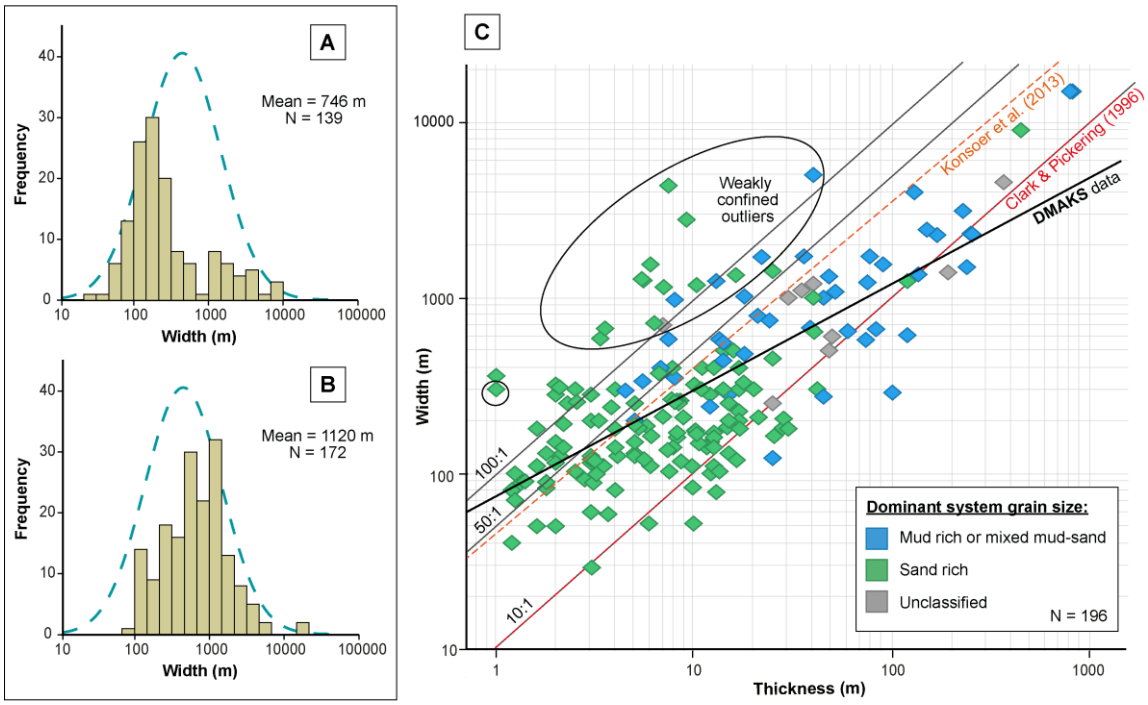

Fig. 4.8. A-B) Histograms of the measured width of channel elements based upon outcrop (A) and seismic and bathymetric data (B). A lognormal distribution curve fitted to a merge of both datasets is plotted in both graphs (dashed line; population mean = 953 m). Note the logarithmic scale and thus the positive skewness of the data. C) Width vs thickness (or depth, in the case of modern forms) of channel elements. The 10:1 width-to-thickness aspect ratio proposed by Clark & Pickering (1996(b); red) is plotted, as well as power-law regression lines for the DMAKS dataset (black), and the study by Konsoer et al. (2013; orange). Channels are classified by the dominant grain size for the system, as sand dominated (green), mud dominated or mixed (blue) or unclassified (grey). Outliers above roughly 100:1 are mostly channels documented as showing weak confinement in the original source-work. N = number of channel elements included in each plot. All measurements are true (maximum) values.

4.3.2 Comparisons of hierarchical organisation

The geological significance of deep-marine hierarchical relationships is not yet fully understood, and its comprehension is in part hindered by the inconsistent use of terminology (cf. Chapter 3; Cullis et al., 2018). The interpretational difficulties become evident when element dimensions are plotted against the terminology adopted in the original sources, as in Fig. 4.9, which demonstrates the size range observed in channel and lobate features sharing the same nominal architectural classification. A large spread in the element dimensions can be seen for each term, even when hierarchical parent-child relationships are considered, as terminology can be associated with multiple 'parent' hierarchical orders. Hierarchical

terminology reported in source works can therefore be seen to provide no consistent dimensional constraint to element dimensions.

Fig. 4.9. Channel-element thickness (A) and terminal-deposit width (B) 'true (maximum)' measurements classified by the original source-work terminology. The number of parent elements encapsulating an element is indicated, starting from a known highest-order element (zero).

Often, comparisons between units occurring in different deep-marine systems and associated with hierarchical categories involve re-assignment of reported hierarchical classifications to an alternative scheme (e.g., Sprague et al., 2005; Prélat et al. 2010; Straub & Pyles 2012). These comparisons are arguably largely subjective and inherently uncertain. DMAKS permits assessment of how the original terminology relates to nested parent-to-child relationships between elements, and how these hierarchical relationships are reflected in the relative size of the elements (e.g., Fig. 4.9). Scaling relationships between child and parent elements of

both channels and terminal deposits range between 1:1 and 10:1 (Fig. 4.10). Such information can improve our understanding of the hierarchical organisation of deep-marine systems and has the potential to help inform reservoir models.

DMAKS enables comparisons between architectural elements to be undertaken in a consistent manner, by querying on any combination of empirical attributes, related for example to scale, stratal trends, bounding-surface relationships (Figs. 4.9 and 4.10), or facies and architectural characteristics associated with a particular sub-environment. Therefore, DMAKS can be used to make objective comparisons between case studies that use different terminologies or hierarchical definitions. This arguably results in more meaningful analyses of the organisation of sedimentary architecture in deep-marine clastics than what can typically be attempted on the basis of terminologies or the re-assignment of data to classification schemes.

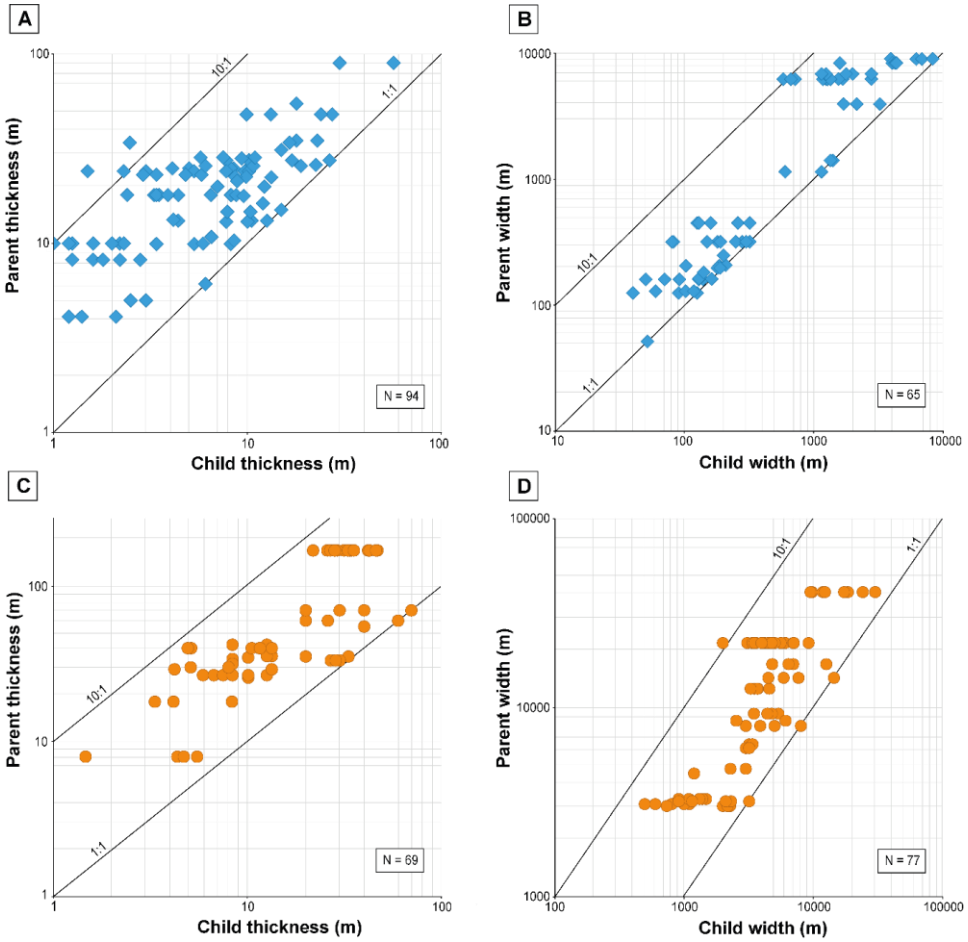

Fig. 4.10. Relationships between the geometry of 'child' elements and the geometry of the 'parent' elements in which they are contained, for channel elements (blue diamonds, A-B) and terminal deposits (orange circles, C-D). Data are plotted for element thickness (A, C) and width (B, D). Only true (maximum) measurements are considered.

4.3.3 Characterisation of architectural spatial arrangements

DMAKS allows spatial relationships between architectural units to be recorded in 3D, along the vertical, strike and dip directions. These data can be used to produce information on scaling relationships between co-genetic deposits. For example, Fig. 4.11 describes the scaling relationship between the width of channel elements and the width of genetically-related laterally adjacent levees. A positive relationship between master levees (i.e., a levee not contained in a larger channel body, see Table 4.3) and their adjacent channels is depicted (r^2 = 0.62), in agreement with the findings of Skene et al. (2002) and Nakajima & Kneller (2013). Filtering the data by physiographic setting suggests that basin-plain environments are associated with wider master levees and channels compared to their slope counterparts, supporting the notion that shallower slopes result in wider master levees (Nakajima & Kneller 2013). These outputs can be utilised as predictive tools, for example for prediction of thin-bedded volumes and in reservoir modelling.

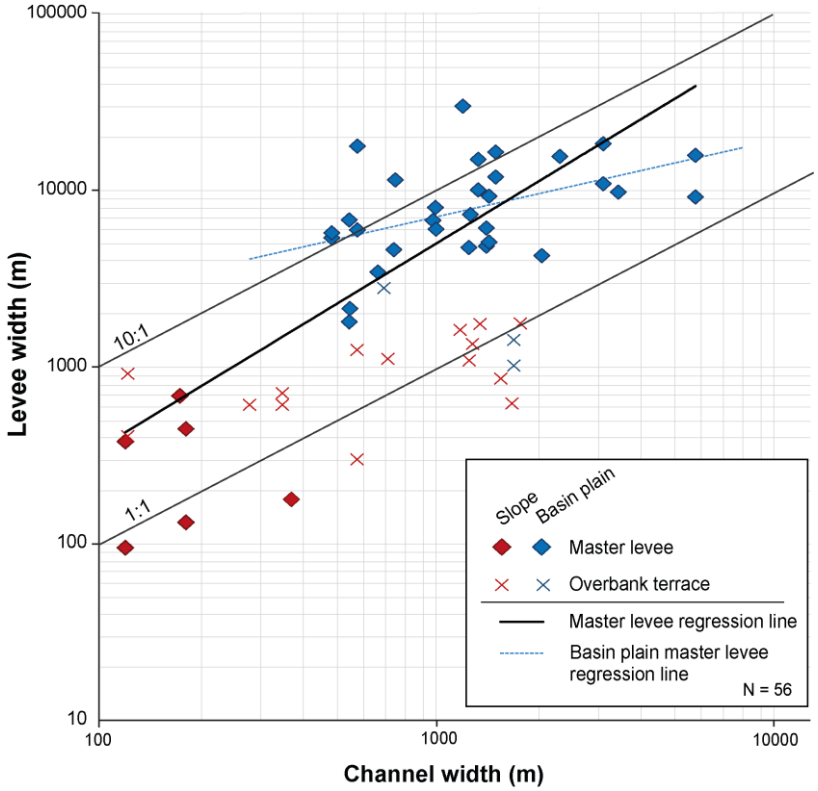

Fig. 4.11. Cross-plot of the width of channel elements and genetically-related laterally adjacent levees. Levees are further categorised as master levees or overbank terraces (see detailed element type descriptions, Table 4.3). Elements are classified by depositional setting (red: slope; blue: basin plain). All widths are 'true (maximum)' values. A power-law regression line associated with master levee-channel relationships is shown (bold black line; $y = 1.6x^{1.16}$), as well as a power law regression line for master levee-channel relationships located on the basin plain (blue dashed line; $y = 356.2x^{0.43}$, r^2 = 0.22).

Additionally, DMAKS can produce outputs that describe the likelihood of occurrence of a certain architectural element away from a known point, as in Fig. 4.12. Such outputs serve as predictive models that can be used to support conceptual models of the subsurface and guide reservoir-development planning, especially in data-poor situations.

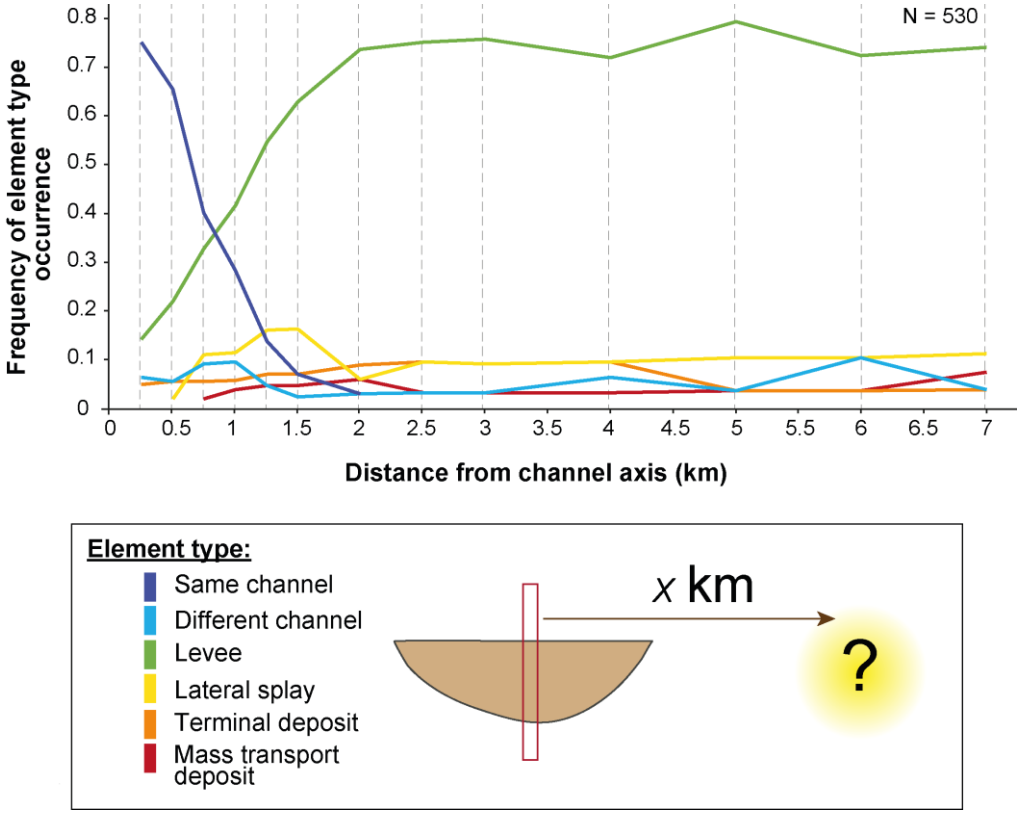

Fig. 4.12. Plot showing the frequency of different element-type occurrences as a function of the lateral (strike) distance away from the axis of a channel. The channel elements at the origin do not include modern channel forms and are not described in the source-work as a 'complex' or 'storey'. Lateral along-strike transitions (in both directions away from the channel axis) are counted between highest-order elements. N records the total number of element transitions. Grey dashed lines mark the distances at which frequencies were calculated.

4.3.4 Temporal variations in architecture

Geochronological dating of deep-marine deposits is usually limited with respect to sampling density and resolution, limiting the ability to constrain absolute ages of individual elements. However, the relative depositional age of deposits can often be inferred based upon geological principles of succession. Data on the relative timing of deposition are stored for elements in DMAKS, allowing derivation of outputs that describe how architectural attributes vary in a relative time frame. For example, Fig. 4.13 shows the change in lobate terminal deposit geometry in terms of length-to-width ratio over time for a number of different subsets. An oscillation through time between more elongate and more equant deposits can

be seen in some of the examples, e.g., the South Golo lobe and Kutai basin-plain fan, Fig. 4.13 A-B. Additional data might provide the basis for testing whether this apparent cyclicity is common in the architecture of turbidite lobes and sheets, and might elucidate whether this could reflect a form of autogenic organisation.

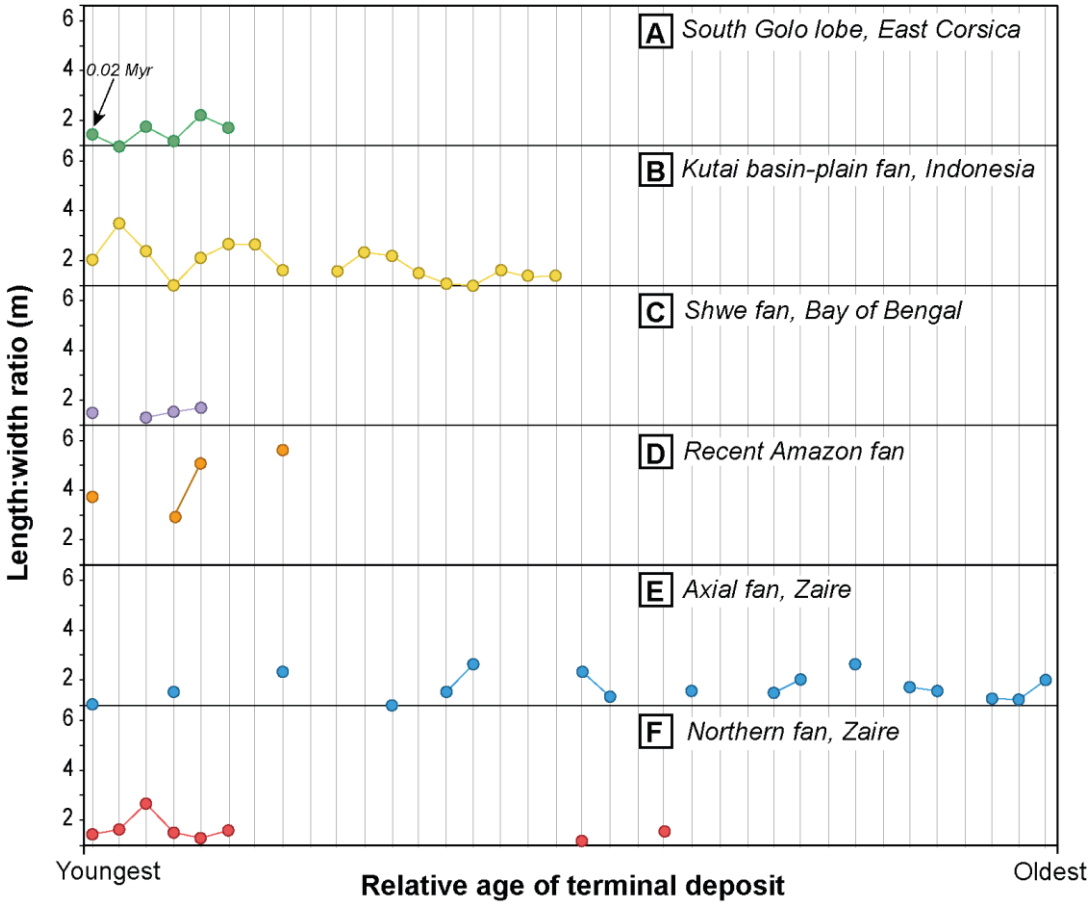

Fig. 4.13. Changes in lobate terminal deposit length-to-width ratios (vertical axes), over relative time scales (horizontal axis). Each box corresponds to a different subset, where terminal deposits are either i) contained in a larger parent terminal deposit (i.e., the South Golo fan, Kutai fan and Shwe fan) or ii) are the largest known lobate terminal deposits on the basin-floor in the entire fan (i.e., the Amazon and Zaire deposits). For each subset, the comparison only includes 'true' widths and lengths of deposits of the same hierarchical order. Each point reflects a terminal deposit; lines are broken where intervening deposits exist but suitable data on their dimensions are lacking. Total duration of deposition for each subset is typically over 10^4 yr timescales, except for the Zaire (10^5 yr); the time scale is unknown for the Shwe fan. Absolute age is shown for the youngest terminal deposit of the South Golo lobe (A).

4.3.5 Synthetic facies models

Synthetic facies models that account for the proportion of deposits of different types and for trends and distributions in lithologies can be built at a variety of geological scales, i.e., for

bed, element or depositional environments. Figure 4.14 shows the relative proportion of sedimentary structures found in the sandstone intervals of different element types. Output on the proportion of sedimentary units can be generated based on the synthesis of data from many elements, and with consideration of biases related to variations in size and representativeness of the available samples. For example, in Fig. 4.14 facies proportions are presented based on both (i) scaled averages that assign equal weight to each element to account for sampling biases (darker), and (ii) the total sum of their thickness (lighter).

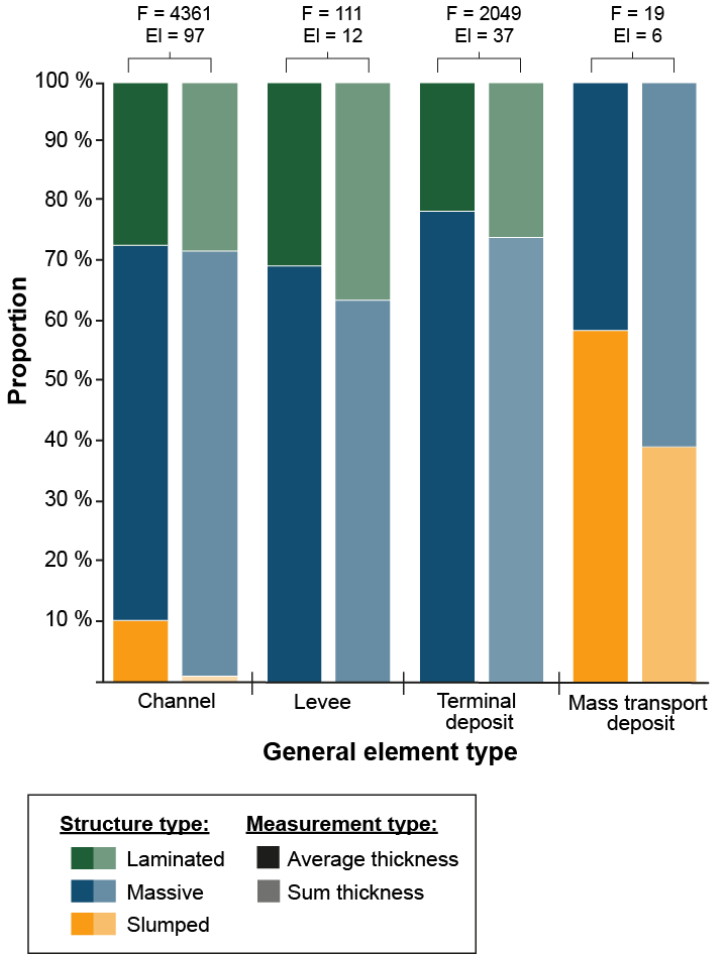

Fig. 4.14. Bar chart showing the different sedimentary structures found in sandstone intervals observed in different general element types (see Table 4.2 for element type descriptions). Two different proportional measures are shown: i) scaled averages of proportions, where each element is given an equal weight (darker bars) and ii) proportions based on the total sum of facies thickness in all elements (lighter bars). F = number of facies, El = number of elements.

Facies models can be tailored to specific environmental scenarios, e.g., system parameters, architectural or facies characteristics, bed relationships, or position in a sub-environment. For example, Fig. 4.15 compares the grain size and sedimentary structures of the sandstone intervals found in channel-related detailed element types (see Table 4.3) associated with

sandy systems. Similar proportional grain-size and sedimentary structure trends can be identified for both lateral accretion packages (LAPs) and aggradational channel fills. For example, over 50% of the classified facies units for both element types are 'massive'. LAPs are seen to contain a higher proportion of gravel, as well as of cross-stratification compared to aggradational channel fills (Fig. 4.15). This trend is also identified when considering only systems that include data for both LAPs and aggradational channel fills. In these systems, the total proportion of gravel is equal to 47% in LAPs (N = 1224 facies, 10 elements), compared to 36% in aggradational channel fills (N = 1061 facies, 30 elements), whereas the proportion of cross-stratified sands is equal to 17% in LAPs (N = 791 facies, 10 elements), compared to 6% (N= 547 facies, 23 elements). As new data is added to the database and the sample size is increased, further investigation can take place to verify the statistical significance of these results, as well as use them to analyse experimental or numerical process models. Quantified facies models of this type can also be used as 'synthetic analogues' for interpretations and predictions in subsurface studies.

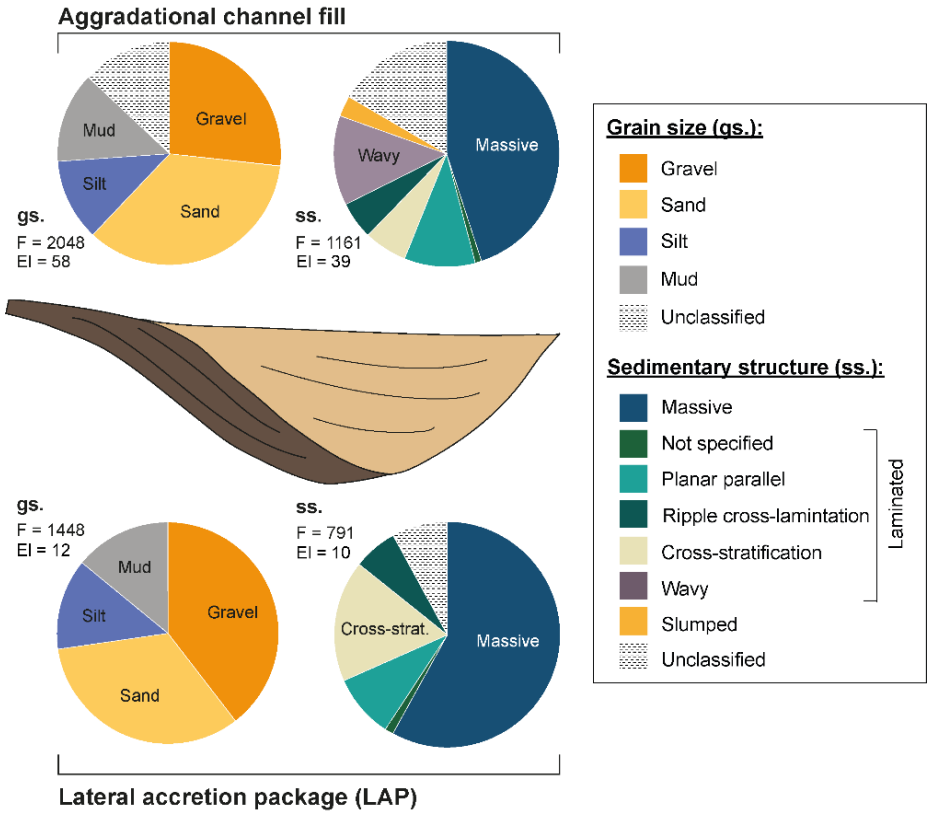

Fig. 4.15. Facies proportion models for deep-marine channel-related architecture. Scaled average proportions based on facies thicknesses are shown for grain size (gs.) and sedimentary structure, including lamination types, from sand/sandstone facies (ss.). Note that the drawing is for illustration only and it does not imply that the element proportions shown are based upon spatial relations. F = number of facies, El = number of elements.

4.3.6 Vertical organisation of facies

Quantitative descriptions of the vertical distribution of facies can be built using facies transitions and 1D facies ordering information stored in DMAKS. For instance, Fig. 4.16 shows high probability (>60%) for fining upwards grain size trends in sandstones and gravels in channel elements of sandy systems. Silty facies, however, are more likely to transition upwards to coarser fractions, suggesting that complete fining upwards sequences are rarely deposited or preserved in the considered dataset. Such outputs on quantitative facies analysis can be used to inform stochastic facies models (e.g., Markov chain analysis), similar to the deep-marine facies studies of Falivene et al. (2006) and Li et al. (2018).

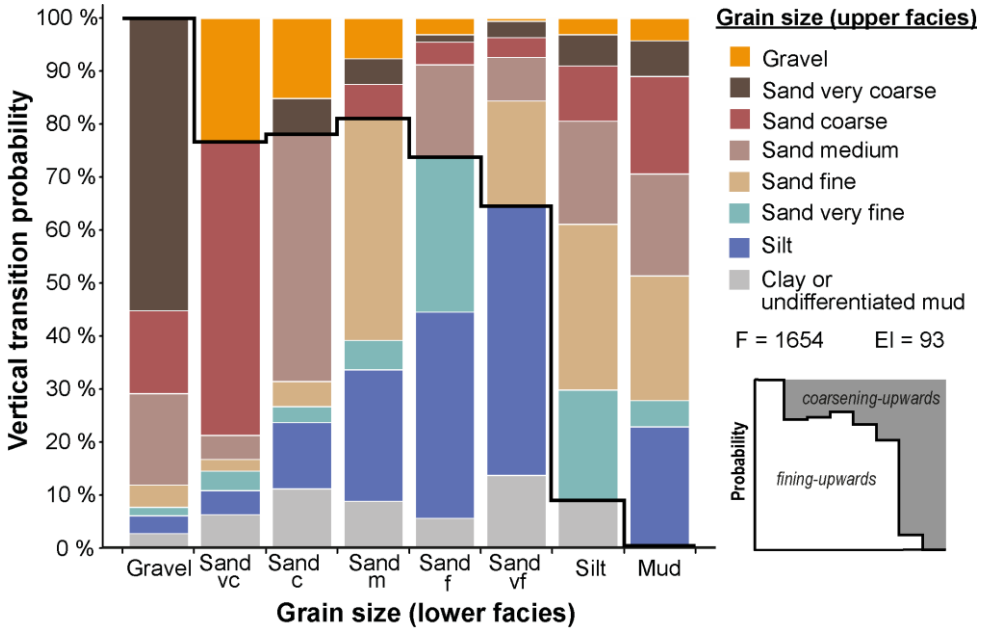

Fig. 4.16. Vertical transition probability for grain-size classes of in-channel facies units, from the starting (lower) facies type indicated on the horizontal axis. Transitions between facies of the same grain size are not included. Only facies from channel elements in sandy systems are considered. The vertical transition grain size classes are presented in a manner whereby coarser classes are at the top. A continuous black line marks the position of the grain size of the starting lower facies and therefore facies transitions counts above the line indicate a transition to coarser sediments (coarsening-upward), while facies transition counts below the line show the probability of vertically passing to a finer sediment (fining-upward), see illustration in bottom-right corner. F = number of facies, El = number of elements.

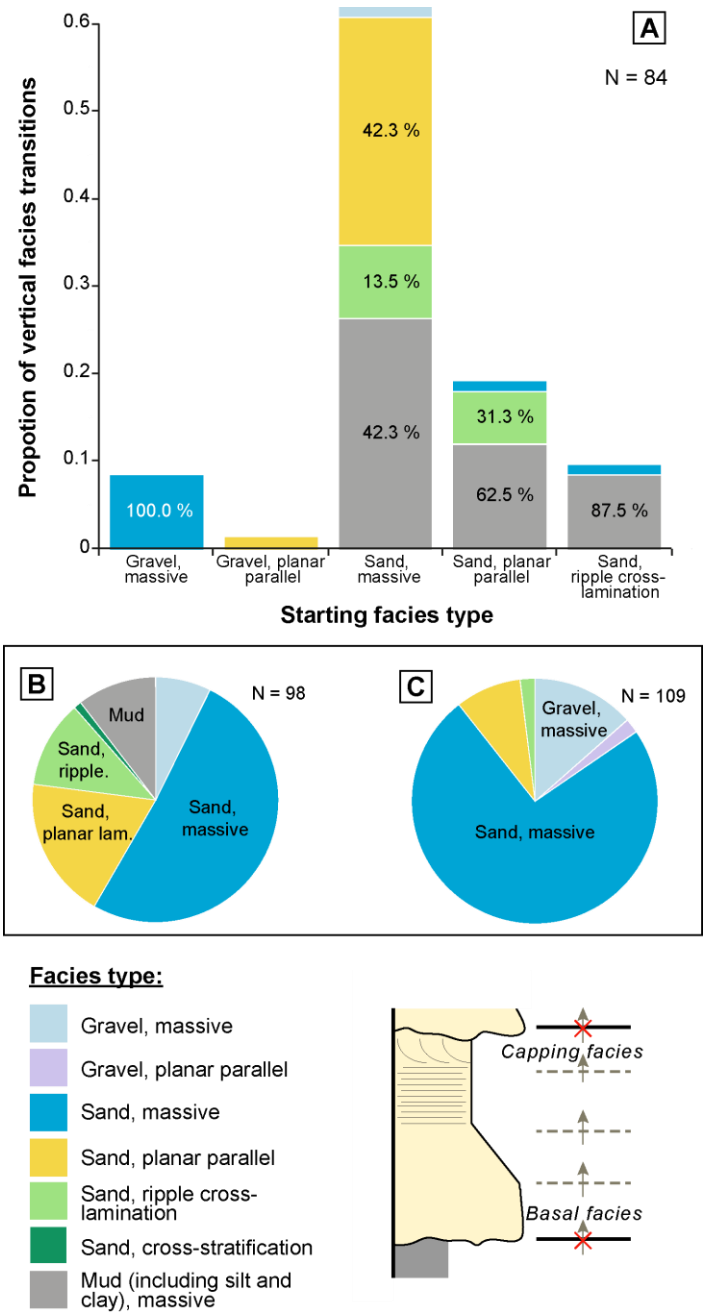

Fig. 4.17. Facies proportions derived from beds contained in channel deposits of the San Clemente case study (Li et al., 2016; Table 4.1). A) Facies-type vertical transitions contained in units described as beds in the original source. Transitions across bedding surfaces are excluded (see illustration in key). X-axis categories represent the lower facies and colours represent the upper facies. Capping (B) and basal (C) facies-type proportions calculated based upon their sum thickness. Only beds containing more than one facies are included in B, while C also includes beds with only one facies. Facies types are classified based upon grain size, sedimentary structures and lamination type, if applicable.

The recurrence of specific facies trends in beds can also be investigated. For example, Fig. 4.17 depicts facies trends in bed units identified in a specific case study, the San Clemente slope channel-system (Capistrano Formation, Li et al., 2016). The modelling of facies distribution within beds can be used to improve characterisation of reservoir quality at the bed scale. Facies distributions can also be used to model the cyclicity of depositional patterns, which in turn can be used to inform geological modelling efforts. For instance, DMAKS could be used to evaluate, statistically, the occurrence and distribution of facies as represented in proposed facies models (e.g., in the classification of hybrid event beds; Haughton et al., 2009; Fonnesu et al., 2018); such approaches would help inform process interpretations via the analysis of large sets of standardised data.

4.3.7 Net-to-gross ratios

Outputs on the proportion of facies in specific types of elements can be used to calculate sandstone proportions or net-to-gross ratios, and the variability in these values can be quantified through consideration of multiple elements. For example, Fig. 4.18 shows the distribution in the proportion of sand and gravel observed in different element types. Net-to-gross values can be tailored to user-defined 'net' specifications and obtained by filtering data based on the attributes on which the systems are classified, to enable consideration of relevant analogues. For instance, Fig. 4.19 considers only channels found on the slope, in sandy systems (i.e., in which the dominant grain size was reported as mixed or sand-rich in the original sources). Metrics of this type can inform predictions relating to total reservoir volume and, when paired with information on spatial variations in lithological heterogeneity (e.g., transition data, or position classifiers), its distribution. For example, Fig. 4.19 depicts a base case for the decrease in net-to-gross ratio seen from the axis of channel elements to their margin – supporting the slope models of Richards & Bowman (1998) and Hubbard et al. (2014), as well as the outcrop studies of Campion et al. (2000; Capistrano Formation) and Macauley & Hubbard (2013; Tres Pasos Formation). The ability to link facies records (and their bed bounding-surface relationships; demonstrated in Section 4.3.6) to a position within their sub-environment could further be used to characterise likely process-product relationships.

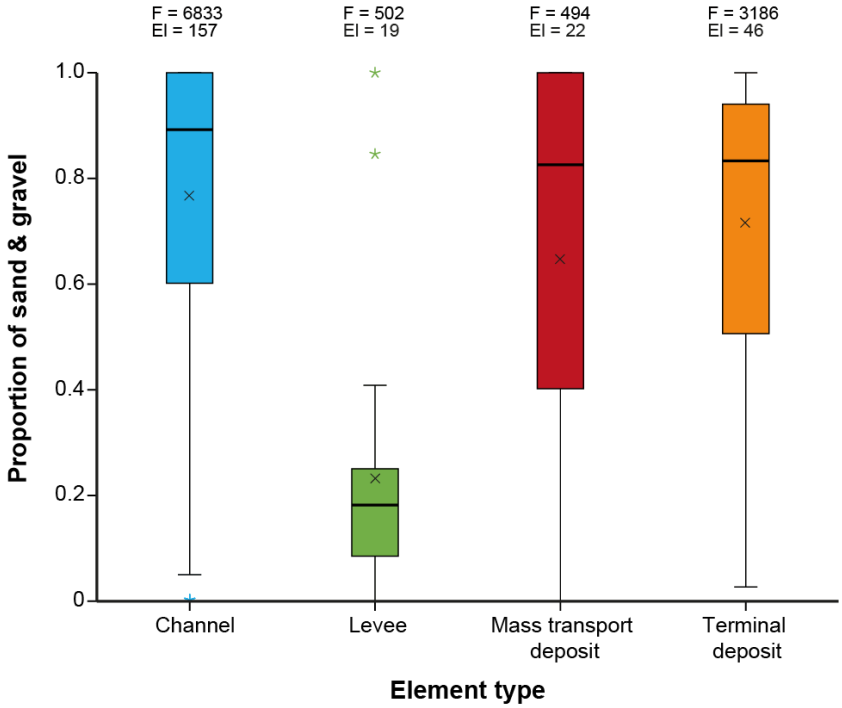

Fig. 4.18. Proportion of sand and gravel found in different element types. Proportions are calculated based on the thickness of sandstone and conglomerate intervals divided by the full thickness of each element. A facies may be counted more than once if contained in elements that are organised hierarchically. Each box represents the interquartile range and includes a median line. Crosses show mean values; stars denote outliers. F = number of facies; El = number of elements.

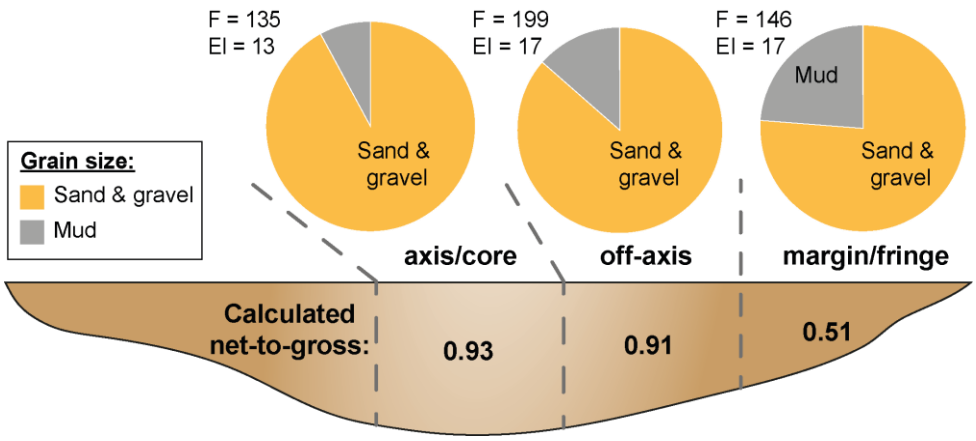

Fig. 4.19. Relative proportion of sand and gravel vs mud specified by lateral position in channel elements. Proportions calculated by averaging the sum of the thicknesses of a grain size against each facies sequences total vertical thickness. Only facies descriptions with a DQI rating of 'A' or 'B' have been considered. 'Mud' includes silt and clay. Data are filtered to include only slope channels found in dominantly sandy systems. F = number of facies; El = number of elements.

4.4 Discussion

DMAKS enables the effective integration of data from the modern seafloor, ancient subsurface and outcropping deep-marine successions, facilitating a comprehensive characterisation and comparison of deep-marine systems (e.g., Fig. 4.8 A and B; Slatt, 2000; Gamberi et al., 2013). The scope of this databasing effort is deliberately wide, aiming to cover both the broad range of environmental settings found in deep-marine systems, together with associated hierarchical and spatial relationships between and within geological entities; this breadth of scope distinguishes it from other approaches (e.g., Cossey & Associates Inc., 2004; Baas et al., 2005; Moscardelli & Wood, 2015; Clare et al., 2018). DMAKS facilitates the characterisation of deep-marine systems by producing quantitative information on the geometries, spatial arrangements and lithological organization of modern landforms and preserved deposits, which can be derived from single or multiple case studies. It can therefore be used to conduct fundamental research, based upon meta-analysis and synthesis of legacy data, or be employed as a resource in subsurface applications that benefit from quantification of sedimentological properties. DMAKS demonstrates the benefits of data standardisation in deep-marine sedimentology, as data integration from multiple sources improves the significance of statistical outputs. The wide range of geological parameters considered allows data to be filtered by multiple variables, to produce outputs that are relevant to specific academic research questions or that can act as synthetic analogues to particular hydrocarbon reservoirs. Through quantification of intra- and inter-system variability in sedimentary architecture, DMAKS enables the geological uncertainties affecting subsurface workflows to be accounted for, and to some extent, reduced.

The database is designed to be refined and extended, in response to scientific progress in the field of deep-marine sedimentology. It complements existing databases for fluvial (Colombera et al., 2012(a)) and paralic and shallow-marine depositional systems (Colombera et al., 2016); a longer-term goal is database integration, to facilitate linked analysis of sedimentary architectures across a range of connected clastic environments.

4.5 Summary

DMAKS is a database storing field- and literature-derived standardised sedimentological data pertaining to siliciclastic deep-marine depositional systems. DMAKS integrates data from multiple studies, and considers the geometry, spatial and hierarchical arrangements, and internal facies properties of deposits and landforms, assigned to systems and case studies classified on boundary conditions, descriptions of the context of deposition, and other

metadata. DMAKS can be queried flexibly to produce quantitative outputs that can be used to (i) undertake quantitative comparative analyses between multiple studies and to (ii) produce syntheses of datasets that act as quantitative facies models or composite analogues. DMAKS finds application in both pure and applied research, particularly for testing process-product relationships via a meta-analytical approach, and for enabling subsurface predictions that are realistic and effectively account for geological uncertainty.

Annex 1. Entity-relationship diagram of the DMAKS database, including look-up tables. Each table (box) is shown including a list of its attributes. Relationships between the tables are shown by connecting lines associated with Primary key (PK) or Foreign key (FK) attributes. Unique keys (UK) are also annotated in each table, meaning data stored in such attributes is unique to a single entry within that table. The cardinality between the tables binary relationships are also noted as either one (1) or many (∞).

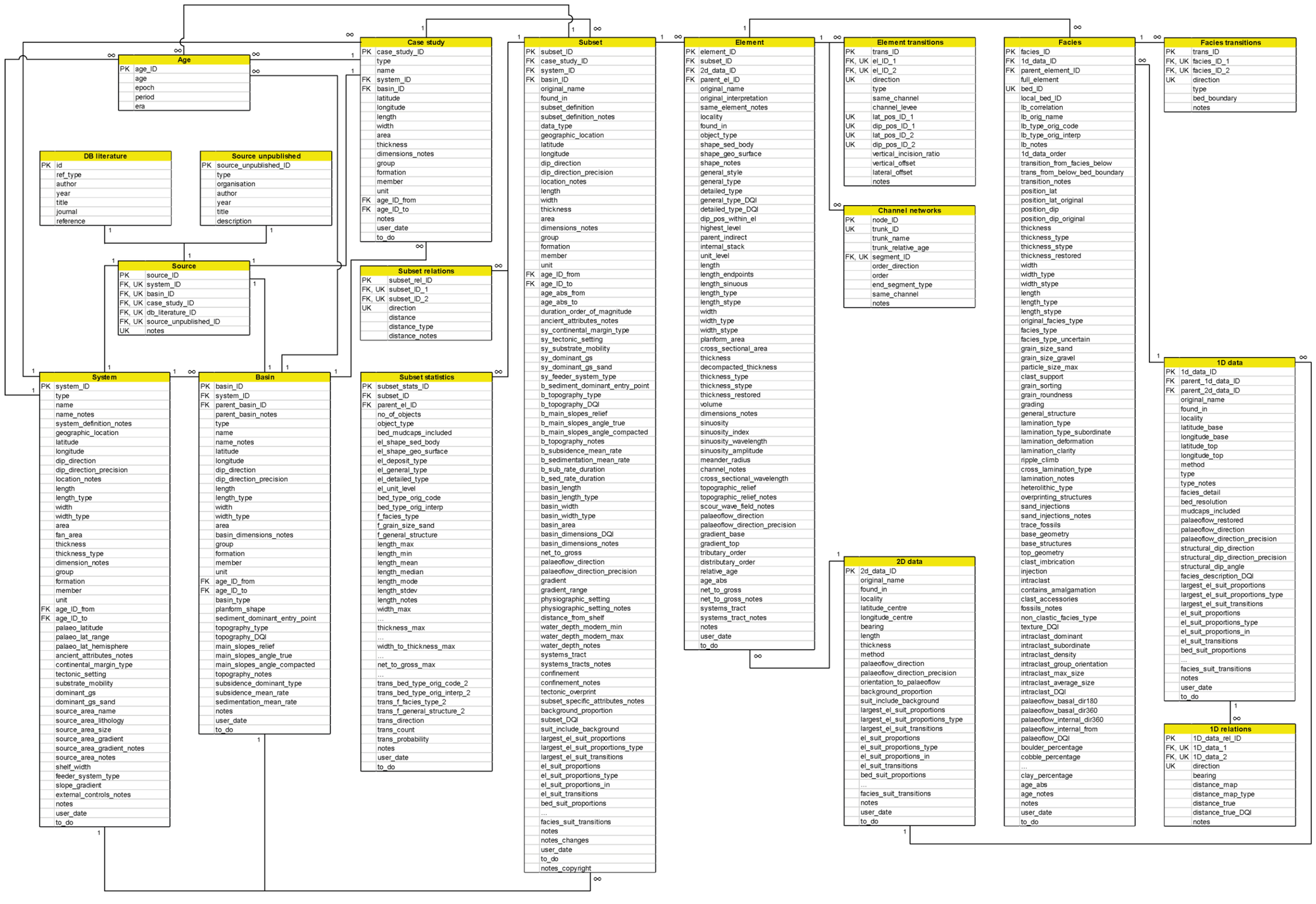

Annexes 2-5. The following worked examples show how information is extracted from different data types and codified into the DMAKS tables. Each Annex is associated with a single case study. Data types examined are i) bathymetric data from the modern sea-floor (Annex 2), ii) seismic data imaging the sub-surface (Annex 3), iii) a cross plot containing data from multiple elements (Annex 4), iv) an architectural panel from outcrop (Annex 5a), and v) sedimentary logs (Annex 5b). All worked examples are derived from the published literature and case study identifiers match those shown in Table 4.1. Geological units are given unique numerical identifiers which allow them to be traced and related between connected tables. For example, an element's identifier can be used to characterise the unit in the Element table, record spatial relationships with other elements in the Element transition and Channel Networks tables, contain associated facies units and beds in the Facies table, while being part of a particular stratigraphic window or of a more specific 2D architectural panel digitised in the Subset and 2D data tables, respectively. Partially filled example data entry tables are shown to demonstrate how unique identifiers are used across multiple tables, as well as some of the different attributes DMAKS captures; Annex 1 contains a comprehensive list of database attributes.

Annex 2. Worked Example: Bathymetric dataset

Case study

case_study_ID	type	name
36	single system dataset	Active channel-mouth lobe complex, Congo-Angola margin, Zaire turbidite system

Figures taken from Dennielou et al., 2017

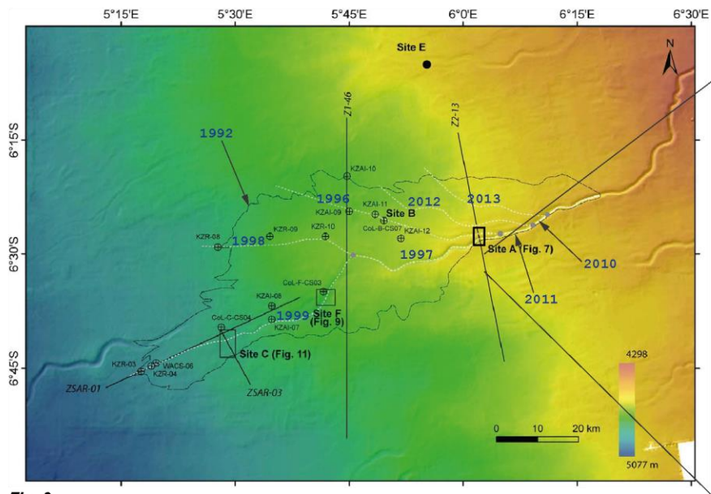

Fig. 2 .

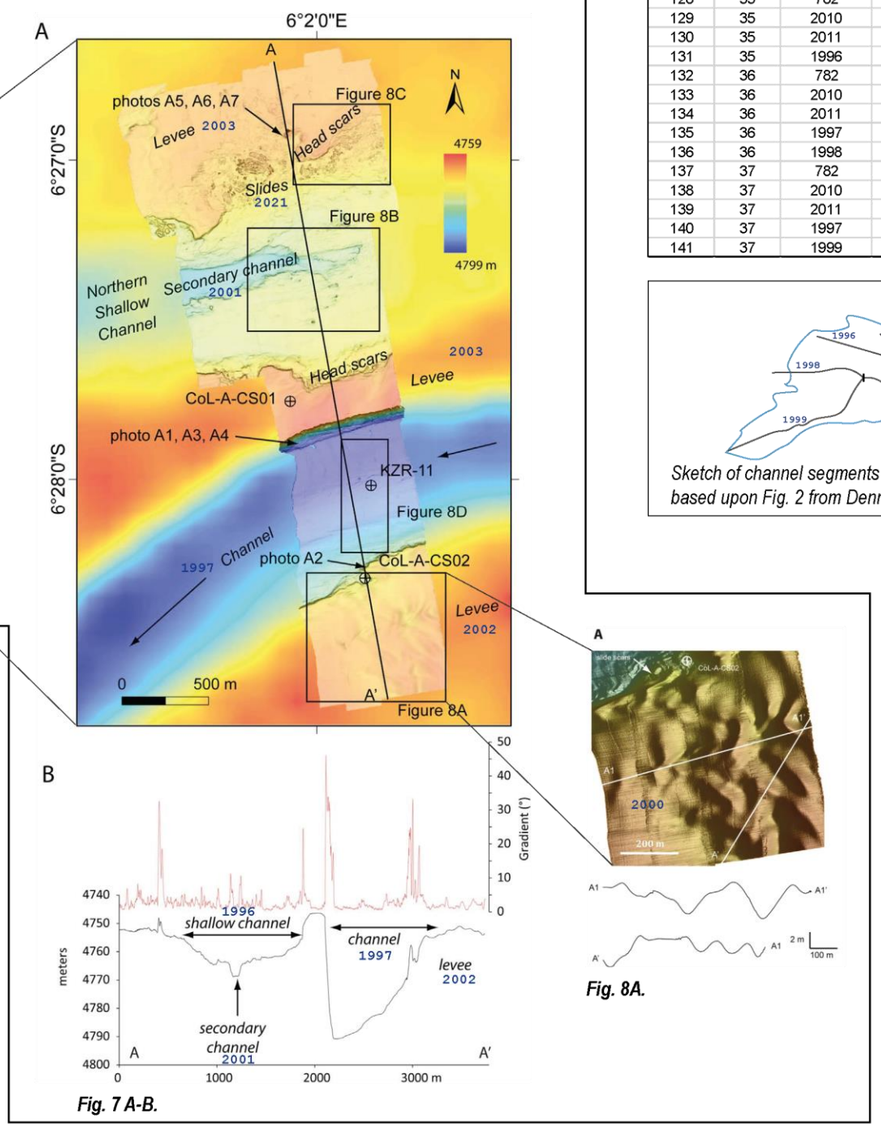

Fig. 7 A-B.

Fig. 8A.

Channel networks

node_ID	trunk_ID	segment_ID	order	order_direction	end_segment_type
123	33	782	1	downstream	-
124	33	2013	2	downstream	distal termination
125	34	782	1	downstream	-
126	34	2010	2	downstream	-
127	34	2012	3	downstream	distal termination
128	35	782	1	downstream	-
129	35	2010	2	downstream	-
130	35	2011	3	downstream	-
131	35	1996	4	downstream	distal termination
132	36	782	1	downstream	-
133	36	2010	2	downstream	-
134	36	2011	3	downstream	-
135	36	1997	4	downstream	-
136	36	1998	5	downstream	distal termination
137	37	782	1	downstream	-
138	37	2010	2	downstream	-
139	37	2011	3	downstream	-
140	37	1997	4	downstream	-
141	37	1999	5	downstream	distal termination

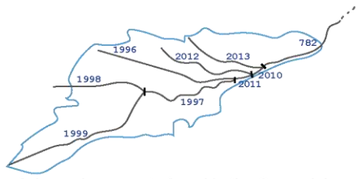

Sketch of channel segments found in the Congo lobe complex based upon Fig. 2 from Dennielou et al., 2017.

Example sketches showing how channel 'trunks' are digitised using individual channel segment ID's

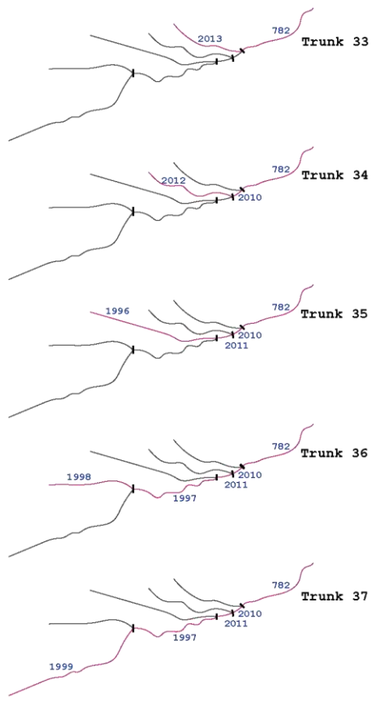

Elements

el_ID	subset_ID	parent_el_ID	highest_level	object_type	shape_geo_surface	general_type
1992	57	-	Y	mixed	mound	terminal deposit
1996	57	-	Y	geosurface	channel	channel
1997	57	-	Y	geosurface	channel	channel
1998	57	-	Y	geosurface	channel	channel
1999	57	-	Y	mixed	channel	channel
2000	57	-	Y	geosurface	wave field	-
2001	57	1996	-	geosurface	channel	channel
2002	57	-	Y	sed body	-	levee
2003	57	-	Y	sed body	-	levee
2010	57	-	Y	geosurface	channel	channel
2011	57	-	Y	geosurface	channel	channel
2012	57	-	Y	sed body	-	channel
2013	57	-	Y	geosurface	channel	channel
2021	57	-	Y	sed body	-	mass transport deposit

Element transitions

trans_ID	el_ID_1	el_ID_2	direction	type	channel_levee	lat_pos_ID_1	dip_pos_ID_1	lat_pos_ID_2	dip_pos_ID_1
3898	2002	2000	vertical	-	-	inner crest	-	-	-
3899	2002	1997	lateral	sharp	Y	inner crest	-	margin/fringe	proximal
3900	1997	2003	lateral	sharp	Y	margin/fringe	proximal	inner crest	-
3901	2003	1996	lateral	sharp	-	crest	-	-	proximal
3902	1996	2001	lateral	sharp (erosional)	-	axis/core	proximal	margin/fringe	proximal
3903	2001	1996	lateral	sharp (erosional)	-	margin/fringe	proximal	axis/core	proximal
3904	1996	2021	lateral	sharp	-	margin/fringe	proximal	-	-
3905	2021	2003	lateral	sharp	-	-	-	crest	-

Annex 3. Worked Example: Seismic dataset

Case study

case_study_ID	type	name
1	single system dataset	Late Pleistocene deposits offshore East Corsica, Golo turbidite system

Figures taken from Gervais et al., 2006(a)

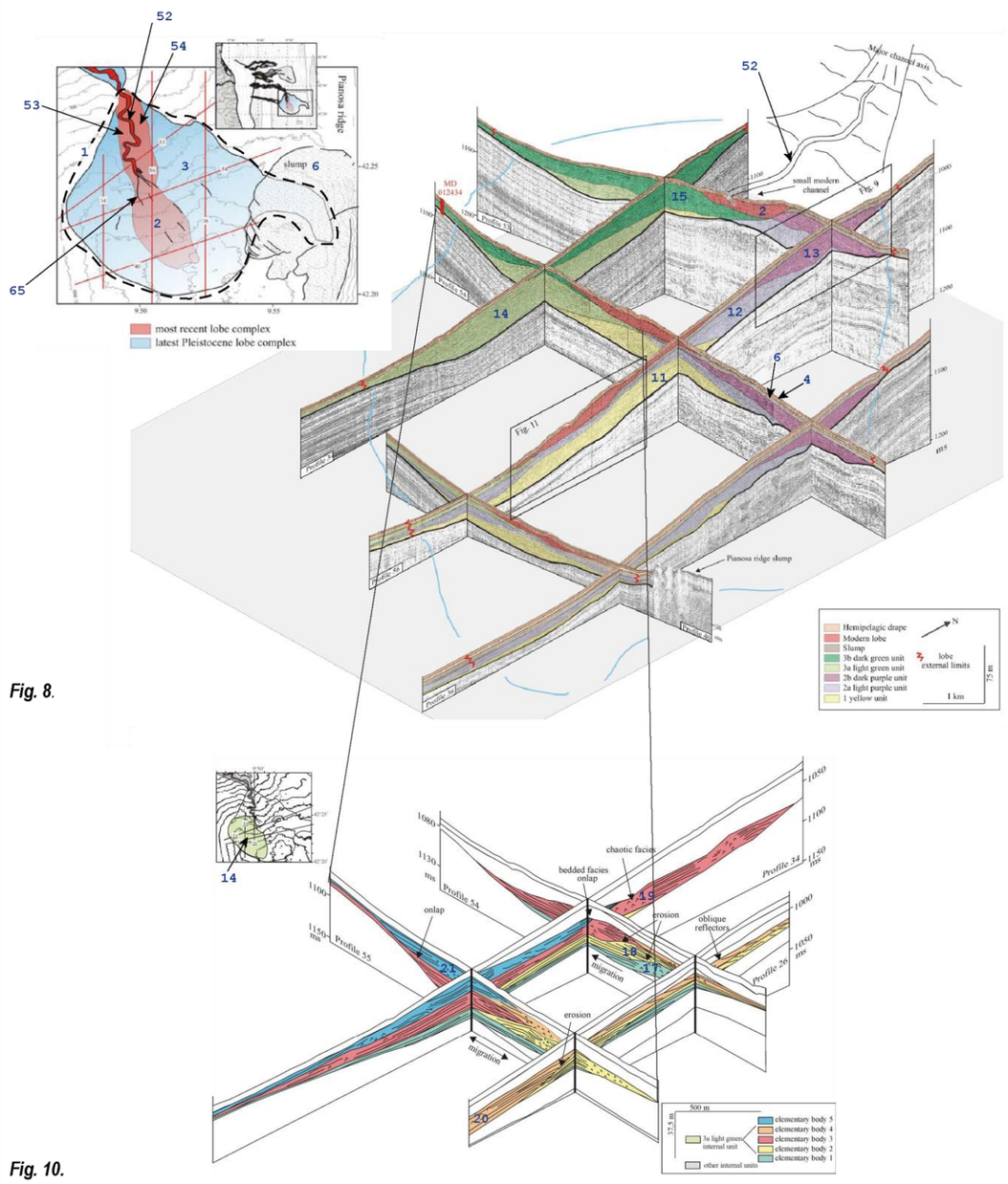

Fig. 8.

Fig. 10.

Elements

el_ID	parent_ el_ID	highest _level	general_type	length (m)	length_type	width (m)	width_type (m)	thickness (m)	thickness_type
1	-	Y	terminal deposit	20240.00	true (maximum)	17016.00	true (maximum)	60.00	true (maximum)
2	1	-	terminal deposit	7150.00	true (maximum)	4800.00	true (maximum)	20.00	true (maximum)
3	1	-	terminal deposit	20240.00	true (maximum)	12650.00	true (maximum)	60.00	true (maximum)
4	-	Y	background	-	-	-	-	17.00	true (maximum)
6	-	Y	mass transport deposit	710.00	apparent	525.00	apparent	22.50	true (not maximum)
11	3	-	terminal deposit	6261.00	true (maximum)	3502.00	true (maximum)	33.00	true (not maximum)
12	3	-	terminal deposit	8502.00	true (maximum)	3740.00	true (maximum)	28.00	true (not maximum)
13	3	-	terminal deposit	4577.00	true (maximum)	3707.00	true (maximum)	35.00	true (not maximum)
14	3	-	terminal deposit	5923.00	true (maximum)	3290.00	true (maximum)	45.00	true (not maximum)
15	3	-	terminal deposit	4601.00	true (maximum)	4558.00	true (maximum)	33.00	true (not maximum)
17	14	-	terminal deposit	2615.00	true (maximum)	1480.00	true (maximum)	11.53	true (maximum)
18	14	-	terminal deposit	1480.00	true (maximum)	1090.00	true (maximum)	12.50	true (maximum)
19	14	-	terminal deposit	3980.00	true (maximum)	1390.00	true (maximum)	17.00	true (maximum)
20	14	-	terminal deposit	2250.00	true (maximum)	910.00	true (maximum)	15.00	true (maximum)
21	14	-	terminal deposit	2680.00	true (maximum)	1320.00	true (maximum)	12.00	true (maximum)
52	-	Y	channel	*	true (maximum)	1320.00	true (maximum)	48.00	true (maximum)
53	-	Y	levee	14378.00	apparent	-	-	-	-
54	-	Y	levee	13000.00	apparent	-	-	-	-
65	2	-	channel	-	-	-	-	-	-

For sinuous elements like a channel, DMAKS records both the sinuous length, as well as the length of a straight line between the elements endpoints

Element transitions

trans_ID	el_ID_1	el_ID_2	direction	type	lat_pos_ID_1	dip_pos_ID_1	lat_pos_ID_2	dip_pos_ID_1
121	17	18	vertical	sharp (erosional)	axis/core	proximal	axis/core	proximal
122	17	18	lateral	sharp (erosional)	axis/core	proximal	axis/core	proximal
123	18	2	vertical	sharp	margin/fringe	distal	axis/core	mid
124	14	2	vertical	sharp	off-axis, margin/fringe	mid	axis/core	mid
125	14	2	vertical	sharp	margin/fringe	distal	off-axis, margin/fringe	distal
126	15	14	dip	sharp	off-axis	distal	axis/core	mid

Annex 4. Worked Example: Cross-plot data

Case study

case_study_ID	type	name
2	single system dataset	Ross Sandstone, Loop Head Peninsula and Ballybunnion, Ross Formation

2D data

2D_data_ID	original_name	found_in	method
9	Cross-section of Rinevella Point exposure	Fig 6, Pyles, 2007	lidar scan

Figures taken from Pyles, 2007

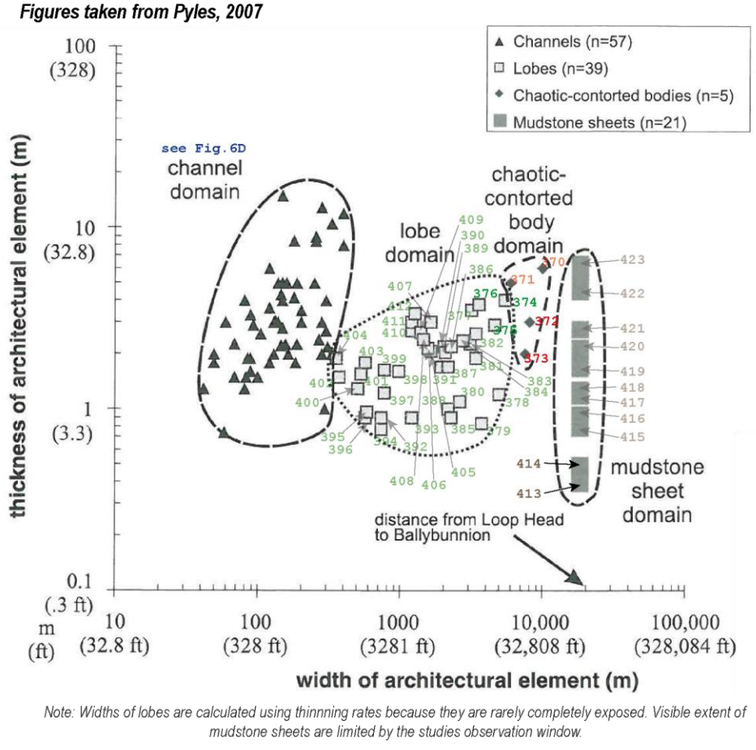

Note: Widths of lobes are calculated using thinnning rates because they are rarely completely exposed. Visible extent of mudstone sheets are limited by the studies observation window.

Fig. 5.

2D data 9

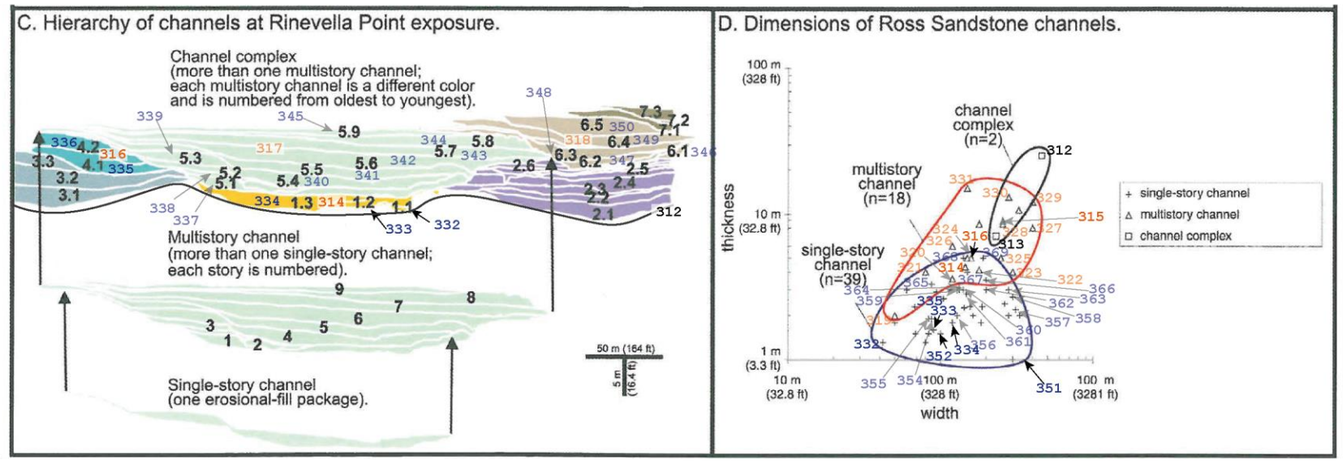

Fig. 6 C-D.

**ID labeling is faded out if not included in the example Element table*

Elements

el_ID	subset_ID	2D_data_ID	parent_el_ID	highest_level	original_interpretation	general_type	width (m)	width_type	thickness (m)	thickness_type
312	2	9	-	Y	channel complex	channel	450.00	true (maximum)	25.00	true (maximum)
313	2	-	-	Y	channel complex	channel	210.00	true (maximum)	7.00	true (maximum)
314	2	9	312	-	multistory channel	channel	125.00	true (maximum)	4.10	true (maximum)
315	2	-	-	-	multistory channel	channel	260.00	true (maximum)	8.50	true (maximum)
316	2	9	312	-	multistory channel	channel	130.00	true (maximum)	5.00	true (maximum)
332	2	9	314	-	single-story channel	channel	40.00	true (maximum)	1.20	true (maximum)
333	2	9	314	-	single-story channel	channel	90.00	true (maximum)	1.40	true (maximum)
334	2	9	314	-	single-story channel	channel	125.00	true (maximum)	2.10	true (maximum)
335	2	9	316	-	single-story channel	channel	102.00	true (maximum)	2.50	true (maximum)
351	2	-	-	-	single-story channel	channel	360.00	true (maximum)	1.00	true (maximum)
352	2	-	-	-	single-story channel	channel	100.00	true (maximum)	1.25	true (maximum)
372	2	-	-	Y	chaotic-contorted body	mass transport deposit	8000.00	true (maximum)	3.00	true (maximum)
373	2	-	-	Y	chaotic-contorted body	mass transport deposit	7500.00	true (maximum)	2.00	true (maximum)
374	2	-	-	Y	lobe	terminal deposit	5500.00	*calculated	4.00	true (maximum)
375	2	-	-	Y	lobe	terminal deposit	4500.00	*calculated	3.00	true (maximum)
376	2	-	-	Y	lobe	terminal deposit	3500.00	*calculated	3.90	true (maximum)
413	2	-	-	Y	mudstone sheet	background	18000.00	partial observed	0.36	true (maximum)
414	2	-	-	Y	mudstone sheet	background	18000.00	partial observed	0.50	true (maximum)

** The lobe widths are not actual measurements (see 'Note' from Pyles, 2007 in Figures above) and so these estimates are recorded separately in the 'dimensions_notes' attribute.*

Annex 5a. Worked Example: Architectural panel

Case study

case_study_ID	type	name
20	single system dataset	San Clemente channel system, California, Capistrano Formation

2D data

2D_data_ID	original_name	found_in	method	bearing	palaeoflow_direction	palaeoflow_direction_precision	orientation_to_palaeoflow
5	Photomosaic and interpretation of the Capistrano Formation	Fig 5, Li et al., 2016	photopanel	340	319	exact value	oblique

Figures taken from Li et al., 2016

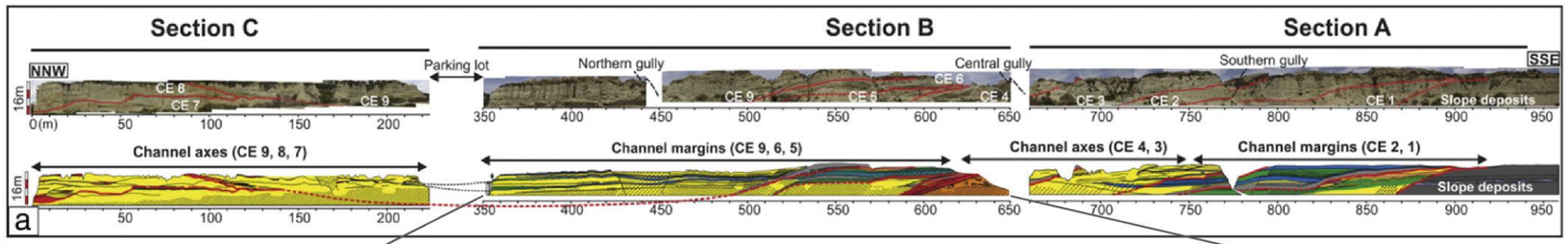

Fig. 5A.

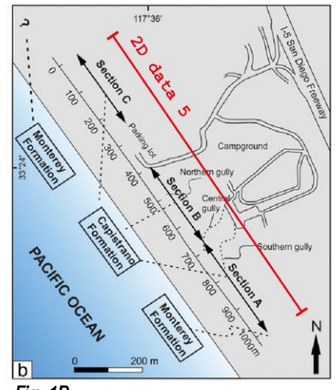

Fig. 1B.

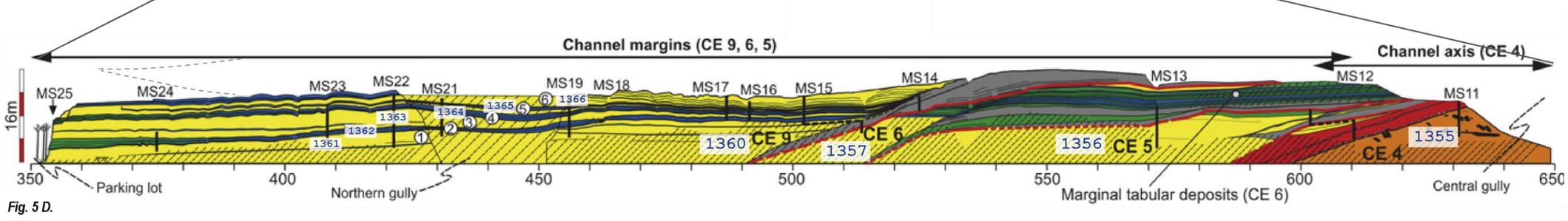

Fig. 5 D.

Elements

el_ID	2D_data_ID	parent_el_ID	original_name	object_type	general_type	width (m)	width_type	thickness (m)	thickness_type
1355	5	1350	CE 4	sed body	channel	70.00	partial eroded	9.60	unlimited eroded
1356	5	1351	CE 5	sed body	channel	72.00	partial eroded	9.90	partial eroded
1357	5	1351	CE 6	sed body	channel	89.00	partial eroded	6.60	true (not maximum)
1360	5	1351	CE 9	sed body	channel	510.00	apparent	14.70	unlimited eroded
1361	5	1360	1	sed body	-	-	-	2.87	partial observed
1362	5	1360	2	sed body	-	-	-	1.30	true (maximum)
1363	5	1360	3	sed body	-	-	-	3.83	true (maximum)
1364	5	1360	4	sed body	-	-	-	1.00	true (maximum)
1365	5	1360	5	sed body	-	-	-	0.90	true (maximum)

Element transitions

trans_ID	el_ID_1	el_ID_2	direction	type	lat_pos_el_ID_1	lat_pos_el_ID_2
3133	1355	1356	vertical	sharp (erosional)	axis/core,off-axis,margin/fringe	margin/fringe
3134	1355	1356	lateral	sharp (erosional)	axis/core,off-axis,margin/fringe	margin/fringe
3135	1356	1357	vertical	sharp (erosional)	all	all
3136	1356	1357	lateral	sharp (erosional)	all	all
3137	1357	1360	vertical	sharp (erosional)	axis/core,off-axis,margin/fringe	margin/fringe
3138	1357	1360	lateral	sharp (erosional)	axis/core,off-axis,margin/fringe	margin/fringe
3154	1361	1362	vertical	sharp	off-axis	margin/fringe
3159	1361	1362	vertical	sharp	axis/core,off-axis,margin/fringe	all
3160	1362	1363	vertical	sharp	all	all
3161	1362	1363	lateral	sharp	all	all
3162	1363	1364	vertical	sharp	all	all
3163	1364	1365	vertical	sharp	all	all

Annex 5b. Worked Example: Facies data

Using Case study 20, the San Clemente channel system, California, Capistrano Formation

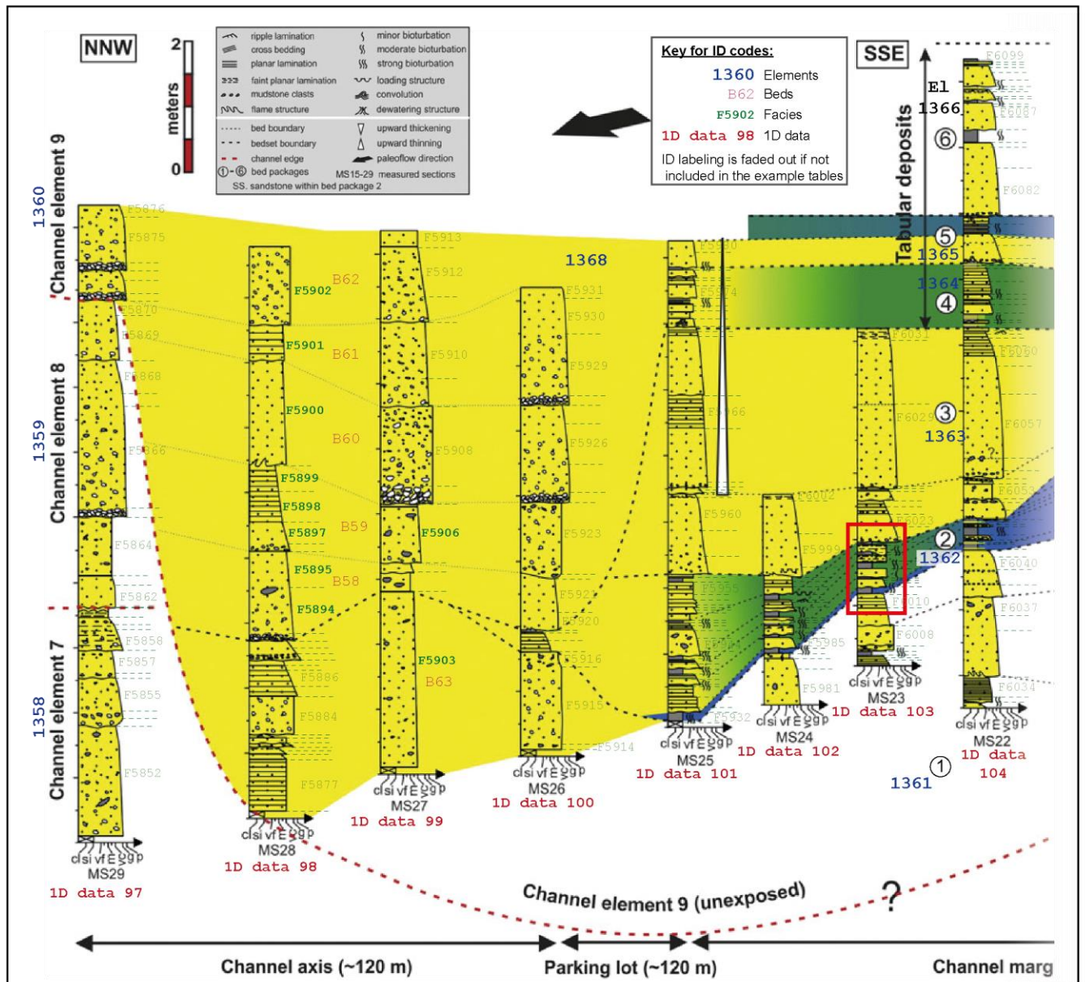

Fig. 6, taken from Li et al., 2016.

Facies

facies_ID	1D_data_ID	parent_element_ID	full_element	bed_ID	local_bed_ID	lb_correlation	1d_data_order	transition_from_facies_below	thickness (m)	thickness_type	facies_type	grain_size_sand	grading	general_structure
5893	98	1368	N	58	58	new bed	16	sharp	0.10	true (maximum)	_G	-	non-graded	massive
5894	98	1368	N	-	58	-	17	gradational	0.69	true (maximum)	_G	-	normally graded	massive
5895	98	1368	N	-	58	-	18	gradational	0.55	true (maximum)	_G	-	normally graded	massive
5896	98	1368	N	59	59	new bed	19	sharp	0.14	true (maximum)	_S	very coarse	normally graded	massive
5897	98	1368	N	-	59	-	20	gradational	0.34	true (maximum)	_S	very coarse	normally graded	massive
5898	98	1368	N	-	59	-	21	sharp	0.48	true (maximum)	_S	coarse	normally graded	laminated
5899	98	1368	N	-	59	-	22	sharp	0.41	true (maximum)	_S	medium	normally graded	laminated
5900	98	1368	N	60	60	new bed	23	sharp	1.60	true (maximum)	_S	very coarse	normally graded	massive
5901	98	1368	N	61	61	new bed	24	sharp	0.55	true (maximum)	_S	very coarse	normally graded	laminated
5902	98	1368	N	62	62	new bed	25	sharp	1.24	true (maximum)	_G	-	non-graded	massive
5903	99	1361	Y	63	63	new bed	1	sharp	2.72	true (maximum)	_S	very coarse	normally graded	massive
5904	99	1368	N	-	58	observed	2	sharp	0.28	true (maximum)	_S	medium	non-graded	massive
5905	99	1368	N	-	-	-	3	sharp	0.14	true (maximum)	_S	coarse	normally graded	massive
5906	99	1368	N	-	59	observed	4	sharp	0.90	true (maximum)	_G	-	normally graded	massive
5907	99	1368	N	-	60	observed	5	sharp	0.28	true (maximum)	_G	-	non-graded	massive

1D data

1D_data_ID	parent_2D_data_ID	original_name	method	type
97	5	MS29	stratigraphic	normal
98	5	MS28	stratigraphic	normal
99	5	MS27	stratigraphic	normal
100	5	MS26	stratigraphic	normal
101	5	MS25	stratigraphic	normal
102	5	MS24	stratigraphic	normal
103	5	MS23	stratigraphic	normal
104	5	MS22	stratigraphic	normal

1D data relations

1D_data_rel_ID	1D_data_1	1D_data_2	direction	bearing	distance_map	distance_map_type
20	98	97	oblique right	340	48	undeformed
21	99	98	oblique right	340	36	undeformed
22	100	99	oblique right	340	28	undeformed
23	101	100	oblique right	340	151	undeformed
24	102	101	oblique right	340	20	undeformed
25	103	102	oblique right	340	34	undeformed
26	104	103	oblique right	340	13	undeformed

Facies transitions

trans_ID	facies_ID_1	facies_ID_2	direction	type
245	6018	6020	vertical	sharp (erosional)

Transition stored in Facies table via 1D data order
Transition stored in Facies transition table

(insert taken from 1D 103, see red box in Fig. 6)

Chapter 5:

A multi-scale evaluation of relationships between external parameters and terminal-deposit geometries in deep-marine clastic systems

---

Chapter synopsis

Using the Deep-Marine Architecture Knowledge Store (DMAKS), a comparative analysis exploiting modern, subsurface and outcrop datasets has been undertaken to explore the importance of system-scale parameters, such as margin type, shelf width, slope gradient and maximum water depth (over the domain of the depositional system), as controls upon the architecture of lobate terminal deposits at multiple scales. The scale of a deep-marine system is seen to correlate positively with wider shelves, decreasing grain size, shallower slope gradients and deeper water depths; larger systems are also associated with passive margin settings. Such associations corroborate relationships as described in the literature, which often attribute these system-scale characteristics as being related in some way to tectonic controls. A non-linear relationship is found to exist between the depositional-system scale, its inter-related parameters (i.e., associated margin type, shelf width and slope gradient), and the size of its largest (i.e., of highest hierarchical order) terminal deposits. When considered collectively across all the studied systems, width and length distributions of the highest-order terminal deposits show two peaks; the variability observed between the system-scale end-members and their associated system parameters compliment these non-normal distributions. A general trend can be seen, whereby dimensionally smaller highest-order elements with lobate planform geometries are deposited in 'small' systems (<100 km) associated with steeper slope gradients (>0.03 m/m), shorter shelves (<30,000 m), shallower water depths (<2500 m) and tectonically active margins, while larger highest-order terminal deposits are typical in 'large' systems (>100 km) and their associated shallower slope gradients (<0.03 m/m), longer shelves (>30,000 m), deeper water depths (>2500 m) and tectonically passive margins. However this study suggests that the local depositional gradient, coupled with the local depositional water depth, is a statistically more accurate predictor of terminal deposit planform geometry at all hierarchical scales: gradients shallower than 0.01 m/m at water depths greater than 2500 m are associated with larger planform geometries, as opposed to smaller planform geometries which are predominantly found upon steeper gradients (>0.01 m/m) and shallower water depths (<2500 m). The local depositional gradient

and water depth can be seen to be preferentially associated with the allogenic system parameters; thus, the tectonic regime is seen to exert influence, albeit subtly, upon element-scale deposition. Widths and lengths of terminal-deposits can be seen to be influenced by system-scale and local parameters (both allogenic and autogenic). However, terminal-deposit volumes show a common upper limit, regardless of any controlling parameters considered in this study, suggesting that internal flow dynamics may act to limit the 3D morphology of terminal deposits.

5.1 Introduction

Organisation in clastic systems can be investigated through the study of quantitative relationships between the sedimentary environments along the depositional profile, e.g., Sømme et al., 2009; Martinsen et al., 2011; Bhattacharya et al., 2016; Xu et al., 2017; Nyberg et al., 2018; Snedden et al., 2018. Deep-marine siliciclastic systems show scaling-relationships between their architectural building blocks; for instance, levee thinning rates downstream and across the levee crest are statistically related to the geometry of their genetically-associated channel (Skene et al., 2002; Nakajima & Kneller, 2013), while upstream channel dimensions are also seen to correlate to the morphology of genetically-related lobate terminal deposits (Pettinga et al., 2018) and relationships are also observed between nested parent and child channelised and lobate architectures (Fig. 4.10 in Chapter 4; Cullis et al., *accepted*). These geometrical relationships suggest that common controls may possibly affect the deep-marine sedimentary environment or at least some portions thereof. Deep-marine systems, and their depositional geometries, are commonly thought to be controlled by sediment supply, sea-level, climate and regional tectonics (Stow et al., 1996; Richards et al., 1998; Bouma, 2004; Covault & Graham, 2010). At the largest architectural-element scale allogenic controls are believed to dominate, while at smaller scales autogenic controls are thought to prevail. However, the relative influence of these controls, as well as their precise roles, remain unclear (Prélat et al., 2009; Terlaky et al., 2016; Picot et al., 2016; Jerolmack & Paola, 2010).

The DMAKS database has been employed to assess multiple system variables across different scales of deposition. DMAKS stores a wide range of standardised data, enabling multi-factor analysis to compare the significance of system relationships. Typical published investigations into allogenic controls focussed upon either the overall system-scale (e.g., Reading & Richards, 1994; Nelson et al., 2009; Covault & Romans, 2009; Sømme et al., 2009; Snedden et al., 2018) or element-scale deposition (e.g., Marsset et al., 2009; Picot et al., 2016; Zhang et

al., 2018). Here, DMAKS' ability to store data on nesting relationships between geological units allows analysis of architectural characteristics across multiple scales. A multi-scale assessment of system-scale characteristics will additionally serve as a test of whether large-scale allocyclic signals are 'shredded' at smaller depositional scales (e.g., Jerolmack & Paola, 2010).

The immediate aim of this study is to investigate the importance of system-scale parameters upon the depositional geometry of terminal deposits, via a comparative analysis of multiple systems. Quantitative database outputs allow the relationships between system-scale variables and element-scale lobate geometries to be characterised. The aim of this Chapter will be achieved through: i) a preliminary evaluation of the effects of a system's regional characteristics and configuration upon the resultant scale of the deep-marine system, and ii) a subsequent examination of the effects of the observed system-scale parameters upon the geometry of associated terminal deposits, with particular focus on the dimensions of the largest terminal deposits together with the geometrical relationships between the different hierarchical levels of nested terminal deposits.

5.2 Methodology

To assess the effect of deep-marine system variables upon terminal deposit geometry, data have been collated into DMAKS from 17 modern and ancient siliciclastic deep-marine systems characterised by a range of scales and external controls (summary in Table 5.1). This dataset has been derived from the literature and has been standardised following systematic entry into DMAKS using the database definitions and workflow outlined in Chapter 4 (Cullis et al., *accepted*). Data standardisation enables joint quantitative interrogation and comparison of deep-marine datasets sourced from bathymetric, seismic and outcrop studies. To evaluate the 'goodness of fit' for the database trends presented in this study confidence intervals to regression and correlation coefficients have been calculated for the original DMAKS dataset (taken from DMAKS October 2018), as well as an extended dataset which includes a further 11 systems input into DMAKS by May 2019. The additional 11 systems are summarised in Appendix D.

The database stores information concerning multiple parameters at different scales. The external controls considered within the scope of this study are largely captured at the 'system' scale and are concerned with the regional configuration of the system, i.e., the overall system dimensions, dominant grain size (as described by the source-work), average shelf width along the width of the system, average slope gradient, maximum water depth at

time of deposition, and continental margin type/tectonic regime (Fig. 5.1). Following the DMAKS standard, a deep-marine system is considered as the complete erosional and depositional expression of deep-marine sediment-gravity flows, from the shelf-break to their most distal reaches (Fig. 5.1). A system may be associated with a topographic depression (i.e., a 'basin' in DMAKS; Table 5.1), resulting in the preferential location of sedimentary deposition for part of or all of a system's lifetime. Local changes upon element-scale deposition, such as water depth and the sea-floor gradient, are recorded in the DMAKS 'subset' table – which can be used to capture the variability of controls on individual systems, across temporal and spatial scales.

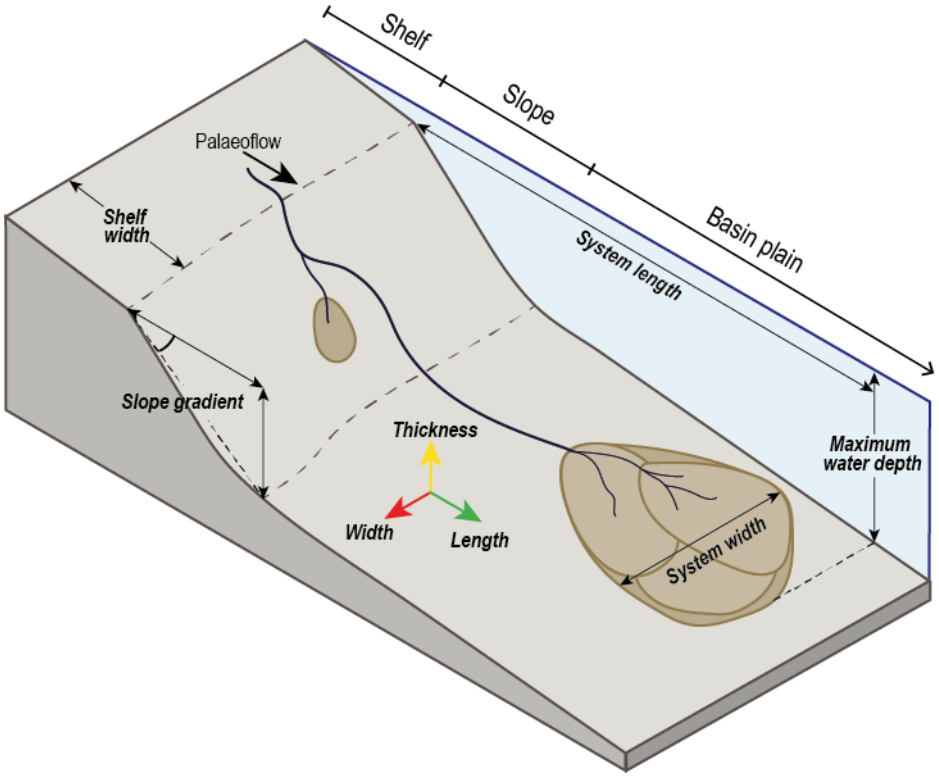

Fig. 5.1. A summary diagram showing a deep-marine system and its system-scale morphological parameters analysed in this study. Two highest-order terminal deposit architectures are shown of different hierarchical complexity, this hierarchical variance between highest-order deposits is common in the systems studied. Dimensions are measured with respect to a reference system orientated relative to the dominant (palaeo-) flow direction. No scale implied.

At the architectural 'element' scale this study focuses upon lobate 'terminal deposits', irrespective of their hierarchical assignation. A 'terminal deposit', as defined in DMAKS, is regarded as a depositional body located at the terminus of a genetically-related channel architecture, as sediment gravity flows decelerate due to the change in flow confinement (Posamentier & Kolla, 2003; Weimer & Slatt, 2007(d)). Sheet-like terminal geometries are not

considered in this study. Dimensional data derived from DMAKS associated with 321 terminal deposits have been considered in this investigation. Hierarchical units are discerned based upon the consideration of bounding-surface relationships, whereby “highest-order” terminal deposits depict the largest hierarchical order, as they are not contained within any other terminal deposit. Element (and system) dimensions are measured relative to the dominant (palaeo-) flow direction for the object being measured; length is taken as a straight-line measurement along (palaeo-) flow and width is taken orthogonal to (palaeo-) flow (Fig. 5.1). To ensure data quality, only ‘true (maximum)’ terminal deposit thicknesses have been considered (*sensu* Geehan & Underwood, 1993; Fig. 4.6, Chapter 4). Terminal deposit width and length dimensions are ‘true’ or ‘estimated’ values. An ‘estimated’ value is an inferred measurement, based upon the extrapolation of thinning rates from known pinchouts; such measurements are typical in extensive but incomplete outcrops (e.g., the Karoo depocentre, Prélat et al., 2009). All dimensions are taken from datasets that are of either 2D or 3D spatial type (Fig. 4.6, Chapter 4). The data considered in this study have also been filtered to account for their suitability for geometric analysis, as recorded in metadata fields in the database.

The scope of this study is limited by the available data sourced from the literature. This study focuses in particular upon the regional configuration of the systems (i.e., margin type, morphology and scale), which might arise from self-organization; the impact of other external controls (e.g., climate, sea-level and sediment supply) has not been considered. The system-scale parameters examined in this study only characterise the state of a system for a relatively restricted time interval; temporal variations in the overall system size or in external controls are not captured in this study due to limited data availability of such changes for some systems considered in this study. Therefore, the parameters on which the systems are classified are the dominant or average conditions exhibited during either a preserved sedimentary package or a modern system with a sea-floor expression. The results of this study do not account for differential sediment compaction, for inherent variations in preservation potential (Sadler, 1981; Miall, 2015), or for the fact that studied units of ‘active’ systems may not have reached a terminal configuration (Table 5.1).

ID	System name and locality	Data collection method	Duration	Length (km)	Width (km)	Basin topography	Margin type (tectonic regime)	Dominant system grain size	Feeder system type	Shelf width (m)	Slope gradient (m/m)	Maximum water depth (m)	References
1	**Al Batha Turbidite System**, Gulf of Oman, North-west Indian Ocean	bathymetry and 2D seismic	? - active	3,35	91.5	no	passive margin	mixed	single	15,000	0.027	3,330	Bourget et al., 2010
2	**Amazon Turbidite System**, offshore Northern Brazil, Western Atlantic	bathymetry and 2D seismic	Pleistocene - *active*	700	700	no	passive margin	mud rich	single	300,000	0.014	4,700	Flood et al., 1987; Flood et al., 1991; Piper & Normark, 2001; Jegou et al., 2008; Sømme et al., 2009
3	**Bengal System**, Bay of Bengal, North-east Indian Ocean	3D seismic	Eocene - *active*	3,000	1,430	no	passive margin	mud rich	single	190,000	0.023	5,000	Barnes & Normark, 1985; Emmel & Curray, 1985; Pickering et al., 1989; Curray et al., 2003; Schwenk & Speiss, 2009; Yang & Kim, 2014
4	**Bjørnsonfjellet Member Turbidite System**, Spitsbergen, Svalbard archipelago, Norway	outcrop	Eocene	14(?)	5.5(?)	yes	(strike-slip)	sand rich	-	-	-	-	Plink-Björklund et al., 2001; Plink-Björklund & Steel, 2004; Grundvåg et al., 2014
5	**Gendalo Field**, offshore East Kalimantan, Indonesia	3D seismic	Miocene	17	10	yes	(convergent)	sand rich	-	-	-	1,680	Sugiaman et al., 2007; Saller et al., 2008
6	**Golo Turbidite System**, offshore East Corsica, France	bathymetry and 2D seismic	Upper Pleistocene - Holocene	32	44	yes	(extensional)	mixed	multiple	12,000	0.0524	860	Pichevin et al., 2003; Gervais et al., 2006(a); Gervais et al., 2006(b); Deptuck et al., 2008; Prélat et al., 2010; Sømme et al., 2011
7	**Joshua Channel System**, DeSoto canyon area, Gulf of Mexico	3D seismic	Pleistocene	-	-	no	passive margin	-	single	-	0.0306	-	Posamentier, 2003
8	**Kutai Pleistocene System**, offshore East Kalimantan, Indonesia	3D seismic	Pleistocene	77.4	22	yes	(convergent)	sand rich	single	-	0.0366	2,000	Saller et al., 2004; Sugaiman et al., 2007; Saller et al., 2008; Prélat et al., 2010
9	**Mississippi System**, offshore Southern United States, Gulf of Mexico	bathymetry and 2D seismic	Pliocene - Pleistocene	685	615	no	passive margin	mixed	single	115,000	0.016	3,300	Weimer, 1991; Twichell et al., 1995; Schwab et al., 1996; Sømme et al., 2009
10	**Mizala Turbidite System**, Mizala, Beltic Cordilleras, SE Spain	outcrop	Miocene	18(?)	4.5(?)	yes	-	sand rich	single	-	0.05	2,000*	Postma & Kleverlaan, 2018
11	**Navy System**, Southern California continental borderland, West of San Diego, USA	bathymetry and 2D seismic	Pleistocene - Holocene	45	45	yes	active margin (transform)	sand rich	single	15,000	0.089	1,900	Normark et al., 1979; Normark & Piper, 1985; Normark et al., 2009
12	**Niger Delta System**, Niger Delta Basin, offshore West Africa	2D and 3D seismic	Eocene - *active*	741	550	no	passive margin	mixed	multiple	65,000	0.018	4,500	Damuth, 1994; Konyuklov et al., 2008; Some et al., 2009; Prélat et al., 2010; Zhang et al., 2016
13	**Santa Monica Basin**, California continental borderland, West of Los Angeles, USA	bathymetry and 2D seismic	Pleistocene - Holocene	70.5	36.5	yes	active margin (transform)	sand rich	multiple	6,600	0.061	900	Normark et al., 1998; Piper et al., 1999; Piper & Normark, 2001; Normark et al., 2009

14	**Tanqua Karoo Turbidite System**, Cape Province, South Africa	outcrop	Cisuralian – Guadalupian	200 (?)	50.7(?)	yes	(convergent)	sand rich	-	-	-	-	Hodgson et al., 2006; Bouma & Delery, 2007; Prélat et al., 2009; Prélat et al., 2010
15	**Tres Pasos Deep-Water Slope System**, Ultima Esperanza District, Southern Chile	outcrop	Upper Cretaceous	50(?)	40(?)	yes	active margin (convergent)	sand rich	-	-	-	900*	Bouma, 1982; Armitage et al., 2009; Romans et al., 2011
16	**Villafranca Deep-Sea System**, offshore NE Sicily, Southeastern Tyrrhenian Sea	bathymetry and 2D seismic	? - active	36.8	13.3	yes	(extensional)	sand rich	single	3,600	0.063	1,250	Gamberi & Marani, 2006; Gamberi et al., 2014
17	**Zaire System**, Congo-Angola margin, Southeast Atlantic	bathymetry and 2D seismic	Pleistocene - *active*	860	550	no	passive margin	mud rich	single	90,000	0.02	5,200	Babonneau et al., 2002; Droz et al., 2003; Marsset et al., 2009; Picot et al., 2016; Dennielou et al., 2017

Table 5.1. List of the deep-marine systems and their regional characteristics analysed in this study. Systems are organised in alphabetical order. System durations are shown as 'epoch' chronostratigraphic divisions; unknown age boundaries are shown by a question mark (?). The Bjørnsonfjellet, Mizala, Tanqua and Tres Pasos system dimensions are estimated from projected schematic models, shown by (?) notation, all other systems are 'true (maximum)' measurements. A system associated with a topographic 'basin' depression, resulting in the preferential catchment of some or all sedimentary deposits, is noted in the field 'basin topography'. The dominant grain-size is classified using the source-work descriptions. Feeder-system types are classified following the approach of Reading & Richards (1994). If a system is not found along a continental margin the overarching tectonic regime is recorded in brackets. Shelf width is an average value, calculated along the width of the system, using the shelf break position as defined by the source-work. 'Maximum water depth' corresponds to the maximum bathymetric water depth observed across the area covered by the system. An asterisk (*) in this column marks the estimated maximum depths for ancient successions, based upon sedimentological inference or gravity modelling (e.g., Postma & Kleverlaan, 2018).

5.3 Results

5.3.1 System-scale variables

The modern and ancient (subsurface and outcrop) deep-marine systems analysed in this study show a strong correlation based upon Spearman's rank correlation coefficient for both the DMAKS-derived October 2018 dataset and the May 2019 dataset ($r_s(16) = 0.89$, $p < 0.001$, $r_s(27) = 0.89$, $p < 0.001$) between their length and width, as measured relative to the average (palaeo-) flow direction (Fig. 5.2). A geometric power-law provides a better fit to the data, in agreement with the findings of Sømme et al. (2009), who studied the scaling relationships of 29 modern and ancient (subsurface) sedimentary systems, including their deep-marine fans. The deep-marine fans considered by Somme et al. (2009) differ to the 'systems' considered in this study, as a fan corresponds with the sedimentary deposits found exclusively on the basin floor. 95% confidence intervals for weighted least-square regression curves for both the October 2018 and May 2019 datasets are seen to overlap (Fig. 5.2).

Among the 17 deep-marine systems derived from the October 2018 dataset, the largest ones (typically those over 100 km in width and length) are found along passive continental margins and are generally fine-grained, mud-rich systems (Fig. 5.3). Fig. 5.3B reports data on systems by feeder type; sediment was supplied to each system by either a 'single feeder' channel or 'multiple' source localities along the coastline based upon the terminology of Reading & Richards (1994). No obvious trend is observed between this variable and system size, possibly because of the limited sample size for systems sourced from multiple points.

Based upon the October 2018 DMAKS dataset, the scale of a system (for which system length is used as a proxy, based upon Fig. 5.3) also correlates with a number of other morphometric parameters, as expected (e.g., see Sømme et al., 2009). For instance, a significant positive log-log relationship between system length and shelf width can be observed (Fig. 5.4A), as system length increases so does the shelf width ($r_s(10) = 0.79$, $p = 0.006$). A significant negative relationship between slope gradient and system length is observed ($r_s(12) = -0.75$, $p = 0.005$), as large systems are characterised by gentle slope gradients (below 0.03 m/m), whereas typically sand-rich, tectonically active, smaller systems are characterised by a wider range of steeper slope gradients between 0.003 to 0.09 m/m (Fig. 5.4B). Similarly to the findings of Sømme et al. (2009), a significant positive correlation, expressed by a power-law relationship, is seen between maximum water depth and system size ($r_s(14) = 0.80$, $p = 0.001$; Fig. 5.4C). For this sample, it is typically large, mud-rich systems that are seen to deposit sediment at depths greater than 2500 m. Analysis of the extended system dataset, taken

from DMAKS version of May 2019, also show similar trends between a system's length and shelf width, slope gradient and maximum water depth, see Fig. 5.4, to the more limited October 2018 data pool, e.g., similar spearman's rank means are observed and the bootstrapped (Efron & Tibshirani, 1986) 95% confidence intervals show a similar data spread. Confidence intervals to the coefficients of determination could not be calculated for the trends shown in Fig. 5.4, because of the limited sample sizes.

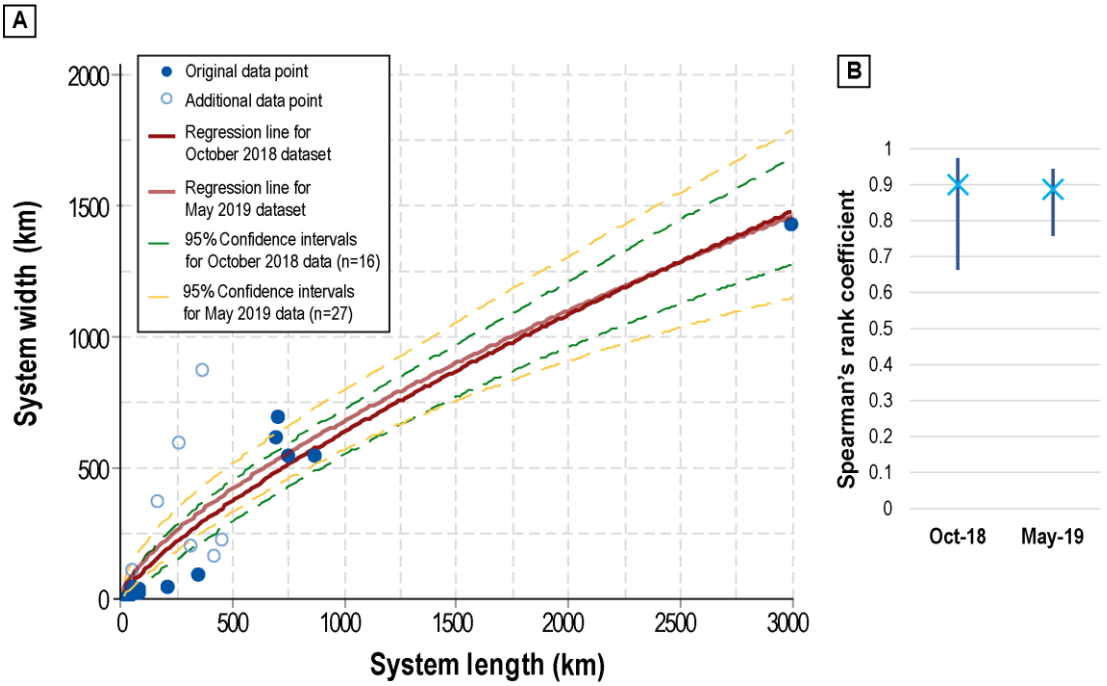

Fig. 5.2. System length versus width power-law regressions and 95% confidence intervals calculated by weighted least-square regression for the October 2018 DMAKS version ($y=17.5x^{0.76}$) and the May 2019 version ($y=43.9x^{0.69}$). B) 95% bootstrapped confidence intervals (method uses percentiles; Efron & Tibshirani, 1986), taken from 1000 samples, for mean Spearman rank correlation values for the original October 2018 (n=16) and extended May 2019 (n=27) datasets. Bar shows extent of 95% confidence intervals, cross (x) marks mean value.

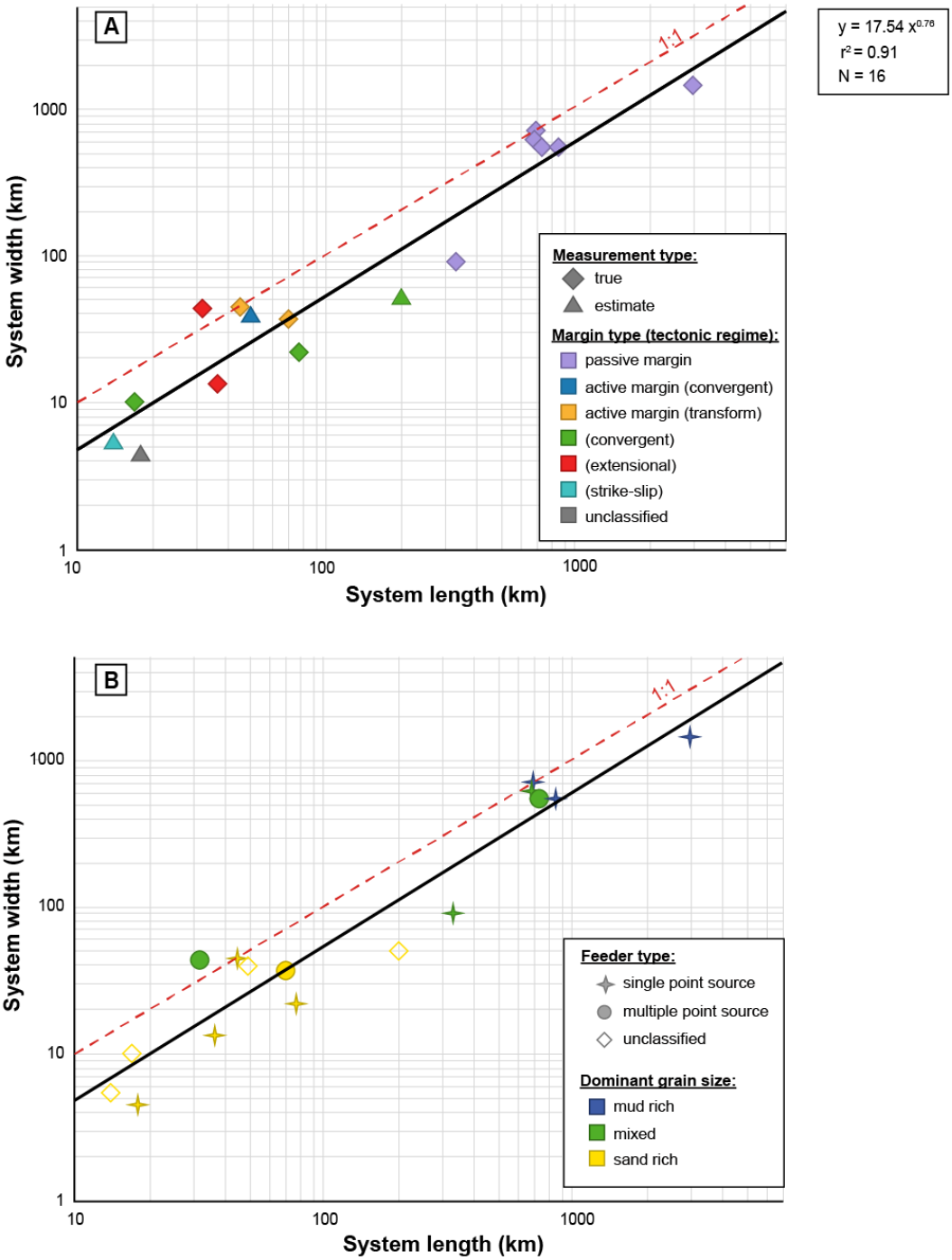

Fig. 5.3. Deep-marine system length and width cross-plot, including 1:1 line (dashed) and exponential best fit (full line). A) Systems are colour-coded by continental margin type, or tectonic setting if the system does not lie near the continental to oceanic crust transition. Measurement types are shown by marker type, as 'estimates' (based upon schematic projections; triangles) or 'true' measurements (diamonds). B) Systems are colour-coded by dominant grain size, while feeder types are denoted by marker shape (based upon the terminology of Reading & Richards, 1994). The N value records the number of systems. The equation of a regression curve and its r^2 value are also reported. Note the logarithmic scales.

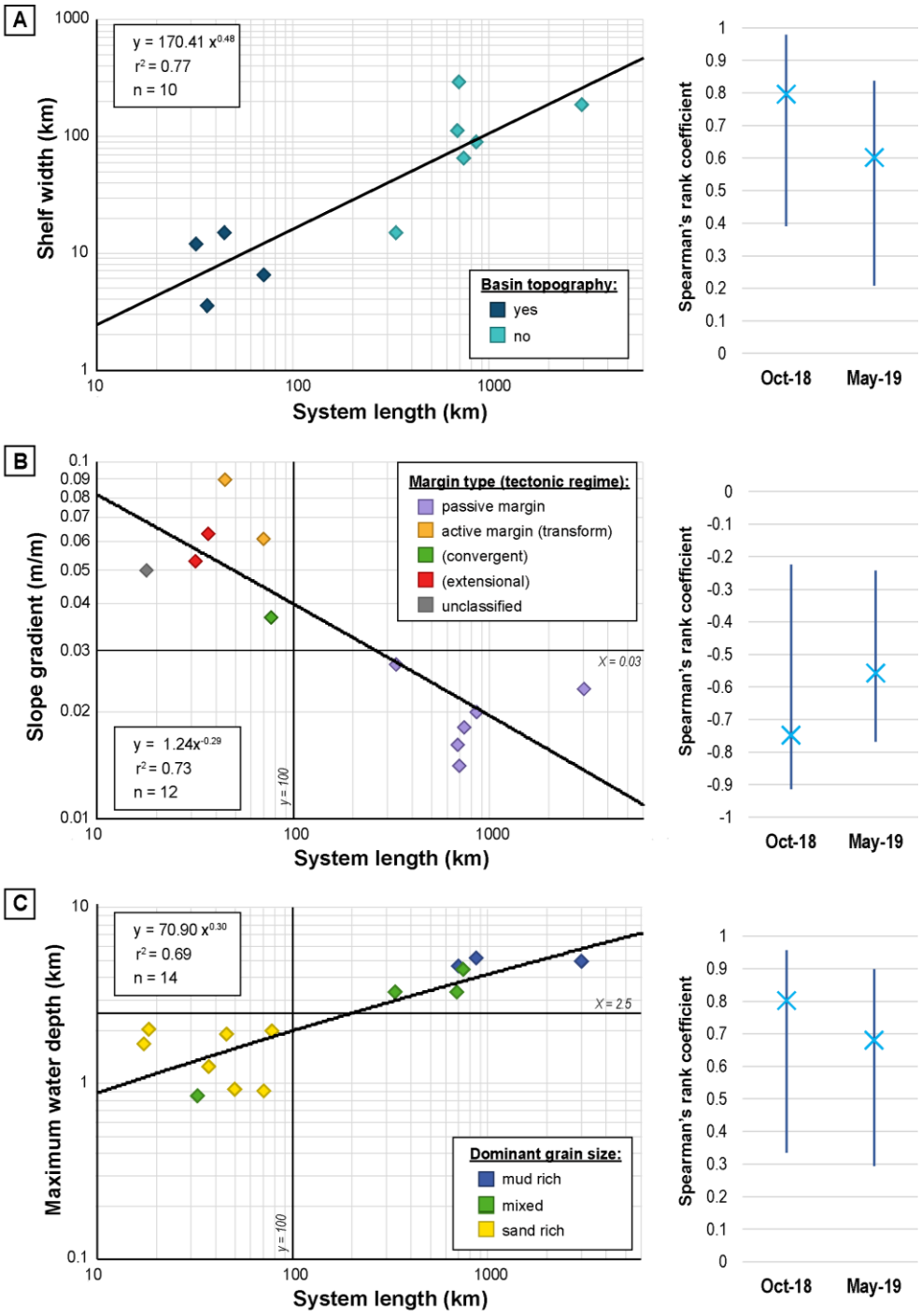

Fig. 5.4. System length plotted against various system morphological characteristics; A) shelf width, classified by the presence of a confining basin topography; B) slope gradient, where systems are classified by margin type (following conventions shown in Fig. 5.3); and C) maximum depositional water depth, classified by dominant grain size. All system length values are 'true' measurements. For each plot, 95% bootstrapped (using percentiles; Efron & Tibshirani, 1986) confidence intervals for Spearman's rank correlation coefficients are also shown for the October 2018 and May 2019 datasets. 1000 bootstrap replications were performed; the bar shows extent of the 95% confidence intervals and the cross (x) marks the mean.

5.3.2 Dimensional relationships of highest-order terminal deposits

A key question is whether the geometry of deep-marine terminal deposits correlates to the examined system-scale parameters. Initial investigation focused upon the dimensions of the highest-order terminal deposits. The width, length and thickness for highest-order terminal deposits all follow a non-Gaussian distribution with a positive skew (Fig. 5.5A, B and C). Both length and width datasets (first and second column of Fig. 5.5) suggest the existence of bimodal distributions if all elements are considered simultaneously, also indicated by kinks observed in their corresponding cumulative frequency curves (Fig. 5.5A and B); these characteristics can be also observed in log-transformed datasets (Appendix E).

The dimensional data have been filtered on a suite of regional parameters that appear to be related to the scale of a system, e.g., slope gradient, shelf width and margin type, Fig. 5.5. Continuous variables have been treated as categorical variables based upon the system-scale findings for this sample of deep-marine systems (cf. Figs. 5.3 and 5.4). For instance, a boundary can be emplaced tentatively between 'large' and 'small' systems for a slope gradient of 0.03 m/m, shelf width exceeding 30,000 m or maximum system water depth of 2,500 m. The margin type has also been categorised into 'passive' and 'other' due to the bias seen in this sample, as all 'large' systems (>100 km in width and length) are found upon passive margins (Fig. 5.3A). System lengths and widths are binned into two categories (< and > 100 km). Although the system scales span four orders of magnitude, this approach has been chosen due to the limited data on terminal deposits associated with systems that are over 1000 km in scale (i.e., the Bengal), or below 10 km (i.e., the Mizala system, Table 5.1).

Distributions of highest-order terminal-deposit length, width and thickness are presented as box plots (first, second and third column of Fig. 5.5, respectively). The data are filtered by depositional-system parameters (Fig. 5.5J-U), data type (Fig. 5.5L) and the "local" water depth and gradient (Fig. 5.5D-H), i.e. the gradient and water depth at the location of the terminal-deposit, while thickness is also categorised by local confinement (*sensu* Prélat et al., 2009; Fig. 5.5I). All distributions are positively skewed, as the mean values lie to the right of the median. For length and width distributions (first and second column of Fig. 5.5), similar trends are identified between each parameter's pair of end-member box plots. For example, each parameter shows one category with a tighter data range, associated with a smaller mean and standard deviation (only system width shows a larger standard deviation, Fig. 5.5T; Appendix E), whereas the second category has a wider spread, and a median typically larger than the 75th percentile of the former category. The medians of the two categories for each parameter

are generally comparable to the two peaks (modes) observed in the global distributions (Fig. 5.5A and B).

To test the difference between the populations of the two categories for each system parameters, the non-parametric Mann-Whitney U statistic has been calculated (Shier, 2004). Smaller 'U' values denote less overlap between mean ranks, and thus a more significant result (i.e. the two populations are more different). The 'local' depositional characteristics, i.e., water depth and gradient at the location of the terminal deposit (Fig. 5.5D, E, G and H), show less overlap between the two data categories based upon the U test results; additionally, the data category associated with a smaller median (i.e., local gradients >0.01 m/m and water depths <2500 m) are seen to align more closely with the first peak in the global bimodal distributions for both length and width.

Smaller terminal deposits are associated with smaller systems (<100 km in width or length), with steeper slope gradients (>0.03 m/m), narrower shelves (<30 km) and shallower water depths (<2500 m); these conditions are usually found along active margins. Larger terminal deposits tend to be associated with larger systems, which are usually found along passive margins, and are characterised by shallower slope gradients, wider shelves, and deeper and gentler (>2500 m, 0.01 m/m) sea-floors. However a much wider range of dimensions characterises the 'large system' category. Outliers to these distributions can be observed; for instance the outlier identified for shelves narrower than 30 km (Fig. 5.5M and N) is associated with the Al Batha system, which is classified as a 'large' system (over 100 km) in relation to its length but as a 'small' system related to its width – suggesting that differences in system size are not easily captured based upon order of magnitude end-members. The ancient Tanqua Karoo, which is thought to be positioned along a convergent margin, is also classified as a 'small' system based upon its inferred system width; however some of its highest-order terminal deposits plot as significant outliers (Fig. 5.5P, Q and T). The cluster of outliers in the terminal deposit length plots, associated with 'large systems' and their related characters, correlate to the Zaire and Amazon. Interestingly, the Bengal, which is the largest system considered in this study, plots its highest-order terminal deposits below the first quartile for both length and width. Therefore the size of a highest-order terminal deposit does not scale directly with the overall system size, supporting the recent findings of Pettinga et al. (2018).

Where available data exists, the thickness of highest-order terminal deposits have also been filtered by depositional-system characters, i.e., system length, margin type, significant basin topography (i.e., where the locality of sediment deposition is influenced by the underlying topography; Fig. 5.5O, R and U), as well as by local confinement (*sensu* Prélat et al., 2010) and local gradient (Fig. 5.5F and I). These plots show no significant distinction between thickness

mean ranks based upon any of the considered parameters, as Mann-Whitney U test 2-tailed p-values exceed the 0.05 significance level. Thickness data has also been categorised by data type to substantiate whether the effects of sediment compaction are significant (Fig. 5.5L); for this particular sample both modern and outcrop results show a similar spread in data.

Fig. 5.5 (A-U). *(overleaf)* Highest-order terminal-deposit dimensions. Width, length and thickness histograms, as well as cumulative frequency curves (red line) shown alongside projected normal distribution curves (black line) are shown in A, B and C respectively. The kinks observed in the width and length cumulative distributions are marked with by an arrow. Population mean (μ), standard deviation (σ), skewness and population size (N) statistics are shown for each global dimension distribution (A, B, C). Box plots for length (blue), width (orange) and thickness (green) categorise the dimensional data by local depositional gradient (D, E, F), local water depth (G, H), slope gradient (J, K), shelf width (M, N), margin type (P, Q, R), system length (S, U) and system width (T). Thickness is further classified by local confinement (I), data type (L) and basin topography (O). A box plot is shown where a category sample size (n) is greater than 7 points. Median lines, mean values (shown by a cross), and asterisks (*) denoting statistically identified outliers are shown for each box plot. Outliers are numbered corresponding to the system ID shown in Table 5.1. Significant Mann-Whitney U test results are recorded in bold, recognised by a 2-tailed p-value below 0.05.

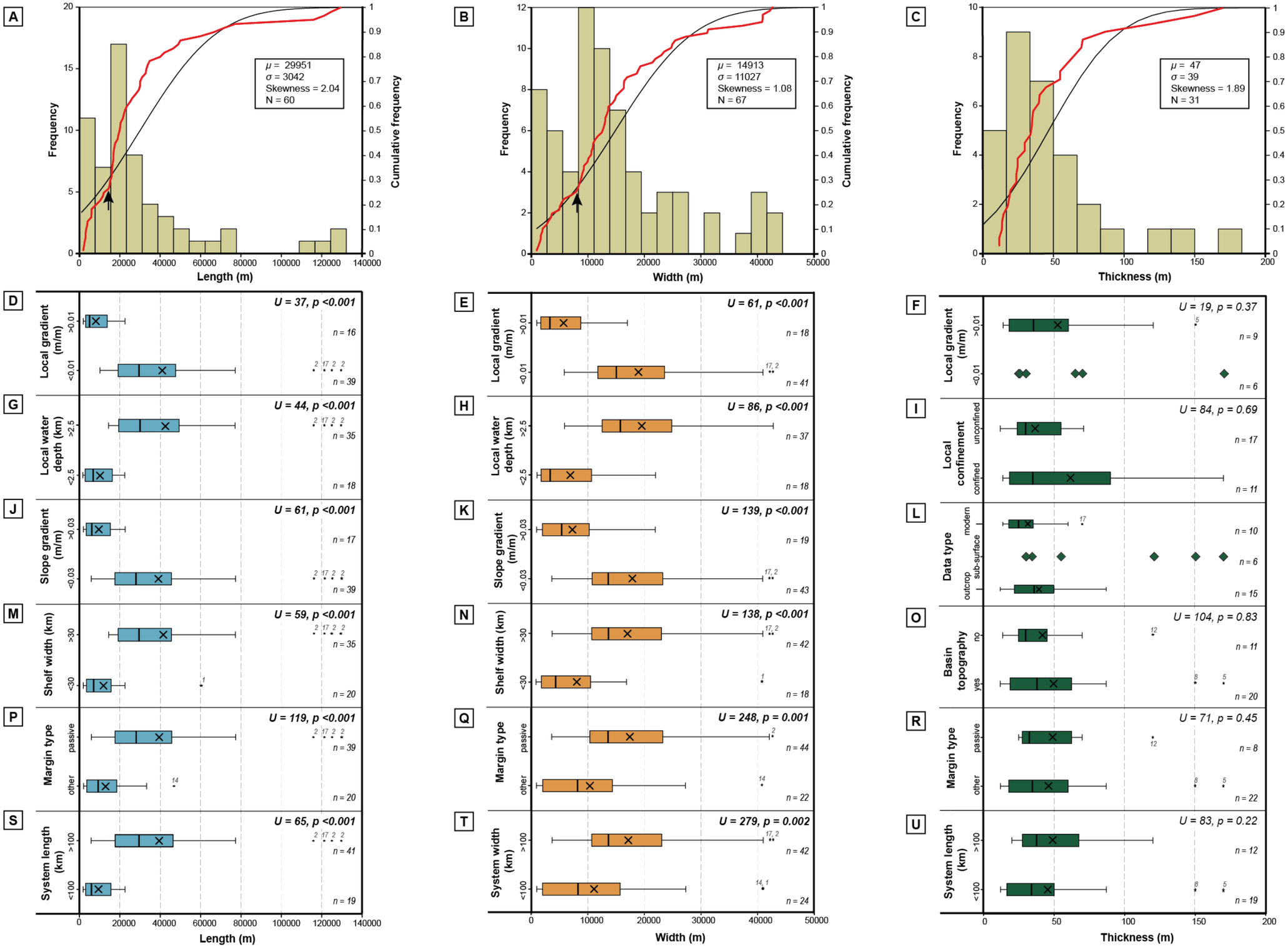
A
μ = 29951
σ = 3042
Skewness = 2.04
N = 60
Frequency
Cumulative frequency
Length (m)
B
μ = 14913
σ = 11027
Skewness = 1.08
N = 67
Frequency
Cumulative frequency
Width (m)
C
μ = 47
σ = 39
Skewness = 1.89
N = 31
Frequency
Cumulative frequency
Thickness (m)
D
Local gradient (m/m)
>0.01
<0.01
U = 37, p <0.001
n = 16
n = 39
E
Local gradient (m/m)
>0.01
<0.01
U = 61, p <0.001
n = 18
n = 41
F
Local gradient (m/m)
>0.01
<0.01
U = 19, p = 0.37
n = 9
n = 6
G
Local water depth (km)
>2.5
<2.5
U = 44, p <0.001
n = 35
n = 18
H
Local water depth (km)
>2.5
<2.5
U = 86, p <0.001
n = 37
n = 18
I
Local confinement
unconfined
confined
U = 84, p = 0.69
n = 17
n = 11
J
Slope gradient (m/m)
>0.03
<0.03
U = 61, p <0.001
n = 17
n = 39
K
Slope gradient (m/m)
>0.03
<0.03
U = 139, p <0.001
n = 19
n = 43
L
Data type
modern
sub-surface
outcrop
U = 104, p = 0.83
n = 10
n = 6
n = 15
M
Shelf width (km)
>30
<30
U = 59, p <0.001
n = 35
n = 20
N
Shelf width (km)
>30
<30
U = 138, p <0.001
n = 42
n = 18
O
Basin topography
no
yes
U = 104, p = 0.83
n = 11
n = 20
P
Margin type
passive
other
U = 119, p <0.001
n = 39
n = 20
Q
Margin type
passive
other
U = 248, p = 0.001
n = 44
n = 22
R
Margin type
passive
other
U = 71, p = 0.45
n = 8
n = 22
S
System length (km)
>100
<100
U = 65, p <0.001
n = 41
n = 19
T
System width (km)
>100
<100
U = 279, p = 0.002
n = 42
n = 24
U
System length (km)
>100
<100
U = 83, p = 0.22
n = 12
n = 19
Length (m)
Width (m)
Thickness (m)

5.3.3 Geometrical relationships of hierarchically nested terminal deposits

In deep-marine clastic systems, terminal deposits are known to develop over a range of scales which can be described in a hierarchical framework (Deptuck et al., 2008; Prélat et al., 2009; Straub & Pyles, 2012; Flint et al., 2011). A strong correlation between the length and width of terminal deposits from all hierarchical levels is observed for both the October 2018 and May 2019 datasets (Fig. 5.6), with nearly all data plotting below the 1:1 line ($r_s(158) = 0.93$, $p < 0.001$; $r_s(193) = 0.94$, $p < 0.001$). The October 2018 DMAKS dataset best fits a power-law regression line, showing tight 95% confidence intervals ($y=14.3x^{0.67}$). However, the extended May 2019 dataset, which includes terminal deposits that are an order of a magnitude larger, displays better fit by a linear regression ($y=0.39x + 2093$), which does overlap the confidence intervals of the smaller dataset from the October 2018 DMAKS version.

Filtering terminal deposit length and width by the local depositional gradient shows that gentler gradients (<0.01 m/m) are associated with a wider spread of geometries and with the largest values of planform sizes (Fig. 5.7; see also Fig. 5.5D and E). This cross-plot (Fig. 5.7) includes all terminal deposits that develop above a 'bed' scale (*sensu* Campbell, 1967), where highest-order terminal deposits are shown in yellow, while grey markers refer to lower-order or deposits of unknown order. The same form of plot also showing a power-law regression line was published by Pettinga et al. (2018; Fig. 5.7B), colour-coding terminal deposit planform geometries based upon the interpreted 'hierarchical ordering' (*sensu* Pettinga et al., 2018). The deposits cannot be seen to discretely cluster based upon hierarchical orders, although their analysis suggests two overlapping hierarchical sequences which they attribute to the deposits degree of confinement; confinement is defined in their study as the existence of lateral and/or frontal topographic relief that affects sediment run-out (*sensu* Prélat et al., 2010); however no guidelines on how to recognise such relief (e.g., scale or extent of a topographic high) is provided. Note that 'highest-order terminal deposits' as defined in DMAKS do not all belong to the same 'hierarchical order', and additionally that a 'H4, lobe complex' is not necessarily the largest terminal deposit expression within a system.

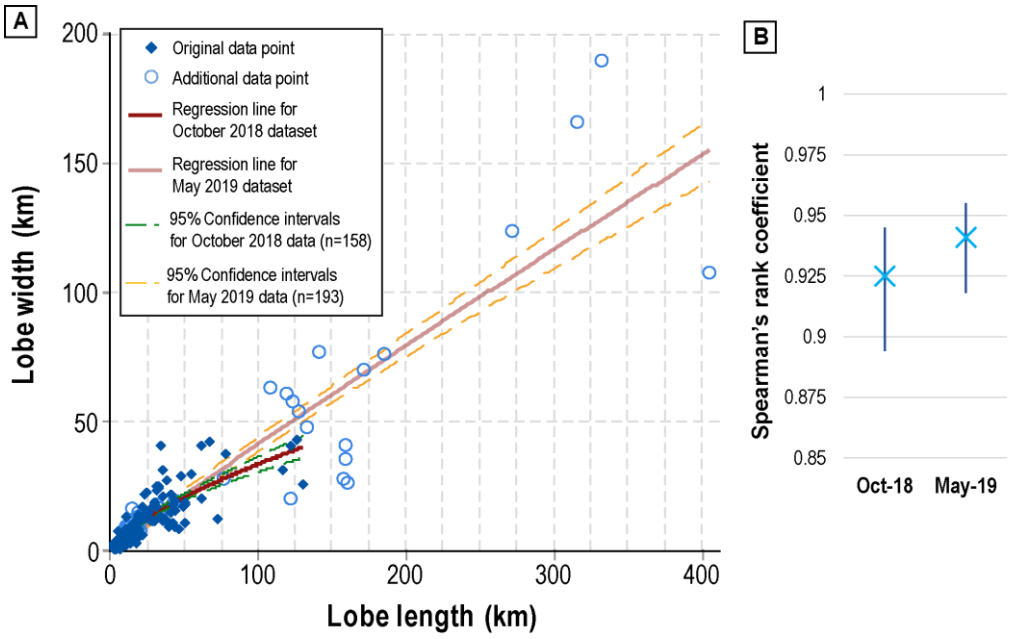

Fig. 5.6. A) Terminal deposit length-versus-width power-law regression lines and 95% confidence intervals calculated by weighted least square regression for the original DMAKS dataset ($y=14.3x^{0.67}$) and the extended dataset ($y=0.8x^{0.94}$). B) Bootstrapped 95% confidence intervals and the mean Spearman rank correlation values for the October 2018 (n=158) and May 2019 (n=193) datasets, based on 1000 samples. Bootstrapping was undertaken using a percentile method, Efron & Tibshirani, 1986.

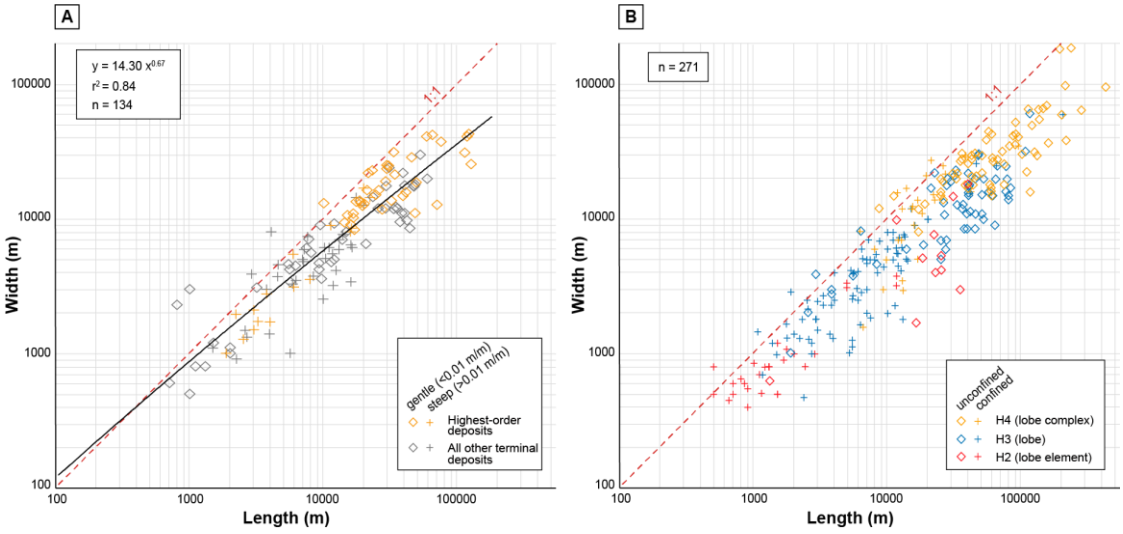

Fig. 5.7. A) Terminal deposit width versus length cross-plot on a logarithmic scale. Only deposits that can be classified by their local depositional gradients are shown, see marker type. Deposits are colour coded by hierarchical order. Power-law regression line and a 1:1 trendline are plotted. B) Length to width plot redrawn from Pettinga et al., 2018; deposits are colour-coded by the source-works own hierarchical classification scheme (H4, H3, H2 annotation) and classified by 'local confinement' by marker type (*sensu* Prélat et al., 2010). A 1:1 trendline is shown.

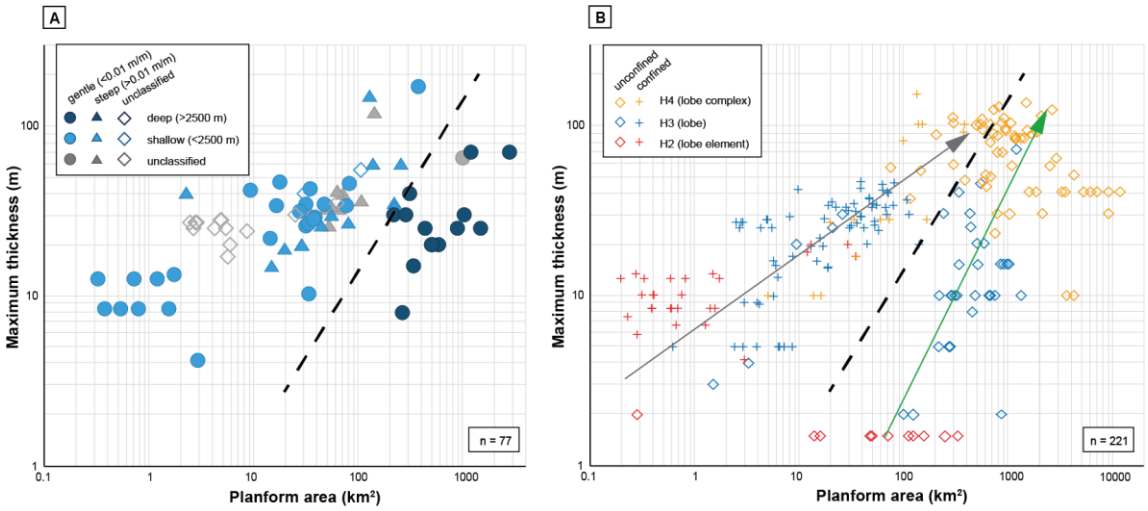

Fig. 5.8. Cross-plots of terminal-deposit maximum thickness against planform area. A) Terminal deposits classified by local gradient (shape) and local water depth (colour). Areas are measured directly from the source-work, while maximum thickness is derived from 2D or 3D data. B) Same type of plot redrawn from Pettinga et al. (2018), with terminal deposits classified by relative confinement and hierarchical order (H2 to H4 *sensu* Pettinga et al., 2018). The two trends identified by Pettinga et al. (2018) are shown by corresponding arrows. Planform areas are either measured from the source-work or calculated based upon the equation for the area of an ellipse. The dashed line separates the data pools related to the local parameters.

Building upon the ideas presented by Prélat et al. (2010), Pettinga et al. (2018) plotted terminal-deposit planform areas against their maximum thickness and identified two distinct hierarchical sequences which they again attribute to confinement (Fig. 5.8B). The October 2018 DMAKS dataset also identifies two discrete data pools that can be more successfully characterised by local depositional parameters (Fig. 5.8A) - albeit from a smaller sample size than Pettinga et al. (2018) as only planform areas measured directly from the source-work are presented, thus the ability to discern smaller-scale geometries within seismic datasets is limited in this sample. The two differing data clusters were attributed to differences in confinement in the studies by both Prélat et al. (2010) and Pettinga et al. (2018) but anomalies to this proposed trend are observed such as the unconfined Bengal Shwe deposits included in the Pettinga et al. (2018; taken from Yang & Kim, 2014) dataset which plot within the 'confined' trend (above the grey arrow in Fig. 5.8B). These anomalies are not observed when classifying the data by alternative local depositional variables, e.g., Fig. 5.8A shows that terminal deposits (of all hierarchical levels) with larger planform areas (>200 km^2) are found in basin plain physiographic settings with gentle local gradients (<0.01 m/m), coinciding with deeper depositional water depths (>2500 m). Terminal deposits with smaller planform areas

(< 400 km^2) are found upon both gentle and steep local depositional gradients, but (where available data permits) are all observed to be deposited at shallower water depths (<2500 m), including the unconfined Bengal terminal deposits. Both datasets, from this study and Pettinga et al. (2018), show the terminal deposit volumes to become more similar as scale increases (>30m thick), an idea also suggested by Prélat et al. (2010).

5.3.4 Multivariate analyses

The ability to extract multiple characteristics for a specific object from DMAKS allows multivariate analyses to be conducted. Only a small sample of data is currently available for such statistical analysis at this time (n = 14), as a limited number of terminal deposits, irrespective of hierarchical significance, contain data for all of the studies key variables. Principal component analysis of terminal deposits (Fig. 5.9) and hierarchical cluster analysis of the selected variables (Fig. 5.10) have been conducted considering 9 main parameters: system length, system width, shelf width, slope gradient, terminal deposit length, terminal deposit width, terminal deposit thickness, local gradient and local water depth.

Principal component analysis suggests that two significant components, with eigenvalues >1 (Fig. 5.9A), account for 89% of the total variance observed within the data. The first component groups variables related to the 'environment' of lobe deposition, i.e., the system width and length, slope gradient, shelf width, local depositional gradient and local water depth; Fig. 5.9B, see variables > +/-0.5. Component 2 is largely a combination of variables that describe individual terminal deposit's geometry (i.e., thickness, width and length). The cluster analysis (see heat map and dendrogram in Fig. 5.10) highlights similarity in the behaviour of slope gradient and local depositional gradient due to their negative polarity (see Fig. 5.9B and C). Within component 1 terminal deposit width and length still show significant component scores (width = 0.47, length = 0.59 based upon the PCA rotated component matrix), unlike terminal deposit thickness, which contributes significantly to component 2 (rotated component matrix score = 0.91) as illustrated in Fig. 5.9D. The score plot shown in Fig. 5.9C suggests that the individual terminal deposits tend to be grouped by tectonic setting (i.e., as being associated with passive margins or not) based upon component 1: as passive margins plot positive component 1 scores along the x axis, while active margin settings produce negative component 1 scores. An anomaly to this trend is seen, as a lobe case from the passive margin of the Al Batha system plots within the negative component 1 'active margin' group.

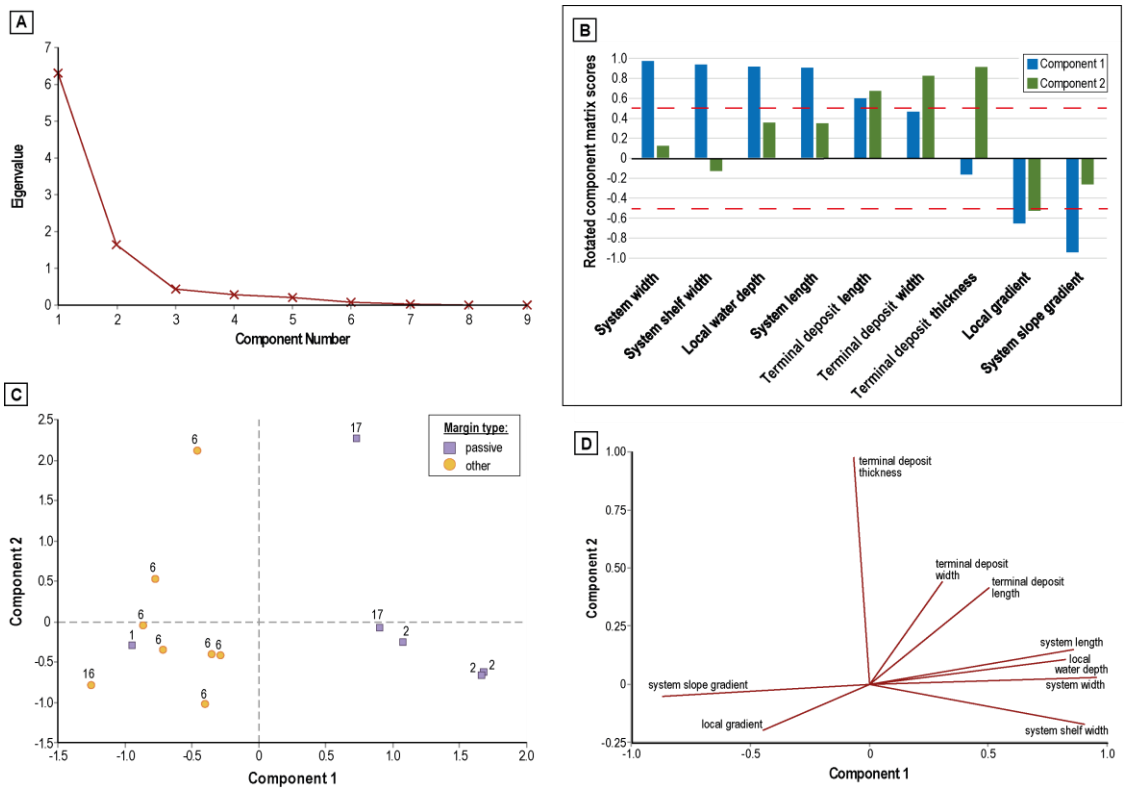

Fig. 5.9. Results of a principal component analysis of 9 continuous variables (system width, system length, system shelf width, system slope gradient, terminal deposit width, terminal deposit length, terminal deposit thickness, local gradient and local water depth). A scree plot for the 14 cases is shown in A) identifying 2 key components with eigenvalues > 1. The bar chart in B) highlights the scores of the variables in each component based upon varimax rotated component matrix scores, red dashed lines highlight scores > +/- 0.5. A score plot is presented in C) classified by margin type (passive or other) and each point is labelled by its system ID (see Table 5.1). D) presents a loading plot for each variable considered.

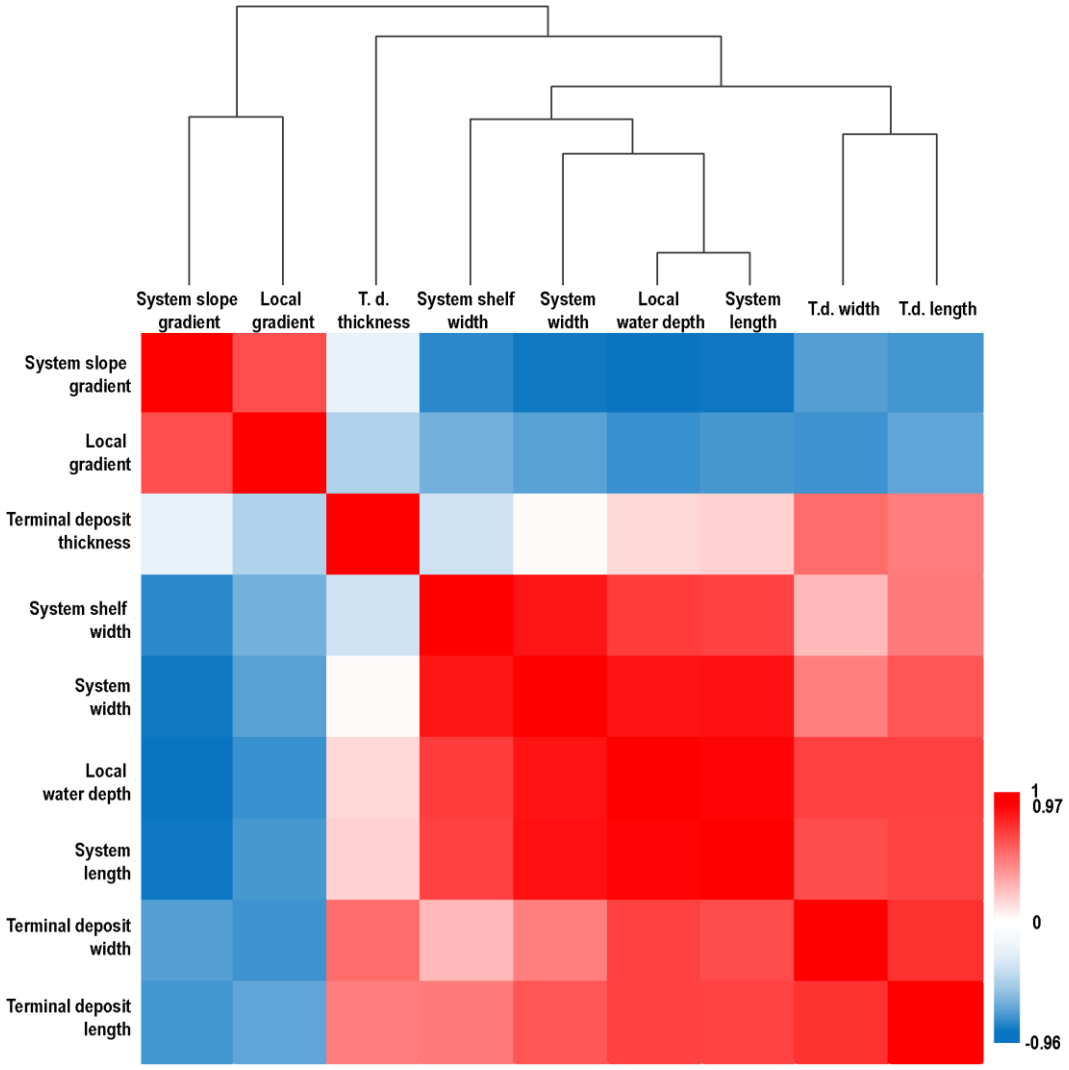

Fig. 5.10. Heatmap of the Pearson's correlation of the studied variables and corresponding dendrogram derived from the hierarchical clustering based on variables' proximity matrix. The heatmap scales from red (highest correlation coefficient, which here equates to the autocorrelation, i.e., diagonal values) to blue (lowest correlation coefficient), the actual maximum R value (0.97) and minimum R value (-0.96) shared between any two distinct variables are annotated on the scale bar. N = 14.

5.4 Discussion

5.4.1 Influences on the scale of deep-marine systems

The width and length of deep-marine systems are positively correlated (Fig. 5.3; Sømme et al., 2009, Snedden et al., 2018). This study shows that modern, subsurface and ancient systems plot along a similar power-law trend. The relationship between system length and width is therefore seen to be independent of its depositional age, or duration; supporting the findings of Wetzel (1993) conducted upon river-fed deep-marine systems. A strong

relationship (based on Spearman's rank correlation) between system length and width is seen in both the smaller October 2018 dataset, as well as the extended May 2019 dataset.

The scale of a system can be inferred based upon a number of regional characteristics, such as slope gradient, shelf width and maximum water depth (Fig. 5.4). A 'large' system (generally over 100 kms in width and length) typically has a shelf width over 30 km, slope gradients below 0.03 m/m, depositing at a maximum water depth over 2500 m (Fig. 5.4) and it is not confined by seafloor 'basin' topography. Larger systems therefore show a gentler shelf to basin plain profile. This longer sediment pathway (from source-to-sink) may help flows to progressively become finer grained due to preferential deposition of coarse grain size fractions, possibly allied with erosion of finer materials, resulting in a deep-marine system dominated by finer-grained deposits (Stow et al., 1985; Milliman & Syvitski, 1992; Michael et al., 2013). All 'large' systems in this study are found along passive continental margins, as opposed to 'small' systems found in tectonically active settings. It should be noted that in the study of Sømme et al. (2009), large fans were not exclusively associated with passive margins: based upon their classification large fans included those that are from margins that cannot be readily classified as passive or active *sensu* Shanmugam & Moiola (1988). The regional characteristics of a system (e.g., shelf width, slope gradient, water depth, basin topography and tectonic setting) can also be used to predict the relative size of a system. Reading & Richards (1994) suggested that deep-marine systems are greatly influenced by the nature of the sediment supply, which is itself related to the type of feeder system. In the present study, the type of feeder system does not show a significant correlation with the size of a system; however this result must be considered provisional, as it needs to be substantiated by the analysis of a larger data pool.

Finer-grained systems relating to relatively wider shelves compared to coarser grained systems have also been documented by Sweet & Blum (2016). Reading & Richards (1994) have also observed gentler slope gradients as grain-size decreases. Paris et al. (2016) show shelf dimensions (width and depth) to be divisible into tectonic setting categories, whereby active settings are characterised by narrower shelves than passive margins (~<120 km based upon global mean averages). Previous research has identified tectonics as a key influence upon deep-marine system bathymetry and morphology (i.e., size and gradients) of shelf, slope and basin topography (Nelson & Nilsen, 1984; Mutti & Normark, 1987; Shanmugam & Moiola, 1988; Richards et al., 1998; Bouma, 2000, 2004; Weimer & Slatt, 2007(a); Nelson et al., 2009; Pickering & Hiscott, 2016). Tectonics also control the configuration of the onshore catchment, including the distance from the sediment source, in turn influencing climate and subsequently rates, modes and calibre of offshore sediment supply (Bouma, 2000; 2004;

Nelson et al., 2009). This would suggest that the tectonic setting can be inferred as the dominant influence upon the regional characteristics of a system (e.g., margin type, shelf width, slope gradient, maximum water depth and dominant grain size) ultimately controlling the system's resultant size.

5.4.2 Influences on the length and width of terminal deposits

DMAKS was used to test whether the parameters observed to influence overall system dimensions are also seen to affect the dimensions of lobate terminal deposits. For each system parameter, two end-member classes were defined, based upon the system-scale findings. Filtering the highest-order terminal deposits by these classes does suggest that terminal deposit length and width are influenced by the system-scale parameters (e.g., margin type, shelf width, slope gradient, and system size), as each parameter shows a significant difference between their two classes mean ranks based on U statistics (Fig. 5.5). The median values for the two classes of each system parameter appear to map with the two modes that confer bimodality to global length and width populations (first and second columns in Fig. 5.5). The length of highest-order terminal deposits are more significantly correlated with these system parameters than the widths, reflected in the length dimensions smaller U test results.

The general trend observed suggests that smaller planform geometries, $\tilde{x}$ (sample median) = 6000 m long and 8275 m wide, are associated with 'small' deep-marine systems (<100 km width and length) typical of active settings, and their generally shallow water depths (<2500 m), steep slopes (>0.03 m/m) and narrower shelves (<30 km), compared to larger systems and their typically larger terminal deposit geometries ($\tilde{x}$ = 29500 m long, 13660 m wide). These 'small' systems are also predominantly sand-rich (Table 5.1). A similar pattern was also identified for deep-marine channel lengths by Covault et al. (2012), as longer canyon-channel systems are typically identified in large, mud-rich, mature systems found along passive margins.

System scale, margin type, slope gradient and shelf type are shown to be interconnected based upon the similar data distributions (data range, median, mean and standard deviation results) that are seen between each parameter's end-member classes (Fig. 5.5). The correlation observed between the system-scale parameters and the resultant terminal-deposit scale could suggest that the overarching tectonic regime acts as a control upon element-scale deposition in a similar manner to what is seen at the system scale. However, outliers are observed. For instance, the ancient Tanqua Karoo system is thought to have been

deposited along a convergent margin (Bouma & Delery, 2007), but its highest-order terminal deposits plot above both the length and width median values for passive margins (see 'other' margin type outliers in Fig. 5.5P and Q). The Tanqua system sediment source was analysed by Scott et al. (2000) who suggested that the system was characterised by a long sediment pathway, similarly to systems hosted on passive margins, resulting in very-fine to fine-grained deposits. They also imply from their findings that the Tanqua was deposited during times of tectonic quiescence, overall suggesting a 'passive margin' style of deposition. This draws attention to the importance of depositional timescales, as the tectonic signal observed in a system, and its duration, is not usually directly comparable to the depositional timescale and its sedimentation rates, made more uncertain by the fragmentary state of the stratigraphic record (Sadler, 1981; 1991; Hawie et al., 2015; Miall, 2015; Nyberg et al., 2018).

With reference to the Tanqua system, Scott et al. (2000) suggested that the tectonic setting is not the most reliable predictor of the sedimentary characteristics of deep-marine systems. Instead, they suggest that grain size has a higher predictive power, leading to the classification of deep-marine systems based on grain size by Bouma et al. (2000). However, a standard and objective classification of depositional systems grain size is not yet readily employed in sedimentological investigations, which makes it difficult to undertake meaningful comparisons between systems based upon their dominant grain-size. For this reason, this qualitative attribute has not been examined as a system parameter at the element-scale. As more data is added to DMAKS, it may become possible to analyse grain-size trends across a system statistically, e.g., if the average grain size could be calculated for a system, based upon facies data from a range of architectural element types along the systems depositional profile.

The regional characteristics (i.e., system scale, shelf width, slope gradient and margin type) end-member categorisations are based upon discretisation of continuous data; consequently, it is the intermediate scale systems, those found mid-way along the system width-to-length power-law regression line, that plot as outliers in the distributions of morphometric parameters (e.g., the Al Batha's <30 km shelf and ≥0.03 m/m slope gradient). The system width outliers are associated with the 'small' Tanqua and Al Batha turbidite systems, which both show system lengths >100 km (Table 5.1). No direct proportionality is therefore observed between system dimensions and those of their corresponding highest-order terminal deposits. The Bengal system and its highest-order terminal deposits again reflect this, as the Bengal, 140 times the area of the Al Batha system, is characterised by terminal deposits with width and length below the median values of the complete dataset. This would suggest that while the systems tectonic setting and associated regional characteristics (i.e.,

shelf width, slope gradient, system scale and margin type) display relationships with the terminal-deposit planform geometries, they are not the primary control upon deposition. There must be other significant controls, or a complex suite of inter-connected relationships. The non-proportional relationship between the scale of a system and its internal element scales is also likely affected by the different methods of sediment distribution in a system, e.g., through flow filtering and sediment bypass processes.

A strong relationship exists between the length and the width of terminal deposits (Fig. 5.6B), seen in both the October 2018 DMAKS dataset and the May 2019 dataset which contains 25% additional terminal deposit measurements. While tight confidence intervals are found for both the October 2018 and May 2019 dataset regressions (Fig. 5.6A), an agreement between the types of regression is not observed: the original dataset is better approximated by a power-law regression, while the extended dataset is better approximated by a linear regression. This discrepancy reflects that fact that the smaller October 2018 dataset was limited to terminal deposits below 1000 km – a bias that is commonly observed in other published lobe studies, e.g., Prélat et al. (2010), Zhang et al. (2017) and Pettinga et al. (2018).

The results from this study suggest that the local depositional gradient may be a more significant predictor of lobate planform dimensions. For instance, small lobate geometries are always found upon steep local gradients (>0.01 m/m: $\tilde{x}$ = 5000 m long, 3325 m wide), irrespective of their overall system size (<0.01 m/m: $\tilde{x}$ = 29500 m long, 15000 m wide). Less overlap is observed between the local gradient mean ranks (length U = 37, width U = 61) compared to the regional characteristics such as margin type (length U = 119, width U = 248; Fig. 5.5). This autogenic parameter (i.e., local depositional gradient) is therefore seen to have a more significant influence upon the highest-order scale of deposition as opposed to the allogenic system-scale variables (i.e., margin type, system size and morphology). The increased significance of 'local gradient' as an improved predictor of terminal deposit dimensions is further recognised by the more discrete data distributions and their larger differences between mean ranks, which align more closely to the apparent bimodality observed in the global length and width populations, compared to the 'system-scale' variables (Fig. 5.5). Experimental work has shown underlying gradients to affect the resultant depositional geometry; for example, a gentler depositional gradient is seen to encourage more elongate geometries (Ouchi et al., 1995). Modern and subsurface studies have also attributed geometrical differences in lobate deposits to physiographic gradient changes, e.g., the Miocene Agbada Formation of the Niger Delta (Zhang et al., 2016) and East Corsican Golo system (Deptuck et al., 2008). Terminal deposits can be deposited anywhere along the slope to basin-plain profile (Gamberi & Rovere, 2011). However, an association can be seen

between system configurations and their local site of deposition. For instance, 'larger' systems (>100 km) and their typically large highest-order terminal deposits are generally found deposited upon basin plain environments and their gentler gradients (>0.01 m/m; Boggs, 1995) at water depths over 2500 m (Figs. 5.7 and 5.8). This preferential association between local gradient and physiographic setting can be inferred to be a likely cause as to why system-scale variables are seen to evoke significant correlations with terminal deposit geometries. However, variations to this general trend are found, e.g., within this study 'small' systems can be seen to deposit upon gentle basin floor topography, as well as the slope, such as the Golo, Santa Monica and Navy, while the 'large' Niger system also deposits upon both the slope and basin plain environments. Thus, a direct link between system scale and the local depositional gradient cannot be established.

Terminal deposit planform geometries, including the highest-orders and their internal hierarchically nested units, show a strong correlation just under the 1:1 width-to-length ratio; this is similar to system width-to-length relationship (Figs. 5.3 and 5.7). This consistent trend is observed across all hierarchical orders, suggesting a similarity between the dominant mechanisms controlling planform geometry across all depositional scales. The highest-order lobate units are not all constrained to a single 'hierarchical order'. For instance, the Bengal highest-order terminal deposits would be recognised as a lower hierarchical class than the Tanqua and Al Batha highest-order terminal deposits due to their lower number of bounding surfaces – possibly accounting for some of the differences seen between these elements' dimensions. The significance of hierarchy has not been considered in detail within the scope of this study and future work would therefore be necessary to study its influence.

5.4.3 Influences on the 3D geometry of terminal deposits at the element-scale

Highest-order terminal deposit thickness data exhibit a unimodal distribution (Fig. 5.5C). In contrast to the highest-order terminal deposit length and width dimensions, the system-scale (i.e., margin type, system scale, basin topography) and local depositional characteristics (i.e., gradient and confinement) considered in this study are not seen to be significantly related to the thickness of the highest-order terminal deposits (validated by the U test statistics, Fig. 5.5, third column). Comparing terminal deposit maximum thicknesses against their corresponding planform areas for terminal deposits of all hierarchical significance (Fig. 5.8) supports the findings of Pettinga et al. (2018) who identified two distinct trends which merge at the largest scale; proportionally thicker deposits relative to their planform areas versus 'thinner' deposits relative to their planform areas (Fig. 5.8B). The coalescence of terminal

deposit volumes at the largest scales supports the findings of Prélat et al. (2010) who attributed this maximum volume to “intrinsic processes”, conceivably related to i) sediment filtering, as material is transported across the deep-marine system, or ii) lobe growth reducing downstream gradients, forcing upstream avulsion. Terminal deposit 3D morphology is thus shown to have a finite upper limit, which may account for the unimodal distribution in highest-order deposits (and a lack of significant end-member controls; Fig 5.5). Lobate geometry thus appears to be scale-dependent, a property that is suggestive of a ‘hierarchical’ organisational style (Straub & Pyles, 2012).

Zhang et al. (2016) proposed that when accommodation space is limited laterally, stacking patterns are altered resulting in thicker terminal deposits. Covault & Romans (2009) also suggested such a link between accommodation space and the overall system thickness, as thicker deposits were identified where sediment run-out was blocked by basin topography (e.g., in the California borderlands or Gulf of Mexico intraslope basins). ‘Confinement’ has been identified by many as a key control upon deposition of lobate units (Covault & Romans, 2009; Prélat et al., 2010; Pettinga et al., 2018; Fig. 5.8B). Local topography is seen to affect the stacking patterns and thus resultant terminal geometry of deep-marine deposits (e.g., Satur et al., 2000; Brunt et al., 2013; Picot et al., 2016; Pemberton et al., 2016). ‘Confinement’ is described as lateral and/or frontal topographic relief, such as a basin or structural high, that affects sediment run-out (following the definition used by Prélat at al., 2010 and Pettinga et al., 2018). Confinement is often classified from a limited view of the relief underlying a system and not constrained to a specific scale and so can be a subjective term. The subjectivity of this variable and the lack of a standardised, quantitative and broadly applicable classification has led to its limited usage in this study. However, it is necessary to remember that confinement is heavily influenced by the large-scale system configuration, e.g., basin-scale ‘confinement’ is preferentially seen in active margins or tectonic settings, where significant relief in basin topography exists (e.g., within this study the Gendalo, Golo, Kutai, Navy, Santa Monica and Villafranca all contain ‘confined’ deposits, all of which are tectonically ‘active’ systems). Typically, these confined systems show shorter flow run-outs, which can be related to catchment area scaling relationships (Sømme et al., 2009), as these smaller systems generally deposit more immature, coarser sediment (Bouma, 2000). Outliers to this trend have been identified, for instance Prélat et al. (2010) characterises the ‘large’ passive-margin Niger Delta system deposits as ‘confined’ due to an anticline causing a lateral slope. Confinement has since been used to determine trends in lobe planform geometries by Prélat et al. (2010) and Pettinga et al. (2018) but interestingly, other variables can be used to categorise the lobe planform data into the same groups as those identified (e.g., see Figs. 5.7

and 5.8). For instance, the quantifiable parameters, local depositional gradient and water depth, match the same 'confinement' trends and do not include anomalies within the groupings, unlike 'confinement' (Figs. 5.7 & 5.8). This helps to demonstrate the broader application of DMAKS, as the databases storage of a wide array of variables allows trends to be evaluated against a wide number of parameters, or combinations of parameters. In this particular case it also calls to attention the complex interactions that must exist within the deep-marine depositional environment.

No effects of sediment compaction are apparent in the sample thickness data; Fig. 5.5L shows modern and ancient deposits to span similar data ranges. Case-by-case analysis would be necessary to truly test this conclusion. For example, it is known that the Bengal deposits considered in this study, taken from the Shwe fan, have subsequently been injected into the overlying layers during compaction, potentially altering the preserved geometries (Yang & Kim, 2014).

The multivariate investigations are limited in their application due to the small sample size (n=14), however these preliminary results do complement the univariate findings concerning terminal deposit geometry. For instance, the multivariate analyses (Fig.'s 5.9D and 5.10) suggest that the local depositional characteristics (gradient and water depth) are strongly related to the large-scale system variables (system width, length, shelf width and slope gradient) – again, a trend suggested in the univariate analyses due to the similar data distributions observed between the environmental variables (see box plots in Fig. 5.5). It is thus likely that the large-scale system setting can act as a predictor of the local depositional environment (e.g., large, passive systems typically deposit lobes upon gentler gradients, <0.01 m/m at deeper water depths, >2500 m). However this limited multivariate sample does not represent terminal deposits in other types of environments, e.g., deposition on the shallow slope as seen in the large Niger system. Additional data are needed to undertake a corresponding quantitative characterisation of these depositional settings, i.e., of 'large' systems in shallow (<2500 m), steep (>0.01 m/m) environments, or in 'small' systems associated with gentle gradients.

Tectonics is often attributed as a key influence upon shelf-to-basin plain morphology and bathymetry (Nelson & Nilsen, 1984; Shanmugam & Moiola, 1998; Bouma, 2000; Nelson et al., 2009; Pickering & Hiscott, 2016). Tectonic setting can be used as a predictor of system type; for example, univariate analyses can group terminal deposit length and width dimensions based upon margin type (Fig. 5.5 P and Q), while multivariate principal component 1 scores can be grouped by margin type (Fig. 5.9C). However, anomalies are found in both the univariate and multivariate analyses: for example, even with the small multivariate sample

size, the passive system of the Al Batha plots within the 'other' active margin settings (Fig. 5.9C). The passive Al Batha displays system settings also akin to an active margin, i.e., a small shelf width (<30 km) and system width (<100 km), suggesting that tectonic setting cannot be utilised as the sole predictor of system-scale and element-scale deposition. This suggests again the likely interconnections between variables and thus a more complex suite of geometrical controls.

The data shown in Fig. 5.8 suggest that relatively thicker 'small' lobate geometries are seen to preferentially deposit on steep gradients (>0.01 m/m) at shallower water depths (<2500 m), typically where sediment run-out has been inhibited as a result of basin or structural confinement. Sediment run-out is seen to be associated with gentle gradients (Wetzel, 1993), and subsequently larger terminal deposit geometries arise (Fig. 5.7; Ouchi et al., 1995); conversely, steeper slope gradients are seen to result in smaller lobate geometries (Fig. 5.5J and K). The change between slope and basin plain gradient is interpreted to lead to a deceleration in flow velocity and thus deposition; a gentler angle (flatter gradient) between the slope and basin plain will carry material further downdip before finally depositing (Fernandez et al., 2014; Adeogba et al., 2005). The important role of the underlying deep-marine topography is not only observed at the system scale but also at the individual element-scale, as depositional topography can influence lobe stacking patterns (Groenenberg et al., 2010). The relative change between deep-marine system and element-scale gradients, are possible variables to track with DMAKS, suggesting a direction for future work to be carried out with a larger data pool. Terminal deposits are found upon both slope and basin-plain environments, suggesting an enquiry into what may be controlling the locality of deposition upon 'steep' slope gradients (>0.01 m/m) instead of reaching the basin plain, or the topographic basin-floor for confined deposits.

Experimental work shows more areally-expansive deposits to be the result of high-density turbidite currents (Al Ja' Aidi et al., 2004; Fick et al., 2017). Flow run-out can also be encouraged by increased flow volumes and a higher proportion of fines in suspension (see Alexander & Mulder, 2002; Hamilton et al., 2017). Study in single depositional systems, e.g., the Zaire Axial fan, also argues that changes in sediment rate and supply, driven by climate or sea-level changes, are the cause for variation in terminal-deposit volumes (Picot et al., 2016). Sediment-gravity flow properties are therefore likely to have a significant influence upon the style of deposition observed and perhaps the locality of deposition (e.g., slope or basin-plain setting). This study did not consider smaller-scale, temporal changes associated with flow properties. However, it would be possible to conduct such studies through the use of DMAKS

via the construction of ‘subsets’ that would capture any such changes observed in the system. However, such investigation would be subject to the availability of data.

It is important to note that while both the univariate and multivariate analyses conducted in this study suggest correlations to exist between the considered variables, the DMAKS-derived data cannot be used to ascertain the causes behind these relationships, i.e., no comment can be made upon whether these relationships are the result of direct or indirect causes, a common response to an alternative variable, or the result of co-variance. The database approach is thus limited in its application as causality cannot be reliably determined based upon the interrogation of the database alone, external information and further research is necessary in order to evaluate the real-world application of the statistical relationships observed between the studied variables.

5.5 Conclusion

DMAKS has been applied to explore some of the complex relationships between deposit geometries and their deep-marine system controls. The significance of multiple system parameters (e.g., shelf width, slope gradient, margin type) as predictors of sedimentary architecture at the system- and element- scales has been examined based on data from multiple deep-marine studies. Larger systems tend to be associated with passive margins and typically exhibit gentler slope gradients (<0.03 m/m), a wider shelf (>30 km), maximum water depths above 2500 m, leaving finer-grained deposits. Overarching tectonic controls have previously been determined, directly, or indirectly, to influence these system-scale characteristics. A non-linear relationship between the scale of a system and the size of its highest-order terminal deposit is observed. However, the system-scale parameters (i.e., system scale, margin type, shelf width and slope gradient) are seen to be linked to an apparent bimodality in the distributions of highest-order terminal deposit length and width. For example, output from this study shows ‘smaller’ systems (<100 km, and their interconnected suite of characteristics) to deposit relatively smaller terminal deposits in planform, as opposed to ‘larger’ systems and their wider data range representing typically larger deposits (Fig. 5.5). Local depositional variables examined in this study (i.e., local gradients and water depth) demonstrate statistically stronger reasoning for the observed bimodality in the highest-order terminal deposit width and length dimensions (Mann-Whitney U test statistics show associations with end-member classes that are more discrete compared to the system-scale parameters). Therefore, local parameters can be seen to more closely predict the resultant geometry of terminal deposits. Overall, it can be concluded that

the variables recognised to affect the system-scale are not completely shredded at the element-scale (cf. Jerolmack and Paola, 2010), as both allogenic and autogenic influenced characteristics can be statistically related to the resultant highest-order terminal deposit geometry.

Both univariate and multivariate outputs show local depositional characteristics (water depth and gradient) to be strongly associated with the system configuration. For instance, long sediment run-out and higher volume deposits are typically the result of large, unconfined systems, with gentle slope gradients. Short sediment run-out distances, which may be induced by slope irregularities, result in smaller planform geometries; such deposits are generally found upon steeper gradients (>0.01 m/m), which are preferentially found on the continental slope and thus are closer to the shelf and at shallower water depths (<2500 m; Fig. 5.8). Local depositional gradient and water depth can be extracted from subsurface and modern datasets, providing a more reliable variable than the currently subjective measure of confinement to predict terminal deposit geometries. Sediment run-out distances can be shortened because of basin or structural confinement, as well as variations in sediment supply – both variables known to be associated with the overarching tectonic setting. Overall, it can be concluded that a complicated suite of inter-related parameters acts to control lobate terminal deposition. A more detailed study into the local and system-wide effects of grain-size would help to better refine understanding, as grain-size is often coupled with system-wide and depositional characteristics. Such investigation would be possible using DMAKS, as and when methods to quantitatively assess grain-size become achievable. Understanding the role played by local, autogenic controls may also help to uncover what mechanisms dictate the upper limit of terminal deposit 3D geometry that has been documented.

Chapter 6:

Conclusions

6.1 Summary

This Thesis has presented an improved database approach for the characterisation of siliciclastic deep-marine depositional systems, with regards to their architectural and facies properties in a spatial, temporal and hierarchical framework. It has been implemented as DMAKS, the Deep-Marine Architecture Knowledge Store. The methodology has been informed by a critical review of current practice in deep-marine sedimentological studies, with particular attention being paid to the hierarchical organisation of deep-marine sediments (Chapter 3). This approach has enabled the database to be designed in a way that allows the complex spatio-temporal relationships found between and within deposits to be captured. The consideration of hierarchical organisation, as well as the wide scope of the database, makes this approach stand apart from previous database systems for deep-marine siliciclastics (e.g., Cossey & Associates Inc., 2004; Baas et al., 2005; Moscardelli & Wood, 2015; Clare et al., 2018). The approach improves upon classical comparative techniques (e.g., facies models and analogues), which are typically oversimplified as they can only be undertaken with consideration of a limited number of system attributes. The standardised storage of numerous parameters from a diverse range of systems within DMAKS encourages wider examination of the possible relationships between parameters. It also allows the sedimentological data to be more readily analysed, making it a more efficient comparative tool than typical 'case-by-case' re-interpretations. Systematic data entry ensures that DMAKS can reconcile sedimentary datasets from both modern and ancient systems (Chapter 4). The functionality of DMAKS as a research tool has also been examined on both pure and applied research fronts (Chapter 4 & 5). The use of DMAKS arguably augments the value of data on deep-marine systems, as relationships implicit or hidden in individual studies can be recognised within data compounded from many studies. In addition data derived from analogous datasets can be used to assess both the data quality and interpretational rigour of individual sedimentological investigations. The key outcomes from each data Chapter are summarised below.

6.1.1 Chapter 3

In studies of deep-marine systems, modern forms and sedimentary bodies are often arranged into a hierarchical framework. **Chapter 3** reviewed a selection of the most significant

hierarchical classifications, based upon their original design and/or wide popularity, e.g., Mutti & Normark (1987), Sprague et al. (2005), Prélat et al. (2009) and Pickering & Cantalejo (2015). This review examined the similarities and differences between the considered approaches describing each classification's aims, environmental context and methods of data collection, along with the diagnostic characteristics used to discern discrete hierarchical orders. Generally, newly-proposed classifications were only applied to – and established on – single systems. This fact begs the question as to whether classifications are robust; certainly this has contributed to the proliferation of hierarchical schemes. Reconciliation between the classifications was hindered due to the wide variety found between the classification schemes, e.g., in the number of significant orders recognised, dimensions, temporal scales, terminology and diagnostic criteria.

Differences between hierarchical classifications can be associated with each study's focus on certain environments and different methods of data collection. For example, studies focused upon the classification of channelised architecture recognised more significant hierarchical orders (3-10) than schemes devised for distal terminal deposits (3-4 orders). This difference suggests that organisational complexity appears to reduce down-system. The existence of systematic hierarchical differences between channelised and lobate environments suggests that it might not be possible to devise a unified hierarchical approach across systems; hierarchical levels in one environment may not be equivalent to the hierarchical orders in the other. Contrary to popular belief, architecture characterised in outcrop can be equivalent in size to basin-scale architecture characterised using seismic. However reconciliation between seismic and outcrop datasets is hampered by the limited resolution of smaller architectural scales in seismic datasets. Hierarchical relationships are commonly inferred 'bottom-up', therefore poor seismic resolution reduces the confidence with which lower-hierarchical scales can be assigned in these datasets, leading to associated uncertainties in assigning hierarchical levels at larger scales. Further comparison between outcrops exposed at basin-scale and seismic datasets could help to remedy this problem. Comparisons between hierarchical classifications are further impeded by the wide variety of nomenclature used, as well as by inconsistent definitions. These terminological discrepancies can be seen to arise in part as a product of scientific advancement, as ideas are refined. However, ultimately this wealth of terminology leads to complications when trying to confidently reconcile classifications, especially when the heritage of these terms is not well-documented; this is a common problem also experienced in the study of other sedimentary environments (e.g., Miall, 1995; Catuneanu et al., 2011; Bruno & Ruban, 2017; Fryirs & Brierley, 2018).

Common criteria to all the schemes considered were observed and help define hierarchical orders based upon key sedimentological features, i.e., facies association, architectural geometry, and bounding surface relationships. As a general rule, architectural complexity increases in line with the spatio-temporal scale of deposition, associated with the increased internal complexity of compound and diachronous deposits. Common formative processes are also interpreted for each hierarchical order in both channelised and distributary environments: each hierarchical order is seen to reflect a single cycle of waxing and waning energy, from initiation, to growth and retreat. A universal genetic hierarchy would ideally relate deposits to processes that are exclusive to a specific scale, but such a hierarchy cannot be discerned currently. A related difficulty is the lack of consensus regarding process-to-product relationships, compounded by the difficulties observed in attributing auto- or allogenic controls to a particular depositional scale (e.g., Shanmugam, 2000; Prélat et al., 2009; McHargue et al., 2011(a); Terlaky et al., 2016). In the current state of knowledge, a fractal (i.e., scale-invariant) organisational principle is arguably as valid as a truly hierarchical order to describe channelised and lobate architectures. Establishment of a unified hierarchical framework therefore awaits improved understanding of formative processes at different scales. Based upon this review, the common descriptive characteristics used to discern architecture (i.e., facies associations, geometry and bounding surface relationships) should be relied upon in order to objectively examine the reality of hierarchical architectural relationships.

6.1.2 Chapter 4

The Deep-Marine Architecture Knowledge Store (DMAKS) contains data from deep-marine siliciclastic sedimentary systems derived from the peer-reviewed literature. **Chapter 4** presented this database methodology, where data is codified in a consistent manner through the adoption of a database standard which specifies definitions of the database entities and the data-entry workflow. Based upon the findings in Chapter 3, DMAKS can characterise nested architectural hierarchical organisation in a number of ways. For example, the database contains a bespoke classification scheme derived from the observed similarities between both channelised and lobate architectural units and their associated interpretations (described in Chapter 3). Objective approaches to describe hierarchical organisation, without the need of re-interpretation, have also been implemented, e.g., bounding-surface relationships between parent and child architecture are captured allowing nested relationships to be objectively traced, and highest-order architectural elements (i.e., the largest hierarchical units of a particular element type) are also identified. Currently DMAKS contains 18 tables. The types of information codified in DMAKS relate to: i) the regional

context of deposition, e.g., describing external system controls or basin topography; ii) the geological region under investigation (i.e., the case study) which may be further subdivided into subsets in order to capture variability within a system; iii) the geometry of geomorphic surfaces and sedimentary bodies, including their hierarchical relationships; iv) lithological facies descriptions and their bed bounding-surface relationships; v) spatial transitions between the geological entities in 3D; and vi) the quality of the primary data which helps to refine the suitability of data for particular interrogation.

Furthermore, Chapter 4 presented a selection of general applications demonstrating the scope of analysis feasible using DMAKS, along with their potential applications to hydrocarbon-reservoir characterisation. For example, the ability to integrate data from ancient outcrop, subsurface and modern studies allows DMAKS to bridge the gap between studies conducted at different scales of observation and resolution. This enabled trends in channel cross-sectional geometries to be tested against a much wider data pool than hitherto, revealing a narrower variability in channel width than previously modelled by Clark & Pickering, 1996(b) and Konsoer et al., 2013. In addition, filtering the data by the dominant system grain-size further supported the ideas of Reading & Richards (1994) and Normark & Piper (1991), as sand-dominated systems favoured thinner and narrower channel forms. The database demonstrated its potential as a tool with which to undertake fundamental research, as the temporal and hierarchical organisation of deposits were explored; for example, initial interrogation into the temporal changes in the length-to-width ratio of terminal deposits suggests that by this measure their geometry may oscillate over time across a range of systems, while scaling-relationships between child and parent channel and terminal deposits dimensions can also be inferred. Understanding the geometry and internal arrangement of deposits can be used to better inform architectural models, as the evolution of a system can be mapped through time and space. Spatial relationships between architectural units and their associated characteristics were also analysed using DMAKS-derived output; e.g., the spatial scaling between genetically-related levee and channel architecture showed a positive relationship between their width measurements whereby changes in physiographic setting show basin-plain environments to result in wider levee and channel widths, compatible with the findings of Skene et al. (2002) and Nakajima & Kneller (2013). Based upon analogous data, spatially-related object models can be developed, such models are especially useful predictive tools in limited data environments. Proportional facies models were built related to particular system parameters, architectural or facies characteristics, bed relationships or positions within a sub-environment. For example, the net-to-gross value (proportion of sand and gravel) was seen to decrease from the channel-axis to channel-margin in slope settings.

These calculations can be used to model reservoir quality and when paired with spatial information can be used to analyse the distribution of reservoir material.

DMAKS output can be tailored to suit specific real-world examples, or particular research interests (cf. Chapter 5). Data were interrogated to assess the variability between deep-marine sedimentary environments under different combinations of boundary condition, in both pure and applied research environments. DMAKS demonstrated its ability to aid reservoir characterisation by validating or expanding upon geological models, building statistically accurate predictive models, as well as produce synthetic and statistically founded analogues.

6.1.3 Chapter 5

The research capability of DMAKS was tested further in **Chapter 5** through its ability to facilitate meta-analysis and provide quantitative outputs from modern, subsurface and outcrop deep-marine systems, focused on a single problem. The database was employed to quantify the significance of relationships between multiple system parameters and the geometry of terminal deposits at multiple scales. Typically, the deep-marine literature examines the effects of external boundary conditions at either the system- or element- scale; the nested organisation of geological units in DMAKS allowed for a multi-scale analytical approach to be undertaken in this study (i.e., across system to element scales of deposition). Terminal deposit geometry was examined at its largest spatial expression (i.e., via the recognition of highest-order deposits), as well as across hierarchical orders based upon the recognition of parent-child nested architectural relationships.

At the system-scale, DMAKS output was consistent with the relationships observed between external parameters (e.g., margin type, grain size, system size and morphology) that are already identified in the literature (e.g., Reading & Richards, 1994; Sømme et al., 2009, Sweet & Blum, 2016 and Snedden et al. 2018). For example, this study confirmed that larger deep-marine systems are associated with passive margins, finer-grained deposits, a gentle slope gradient (<0.03 m/m), wider shelf (>30 km) and deeper maximum depositional water depth (>2500 m). Arguably, the compatibility between the long-held results observed in the literature and the DMAKS-derived output confirms the reliability of DMAKS as a research tool. A consistency between modern, subsurface and outcrop system scales and their boundary conditions is also revealed by the DMAKS output.

No proportional scaling-relationship is observed between deep-marine systems and their genetic highest-order terminal deposit dimensions, similar to the findings of Covault et al. (2012) in their study on deep-marine channel geometries. However, two clusters are

identified for the width and length of terminal deposits which can be statistically related to 'small' or 'large' system scales and their associated allogenic characteristics. Results show that smaller lobate planform geometries (~ <10,000 m in length and width) are typically deposited in smaller systems (<100 km) with an active margin, steeper slope gradient (>0.03 m/m) and smaller shelf width (<30km). Multi-factor analysis showed autogenic variables, (i.e., the local depositional gradient and water depth), to be statistically more significant predictors of terminal deposit widths and lengths, for all hierarchical scales; for instance, gentle local depositional gradients (>0.01 m/m) and deeper water depths (>2500 m) result in larger terminal deposit planform geometries. It has often been noted that there are difficulties in attributing autogenic or allogenic controls to a particular architectural scale and often the relative dependency upon these depositional controls is proposed to alter across the hierarchical sequence (e.g., Prélat et al., 2009; McHargue et al., 2011(a); Picot et al., 2016; Terlaky et al., 2016). The database cannot be used alone to determine causality between any relationships found. However, this study has shown through statistical reasoning that the local depositional environment has a stronger influence upon the planform geometry of terminal deposits at the highest-order of deposition. Nevertheless, these localised parameters are strongly associated with the overarching system-scale boundary conditions and in turn any associated allogenic forcing's – thus the effects of the system-scale parameters are still visible at all hierarchical scales of terminal deposition. The thickness of terminal deposits was shown not to be significantly affected by the system-scale or local parameters examined in this study. Nevertheless, a common limit to the maximum terminal deposit volume was observed.

6.2 Recommendations for future research

The research presented in this Thesis has highlighted several areas of study that would benefit from the use of a standardised database approach. For example:

- A truthful representation of hierarchical organisation and of its variability within a deep-marine system is not yet fully established, as exemplified through the numerous hierarchical classification schemes present in the literature (Chapter 3; Cullis et al., 2018 and references therein). DMAKS can facilitate objective comparisons between nested architectural units based upon the digitisation of common architectural observations, e.g., bounding surface relationships, geometry, scale and internal facies relationships. DMAKS can therefore be used to analyse nested architectural relationships to develop a statistically-informed understanding of these organisational patterns. Preliminary work in this Thesis has suggested both

fractal (i.e., scale-invariant) and hierarchical (i.e., scale-dependent) modes of organisation may exist in deep-marine systems. This conclusion is consistent with the findings of Straub & Pyles (2012) who suggest a mix of fractal and hierarchical organisation styles are possible in deep-marine environments. For example, the cyclic nature of initiation, growth and retreat phases in the formation of both channelised and lobate geometries at all scales suggests a fractal control upon deep-marine depositional processes; meanwhile, a common limit to terminal-deposit volumes, regardless of the variable controlling parameters, implies a finite scale (and thus scale-dependent limit) to the size of terminal deposition. DMAKS can be used to further unravel these complex relationships in deep-marine organisation, to produce a more rigorous understanding of deep-marine spatial and temporal relationships. Furthermore, the digitisation of data from different deep-marine environments and their interconnected spatial relationships would allow DMAKS to evaluate how architectural organisation varies along the depositional profile and through different environments.

- Typically, caution is advised when comparing systems of differing geological age analysed using differing methods of data collection (Mutti & Normark, 1987; Bouma et al., 1985). DMAKS can be used to aid comparison between modern and ancient systems, as the database enables the reconciliation of datasets derived from 1D, 2D cross-section, 2D planform and 3D sources (e.g., wireline log, core, outcrop, subsurface seismic and bathymetric). For example, DMAKS has revealed similarities between the scale of modern and ancient systems; e.g., deep-marine system planform areas plot along the same power-law trend (Chapter 5), whereas similar maximum dimensions for channel widths (Chapter 4) and 'basin-scale' hierarchical orders (Chapter 3) have also been identified. Yet, this result needs to be evaluated in more detail. For example, closer interrogation of datasets of both modern and ancient systems might permit analysis of whether systems have evolved through time, e.g., what boundary conditions have controlled deep-marine organisation at multiple scales through geological history, thus whether caution is indeed warranted when comparing characteristics of modern vs. ancient deep-marine systems.
- The value and accuracy of DMAKS-derived quantitative outputs for the characterisation of deep-marine systems is inherently linked to the quantity and quality of data DMAKS contains; data upload is an ongoing process. The data entered into DMAKS is largely taken from peer-reviewed sources (e.g., journal articles, books and thesis material) and thus data quality is intrinsically related to the available data

in the published domain. As data entry continues, DMAKS can in turn be used as a feedback system to identify areas where gaps in the primary data are noticed. Examples may be the current restricted ability to objectively categorise the dominant system grain-size (Chapter 5), or the relative paucity of facies descriptions of levees and MTDs (see Figs. 4.14 and 4.18, Chapter 4). Therefore, while DMAKS has been designed primarily as a resource to enable comparative analysis, it can also be used to inform the direction of future deep-marine sedimentological investigations.

DMAKS is flexible in its design, allowing the extension and refinement of tables and their parameters as scientific understanding progresses. Several possible methodological improvements are described below related to the way DMAKS handles data, as well as the information it contains.

- The introduction of an 'estimated' spatial type for element and system measurements would enable projected width and length dimensions to be included within the database. Estimated measurements are typically inferred in incomplete exposures, calculated using extrapolated thinning rates away from a maximum thickness, e.g., for lobate geometries in the studies of Pyles, 2007 and Prélat et al., 2009. This measurement type would improve upon the data quality of otherwise 'partial' or 'unlimited' dimensions, as an estimated complete measurement type could be recorded.
- The ability to objectively classify the dominant system grain-size would greatly enhance the investigation of deep-marine organisation. Currently, this is a subjective term and thus its reliability in comparative studies is limited. As data-entry continues and more complete system profiles are digitised within DMAKS (i.e., facies data from proximal to distal element architecture), a statistical method could be established to quantitatively compare system grain-size.
- The database would benefit from the inclusion of petrophysical information. The addition of porosity and permeability data would increase the ability to analyse reservoir quality at different scales, as well as to model fluid flow properties and their distributions using associated spatial transition records.
- To aid the quantification of confinement the introduction of a '% covered' attribute would help to quantify the total amount of sedimentary cover that exists within the basin topography. Currently 'slope relief' and 'slope angle' attributes are recorded for the main basin wall only, the inclusion of these measurements for each wall would help to better constrain the basin topography allowing lateral or frontal basin confinement to be assessed in a quantitative manner.

- To enable the database to better capture the geomorphology of scours and contourite deposits the geomorphic surface classifiers should be extended to include lineation geometries, e.g., chevron, spoon, wavy or linear plan-view descriptors. This would ensure better-handling of such geomorphological datasets (e.g., Wynn & Stow, 2002; Stow et al., 2009).
- The database would benefit from the inclusion of additional source-to-sink descriptive attributes, e.g., onshore climate, shelf gradient, catchment length, marginal-marine process influences. DMAKS is part of a suite of complementary database approaches, individually designed for distinct sedimentary environments, i.e., fluvial (FAKTS; Colombera et al., 2012(a)), paralic and shallow-marine (SMAKS; Colombera et al., 2016) and deep-marine environments (DMAKS; Cullis et al., *accepted*). The integration of these three databases would enable analysis of the complete source-to-sink sedimentary profile, i.e., analysis of sedimentary architecture across a range of connected siliciclastic-environments and their interconnected boundary conditions. Relationships between the sedimentary environments are well documented (e.g., Sømme et al., 2009; Martinsen et al., 2011; Bhattacharya et al., 2016), however such an integrated database approach could more readily examine trends along the complete sediment pathway, e.g., comparing similarities and differences between modern and ancient systems, testing how far allogenic signals are propagated down-dip along the sedimentary profile, or to analyse the complexity in sedimentary hierarchical arrangements along the complete depositional profile.

DMAKS is an actively evolving research tool, able to adapt and update as the complexities of deep-marine sedimentary environments are unravelled. The methodology presented in this Thesis is specific to siliciclastic deep-marine systems but it would be possible to use this approach as a template to inform the development of similar repositories for other geological environments, such as carbonate systems. A wider application of DMAKS could see it being employed to compare deep-marine systems to other terrestrial, or interplanetary, sedimentary environments.

References

Abreu, V., Sullivan, M., Pirmez, C. & Mohrig, D., 2003. Lateral accretion packages (LaPs): an important reservoir element in deep water sinuous channels. Marine and Petroleum Geology, 20, pp.631-648.

Adeogba, A. A., McHargue, T. R. & Graham, S. A., 2005. Transient fan architecture and depositional controls from near-surface 3-D seismic data, Niger Delta continental slope. AAPG Bulletin, 89(5), pp. 627-643.

Alexander, J. & Mulder, T., 2002. Experimental quasi-steady density currents. Marine Geology, 186(3-4), pp. 195-210.

Allen, J.R.L., 1983. Studies in fluviatile sedimentation: Bars, bar-complexes and sandstone sheets (low-sinuosity braided streams) in the brownstone (L. Devonian), Welsh Borders. Sedimentary Geology, 33, pp. 237-293.

Albouy, E., Deschamps, R., Euzen, T. & Eschard, R., 2007. Stratigraphic architecture of a channel complex in the canyon-mouth setting of the Lower Pab Basin-Floor Fan, Drabber Dhora, Pakistan. *In*: Nilsen, T. H., Shew, R. D., Steffens, G. S. & Studlick, J. R. J. (Eds). Atlas of Deep-Water Outcrops. AAPG Studies in Geology, 56, pp. 295-298.

Alonso, B. & Ercilla, G., 2003. Small turbidite systems in a complex tectonic setting (SW Mediterranean Sea); morphology and growth patterns. Marine and Petroleum Geology 19(10), pp. 1225-1240.

Al Ja'Aidi, O. S., McCaffrey, W. D. & Kneller, B. C., 2004. Factors influencing the deposit geometry of experimental turbidity currents: implications for sand-body architecture in confined basins. *In*: Lomas, S. A. and Joseph, P. (Eds). Confined Turbidite Systems. Geological Society of London Special Publication, 222, pp. 45-58.

Arbues, P., Mellere, D., Falivene, O., Fernández, O., Munoz, J. A., Marzo, M. & de Gibert, J. M., 2007. Context and Architecture of the Ainsa-1-Quarry Channel Complex, Spain. *In*: Nilsen, T. H., Shew, R. D., Steffens, G. S. & Studlick, J. R. J. (Eds). Atlas of Deep-Water Outcrops, CD-ROM. AAPG Studies in Geology, 56, pp. 1-20.

Armitage, D. A., Romans, B. W., Covault, J. A. & Graham, S. A., 2009. The Influence of Mass-Transport-Deposit Surface Topography on the Evolution of Turbidite Architecture: the Sierra Contreras, Tres Pasos Formation (Cretaceous), Southern Chile. Journal of Sedimentary Research, 79 (5-6), pp. 287-301.

Arnot, M. J., Browne, G. H. & King, P. R., 2007(a). Thick-bedded sandstone facies in a middle basin-floor fan setting, Mount Messenger Formation, Mohakatino Beach, New Zealand. *In*: Nilsen, T. H., Shew, R. D., Steffens, G. S. & Studlick, J. R. J. (Eds). Atlas of Deep-Water Outcrops. AAPG Studies in Geology, 56, pp. 241-244.

Arnot, M. J., King, P. R., Browne, G. H. & Helle, K., 2007(b). Channelized, Innermost, Basin-Floor-Fan Morphologies, Mount Messenger Formation, Waikiekie South Beach and Inland, New Zealand. *In*: Nilsen, T. H., Shew, R. D., Steffens, G. S. & Studlick, J. R. J. (Eds). Atlas of Deep-Water Outcrops. AAPG Studies in Geology, 56, pp. 249-256.

Arnott, R. W. C., 2007(a). Architecture of lateral-accretion deposits in two stacked, deep-water, sinuous channel fills: relationship between coarse channel-fill and adjacent inner-bend leveee deposits, Isaac Channel 2, Castle Creek South, Windermere Supergroup, British Columbia, Canada. *In*: Nilsen, T. H., Shew, R. D., Steffens, G. S. & Studlick, J. R. J. (Eds). Atlas of Deep-Water Outcrops. AAPG Studies in Geology, 56, pp. 89-92.

Arnott, R. W. C., 2007(b). Stratal architecture and origin of lateral accretion deposits (LADs) and conterminuous inner-bank levee deposits in a base-of-slope sinuous channel, lower Isaac Formation (Neoproterozoic), East-Central British Columbia, Canada. Marine and Petroleum Geology, 24, pp. 515-528.

Arnott, R. W. C. & Ross, G. M., 2007. Overview: Outcrop Analysis of an Ancient, Passive Margin, Turbidite System: Windermere Supergroup, British Columbia, Canada. *In*: Nilsen, T. H., Shew, R. D., Steffens, G. S. & Studlick, J. R. J. (Eds). Atlas of Deep-Water Outcrops. AAPG Studies in Geology, 56, pp. 81-84.

Baas, J.H., McCaffrey, W.D. & Knipe, R.J., 2005. The Deep-Water Architecture Knowledge Base: towards an objective comparison of deep-marine sedimentary systems. Petroleum Geoscience, 11, pp. 309-320.

Baas, J. H., Best, J. L., Peakall, J. & Wang, M., 2009. A Phase Diagram for Turbulent, Transitional, and Laminar Clay Suspension Flows. Journal of Sedimentary Research, 79 (3-4), pp. 162-183.

Baas, J. H., Best, J. L. & Peakall, J., 2011. Depositional processes, bedform development and hybrid bed formation in rapidly decelerated cohesive (mud-sand) sediment flows. Sedimentology, 58 (7), pp. 1953-1987.

Babonneau, N., Savoye, B., Cremer, M. & Klein, B., 2002. Morphology and architecture of the present canyon and channel system of the Zaire deep-sea fan. Marine and Petroleum Geology, 19 (4), pp. 445-467.

Babonneau, N., Savoye, B., Cremer, M. & Bez, M., 2010. Sedimentary architecture in meanders of a submarine channel; detailed study of the present Congo turbidite channel (Zaiango Project). Journal of Sedimentary Research, 80 (9-10), pp. 852-866.

Bagnold, R. A., 1954. Experiments on a gravity-free dispersion of large solid spheres in a Newtonian fluid under shear. Proceedings of the Royal Society of London, Series A: Mathematical and Physical Sciences, 225, pp. 49-63.

Bakke, K., Kane, I. A., Martinsen, O. J., Petersen, S. A., Johansen, T. A., Hustoft, S., Jacobsen, F. H. & Groth, A., 2013. Seismic modeling in the analysis of deep-water sandstone termination styles. AAPG Bulletin, 97 (9), pp. 1395-1419.

Barker, S. P., Haughton, P. D. W., McCaffrey, W. D., Archer, S. G. & Hakes, B., 2008. Development of rheological heterogeneity in clay-rich high-density turbidity currents: Aptian Britannia Sandstone Member, UK continental shelf. Journal of Sedimentary Research, 78 (1-2), pp. 45-68.

Barnes, N. E. & Normark, W. R., 1985. Diagnostic parameters for comparing modern submarine fans and ancient turbidite systems. *In*: Bouma, A. H., Normark, W. R. & Barnes, N. E. (Eds). Submarine Fans and Related Turbidite Systems, pp. 13-14.

Barton, M. D. & Dutton, S. P., 2007. A sand-rich, basin-floor turbidite system, Willow Mountain, Texas, USA. *In*: Nilsen, T. H., Shew, R. D., Steffens, G. S. & Studlick, J. R. J. (Eds). Atlas of Deep-Water Outcrops. AAPG Studies in Geology, 56, pp. 418-421.

Barton, M. D., O'Byrne, C. J., Steffens, G. S., Pirmez, C. & Buergisser, H., 2007(a). Architecture of an aggradational deep-water channel complex: Channel Complex 2, Isaac Formation, Windermere Supergroup, British Columbia, Canada. *In*: Nilsen, T. H., Shew, R. D., Steffens, G. S. & Studlick, J. R. J. (Eds). Atlas of Deep-Water Outcrops. AAPG Studies in Geology, 56, pp. 106-110.

Barton, M. D., Craig, P., Prather, B. E. & Copus, J., 2007(b). Facies architecture of channel-levee deposits, Lago Nordenskjold and Laguna Mellizas Sur, Cerro Toro Formation, Chile. *In*: Nilsen, T. H., Shew, R. D., Steffens, G. S. & Studlick, J. R. J. (Eds). Atlas of Deep-Water Outcrops. AAPG Studies in Geology, 56, pp. 157-161.

Barton, M. D., Steffens, G. S. & O'Byrne, C. J., 2007(c). Facies architecture of a submarine-slope channel complex, Condor West Channel, Cerro Toro Formation, Chile. *In*: Nilsen, T. H., Shew, R. D., Steffens, G. S. & Studlick, J. R. J. (Eds). Atlas of Deep-Water Outcrops. AAPG Studies in Geology, 56, pp. 149-153.

Bayliss, N. J. & Pickering, K. T., 2015(a). Transition from deep-marine lower-slope erosional channels to proximal basin-floor stacked channel-levee-overbank deposits, and syn-sedimentary growth structures, Middle Eocene Banaston System, Ainsa Basin, Spanish Pyrenees. Earth-Science Reviews, 144, pp. 23-46.

Bayliss, N.J. & Pickering, K.T., 2015(b). Deep-marine structurally confined channelized sandy fans: Middle Eocene Morillo Systen, Ainsa Basin, Spanish Pyrenees. Earth Science Reviews, 144, pp. 82-106.

Beaubouef, R. T., Rossen, C., Zelt, F. B., Sullivan, M. D., Mohrig, D. C. & Jennette, D. C., 1999. Deep-Water Sandstones, Brushy Canyon Formation, West Texas, Field Guide, American Association of Petroleum Geologists, Hedberg Field Research Conference, April 15-20, pp. 48.

Beaubouef, R. T. & Friedmann, S. J., 2000. High resolution seismic/ sequence stratigraphic framework for the evolution of Pleistocene intra slope basins, Western Gulf of Mexico: Depositional models and reservoir analogs. *In*: GCSSEPM Foundation 20th Annual Research Conference, Deep-Water Reservoirs of the World, pp. 40-60.

Beaubouef, R. T., Abreu, V. & Van Wagoner, J. C., 2003. Basin 4 of the Brazos-Trinity slope system, western Gulf of Mexico: The terminal portion of a late Pleistocene lowstand systems tract. *In*: Roberts, H. H., Rosen, N. C., Fillon, R. H. & Anderson, J. B. (Eds). GCSSEPM Foundation 23rd Annual Research Conference, Shelf Margin Deltas and Linked Down Slope Petroleum Systems: Global Significance and Future Exploration Potential, pp. 45-66.

Beaubouef, R.T., 2004. Deep-water leveed-channel complexes of the Cerro Torro Formation, Upper Cretaceous, southern Chile. AAPG Bulletin, 88 (11), pp. 1471-1500.

Beaubouef, R. T., Rossen, C. & Lovell, R. W. W., 2007. The Beacon Channel: a newly recognized architectural type in the Brushy Canyon Formation, Texas, USA. *In*: Nilsen, T. H., Shew, R. D., Steffens, G. S. & Studlick, J. R. J. (Eds). Atlas of Deep-Water Outcrops. AAPG Studies in Geology, 56, pp. 432-443.

Bhattacharya, J.P., Copeland, P., Lawton, T.F. & Holbrook, J., 2016. Estimation of source area, river paleo-discharge, paleoslope, and sediment budgets of linked deep-time depositional systems and implications for hydrocarbon potential. Earth Science Reviews, 153, pp. 77-110.

Biscara, L., Mulder, T., Martinez, P., Baudin, F., Etcheber, H., Jouanneau, J.-M. & Garlan, T., 2011. Transport of terrestrial organic matter in the Ogooue deep sea turbidite system (Gabon). Marine and Petroleum Geology, 28(5), pp. 1061-1072.

Boggs Jr., S., 1995. Principles of sedimentology and stratigraphy. 2nd ed. Prentice Hall, Englewood Cliffs, New Jersey, p. 439.

Bouma, A. H., 1962. Sedimentology of some Flysch deposits; a graphic approach to facies interpretation. Amsterdam, Elsevier, p.168.

Bouma, A. H., 1982. Intraslope basins in Northwest Gulf of Mexico; a key to ancient submarine canyons and fans. *In:* Watkins, J. S. & Drake, C. L. (Eds), Studies in continental margin geology. AAPG Memoir, Tulsa, OK, United States, American Association of Petroleum Geologists, 34, pp. 567-581.

Bouma, A. H., Normark, W. R. & Barnes, N. E., 1985. COMFAN: needs and initial results. *In*: Bouma, A. H., Normark, W. R. & Barnes, N. E. (Eds). Submarine Fans and Related Turbidite Systems. New York, NY, United States, Springer-Verlag, pp. 7-10.

Bouma, A. H., 2000. Fine-grained, mud-rich turbidite systems: model and comparison with coarse-grained, sand-rich systems. *In*: Bouma, A. H. & Stone, C. G. (Eds). Fine-grained turbidite systems. AAPG Memoir 72/SEPM Special Publication, 68, pp. 9-20.

Bouma, A. H., 2004. Key controls on the characteristics of turbidite systems. *In*: Lomas, S. A. & Joseph, P. (Eds). Confined Turbidite Systems. Geological Society of London Special Publication, 222, pp. 9-22.

Bouma, A. H. & Delery, A. M., 2007. Fine-grained Permian Turbidites of Southwestern South Africa: Tanqua Karoo and Laingsburg Deep-water Basins. *In*: Nilsen, T. H., Shew, R. D., Steffens, G. S. & Studlick, J. R. J. (Eds). Atlas of Deep-Water Outcrops, CD-ROM. AAPG Studies in Geology, 56, pp. 1-19.

Bouma, A. H., Delery, A. M. & Scott, E. D., 2007. Introduction to Deep-water Deposits of the Tanqua Karoo, South Africa. *In*: Nilsen, T. H., Shew, R. D., Steffens, G. S. & Studlick, J. R. J. (Eds). Atlas of Deep-Water Outcrops. AAPG Studies in Geology, 56, pp. 302-304.

Bourget, J., Zaragosi, S., Mulder, T., Schneider, J. L., Garlan, T., Van Toer, A., Mas, V. & Ellouz-Zimmermann, N., 2010. Hyperpycnal-fed turbidite lobe architecture and recent sedimentary processes: A case study from the Al Batha turbidite system, Oman margin. Sedimentary Geology, 229 (3), pp. 144-159.

Bourillet, J.-F., Reynaud, J.-Y., Baltzer, A. & Zaragosi, S., 2003. The 'Fleuve Manche'; the submarine sedimentary features from the outer shelf to the deep-sea fans. Journal of Quaternary Science, 18(3-4), pp. 261-282.

Brocheray, S., Cremer, M., Zaragosi, S., Schmidt, S., Eynaud, F., Rossignol, L. & Gillet, H., 2014. 2000 years of frequent turbidite activity in the Capbreton Canyon (Bay of Biscay). Marine Geology, 347, pp. 136-152.

Brookfield, M.E., 1977. The origin of bounding surfaces in ancient aeolian sandstone. Sedimentology, 24 (3), pp. 303-332.

Brooks, H. L., Hodgson, D. M., Brunt, R. L., Peakall, J. & Flint, S. S., 2018. Exhumed lateral margins and increasing flow confinement of a submarine landslide complex. Sedimentology, 65 (4), pp. 1067-1096.

Browne, G. H., Slatt, R. M. & King, P. R., 2000. Contrasting Styles of Basin-Floor Fan and Slope Fan Deposition: Mount Messenger Formation, New Zealand. *In*: Bouma, A. H. and Stone, C. G. (Eds). Fine-grained turbidite systems. AAPG Memoir 72/SEPM Special Publication, 68, pp. 143-152.

Browne, G. H., King, P. R., Higgs, K. E. & Slatt, R. M., 2005. Grain-size characteristics for distinguishing basin floor fan and slope fan depositional settings: outcrop and subsurface examples from the late Miocene Mount Messenger Formation, New Zealand. New Zealand Journal of Geology and Geophysics, 48 (2), pp. 213-227.

Browne, G. H., King, P. R., Arnot, M. J. & Helle, K., 2007(a). A complete middle-to-inner basin-floor-fan cycle, Mount Messenger Formation, Tongaporutu, New Zealand. *In*: Nilsen, T. H., Shew, R. D., Steffens, G. S. & Studlick, J. R. J. (Eds). Atlas of Deep-Water Outcrops. AAPG Studies in Geology, 56, pp. 245-248.

Browne, G. H., King, P. R., Arnot, M. J. & Slatt, R. M., 2007(b). Architecture of base-of-slope fans, Mount Messenger Formation, Pukearuhe Beach, New Zealand. *In*: Nilsen, T. H., Shew, R. D., Steffens, G. S. & Studlick, J. R. J. (Eds). Atlas of Deep-Water Outcrops. AAPG Studies in Geology, 56, pp. 257-261.

Bruno, D. E. & Ruban, D. A., 2017. Something more than boulders: A geological comment on the nomenclature of megaclasts on extraterrestrial bodies. Planetary and Space Science, 135, pp.37-42.

Brunt, R.L., 2003. Vertical transitions in turbidite facies and sedimentary architecture: insights from the Grès du Champsaur, SE France, and from laboratory experiments. Doctoral Thesis, University of Leeds.

Brunt, R. L. & McCaffrey, W. D., 2007. Heterogeneity of fill within an incised channel: The Oligocene Gres du Champsaur, SE France. Marine and Petroleum Geology, 24, pp. 529-539.

Brunt, R. L., McCaffrey, W. D. & Butler, R. W. H., 2007. Setting and architectural elements of the Champsaur Sandstones, France. *In*: Nilsen, T. H., Shew, R. D., Steffens, G. S. & Studlick, J. R. J. (Eds). Atlas of Deep-Water Outcrops. AAPG Studies in Geology, 56, pp. 188-191.

Brunt, R. L., Hodgson, D. M., Flint, S. S., Pringle, J. K., Di Celma, C. N., Prélat, A. & Grecula, M., 2013. Confined to unconfined: Anatomy of a base of slope succession, Karoo Basin, South Africa. Marine and Petroleum Geology, 41, pp. 206-221.

Butterworth, P. J., Crame, J. A., Howlett, P. J. & Macdonald, D. I. M., 1988. Lithostratigraphy of Upper Jurassic-Lower Cretaceous strata of eastern Alexander Island, Antarctica. Cretaceous Research, 9 (3), pp. 249-264.

Butterworth, P. J. & MacDonald, D. I. M., 2007. Channel-levee complexes of the Fossil Bluff Group, Antarctica. *In*: Nilsen, T. H., Shew, R. D., Steffens, G. S. & Studlick, J. R. J. (Eds). Atlas of Deep-Water Outcrops. AAPG Studies in Geology, 56, pp. 36-41.

Burgreen, B. & Graham, S., 2014. Evolution of a deep-water lobe system in the Neogene trench-slope setting of the East Coast Basin, New Zealand: Lobe stratigraphy and architecture in a weakly confined basin configuration. Marine and Petroleum Geology, 54, pp. 1-22.

Callow, R. H. T., McIlroy, D., Kneller, B. & Dykstra, M., 2013(a). Ichnology of Late Cretaceous Turbidites from the Rosario Formation, Baja California, Mexico. Ichnos-an International Journal for Plant and Animal Traces, 20 (1), pp. 1-14.

Callow, R. H. T., McIlroy, D., Kneller, B. C. & Dykstra, M., 2013(b). Integrated ichnological and sedimentological analysis of a Late Cretaceous submarine channel-levee system: The Rosario Formation, Baja California, Mexico. Marine and Petroleum Geology, 41, pp. 277-294.

Campbell, C. V., 1967. Lamina, Laminaset, Bed and Bedset. Sedimentology, 8, pp. 7-26.

Campion, K. M., Sprague, A. R. G., Mohrig, D. C., Sullivan M. D., Ardill, J., Jensen, G. N., Drzewiecki, P. A., Lovell, R. W., & Sickafoose, D. K., 2000. Outcrop expression of confined channel complexes. *In*: Weimer, P., Slatt, R. M., Bouma, A. R., & Lawrence, D. T., eds., Gulf Coast Section, SEPM, 20th Annual Research Conference: Deep-Water Reservoirs of the World, December 3-6, 2000, Houston, pp. 127-151.

Campion, K. M., Sprague, A. R. & Sullivan, M. D., 2007. Architecture and lithofacies of the Miocene Capistrano Formation, San Clemente State Beach, California, USA. *In*: Nilsen, T. H., Shew, R. D., Steffens, G. S. & Studlick, J. R. J. (Eds). Atlas of Deep-Water Outcrops. AAPG Studies in Geology, 56, pp. 395-400.

Campion, K., Sprague, A. & Sullivan, M., 2011. Architectural hierarchy and lithofacies distribution of deep-water channels in the Capistrano Formation: A model for prediction of reservoir elements in confined channel systems. Internal architecture, bedforms and geometry of turbidite channels, oral and poster abstracts, Geological Society, London, June 20-21st, 2011.

Cartigny, M. J. B., Ventra, D., Postma, G. & van den Berg, J. H., 2014. Morphodynamics and sedimentary structures of bedforms under supercritical-flow conditions: New insights from flume experiments. Sedimentology, 61 (3), pp. 712-748.

Catuneanu, O., Galloway, W. E., Kendall, C. G. St. C, Mial, A. D., Posamentier, H. W., Strasser, A. & Tucker, M.E., 2011. Sequence Stratigraphy: Methodology and Nomenclature. Newsletters on Stratigraphy, 44 (3), pp.173-245.

Clare, M., Chaytor, J., Dabson, O., Gamboa, D., Georgiopoulou, A., Eady, H., Hunt, J., Jackson, C., Katz, O., Krastel, S., León, R., Micallef, A., Moernaut, J., Moriconi, R., Moscardelli, L., Mueller, C., Normandeau, A., Patacci, M., Steventon, M., Urlaub, M., Völker D., Wood, L. & Jobe, Z., 2018. A consistent global approach for the morphometric characterization of subaqueous landslides. Geological society, London, Special Publications, 477.

Clark, J. D. & Pickering, K. T., 1996(a). Architectural elements and growth patterns of submarine channels: Application to hydrocarbon exploration. AAPG Bulletin, 80 (2), pp.194-221.

Clark, J. D. & Pickering, K. T., 1996(b). Submarine channels. Processes and architecture. Vallis Press, London.

Chapin, M. A., Davies, P., Gibson, J. L. & Pettingill, H. S., 1994. Reservoir architecture of turbidite sheet sandstones in laterally extensive outcrops, Ross Formation, western Ireland. *In*: Weimer, P., Bouma, A. H. & Perkins, B. F. (Eds). GCSSEPM Foundation 15th Annual Research Conference, Submarine Fans and Turbidite Systems: Sequence Stratigraphy, Reservoir Architecture and Production Characteristics, Gulf of Mexico and International, pp. 53-68.

Colombera, L., Mountney, N.P. & McCaffrey, W.D., 2012(a). A relational database for the digitisation of fluvial architecture: concepts and example applications. Petroleum Geoscience, 18, pp. 129-140.

Colombera, L., Felletti, F., Mountney, N.P. & McCaffrey, W.D., 2012(b). A database approach for constraining stochastic simulations of the sedimentary heterogeneity of fluvial reservoirs. AAPG bulletin, 96 (11), pp.2143-2166.

Colombera, L., Mountney, N.P. & McCaffrey, W.D., 2015. A meta-study of relationships between fluvial channel-body stacking pattern and aggradation rate: Implications for sequence stratigraphy. Geology, 43 (4), pp. 283–286.

Colombera, L., Mountney, N.P., Hodgson, D.M., & McCaffrey, W.D., 2016. The Shallow-Marine Architecture Knowledge Store: A database for the characterization of shallow-marine and paralic depositional systems. Marine and Petroleum Geology, 75, pp. 83-99.

Cossey, S.P.J., 2005. Turbidite databases [online]. Available at: http://cosseygeo.com/databases/databases.htm [Accessed 12/06/2018]

Cossu, R., Wells, M. G. & Peakall, J., 2015. Latitudinal variations in submarine channel sedimentation patterns: the role of Coriolis forces. Journal of the Geological Society 172 (2), pp. 161-174.

Covault, J. A. & Romans, B. W., 2009. Growth patterns of deep-sea fans revisited: Turbidite-system morphology in confined basins, examples from the California Borderland. Marine Geology, 265(1-2), pp. 51-66

Covault, J. A. & Graham, S. A., 2010. Submarine fans at all sea-level stands: Tectono-morphologic and climatic controls on terrigenous sediment delivery to the deep sea. Geology, 38(10), pp. 939-942.

Covault, J. A., Shelef, E., Traer, M., Hubbard, S. M., Romans, B. W. & Fildani, A., 2012. Deep-Water Channel Run-Out Length: Insights from Seafloor Geomorphology. Journal of Sedimentary Research, 82(1-2), pp. 21-36.

Cremer, M., Orsolini, P. & Ravenne, C., 1985. Cap-Ferret Fan, Atlantic Ocean. *In*: Bouma, A. H., Normark, W. R. & Barnes, N. E. (Eds). Submarine Fans and Related Turbidite Systems. New York, NY, United States, Springer-Verlag, pp. 113-119.

Crevello, P. D., Johnson, H. D., Tongkul, F. & Wells, M. R., 2007(a). Overview of Mixed Braided- and Leveed-channel Turbidites, West Crocker Fan System, Northwest Borneo. *In*: Nilsen, T. H., Shew, R. D., Steffens, G. S. & Studlick, J. R. J. (Eds). Atlas of Deep-Water Outcrops. AAPG Studies in Geology, 56, pp. 50-52.

Crevello, P. D., Johnson, H. D., Tongkul, F. & Wells, M. R., 2007(b). Lobe and channel deposits, Papar Highway, Northwest Borneo. *In*: Nilsen, T. H., Shew, R. D., Steffens, G. S. & Studlick, J. R. J. (Eds). Atlas of Deep-Water Outcrops. AAPG Studies in Geology, 56, pp. 67-69.

Crevello, P. D., Johnson, H. D., Tongkul, F. & Wells, M. R., 2007(c). Mixed Braided and Leveed-channel Turbidites, West Crocker Fan System, Northwest Borneo. *In*: Nilsen, T. H., Shew, R. D., Steffens, G. S. & Studlick, J. R. J. (Eds). Atlas of Deep-Water Outcrops, CD-ROM. AAPG Studies in Geology, 56, pp. 1-32.

Cronin, B. T. & Kidd, R. B., 1998. Heterogeneity and lithotype distribution in ancient deep-sea canyons; Point Lobos deep-sea canyon as a reservoir analogue. Sedimentary Geology, 115 (1-4), pp. 315-349.

Cullis, S., Colombera, L., Patacci, M. & McCaffrey, W.D., 2018. Hierarchical classifications of the sedimentary architecture of deep-marine depositional systems. Earth-Science Reviews, 179, pp. 38-71.

Cullis, S., Patacci, M., Colombera, L., Bührig, L. & McCaffrey, W.D., *accepted*. A database solution for the quantitative characterisation and comparison of deep-marine siliciclastic depositional systems. Marine and Petroleum Geology.

Curray, J. R., Emmel, F. J. & Moore, D. G., 2003. The Bengal Fan: morphology, geometry, stratigraphy, history and processes. Marine and Petroleum Geology, 19(10), pp. 1191-1223.

Damuth, J. E., 1994. Neogene gravity tectonics and depositional processes on the deep Niger Delta continental margin. Marine and Petroleum Geology, 11 (3), pp. 320-346.

Delery, A. M. & Bouma, A. H., 2003. Aspect ratios of coarse-grained and fine-grained submarine fan channels. Transactions - Gulf Coast Association of Geological Societies, 53, pp. 170-182.

Dennielou, B., Droz, L., Babonneau, N., Jacq, C., Bonnel, C., Picot, M., Le Saout, M., Saout, Y., Bez, M., Savoye, B., Olu, K. & Rabouille, C., 2017. Morphology, structure, composition and build-up processes of the active channel-mouth lobe complex of the Congo deep-sea fan with inputs from remotely operated underwater vehicle (ROV) multibeam and video surveys. Deep-Sea Research Part II-Topical Studies in Oceanography, 142, pp. 25-49.

Deptuck, M. E., Steffens, G. S., Barton, M. & Pirmez, C., 2003. Architecture and evolution of upper fan channel-belts on the Niger Delta slope and in the Arabian Sea. Marine and Petroleum Geology, 20 (6-8), pp. 649-676.

Deptuck, M. E., Sylvester, Z., Pirmez, C. & O'Byrne, C., 2007. Migration-aggradation history and 3-D seismic geomorphology of submarine channels in the Pleistocene Benin-major Canyon, western Niger Delta slope. Marine and Petroleum Geology, 24, pp. 406-433.

Deptuck, M. E., Piper, D. J. W., Savoye, B. & Gervais, A., 2008. Dimensions and architecture of late Pleistocene submarine lobes off the northern margin of East Corsica. Sedimentology, 55 (4), pp. 869-898.

Deptuck, M. E., Sylvester, Z. & O'Byrne, C., 2012. Pleistocene seascape evolution above a 'simple' stepped slope - western Niger delta. *In*: Prather, B. E., Deptuck, M. E., Mohrig, D., Van Hoorn, B. & Wynn, R. B. (Eds). Application of the Principles of Seismic Geomorphology to Continental-Slope and Base-of-Slope Systems: Case Studies from Seafloor and Near-Seafloor Analogues. SEPM Special Publication, 99, pp. 199-222.

Di Celma, C. N., Cantalamessa, G., Didaskalou, P. & Lori, P., 2010. Sedimentology, architecture, and sequence stratigraphy of coarse-grained, submarine canyon fills from the Pleistocene (Gelasian-Calabrian) of the Peri-Adriatic basin, central Italy. Marine and Petroleum Geology, 27 (7), pp. 1340-1365.

Di Celma, C. N., 2011. Sedimentology, architecture, and depositional evolution of a coarse-grained submarine canyon fill from the Gelasian (early Pleistocene) of the Peri-Adriatic basin, Offida, central Italy. Sedimentary Geology, 238 (3-4), pp. 233-253.

Di Celma, C. N., Brunt, R. L., Hodgson, D. M., Flint, S. S. & Kavanagh, J. P., 2011. Spatial and Temporal Evolution of a Permian Submarine Slope Channel-Levee System, Karoo Basin, South Africa. Journal of Sedimentary Research, 81 (7-8), pp. 579-599.

Di Celma, C. N., Cantalamessa, G. & Didaskalou, P., 2013. Stratigraphic organization and predictability of mixed coarse-grained and fine-grained successions in an upper slope Pleistocene turbidite system of the Peri-Adriatic basin. Sedimentology, 60 (3), pp. 763-799.

Di Celma, C., Teloni, R. & Rustichelli, A., 2014. Large-scale stratigraphic architecture and sequence analysis of an early Pleistocene submarine canyon fill, Monte Ascensione succession (Peri-Adriatic basin, eastern central Italy). International Journal of Earth Sciences, 103 (3), pp. 843-875.

Dott, R. H. J., 1963. Dynamics of subaqueous gravity depositional processes. AAPG Bulletin, 47 (1), pp. 104-128.

Doughty-Jones, G., Mayall, M. & Lonergan, L., 2017. Stratigraphy, facies, and evolution of deep-water lobe complexes within a salt-controlled intraslope minibasin. AAPG Bulletin, 101 (11), pp. 1879-1904.

Dreyer, T., Fält, L.-M., Høy, T., Knarud, R., Steel, R. & Cuevas, J. L., 1993. Sedimentary architecture of field analogues for reservoir information (SAFARI): a case study of the fluvial Escanilla Formation, Spanish Pyrenees. *In*: Flint, S. S. & Bryant, I. D. (eds), The Geological Modelling of Hydrocarbon Reservoirs and Outcrop Analogues. IAS Special Publication, 15, pp. 57-80.

Droz, L., Marsset, T., Ondreas, H., Lopez, M., Savoye, B. & Spy-Anderson, F.-L., 2003. Architecture of an active mud-rich turbidite system; the Zaire Fan (Congo-Angola margin Southeast Atlantic); results from ZaiAngo 1 and 2 cruises. AAPG Bulletin, 87 (7), pp. 1145-1168.

Du, X. J., Hendy, I. & Schimmelmann, A., 2018. A 9000-year flood history for Southern California: A revised stratigraphy of varved sediments in Santa Barbara Basin. Marine Geology, 397, pp. 29-42.

Ducassou, E., Migeon, S., Mulder, T., Murat, A., Capotondi, L., Bernasconi, S. M. & Mascle, J., 2009. Evolution of the Nile deep-sea turbidite system during the Late Quaternary: influence of climate change on fan sedimentation. Sedimentology, 56(7), pp. 2061-2090.

Dykstra, M. & Kneller, B. C., 2007. Canyon San Fernando, Baja California, Mexico: A deep-water channel-levee complex that evolved from submarine canyon confinement to unconfined deposition. *In*: Nilsen, T. H., Shew, R. D., Steffens, G. S. & Studlick, J. R. J. (Eds). Atlas of Deep-Water Outcrops, CD-ROM. AAPG Studies in Geology, 56, pp. 1-14.

Efron, B. & Tibshirani, R., 1986. Bootstrap methods for standard errors, confidence intervals, and other measures of statistical accuracy. Statistical Science, 1 (1), pp.54-75.

Elliott, T., 2000. Megaflute erosion surfaces and the initiation of turbidite channels. Geology, 28 (2), pp. 119-122.

Emmel, F. J. & Curray, J. R., 1985. Bengal Fan, Indian Ocean. *In*: Bouma, A. H., Normark, W. R. & Barnes, N. E. (Eds). Submarine Fans and Related Turbidite Systems. New York, NY, United States, Springer-Verlag, pp. 107-112.

Ercilla, G., Casas, D., Estrada, F., Vazquez, J. T., Iglesias, J., Garcia, M., Gomez, M., Acosta, J., Gallart, J., Maestro-Gonzalez, A. & Team, M., 2008. Morphosedimentary features and recent depositional architectural model of the Cantabrian continental margin. Marine Geology, 247 (1-2), pp. 61-83.

Eschard, R., Albouy, E., Gaumet, F. & Ayub, A., 2004. Comparing the depositional architecture of basin floor fans and slope fans in the Pab Sandstone, Maastrichtian, Pakistan. *In*: Lomas, S. A. & Joseph, P. (Eds). Confined Turbidite Systems. Geological Society of London Special Publication, 222, pp. 159-185.

Eschard, R., Deschamps, R., Doligez, B., Lerat, O., Langlais, V. & Euzen, T., 2014. Connectivity estimation between turbiditic channels and overbank deposits from the modelling of an outcrop analogue (Pab Formation, Maastrichtian, Pakistan). *In*: Sediment-Body Geometry and Heterogeneity: Analogue Studies for Modelling the Subsurface. Geological Society of London Special Publication, 387, pp. 203-231.

Euzen, T., Eschard, R. & Albouy, E., 2007(a). Stratigraphic architecture of a channel complex in the midfan setting of the Lower Pab Basin Floor Fan, North Baddho Dhora, Pakistan. *In*: Nilsen, T. H., Shew, R. D., Steffens, G. S. & Studlick, J. R. J. (Eds). Atlas of Deep-Water Outcrops. AAPG Studies in Geology, 56, pp. 290-294.

Euzen, T., Eschard, R., Albouy, E. & Deschamps, R., 2007(b). Reservoir Architecture of a Turbidite Channel Complex in the Pab Formation, Pakistan. *In*: Nilsen, T. H., Shew, R. D., Steffens, G. S. & Studlick, J. R. J. (Eds). Atlas of Deep-Water Outcrops, CD-ROM. AAPG Studies in Geology, 56, pp. 1-20.

Evangelinos, D., Nelson, C. H., Escutia, C., De Batist, M. & Khlystov, O., 2017. Late Quaternary climatic control of Lake Baikal (Russia) turbidite systems: Implications for turbidite systems worldwide. Geology, 45 (2), pp. 179-182.

Falivene, O., Arbues, P., Gardiner, A., Pickup, G., Munoz, J. A. & Cabrera, L., 2006. Best practice stochastic facies modeling from a channel-fill turbidite sandstone analog (the Quarry outcrop, Eocene Ainsa basin, northeast Spain). AAPG Bulletin, 90 (7), pp. 1003-1029.

Falivene, O., Arbues, P., Ledo, J., Benjumea, B., Munoz, J. A., Fernandez, O. & Martinez, S., 2010. Synthetic seismic models from outcrop-derived reservoir-scale three-dimensional facies models: The Eocene Ainsa turbidite system (southern Pyrenees). AAPG Bulletin, 94 (3), pp. 317-343.

Faugeres, J. C. & Stow, D. A. V., 1993. Bottom-current-controlled sedimentation; a synthesis of the contourite problem. Sedimentary Geology, 82 (1-4), pp. 287-297.

Felletti, F., 2016. Depositional architecture of a confined, sand-rich submarine system: the Bric la Croce-Castelnuovo turbidite system (Tertiary Piedmont Basin, Oligocene, NW Italy). Italian Journal of Geosciences, 135 (3), pp. 365-382.

Fernandez, R. L., Cantelli, A., Pirmez, C., Sequeiros, O. & Parker, G., 2014. Growth Patterns of Subaqueous Depositional Channel Lobe Systems Developed Over A Basement With A Downdip Break In Slope: Laboratory Experiments. Journal of Sedimentary Research, 84(3), pp. 168-182.

Fick, C., Manica, R. & Toldo, E. E., 2017. Autogenic influence on the morphology of submarine fans: an approach from 3D physical modelling of turbidity currents. Brazilian Journal of Geology, 47(3), pp. 345-368.

Figueiredo, J.J.P, Hodgson, D.M., Flint, S.S. & Kavanagh, J.P., 2013. Architecture of a channel complex formed and filled during long-term degradation and entrenchment on the upper submarine slope, Unit F, Fort Brown Fm., SW Karoo Basin, South Africa. Marine and Petroleum Geology, 41, pp. 104-116.

Fildani, A., Drinkwater, N. J., Weislogel, A., McHargue, T., Hodgson, D. M. & Flint, S. S., 2007. Age controls on the Tanqua and Laingsburg deep-water systems: New insights on the evolution and sedimentary fill of the Karoo basin, South Africa. Journal of Sedimentary Research, 77, pp. 901-908.

Flint, S., Hodgson, D., Sprague, A. & Box, D., 2008. A physical stratigraphic hierarchy for deep-water slope system reservoirs 1: super sequences to complexes. American Association of Petroleum Geologists International Conference and Exhibition, Cape Town, South Africa, Abstracts.

Flint, S.S., Hodgson, D.M., Sprague, A.R., Brunt, R.L., Van der Merwe, W.C., Figueiredo, J., Prélat, A., Box, D., Di Celma, C. & Kavangh, J.P., 2011. Depositional architecture and sequence stratigraphy of the Karoo basin floor to shelf edge succession, Laingsburg depocentre, South Africa. Marine and Petroleum Geology, 28, pp.658-674.

Flood, R. D. & Damuth, J. E., 1987. Quantitative characteristics of sinuous distributary channels on the Amazon deep-sea fan. Geological Society of America Bulletin, 98, pp. 728-738.

Flood, R. D., Manley, P. L., Kowsmann, R. O., Appi, C. J. & Pirmez, C., 1991. Seismic facies and late Quaternary growth of Amazon submarine fan. *In*: Weimer, P. and Link, M. H. (Eds).

Seismic facies and sedimentary processes of submarine fans and turbidite systems, New York, NY, United States, Springer-Verlag, pp. 415-433.

Folk, R.L., 1980. Petrology of Sedimentary Rocks. Hemphill, Austin, p.182.

Friend, P.F., Slater, M.J. & Williams, R.C., 1979. Vertical and lateral building of river sandstone bodies, Ebro Basin, Spain. The Geological Society London, 136, pp.39-46.

Fonnesu, M., Haughton, P. D. W., Felletti, F. & McCaffrey, W. D., 2015. Short length-scale variability of hybrid event beds and its applied significance. Marine and Petroleum Geology, 67, pp. 583-603.

Fonnesu, M., Felletti, F., Haughton, P. D., Patacci, M. & McCaffrey, W. D., 2018. Hybrid event bed character and distribution linked to turbidite system sub-environments: The North Apennine Gottero Sandstone (north-west Italy). Sedimentology, 65, pp. 151-190.

Fryirs, K. A. & Brierley, G. J., 2018. What's in a name? A naming convention for geomorphic river types using the River Styles Framework. PloS one, 13 (9), p.e0201909.

Galloway, W. E. 1989. Genetic stratigraphic sequences in basin analysis. Architecture and genesis of flooding-surface bounded depositional units. AAPG Bulletin, 73, pp.125–142.

Gamberi, F. & Marani, M., 2006. Hinterland geology and continental margin growth: the case of the Gioia Basin (southeastern Tyrrhenian Sea). *In*: Moratti, G. and Chalouan, A. (Eds). Tectonics of the Western Mediterranean and North Africa. Geological Society, London, Special Publication, 262, pp. 349-363.

Gamberi, F. & Rovere, M., 2011. Architecture of a modern transient slope fan (Villafranca fan, Gioia basin-Southeastern Tyrrhenian Sea). Sedimentary Geology, 236(3-4), pp. 211-225.

Gamberi, F., Rovere, M., Dykstra, M., Kane, I. A. & Kneller, B. C., 2013. Integrating modern seafloor and outcrop data in the analysis of slope channel architecture and fill. Marine and Petroleum Geology, 41, pp. 83-103.

Gamberi, F., Rovere, M., Mercorella, A. & Leidi, E., 2014. The Influence of a lateral slope on turbidite lobe development on a modern deep-sea slope fan (Villafranca deep-sea fan, Tyrrhenian Sea). Journal of Sedimentary Research, 84(6), pp. 475-486.

Garcia, M., Ercilla, G., Alonso, B., Estrada, F., Jane, G., Mena, A., Alves, T. & Juan, C., 2015. Deep-water turbidite systems: a review of their elements, sedimentary processes and depositional models. Their characteristics on the Iberian margins. Boletin Geologico y Minero 126(2-3), pp. 189-218.

Gardner, M. H. & Borer, J. M., 2000. Submarine channel architecture along a slope to basin profile, Brushy canyon formation, West Texas. *In*: Bouma, A. H. & Stone, C. G., eds., Fine-grained turbidite systems, AAPG Memoir 72/SEPM Special Publication 68, pp.195–214.

Gardner, M.H., Borer, J.M., Melik, J.J., Mavilla, N., Dechesne, M. & Wagerle, R.D., 2003. Stratigraphic process-response model for submarine channels and related features from studies of Permian Brushy Canyon outcrops, West Texas. Marine and Petroleum Geology, 20, pp. 757–788.

Geehan, G. & Underwood, J., 1993. The use of length distributions in geological modelling. *In*: Flint, S.S. & Bryant, I.D. (Eds.). The geological modelling of hydrocarbon reservoirs and outcrop analogues, 15, IAS Special Publication, pp. 205-212.

Gervais, A., 2002. Analyse multi-échelles de la morphologie, de la géométrie et de l'architecture d'un systéme turbiditique sableux profond (Systéme du Golo, Marge est-Corse, Mer méditérannée). Doctoral Thesis, L'Universite Bordeaux, Bordeaux, p.315.

Gervais, A., Savoye, B., Piper, D.J.W., Mulder, T., Cremer, M. & Pichevin, L., 2004. Present morphology and depositional architecture of a sandy confined submarine system: the Golo turbidite system (eastern margin of Corsica). *In*: Lomas, S.A. and Joseph, P. (eds), Confined Turbidite Systems. Geological Society, London Special Publications, 222, pp. 59-89.

Gervais, A., Savoye, B., Mulder, T. & Gonthier, E., 2006(a). Sandy modern turbidite lobes: A new insight from high resolution seismic data. Marine and Petroleum Geology, 23 (4), pp. 485-502.

Gervais, A., Mulder, T., Savoye, B. & Gonthier, E., 2006(b). Sediment distribution and evolution of sedimentary processes in a small sandy turbidite system (Golo system, Mediterranean Sea): implications for various geometries based on core framework. Geo-Marine Letters, 26 (6), pp. 373-395.

Ghibaudo, G., 1992. Subaqueous sediment gravity flow deposits; practical criteria for their description and classification. Sedimentology, 39 (3), pp. 423-454.

Ghosh, B. & Lowe, D., 1993. The architecture of deep-water channel complexes, Cretaceous Venado Sandstone Member, Sacremento Valley, California. *In*: Graham, S. A. & Lowe, D. R. (eds). Advances in the sedimentary geology of the Great Valley Group, Sacremento Valley, California. Pacific Section SEPM, SEPM, pp. 51-65.

Gibling, M. R., 2006. Width and thickness of fluvial channel bodies and valley fills in the geological record: a literature compilation and classification. Journal of Sedimentary Research, 76 (5), pp. 731-770.

Goldhammer, R. K., Wickens, H. d. V., Bouma, A. H. & Wach, G., 2000. Sequence stratigraphic architecture of the Late Permian Tanqua submarine fan complex, Karoo Basin, South Africa. *In*: Bouma, A. H. & Stone, C. G. (Eds). Fine-grained turbidite systems. AAPG Memoir 72/SEPM Special Publication, 68, pp. 165-171.

Gong, C. L., Steel, R. J., Wang, Y. M., Lin, C. S. & Olariu, C., 2016. Shelf-margin architecture variability and its role in sediment-budget partitioning into deep-water areas. Earth-Science Reviews, 154, pp. 72-101.

Grecula, M., Flint, S. S., Wickens, H. d. V. & Johnson, S. D., 2003. Upward-thickening patterns and lateral continuity of Permian sand-rich turbidite channel fills, Laingsburg Karoo, South Africa. Sedimentology, 50 (5), pp. 831-853.

Groenenberg, R. M., Hodgson, D. M., Prélat, A., Luthi, S. M. & Flint, S. S., 2010. Flow-deposit interaction in submarine lobes: insights from outcrop observations and realisations of a process-based numerical model. Journal of Sedimentary Research, 80, pp. 252-267.

Grundvåg, S-A, Johannessen, E. P., Helland-Hansen, W. & Plink-Björklund, P., 2014. Depositional architecture and evolution of progradationally stacked lobe complexes in the Eocene Central Basin of Spitsbergen. Sedimentology, 61, pp. 535-569.

Habgood, E. L., Kenyon, N. H., Masson, D. G., Akhmetzhanov, A., Weaver, P. P. E., Gardner, J. & Mulder, T., 2003. Deep-water sediment wave fields, bottom current sand channels and gravity flow channel-lobe systems; Gulf of Cadiz, NE Atlantic. Sedimentology, 50(3), pp. 483-510.

Hadler-Jacobsen, F., Johannessen, E. P., Ashton, N., Henriksen, S., Johnson, S. D. & Kristensen, J. B., 2005. Submarine fan morphology and lithology distribution: a predictable function of sediment delivery, gross shelf-to-basin relief, slope gradient and basin topography. *In*: Dore, A. G. & Vining, B. A. (Eds). Petroleum Geology: North-West Europe and Global Perspectives - Proceedings of the 6th Petroleum Geology Conference, pp. 1121-1145.

Hall, R., 2013. Contraction and extension in northern Borneo driven by subduction rollback. Journal of Asian Earth Sciences, 76, pp. 399-411.

Hamilton, P., Gaillot, G., Strom, K., Fedele, J. & Hoyal, D., 2017. Linking hydraulic properties in supercritical submarine distributary channels to depositional-lobe geometry. Journal of Sedimentary Research, 87 (9), pp. 935-950.

Hanquiez, V., Mulder, T., Toucanne, S., Lecroart, R., Bonnel, C., Marches, E. & Gonthier, E., 2010. The sandy channel-lobe depositional systems in the Gulf of Cadiz: Gravity processes forced by contour current processes. Sedimentary Geology, 229(3), pp. 110-123.

Hansen, L., Janocko, M., Kane, I. & Kneller, B., 2017(a). Submarine channel evolution, terrace development, and preservation of intra-channel thin-bedded turbidites: Mahin and Avon channels, offshore Nigeria. Marine Geology, 383, pp. 146-167.

Hansen, L., Callow, R., Kane, I. & Kneller, B., 2017(b). Differentiating submarine channel-related thin-bedded turbidite facies: Outcrop examples from the Rosario Formation, Mexico. Sedimentary Geology, 358, pp. 19-34.

Haughton, P. D. W., 1994. Deposits of deflected and ponded turbidity currents, Sorbas Basin, Southeast Spain. Journal of Sedimentary Research, Section A: Sedimentary Petrology and Processes, 64 (2), pp. 233-246.

Haughton, P. D. W., Barker, S. P. & McCaffrey, W. D., 2003. 'Linked' debrites in sand-rich turbidite systems; origin and significance. Sedimentology, 50 (3), pp. 459-482.

Haughton, P. D. W., Davis, C., McCaffrey, W. D. & Barker, S., 2009. Hybrid sediment gravity flow deposits - Classification, origin and significance. Marine and Petroleum Geology, 26 (10), pp. 1900-1918.

Hawie, N., Deschamps, R., Granjeon, D., Nader, F. H., Gorini, C., Müller, C., Montadert, L. & Baudin, F., 2017. Multi-scale constraints of sediment source to sink systems in frontier basins: a forward stratigraphic modelling case study of the Levant region. Basin Research, 29, pp. 418-445.

Heezen, B. C. & Ewing, W. M., 1952. Turbidity currents and submarine slumps, and the 1929 Grand Banks earthquake. American Journal of Science, 250 (12), pp. 849-873.

Heiniö, P. & Davies, R. J., 2007. Knickpoint migration in submarine channels in response to fold growth, western Niger Delta. Marine and Petroleum Geology, 24 (6-9), pp. 434-449.

Hernandez-Molina, J., Llave, E., Somoza, L., Fernandez-Puga, M. C., Maestro, A., Leon, R., Medialdea, T., Barnolas, A., Garcia, M., Diaz del Rio, V., Fernandez-Salas, L. M., Vazquez, J. T., Lobo, F., Alveirinho Dias, J. M., Rodero, J. & Gardner, J., 2003. Looking for clues to paleoceanographic imprints; a diagnosis of the Gulf of Cadiz contourite depositional systems. Geology, 31(1), pp. 19-22.

Hickson, T. A. & Lowe, D. R., 2002. Facies architecture of a submarine fan channel-levee complex: The Juniper Ridge Conglomerate, Coalinga, California. Sedimentology, 49 (2), pp. 335-362.

Ho, V. L., Dorrell, R. M., Keevil, G. M., Burns, A. D. & McCaffrey, W. D., 2018. Pulse propagation in turbidity currents. Sedimentology, 65 (2), pp. 620-637.

Hodgson, D. M., Flint, S. S., Hodgetts, D., Drinkwater, N. J., Johannessen, E. P. & Luthi, S. M., 2006. Stratigraphic evolution of fine-grained submarine fan systems, Tanqua depocenter, Karoo Basin, South Africa. Journal of Sedimentary Research, 76 (1-2), pp. 20-40.

Hofstra, M., Hodgson, D. M., Peakall, J. & Flint, S. S., 2015. Giant scour-fills in ancient channel-lobe transition zones: Formative processes and depositional architecture. Sedimentary Geology, 329, pp. 98-114.

Hofstra, M., Ponten, A. S. M., Peakall, J., Flint, S. S., Nair, K. N. & Hodgson, D. M., 2017. The impact of fine-scale reservoir geometries on streamline flow patterns in submarine lobe deposits using outcrop analogues from the Karoo Basin. Petroleum Geoscience, 23 (2), pp. 159-176.

Hofstra, M., 2016. The stratigraphic record of submarine channel-lobe transition zones. PhD Thesis, University of Leeds, UK.

Howell, J. A., Martinius, A. W. & Good, T. R., 2014. The application of outcrop analogues in geological modelling: a review, present status and future outlook. *In*: Martinius, A. W., Howell, J. A. & Good, T. R. (Eds). Sediment-Body Geometry and Heterogeneity: Analogue Studies for Modelling the Subsurface. Geological Society Special Publication, Bath, Geological Soc Publishing House, 387, pp. 1-25.

Hubbard, S. M., Romans, B. W. & Graham, S. A., 2008. Deep-water foreland basin deposits of the Cerro Toro Formation, Magallanes Basin, Chile; architectural elements of sinuous basin axial channel belt. Sedimentology, 55 (5), pp. 1333-1359.

Hubbard, S. M., Covault, J. A., Fildani, A. & Romans, B. W., 2014. Sediment transfer and deposition in slope channels: Deciphering the record of enigmatic deep-sea processes from outcrop. Geological Society of America Bulletin, 126 (5-6), pp. 857-871.

Hübscher, C., Spieß, V., Breitzke, M. & Weber, M. E., 1997. The youngest channel-levee system of the Bengal Fan; results from digital sediment echosounder data. Marine Geology, 141 (1-4), pp. 125-145.

Ingersoll, R.V., 2012. Chapter 1 - Tectonics of sedimentary basins, with revised nomenclature. *In*: Busby, C. & Azor, A. (eds.), Tectonics of Sedimentary Basins: Recent Advances. John Wiley & Sons, Ltd, Chichester, UK.

Janocko, M., Nemec, W., Henriksen, S. & Warchol, M., 2013. The diversity of deep-water sinuous channel belts and slope valley-fill complexes. Marine and Petroleum Geology, 41, pp. 7-34.

Jegou, I., Savoye, B., Pirmez, C. & Droz, L., 2008. Channel-mouth lobe complex of the recent Amazon Fan: The missing piece. Marine Geology, 252 (1-2), pp. 62-77.

Jenner, K. A., Piper, D. J. W., Campbell, D. C. & Mosher, D. C., 2007. Lithofacies and origin of late Quaternary mass transport deposits in submarine canyons, central Scotian Slope, Canada. Sedimentology, 54 (1), pp. 19-38.

Jerolmack, D. J. & Paola, C., 2010. Shredding of environmental signals by sediment transport. Geophysical Research Letters, 37 (19), L19401.

Jobe, Z. R., Howes, N. C. & Auchter, N. C., 2016. Comparing submarine and fluvial channel kinematics: Implications for stratigraphic architecture. Geology, 44 (11), pp. 931-934.

Johnson, S.D., Flint, S., Hinds, D. & De Ville Wickens, H., 2001. Anatomy, geometry and sequence stratigraphy of basin floor to slope turbidite systems, Tanqua Karoo, South Africa. Sedimentology, 48, pp. 987-1023.

Johnson, K., Waldman, R. & Marsaglia, K.M., 2017. Data report: sedimentary columns with facies and bedding for Units II–IV at IODP Site U1438. Methods, 1, pp.1.

Kane, I. A., Kneller, B. C., Dykstra, M., Kassem, A. & McCaffrey, W. D., 2007. Anatomy of a submarine channel-levee: An example from Upper Cretaceous slope sediments, Rosario Formation, Baja California, Mexico. Marine and Petroleum Geology, 24, pp. 540-563.

Kane, I. A., Dykstra, M., Kneller, B. C., Tremblay, S. & McCaffrey, W. D., 2009. Architecture of a coarse-grained channel-levee system: the Rosario Formation, Baja California, Mexico. Sedimentology, 56 (7), pp. 2207-2234.

Kane, I. A. & Hodgson, D. M., 2011. Sedimentological criteria to differentiate submarine channel levee sub-environments: Exhumed examples from the Rosario Fm. (Upper Cretaceous) of Baja California, Mexico, and the Fort Brown Fm. (Permian), Karoo Basin, S. Africa. Marine and Petroleum Geology, 28 (3), pp. 807-823.

Kane, I. A. & Ponten, A. S. M., 2012. Submarine transitional flow deposits in the Paleogene Gulf of Mexico. Geology, 40 (12), pp. 1119-1122.

Kane, I. A., Ponten, A. S. M., Vangdal, B., Eggenhuisen, J. T., Hodgson, D. M. & Spychala, Y. T., 2017. The stratigraphic record and processes of turbidity current transformation across deep-marine lobes. Sedimentology, 64 (5), pp. 1236-1273.

Kenyon, N. H. & Millington, J., 1995. Contrasting deep sea depositional systems in the Bering Sea. *In:* Pickering, K. T., Hiscott, R. N., Kenyon, N. H., Lucchi, F. R. & Smith, R. D. A. (Eds). Atlas of Deep Water Environments; Architectural Style in Turbidite systems. Chapman and Hall, pp. 196-202.

Keogh, K.J., Leary, S., Martinius, A.W., Scott, A.S., Riordan, S., Viste, I., Gowland, S., Taylor, A.M. & Howell, J., 2014. Data capture for multiscale modelling of the Lourinha Formation, Lusitanian Basin, Portugal: an outcrop analogue for the Statfjord Group, Norwegian North Sea. Geological Society, London, Special Publications, 387, pp. SP387-11.

Khan, Z. A. & Arnott, R. W. C., 2011. Stratal attributes and evolution of asymmetric inner- and outer-bend levee deposits associated with an ancient deep-water channel-levee complex within the Isaac Formation, southern Canada. Marine and Petroleum Geology, 28 (3), pp. 824-842.

King, P.R. & Trasher, G.P., 1992. Post-Eocene development of the Taranaki basin, New Zealand: Convergent overprint of a passive margin. *In*: Watkins, J.S., Zhiqiang, F. & McMillen, K.J. (Eds.) Geology and Geophysics of Continental Margins. AAPG Memoirs, 53, pp. 93-118.

King, P. R., Browne, G. H. & Slatt, R. M., 1994. Sequence architecture of exposed Late Miocene basin floor fan and channel-levee complexes (Mount Messenger Formation), Taranaki basin, New Zealand. *In*: Weimer, P., Bouma, A. H. & Perkins, B. (Eds). GCSSEPM Foundation 15th Annual Research Conference, Submarine Fans and Turbidite Systems: Sequence Stratigraphy, Reservoir Architecture and Production Characteristics, Gulf of Mexico and International., Houston, Tex., United States, GCSSEPM Foundation, pp. 177-192.

King, E. L., Sejrup, H. P., Haflidason, H., Elverhoi, A. & Aarseth, I., 1996. Quaternary seismic startigraphy of the North Sea Fan: glacially-fed gravity flow aprons, hemipelagic sediments, and large submarine slides. Marine Geology, 130, pp. 293-315.

King, P. R., Browne, G. H., Arnot, M. J., Slatt, R. M., Helle, K. & Stromsoyen, I., 2007(a). An Overview of the Miocene Mount Messenger-Urenui Formations, New Zealand: A 2-D, Oblique-dip Outcrop Transect: Through an Entire Third-order, Progradational, Deep-water Clastic Succession. *In*: Nilsen, T. H., Shew, R. D., Steffens, G. S. & Studlick, J. R. J. (Eds). Atlas of Deep-Water Outcrops. AAPG Studies in Geology, 56, pp. 238-240.

King, P. R., Brown, G. H., Arnot, M. J. & Stromsoyen, I., 2007(b). Slope feeder channels, Urenui Formation, Wai-iti and Mimi Beaches, New Zealand. *In*: Nilsen, T. H., Shew, R. D., Steffens, G. S. & Studlick, J. R. J. (Eds). Atlas of Deep-Water Outcrops. AAPG Studies in Geology, 56, pp. 262-264.

King, P. R., Browne, G. H., Arnot, M. J. & Crundwell, M. P., 2007(c). A 2-D, Oblique-dip Outcrop Transect through a Third-order, Progradational, Deep-water Clastic Succession, Urenui-Mount Messenger Formations, New Zealand. *In*: Nilsen, T. H., Shew, R. D., Steffens, G. S. & Studlick, J. R. J. (Eds). Atlas of Deep-Water Outcrops, CD-ROM. AAPG Studies in Geology, 56, pp. 1-42.

King, R. C., Hodgson, D. M., Flint, S. S., Potts, G. J. & Van Lente, B., 2009. Development of subaqueous fold belts as a control on the timing and distribution of deepwater sedimentation: An example from the Southwest Karoo Basin, South Africa. *In*: Kneller, B. C., Martinsen, O. J. & McCaffrey, W. D. (Eds). External Controls on Deep-Water Depositional Systems. Society for Sedimentary Geology Special Publication, 92, pp. 261-278.

King, P. R., Ilg, B. R., Arnot, M., Browne, G. H., Strachan, L. J., Crundwell, M. P. & Helle, K., 2011. Outcrop and seismic examples of mass-transport deposits from a late Miocene deep-water succession, Taranaki Basin, New Zealand. *In*: Shipp, R. C., Weimer, P. & Posamentier, H. W. (Eds). Mass-Transport Deposits in Deepwater Settings. Society for Sedimentary Geology Special Publication, United States (USA), Society for Sedimentary Geology (SEPM), Tulsa, OK, United States (USA), pp. 311-350.

Kneller, B. C. & McCaffrey, W. D., 1999. Depositional effects of flow nonuniformity and stratification within turbidity currents approaching a bounding slope; deflection, reflection, and facies variation. Journal of Sedimentary Research, 69 (5), pp. 980-991.

Kneller, B. C. & Buckee, C., 2000. The structure and fluid mechanics of turbidity currents: a review of some recent studies and their geological implications. Sedimentology, 47, Suppl. 1, pp. 62-94.

Kneller, B. C., Martinsen, O. J. & McCaffrey, W. D., 2009. External controls on deep-water sedimentary systems: Challenges and persectives. *In*: Kneller, B. C., Martinsen, O. J. & McCaffrey, W. D. (Eds). External Controls on Deep-Water Depositional Systems. Society for Sedimentary Geology Special Publication, 92, pp. 5-12.

Kolla, V., Bourges, P., Urruty, J. M. & Safa, P., 2001. Evolution of deep-water Tertiary sinuous channels offshore Angola (West Africa) and implications for reservoir architecture. AAPG Bulletin, 85 (8), pp. 1373-1405.

Kolla, V., Posamentier, H. W. & Wood, L. J., 2007. Deep-water and fluvial sinuous channels - Characteristics, similarities and dissimilarities, and modes of formation. Marine and Petroleum Geology, 24, pp. 388-405.

Konsoer, K., Zinger, J. & Parker, G., 2013. Bankfull hydraulic geometry of submarine channels created by turbidity currents: Relations between bankfull channel characteristics and formative flow discharge. Journal of Geophysical Research: Earth Surface, 118, pp. 216–228.

Konyuklov, A. I., 2008. Sedimentary basins of passive margins filled with sediments of river deltas and submarine fans. Lithology and Mineral Resources, 43 (6), pp. 507-519.

Kuenen, P. H. & Migliorini, C. I., 1950. Turbidity currents as a cause of graded bedding. Journal of Geology, 58 (2), pp. 91-127.

Lamb, M. P., Hickson, T., Marr, J. G., Sheets, B., Paola, C. & Parker, G., 2004. Surging versus continuous turbidity currents: Flow dynamics and deposits in an experimental intraslope minibasin. Journal of Sedimentary Research, 74 (1), pp. 148-155.

Li, P., Kneller, B. C., Hansen, L. & Kane, I. A., 2016. The classical turbidite outcrop at San Clemente, California revisited: An example of sandy submarine channels with asymmetric facies architecture. Sedimentary Geology, 346, pp. 1-16.

Li, P., Kneller, B., Thompson, P., Bozetti, G. & dos Santos, T., 2018. Architectural and facies organisation of slope channel fills: Upper Cretaceous Rosario Formation, Baja California, Mexico. Marine and Petroleum Geology, 92, pp. 632-649.

Loutit, T.S., Hardenbol, J., Vail, P.R. & Baum, G.R., 1988. Condensed sections: the key to age-dating and correlation of continental margin sequences. *In*: Wilgus, C.K., Hastings, B.S.,

Kendall, C.G.St.C., Posamentier, H.W., Ross, C.A., Van Wagoner, J.C. (Eds.), Sea Level Changes—An Integrated Approach, SEPM Special Publication, (42), pp. 183–213.

Lowe, D. R. , 1979. Sediment gravity flows; their classification and some problems of application to natural flows and deposits. *In*: Doyle, L. J. & Pilkey, O. H. (Eds). Geology of continental slopes. Special Publication - Society of Economic Paleontologists and Mineralogists, Tulsa, OK, United States, SEPM (Society for Sedimentary Geology), 27, pp. 75-82.

Lowe, D. R., 1982. Sediment gravity flows: II, Depositional models with special reference to the deposits of high-density turbidity currents. Journal of Sedimentary Petrology, 52 (1), pp. 279-297.

Macauley, R. V. & Hubbard, S. M., 2013. Slope channel sedimentary processes and stratigraphic stacking, Cretaceous Tres Pasos Formation slope system, Chilean Patagonia. Marine and Petroleum Geology, 41, pp.146-162.

MacDonald, D. I. M., Butterworth, P. J. & Crame, J. A., 1995. Deep marine slide and channel deposits from the Jurassic-Cretaceous Fossil Bluff Group. Alexander Island, Antarctica. *In*: Pickering, K. T., Hiscott, R. N., Kenyon, N. H., Lucchi, F. R. & Smith, R. D. A. (Eds). Atlas of Deep Water Environments; Architectural Style in Turbidite systems. Chapman and Hall, pp. 50-55.

Macdonald, H. A., Wynn, R. B., Huvenne, V. A. I., Peakall, J., Masson, D. G., Weaver, P. P. E. & McPhail, S. D., 2011(b). New insights into the morphology, fill, and remarkable longevity (> 0.2 m.y.) of modern deep-water erosional scours along the northeast Atlantic margin. Geosphere, 7 (4), pp. 845-867.

Macdonald, H. A., Peakall, J., Wignall, P. B. & Best, J. L., 2011(b). Sedimentation in deep-sea lobe-elements: implications for the origin of thickening-upward sequences. Journal of the Geological Society of London, 168 (2), pp. 319-331.

Maier, K. L., Fildani, A., Paull, C. K., Graham, S. A., McHargue, T. R., Caress, D. W., & McGann, M., 2011. The elusive character of discontinuous deep-water channels: New insights from Lucia Chica channel system, offshore California. Geology, 39, pp. 327-330.

Marches, E., Mulder, T., Gonthier, E., Cremer, M., Hanquiez, V., Garlan, T. & Lecroart, R., 2010. Perched lobe formation in the Gulf of Cadiz: Interactions between gravity processes and contour currents (Algarve Margin, Southern Portugal). Sedimentary Geology, 229(3), pp. 81-94.

Marsset, T., Droz, L., Dennielou, B. & Pichon, E., 2009. Cycles in the architecture of the Quaternary Zaire turbidite system: A possible link with climate. *In*: Kneller, B. C., Martinsen, O. J. & McCaffrey, W. D. (Eds). External Controls on Deep-Water Depositional Systems. Society for Sedimentary Geology Special Publication, 92, pp. 89-106.

Martinensen, O. J., Sømme, T. O., Thurmond, J. B., Helland-Hansen, W. & Lunt, I., 2011. Source-to-sink systems on passive margins: theory and practise with an example from the Norwegian continental margin. Geological Society, London, Petroleum Geology Conference series, 7, pp. 913-920.

Masalimova, L. U., Lowe, D. R., Sharman, G. R., King, P. R. & Arnot, M. J., 2016. Outcrop characterization of a submarine channel-lobe complex: The Lower Mount Messenger

Formation, Taranaki Basin, New Zealand. Marine and Petroleum Geology, 71, pp. 360-390.

May, J. A. & Warme, J. E., 2007. A rare exposure of an ancient submarine canyon, Black's Beach, California, USA. *In*: Nilsen, T. H., Shew, R. D., Steffens, G. S. & Studlick, J. R. J. (Eds). Atlas of Deep-Water Outcrops. AAPG Studies in Geology, 56, pp. 378-382.

Mayall, M., Jones, E. & Casey, M., 2006. Turbidite channel reservoirs - Key elements in facies prediction and effective development. Marine and Petroleum Geology, 23 (8), pp. 821-841.

Mayall, M., Lonergan, L., Bowman, A., James, S., Mills, K., Primmer, T., Pope, D., Rogers, L. & Skeene, R., 2010. The response of turbidite slope channels to growth-induced seabed topography. AAPG Bulletin, 94 (7), pp. 1011-1030.

McArthur, A. D., Kneller, B. C., Souza, P. A. & Kuchle, J., 2016. Characterization of deep-marine channel-levee complex architecture with palynofacies: An outcrop example from the Rosario Formation, Baja California, Mexico. Marine and Petroleum Geology, 73, pp. 157-173.

McCaffrey, W. D., Gupta, S. & Brunt, R., 2002. Repeated cycles of submarine channel incision, infill and transition to sheet sandstone development in the Alpine foreland basin, SE France. Sedimentology, 49 (3), pp. 623-635.

McGilvery, T. A. & Cook, D. L., 2003. The Influence of Local Gradients on Accommodation Space and Linked Depositional Elements across a Stepped Slope Profile, Offshore Brunei. *In*: Roberts, H. H., Rosen, N. C., Fillon, R. H. & Anderson, J. B. (Eds). GCSSEPM Foundation 23rd Annual Research Conference, Shelf Margin Deltas and Linked Down Slope Petroleum Systems: Global Significance and Future Exploration Potential, pp. 387-419.

McHargue, T., Pyrcz, M. J., Sullivan, M. D., Clark, J. D., Fildani, A., Romans, B. W., Covault, J. A., Levy, M., Posamentier, H. W. & Drinkwater, N. J., 2011(a). Architecture of turbidite channel systems on the continental slope: Patterns and predictions. Marine and Petroleum Geology, 28 (3), pp. 728-743.

McHargue, T., Pyrcz, M. J., Sullivan, M. D., Clark, J. D., Fildani, A., Levy, M., Drinkwater, N. J., Posamentier, H. W., Romans, B. W. & Covault, J. A., 2011(b). Event-based modeling of turbidite channel fill, channel stacking pattern, and net sand volume. *In*: Outcrops Revitalized: Tools, Techniques and Applications. SEPM Concepts in Sedimentology and Paleontology, SEPM (Society for Sedimentary Geology), 10, pp. 163-173.

Meckel, L. D. I., 2011. Reservoir characteristics and classification of sand-prone submarine mass transport deposits. In: Shipp, R. C., Weimer, P. and Posamentier, H. W. (Eds). Mass-Transport Deposits in Deepwater Settings. Society for Sedimentary Geology Special Publication, United States (USA), Society for Sedimentary Geology (SEPM), Tulsa, OK, United States (USA) 96 1060-071X, 1060-071X, pp. 423-452.

Meiburg, E. & Kneller, B. C., 2010. Turbidity Currents and Their Deposits. Annual Review of Fluid Mechanics, 42, pp. 135-156.

Menard, H. W., Jr., 1955. Deep-sea channels, topography, and sedimentation. AAPG Bulletin, 39 (2), pp. 236-255.

Miall, A.D., 1985. Architectural-element analysis: a new method of facies analysis applied to fluvial deposits. Earth Science Reviews, 22, pp. 261–308.

Miall, A. D., 1987. Recent developments in the study of fluvial facies models. *In*: Ethridge, F. G., Flores, R. M. & Harvey, M. D. (eds.), Recent Developments in Fluvial Sedimentology. The Society of Economic Palaeontologists and Mineralogists, 39, pp.1-9.

Miall, A. D., 1989. Architectural elements and bounding surfaces in channelized clastic deposits: Notes on comparisons between fluvial and turbidite system. *In*: Taira, A. & Masuda, F. (eds). Sedimentary facies in the active plate margin: Tokyo, Japan, Terra Scientific Publishing Company, pp. 3-15.

Miall, A.D., 1999. In defense of facies classifications and models. Journal of Sedimentary Research, 69 (1), pp. 2-5.

Miall, A.D., 1995. Description and interpretation of fluvial deposits: a critical perspective. Sedimentology, 42 (2), pp.379-379.

Miall, A. D., 2015. Updating uniformitarianism: stratigraphy as just a set of 'frozen accidents'. Journal of the Geological Society (London). *In*: Smith, D. G., Bailey, R. J., Burgess, P.M. & Fraser, A.J. (eds.), Strata and Time: Probing the Gaps in Our Understanding, Geological Society, London, Special Publications, 404, pp. 11-36.

Miall, A. D., 2016. The valuation of unconformities. Earth Science Reviews, 163, pp. 22-71.

Michael, N. A., Whittaker, A.C. & Allen, P. A., 2013. The Functioning of Sediment Routing Systems Using a Mass Balance Approach: Example from the Eocene of the Southern Pyrenees. The Journal of Geology, 121 (6), pp. 581-606.

Middleton, G. V. & Hampton, M. A., 1973. Sediment Gravity Flows: Mechanics of Flow and Deposition. *In*: Middleton, G. V. & Bouma, A. H. (Eds). Turbidites and deep water sedimentation. SEPM Short Course, Los Angeles, California, Pacific Section SEPM, pp. 1-38.

Migeon, S., Ducassou, E., Le Gonidec, Y., Rouillard, P., Mascle, J. & Revel-Rolland, M., 2010. Lobe construction and sand/mud segregation by turbidity currents and debris flows on the western Nile deep-sea fan (Eastern Mediterranean). Sedimentary Geology, 229 (3), pp. 124-143.

Mignard, S. L. A., Mulder, T., Professor, P. M., Charlier, K., Rossignol, L. & Garlan, T., 2017. Deep-sea terrigenous organic carbon transfer and accumulation: Impact of sea-level variations and sedimentation processes off the Ogooue River (Gabon). Marine and Petroleum Geology, 85, pp. 35-53.

Miller, S. & MacDonald, D.I.M., 2004. Metamorphic and thermal history of a fore-arc basin: the Fossil Bluff group, Alexander Island, Antarctic. Journal of Petrology, 45 (7), pp.1453-1465.

Milliman, J.D. & Syvitski, J.P., 1992. Geomorphic/tectonic control of sediment discharge to the ocean: the importance of small mountainous rivers. The Journal of Geology, 100 (5), pp. 525-544.

Mitchum, R.M., Vail, P.R. & Thompson, S., 1977. Seismic Stratigraphy and Global Changes of Sea Level, Part 2: The Depositional Sequence as a Basic Unit for Stratigraphic Analysis. *In*: Payton, C.E. (ed), AAPG Memoir 26 Seismic Stratigraphy – Applications to Hydrocarbon Exploration, pp. 53-62.

Mitchum, R.M. & Van Wagoner, J.C., 1991. High-frequency sequences and their stacking patterns: sequence-stratigraphic evidence of high-frequency eustatic cycles. Sedimentary Geology, 70, pp.131-160.

Moody, J.D., 2010. Effect of growth structures on slope channel architecture and facies with respect to reservoir characterisation, Eocene Morillo Turbidite System (South-Central Pyrenees, Spain). Msc. Thesis, Colorado School of Mines.

Moody, J. D., Pyles, D. R., Clark, J. D. & Bouroullec, R., 2012. Quantitative outcrop characterization of an analog to weakly confined submarine channel systems: Morillo 1 member, Ainsa Basin, Spain. AAPG Bulletin, 96 (10), pp. 1813-1841.

Moraes, M. A. S., Blaskovski, P. R. & Joseph, P., 2004. The Gres d'Annot as an analogue for Brazilian Cretaceous sandstone reservoirs: comparing convergent to passive-margin confined turbidites. *In*: Joseph, P. & Lomas, S. A. (Eds). Deep-Water Sedimentation in the Alpine Basin of SE France: New Perspectives on the Gres D'Annot and Related Systems. Geological Society of London Special Publication, 221, pp. 419-437.

Morris, W. R. & Busby Spera, C. J., 1988. Sedimentologic evolution of a submarine canyon in a forearc basin, Upper Cretaceous Rosario Formation, San Carlos, Mexico. AAPG Bulletin, 72, pp. 717-737.

Morris, W. & Busby Spera, C. J., 1990. A submarine-fan valley-levee complex in the Upper Cretaceous Rosario Formation; implication for turbidite facies models. Geological Society of America Bulletin, 102 (7), pp. 900-914.

Morris, E., 2014. Stratigraphic record of sedimentary processes in submarine channel-levee systems. PhD Thesis, University of Leeds, UK.

Morris, E. A., Hodgson, D. M., Flint, S., Brunt, R. L., Luthi, S. M. & Kolenberg, Y., 2016. Integrating outcrop and subsurface data to assess the temporal evolution of a submarine channel-levee system. AAPG Bulletin, 100 (11), pp. 1663-1691.

Moscardelli, L., Wood, L. & Mann, P., 2006. Mass-transport complexes and associated processes in the offshore area of Trinidad and Venezuela. AAPG Bulletin, 90 (7), pp. 1059-1088.

Moscardelli, L. & Wood, L., 2015. Morphometry of mass-transport deposits as a predictive tool. Geological Society of America Bulletin, 128 (1-2), pp. 47-80.

Mulder, T. & Syvitski, J. P. M., 1995. Turbidity currents generated at river mouths during exceptional discharges to the world oceans. Journal of Geology, 103 (3), 285-299.

Mulder, T. & Cochonat, P., 1996. Classification of offshore mass movements. Journal of Sedimentary Research, Section A: Sedimentary Petrology and Processes, 66 (1), pp. 43-57.

Mulder, T. & Alexander, J., 2001. The physical character of subaqueous sedimentary density flows and their deposits. Sedimentology, 48 (2), pp. 269-299.

Mulder, T., Syvitski, J. P. M., Migeon, S., Faugeres, J. C., Savoye, B. & Mutti, E., 2003. Marine hyperpycnal flows; initiation, behavior and related deposits; a review. Marine and Petroleum Geology, 20, pp. 861-882.

Mulder, T. & Etienne, S., 2010. Lobes in deep-sea turbidite systems: State of the art. Sedimentary Geology, 229 (3), pp.75-80.

Mutti, E. & Ricci Lucchi, F., 1972. Le torbidit dell'Appenino settentrionale: introduzione all'analisi di facies. Memoir Society of Geology Italy, 11, 161-199. (English translation by Nilsen, T.H., 1978. International Geological Review, 20, pp.125-166)

Mutti, E. & Ricci Lucchi, F., 1975. Turbidite facies and facies association. *In*: IAS, Field Trip Guidebook. Examples of Turbidites Facies and Facies Association from selected Formations of the Northern Appenines, pp. 21-36.

Mutti, E. and Sonnino, M. (1981). Compensation cycles; a diagnostic feature of turbidite sandstone lobes. In: International Association of Sedimentologists abstracts; 2nd European regional meeting, Oxford, United Kingdom, International Association Sedimentology, pp. 120-123.

Mutti, E. & Normark, W.R., 1987. Comparing Examples of Modern and Ancient Turbidite Systems: Problems and Concepts. *In*: Leggett, J.K. & Zuffa, G.G. (eds.), Marine clastic sedimentology: concepts and case studies: London, Graham and Troutman, pp. 1–38.

Mutti, E. & Normark, W.R., 1991. An Integrated Approach to the Study of Turbidite Systems. *In*: Weimer, P. & Link, M.H. (eds.), Seismic facies and sedimentary processes of submarine fans and turbidite systems: New York, Springer-Verlag, pp. 75–106.

Nakajima, T. and Kneller, B. C., 2013. Quantitative analysis of the geometry of submarine external levees. Sedimentology, 60, pp.877-910.

Nardin, T. R., Hein, F. J., Gorsline, D. S. & Edwards, B. D., 1979. A review of mass movement processes, sediment and acoustic characteristics, and contrasts in slope and base-of-slope systems versus canyon-fan-basin floor systems. Special Publication - Society of Economic Paleontologists and Mineralogists, (27), pp. 61-73.

Navarre, J.-C., Claude, D., Librelle, F., Safa, P., Villon, G. & Keskes, N., 2002. Deepwater turbidite system analysis, West Africa: sedimentary model and implications for reservoir model construction. The Leading Edge, 21, 1132–1139.

Navarro, L., Khan, Z. & Arnott, R. W. C., 2007(a). Depositional Architecture and Evolution of a Deep-marine Channel-levee Complex: Isaac Formation (Windermere Supergroup), Southern Canadian Cordillera. *In*: Nilsen, T. H., Shew, R. D., Steffens, G. S. & Studlick, J. R. J. (Eds). Atlas of Deep-Water Outcrops, CD-ROM. AAPG Studies in Geology, 56, pp. 1-22.

Navarro, L., Khan, Z. A. & Arnott, R. W. C., 2007(b). Architecture of a deep-water channel-levee complex: Channel 3, Castle Creek South, Isaac Formation, Windermere Supergroup, British Columbia, Canada. *In*: Nilsen, T. H., Shew, R. D., Steffens, G. S. & Studlick, J. R. J. (Eds). Atlas of Deep-Water Outcrops. AAPG Studies in Geology, 56, pp. 93-96.

Neal, J. & Abreu, V., 2009. Sequence stratigraphy hierarchy and the accommodation succession method. Geology 37, pp.779-782.

Nelson, C. H. & Nilsen, T. H., 1984. Synthesis and applications to petroleum geology. *In*: Nelson, C. H. & Nilsen, T. H. (Eds). Modern and ancient deep sea-fan sedimentation. SEPM Short Course, Tulsa, OK, United States, Society of Sedimentary Geology, 14, pp. 326-376.

Nelson, C. H., Maldonado, A., Coumes, F., Got, H. & Monaco, A., 1984. The Ebro deep-sea fan system. Geo-Marine Letters, 3(2-4), pp. 125-131.

Nelson, C. H., Escutia, C., Goldfinger, C., Karabanov, E., Gutierrez-Pastor, J. & De Batist, M., 2009. External controls on modern clastic turbidite systems: three case studies. *In*: Kneller, B. C., Martinsen, O. J. & McCaffrey, W. D. (Eds). External Controls on Deep-Water Depositional Systems. Society for Sedimentary Geology Special Publication, 92, pp. 57-76.

Newton, C. S., Shipp, R. C., Mosher, D. C. & Wach, G. D., 2004. Importance of mass transport complexes in the Quaternary development of the Nile Fan, Egypt: Offshore Technology Conference proceedings.

Nielsen, T., Knutz, P. C. & Kuijpers, A., 2008. Seismic Expression of Contourite Depositional Systems. *In*: Rebesco, M. & Camerlenghi, A. (Eds). Contourites. Developments in Sedimentology, Amsterdam, Elsevier Science Bv, 60, pp. 301-321.

Normark, W. R., 1970. Growth Patterns of Deep-Sea Fans. AAPG Bulletin, 54, (11), pp. 2170-2195.

Normark, W. R., Piper, D. J. W. & Hess, G. R., 1979. Distributary channels, sand lobes, and mesotopography of Navy submarine fan, California Borderland, with applications to ancient fan sediments. Sedimentology, 26(6), pp. 749-774.

Normark, W. R. & Piper, D. J. W., 1985. Navy Fan, Pacific Ocean. *In*: Bouma, A. H., Normark, W. R. & Barnes, N. E. (Eds). Submarine Fans and Related Turbidite Systems. New York, NY, United States, Springer-Verlag, pp. 87-94.

Normark, W. R. & Piper, D. J. W., 1991. Initiation processes and flow evolution of turbidity currents; implications for the depositional record. *In*: Osborne, R. H. (Eds). From shoreline to abyss; contributions in marine geology in honor of Francis Parker Shepard. Special Publication - Society of Economic Paleontologists and Mineralogists, Tulsa, OK, United States, SEPM (Society for Sedimentary Geology), 46, pp. 207-230.

Normark, W. R., Piper, D. J. W. & Hiscott, R. N., 1998. Sea level controls on the textural characteristics and depositional architecture of the Hueneme and associated submarine fan systems, Santa Monica Basin, California. Sedimentology, 45 (1), pp. 53-70.

Normark, W. R., Piper, D. J. W., Romans, B. W., Covault, J. A., Dartnell, P. & Sliter, R. W., 2009. Submarine canyon and fan systems of the California Continental Borderland. *In*: Lee, H. J. & Normark, W. R. (Eds). Earth Science in the Urban Ocean: The Southern California Continental Borderland. Geological Society of America Special Papers, Boulder, 454, pp. 141-168.

Nyberg, B., Helland-Hansen, W., Gawthorpe, R.L., Sandbakken, P., Eide, C.H., Sømme, T., Hadler-Jacobsen, F. & Leiknes, S., 2018. Revisiting morphological relationships of modern source-to-sink segments as a first-order approach to scale ancient sedimentary systems. Sedimentary Geology, 373, pp. 111-133.

O'Byrne, C. J., Barton, M. D., Prather, B., Pirmez, C., Sylvester, Z., Commins, D. & Coffa, A., 2007(a). Deep-water channel-complex architectures, Popo Fault Block, Brushy Canyon Formation, Texas, USA - Part 1: stratal framework. *In*: Nilsen, T. H., Shew, R. D., Steffens, G. S. & Studlick, J. R. J. (Eds). Atlas of Deep-Water Outcrops. AAPG Studies in Geology, 56, pp. 457-462.

O'Byrne, C. J., Barton, M. D., Steffens, G. S., Pirmez, C. & Buergisser, H., 2007 (b). Architecture of a laterally migrating channel complex: Channel 4, Isaac Formation, Windermere Supergroup, Castle Creek North, British Columbia. *In*: Nilsen, T. H., Shew, R. D., Steffens, G. S. & Studlick, J. R. J. (Eds). Atlas of Deep-Water Outcrops. AAPG Studies in Geology, 56, pp. 115-118.

Olabode, S. O. & Adekoya, J. A., 2008. Seismic stratigraphy and development of Avon canyon in Benin (Dahomey) basin, southwestern Nigeria. Journal of African Earth Sciences, 50 (5), pp. 286-304.

Ortiz-Karpf, A., Hodgson, D. M., Jackson, C. A. L. & McCaffrey, W. D., 2017. Influence of Seabed Morphology and Substrate Composition on Mass-Transport Flow Processes and Pathways: Insights From the Magdalena Fan, Offshore Colombia. Journal of Sedimentary Research, 87 (3), pp. 189-209.

Ouchi, S., Ethridge, F. G., James, E. W. & Schumm, S. A., 1995. Experimental study of subaqueous fan development. *In*: Hartley, A. J. & Prosser, D. J. (eds). Characteriseation of Deep Marine Clastic Systems, Geological Society Special Publication, 94, pp. 13-29.

Paris, P. J., Walsh, J. P., & Corbett, D. R., 2016. Where the continent ends. Geophysical Research Letters, 43 (12), pp. 208–12,216.

Patacci, M., Haughton, P. D. W. & McCaffrey, W. D., 2014. Rheological complexity in sediment gravity flows forced to decelerate against a confining slope, Braux, SE France. Journal of Sedimentary Research, 84 (4), pp. 270-277.

Paull, C. K., Ussler, W. I., Caress, D. W., Lundsten, E., Covault, J. A., Maier, K. L., Xu, J. & Augenstein, S., 2010. Origins of large crescent-shaped bedforms within the axial channel of Monterey Canyon, offshore California. Geosphere, 6 (6), pp. 755-774.

Payros, A. & Martinez-Braceras, N., 2014. Orbital forcing in turbidite accumulation during the Eocene greenhouse interval. Sedimentology, 61 (5), pp. 1411-1432.

Peakall, J., McCaffrey, W. D. & Kneller, B. C., 2000. A process model for the evolution, morphology, and architecture of sinuous submarine channels. Journal of Sedimentary Research, 70 (3), pp. 434-448.

Peakall, J., Kane, I. A., Masson, D. G., Keevil, G. M., McCaffrey, W. D. & Corney, R., 2012. Global (latitudinal) variation in submarine channel sinuosity. Geology, 40 (1), pp. 11-14.

Peakall, J. & Sumner, E. J., 2015. Submarine channel flow processes and deposits: A process-product perspective. Geomorphology, 244, pp. 95-120.

Pemberton, E. A. L., Hubbard, S. M., Fildani, A., Romans, B. & Stright, L., 2016. The stratigraphic expression of decreasing confinement along a deep-water sediment routing system; outcrop example from southern Chile. Geosphere, 12 (1), pp. 114-134.

Pettinga, L., Jobe, Z., Schumaker, L. & Howes, N., 2018. Morphometric scaling relationships in submarine channel–lobe systems. Geology, 46 (9), pp. 819-822.

Pettingill, H. S. & Weimer, P., 2002. Worldwide deepwater exploration and production; past, present, and future. The Leading Edge, 21, pp. 371-376.

Pichevin, L., Mulder, T., Savoye, B., Gervais, A., Cremer, M. & Piper, D. J. W., 2003. The Golo submarine turbidite system (east Corsica margin): morphology and processes of terrace formation from high-resolution seismic reflection profiles. Geo-Marine Letters, 23 (2), pp.117-124.

Pickering, K. T., Stow, D. A. V., Watson, M. P. & Hiscott, R. N., 1986. Deep-water facies, processes and models: a review and classification scheme for modern and ancient sediments. Earth Science Reviews, 23, pp.75-174.

Pickering, K. T., Hiscott, R. N. & Hein, F. J., 1989. Deep Marine Environments: Clastic Sedimentation and Tectonics. London, Unwin Hyman.

Pickering, K. T., Clark, J. D., Smith, R. D. A., Hiscott, R. N., Ricci Lucchi, F. & Kenyon, N. H., 1995. Architectural element analysis of turbidite systems, and selected topical problems for sand-prone deep-water systems. *In*: Pickering, K. T., Hiscott, R. N., Kenyon, N. H., Ricci Lucchi, F. & Smith, R. D. A. (Eds.), Atlas of Deep Water Environments: Architectural Style in Turbidite Systems. Chapman & Hall, London, pp. 1–10.

Pickering, K. T. & Corregidor, J., 2005. Mass-transport complexes, (MTCs) and tectonic control on basin-floor submarine fans, Middle Eocene, South Spanish Pyrenees. Journal of Sedimentary Research, 75, pp.761-783

Pickering, K. T. & Bayliss, N. J., 2009. Deconvolving tectono-climatic signals in deep-marine siliciclastics, Eocene Ainsa basin, Spanish Pyrenees: Seesaw tectonics versus eustasy. Geology, 37 (3), pp. 203-219.

Pickering, K. T. & Cantalejo, B., 2015. Deep-marine environments of the Middle Eocene Upper Hecho Group, Spanish Pyrenees: Introduction. Earth-Science Reviews, 144, pp. 1-9.

Pickering, K. T., Corregidor, J. & Clark, J. D., 2015. Architecture and stacking patterns of lower-slope and proximal basin-floor channelised submarine fans, Middle Eocene Ainsa System, Spanish Pyrenees: An integrated outcrop-subsurface study. Earth-Science Reviews, 144, pp. 47-81.

Pickering, K. T. & Hiscott, R. N., 2016. Deep marine systems: Processes, deposits, environments, tectonics and sedimentation. John Wiley & Sons.

Picot, M., Droz, L., Marsset, T., Dennielou, B. & Bez, M., 2016. Controls on turbidite sedimentation: Insights from a quantitative approach of submarine channel and lobe

architecture (Late Quaternary Congo Fan). Marine and Petroleum Geology, 72, pp. 423-446.

Piper, D. J. W., Hiscott, R. N. & Normark, W. R., 1999. Outcrop-scale acoustic facies analysis and latest Quaternary development of Hueneme and Dume submarine fans, offshore California. Sedimentology, 46 (1), pp. 47-78.

Piper, D. J. W. & Normark, W. R., 2001. Sandy fans; from Amazon to Hueneme and beyond. AAPG Bulletin, 85 (8), pp. 1407-1438.

Piper, D. J. W. & Normark, W. R., 2009. Processes that initiate turbidity currents and their influence on turbidites; a marine geology perspective. Journal of Sedimentary Research, 79 (5-6), pp. 347-362.

Plink-Björklund, P., Mellere, D. & Steel, R. J., 2001. Turbidite variability and architecture of sand-prone, deep-water slopes; Eocene clinoforms in the Central Basin, Spitsbergen. Journal of Sedimentary Research, Section B: Stratigraphy and Global Studies, 71 (6), pp. 895-912.

Plink-Björklund, P. & Steel, R. J., 2004. Initiation of turbidity currents: outcrop evidence for Eocene hyperpycnal flow turbidites. Sedimentary Geology, 165 (1-2), pp. 29-52.

Posamentier, H. W., Meizarwin, M., Wisman, P. S. & Plawman, T., 2000. Deep Water Depositional Systems - Ultra-Deep Makassar Strait, Indonesia. *In:* GCSSEPM Foundation 20th Annual Research Conference, Deep-Water Reservoirs of the World, pp. 806-816.

Posamentier, H. W, 2003. Depositional elements associated with a basin floor channel-levee system: case study from the Gulf of Mexico. Marine and Petroleum Geology, 20 (6-8), pp. 677-690.

Posamentier, H. W. & Kolla, V., 2003. Seismic geomorphology and stratigraphy of depositional elements in deep-water settings. Journal of Sedimentary Research, 73 (3), pp. 367-388.

Posamentier, H. W. & Walker, R. G., 2006. Deep-water turbidites and submarine fans. *In*: Posamentier, H. W. & Walker, R. G. (eds), Facies Models Revisited. SEPM Special Publications, 84, pp. 399 – 520.

Posamentier, H. W. & Martinsen, O. J., 2011. The character and genesis of submarine mass-transport deposits; insights from outcrop and 3D seismic data. *In*: Shipp, R. C., Weimer, P. & Posamentier, H. W. (Eds). Mass-Transport Deposits in Deepwater Settings. Society for Sedimentary Geology Special Publication, United States (USA), Society for Sedimentary Geology (SEPM), Tulsa, OK, United States (USA) 96 1060-071X, 1060-071X, pp. 7-38.

Postma, G. & Kleverlaan, K., 2018. Supercritical flows and their control on the architecture and facies of small-radius sand-rich fan lobes. Sedimentary Geology, 364, pp. 53-70.

Prather, B. E., Booth, J. R., Steffens, G. S. & Craig, P. A., 1998. Classification, lithological calibration, and stratigraphic succession of seismic facies of intraslope basins, deep-water Gulf of Mexico. AAPG Bulletin, 82 (5A), pp.701-726.

Prather, B. E, Keller, F. B. & Chapin, M. A., 2000. Hierarchy of Deep-Water Architectural Elements with Reference to Seismic Resolution: Implications for Reservoir Prediction and Modeling. *In*: GCSSEPM Foundation 20th Annual Research Conference, Deep-water Reservoirs of the World. Houston, December 3-6, 2000.

Prather, B. E., 2003. Controls on reservoir distribution, architecture and stratigraphic trapping in slope settings. Marine and Petroleum Geology, 20 (6-8), pp. 529-545.

Prather, B. E., Pirmez, C. & Winker, C. D., 2012. Stratigraphy of Linked Intraslope Basins: Brazos-Trinity System Western Gulf of Mexico. *In*: Prather, B. E., Deptuck, M. E., Mohrig, D., Van Hoorn, B. & Wynn, R. B. (Eds). Application of the Principles of Seismic Geomorphology to Continental-Slope and Base-of-Slope Systems: Case Studies from Seafloor and Near-Seafloor Analogues. SEPM Special Publication, 99, pp. 83-109.

Prélat, A, Hodgson, D. M & Flint, S. S., 2009. Evolution, architecture and hierarchy of distributary deep-water deposits: a high-resolution outcrop investigation from the Permian Karoo Basin, South Africa. Sedimentology, 56, pp.2132-2154.

Prélat, A., Covault, J. A., Hodgson, D. M., Fíldani, A. & Flint, S. S., 2010. Intrinsic controls on the range of volumes, morphologies, and dimensions of submarine lobes. Sedimentary Geology, 232, pp.66-76.

Prélat, A. & Hodgson, D. M., 2013. The full range of turbidite bed thickness patterns in submarine lobes: controls and implications. Journal of the Geological Society of London, 170 (1), pp. 209-214.

Prior, D. B. & Hooper, J. R., 1999. Sea floor engineering geomorphology: recent achievements and future directions. Geomorphology, 31 (1-4), pp.411-439.

Pringle, J. K., Brunt, R. L., Hodgson, D. M. & Flint, S. S., 2010. Capturing stratigraphic and sedimentological complexity from submarine channel complex outcrops to digital 3D models, Karoo Basin, South Africa. Petroleum Geoscience, 16 (4), pp. 307-330.

Pyles, D. R., 2007. Architectural Elements in a Ponded Submarine Fan, Carboniferous Ross Sandstone, Western Ireland. *In*: Nilsen, T. H., Shew, R. D., Steffens, G. S. & Studlick, J. R. J. (Eds). Atlas of Deep-Water Outcrops, CD-ROM. AAPG Studies in Geology, 56, p. 1-19.

Pyles, D. R., Jennette, D. C., Tomasso, M., Beaubouef, R. T. & Rossen, C., 2010. Concepts learned from a 3D outcrop of a sinuous slope channel complex; Beacon Channel Complex, Brushy Canyon Formation, West Texas, U.S.A. Journal of Sedimentary Research, 80 (1-2), pp. 67-96.

Qin, Y. P., Alves, T. M., Constantine, J. & Gamboa, D., 2016. Quantitative seismic geomorphology of a submarine channel system in SE Brazil (Espirito Santo Basin): Scale comparison with other submarine channel systems. Marine and Petroleum Geology, 78, pp. 455-473.

Reading, H. G. & Richards, M., 1994. Turbidite systems in deep-water basin margins classified by grain size and feeder system. AAPG Bulletin, 78 (5), pp. 792-822.

Reading, H. G. (Ed.), 1996. Sedimentary Environments; Processes, Facies and Stratigraphy. Blackwell Science, Oxford, United Kingdom.

Rebesco, M. & Stow, D., 2001. Seismic expression of contourites and related deposits: a preface. Marine Geophysical Researches, 22 (5-6), pp. 303-308.

Rebesco, M., Hernandez-Molina, F. J., Van Rooij, D. & Wahlin, A., 2014. Contourites and associated sediments controlled by deep-water circulation processes: State-of-the-art and future considerations. Marine Geology, 352, pp. 111-154.

Remacha, E., Fernandez, L. P. & Maestro, E., 2005. The transition between sheet-like lobe and basin-plain turbidites in the Hecho basin (South-Central Pyrenees, Spain). Journal of Sedimentary Research, 75 (5), pp. 798-819.

Richards, M., Bowman, M. & Reading, H., 1998. Submarine-fan systems I: characterization and stratigraphic prediction. Marine and Petroleum Geology, 15 (7), pp. 689-717.

Richards, M. & Bowman, M., 1998. Submarine fans and related systems II: variability in reservoir architecture and wireline log character. Marine and Petroleum Geology, 15 (8), pp. 821-839.

Richter, N., Keogh, K., Howell, J. & Buckley, S., 2009. A global geological outcrop database with a GIS front end. ESRI European PUG Meeting, Stavanger, Norway, 17-18th September.

Riley, T. R., Flowerdew, M. J. & Whitehouse, M. J., 2012. Chrono- and lithostratigraphy of a Mesozoic-Tertiary fore-to intra-arc basin: Adelaide Island, Antarctic Peninsula. Geological Magazine, 149 (5), pp. 768-782.

Romans, B. W., Fildani, A., Hubbard, S. M., Covault, J. A., Fosdick, J. C. & Graham, S. A., 2011. Evolution of deep-water stratigraphic architecture, Magallanes Basin, Chile. Marine and Petroleum Geology, 28 (3), pp. 612-628.

Ross, G. M. & Arnott, R. W. C., 2007. Regional Geology of the Windermere Supergroup, Southern Canadian Cordillera and Stratigraphic Setting of the Castle Creek Study Area, Canada. *In*: Nilsen, T. H., Shew, R. D., Steffens, G. S. & Studlick, J. R. J. (Eds). Atlas of Deep-Water Outcrops, CD-ROM. AAPG Studies in Geology, 56, pp. 1-16.

Rotzien, J. R., Lowe, D. R., King, P. R. & Browne, G. H., 2014. Stratigraphic architecture and evolution of a deep-water slope channel-levee and overbank apron: The Upper Miocene Upper Mount Messenger Formation, Taranaki Basin. Marine and Petroleum Geology, 52, pp. 22-41.

Sadler, P. M., 1981. Sediment accumulation rates and the completeness of stratigraphic sections. The Journal of Geology, 89 (5), pp. 569-584.

Sadler, P. M., 1999. The influence of hiatuses on sediment accumulation rates. GeoResearch Forum, 5, pp. 15–40.

Saller, A. H., Noah, J. T., Ruzuar, A. P. & Schneider, R., 2004. Linked lowstand delta to basin floor fan deposition, offshore Indonesia: An analog for deep-water reservoir systems. AAPG Bulletin, 88 (1), pp. 21-46.

Saller, A. H., Werner, K., Sugiaman, F., Cebastiant, A., May, R., Glenn, D. & Barker, C., 2008. Characteristics of Pleistocene deep-water fan lobes and their application to an upper

Miocene reservoir model, offshore East Kalimantan, Indonesia. AAPG Bulletin, 92 (7), pp. 919-949.

Saller, A. & Dharmasamadhi, I. N. W., 2012. Controls on the development of valleys, canyons, and unconfined channel-levee complexes on the Pleistocene Slope of East Kalimantan, Indonesia. Marine and Petroleum Geology, 29 (1), pp. 15-34.

Satur, N., Hurst, A., Cronin, B. T., Kelling, G. & Gurbuz, K., 2000. Sand body geometry in a sand-rich, deep-water clastic system, Miocene Cingoz Formation of southern Turkey. Marine and Petroleum Geology, 17 (2), pp. 239-252.

Schlager, W., 2004. Fractal nature of stratigraphic sequences. Geology, 32 (3), pp.185-188.

Schlager, W., 2010. Ordered hierarchy versus scale invariance in sequence stratigraphy. International Journal of Earth Science, 99, pp. S139–S151.

Schwab, W. C., Lee, H. J., Twichell, D. C., Locat, J., Nelson, C. H., McArthur, W. G. & Kenyon, N. H., 1996. Sediment mass-flow processes on a depositional lobe, outer Mississippi Fan. Journal of Sedimentary Research, Section A: Sedimentary Petrology and Processes, 66 (5), pp. 916-927.

Schwarz, E. & Arnott, R. W. C., 2007. Anatomy and evolution of a slope channel-complex set (Neoproterozoic Isaac Formation, Windermere supergroup, southern Canadian cordillera): Implications for reservoir characterization. Journal of Sedimentary Research, 77 (1-2), pp. 89-109.

Schwenk, T. & Spieß, V., 2009. Architecture and stratigraphy of the Bengal Fan as response to tectonic and climate revealed from high-resolution seismic data. *In*: Kneller, B. C., Martinsen, O. J. & McCaffrey, W. D. (Eds). External Controls on Deep-Water Depositional Systems. Society for Sedimentary Geology Special Publication, 92, pp. 107-131.

Scotchman, J. I., Bown, P., Pickering, K. T., BouDagher-Fadel, M., Bayliss, N. J. & Robinson, S. A., 2015. A new age model for the middle Eocene deep-marine Ainsa Basin, Spanish Pyrenees. Earth-Science Reviews, 144, pp. 10-22.

Scott, E. D., Bouma, A. H. & Wickens, H. d. V., 2000. Influence of Tectonics on Submarine Fan Deposition, Tanqua and Laingsburg Subbasins, South Africa. *In*: Bouma, A. H. & Stone, C. G. (Eds). Fine-grained turbidite systems. AAPG Memoir 72/SEPM Special Publication, 68, pp. 47-56.

Shanmugam, G. & Moiola, R. J., 1988. Submarine fans: characteristics, models, classification, and reservoir potential. Earth-Science Reviews, 24 (6), pp. 383-428.

Shanmugam, G., 2000. 50 years of the turbidite paradigm (1950s – 1990s): deep-water processes and facies models – a critical perspective. Marine and Petroleum Geology, 17, pp.285-342.

Shanmugam, G., 2002. Ten turbidite myths. Earth-Science Reviews, 58 (3-4), pp. 311-341.

Shanmugam, G., 2016. Submarine fans: a critical retrospective (1950–2015). Journal of Palaeogeography, 5 (2), pp.110-184.

Shier, R., 2004. Statistics: 2.3 The Mann-Whitney U test. Mathematics Learning Support Centre. Available at: http://www.statstutor.ac.uk/resources/uploaded/mannwhitney.pdf [Accessed 01/10/2018]

Shipp, C., Nott, J. & Newlin, J., 2004. Variations in jetting performance in deep-water environments: Geotechnical characteristics and effects of mass transport complexes. Offshore Technology Conference.

Sixsmith, P. J., Flint, S. S., Wickens, H. d. V. & Johnson, S. D., 2004. Anatomy and stratigraphic development of a basin floor turbidite system in the Laingsburg Formation, Main Karoo Basin, South Africa. Journal of Sedimentary Research, 74 (2), pp. 239-254.

Skene, K. I., Piper, D. J. W. and Hill, P. S., 2002. Quantitative analysis of variations in depositional sequence thickness from submarine channel levees. Sedimentology, 49, pp. 1141-1430.

Slatt, R. M., 2000. Why Outcrop Characterization of Turbidite Systems. *In*: Bouma, A. H. & Stone, C. G. (Eds). Fine-grained turbidite systems. AAPG Memoir 72/SEPM Special Publication, 68, pp.181-186.

Snedden, J. W., Galloway, W. E., Milliken, K. T., Xu, J., Whiteaker, T. & Blum, M. D., 2018. Validation of empirical source-to-sink scaling relationships in a continental-scale system: The Gulf of Mexico basin Cenozoic record. Geosphere, 14 (2), pp. 768-784.

Solheim, A., Berg, K., Forsberg, C. F. & Bryn, P., 2005. The Storegga Slide complex: repetitive large scale sliding with similar cause and development. Marine and Petroleum Geology, 22 (1-2), pp. 97-107.

Sømme, T. O., Helland-Hansen, W., Martinsen, O. J. & Thurmond, J. B., 2009. Relationships between morphological and sedimentological parameters in source-to-sink systems: a basis for predicting semi-quantitative characteristics in subsurface systems. Basin Research, 21 (4), pp. 361-387.

Sømme, T. O., Piper, D. J. W., Deptuck, M. E. & Helland-Hansen, W., 2011. Linking onshore-offshore sediment dispersal in the Golo source-to-sink system (Corsica, France) during the Late Quaternary. Journal of Sedimentary Research, 81 (1-2), pp. 118-137.

Soper, D., 2013. Database Lesson – Introduction to Databases 1 of 8 [Online Video]. May 30th. Available from: https://www.youtube.com/watch?v=4Z9KEBexzcM [Accessed: October 13th 2014]

Sprague, A. R. G., Sullivan, M. D., Campion, K. M., Jensen, G. N., Goulding, F. J., Garfield, T. R., Sickafoose, D. K., Rossen, C., Jennette, D. C., Beaubouef, R. T., Abreu, V., Ardill, J., Porter, M. L. & Zelt, F. B., 2002. The physical stratigraphy of deep-water strata: a hierarchical approach to the analysis of genetically related stratigraphic elements for improved reservoir prediction (abstract). American Association of Petroleum Geologists, Annual Meeting, March 10–13, 2002, Houston, Texas, Official Program, p. A167.

Sprague, A. R. G., Garfield, T. R., Goulding, F. J., Beaubouef, R. T., Sullivan, M. D., Rossen, C., Campion, K. M., Sickafoose, D. K., Abreu, V., Schellpeper, M. E., Jensen, G. N., Jennette, D. C., Pirmez, C., Dixon, B. T., Ying, D., Ardill, J., Mohrig, D. C., Porter, M. L., Farrell, M. E. & Mellere, D., 2005. Integrated Slope Channel Depositional Models: The Key to

Successful Prediction of Reservoir Presence and Quality in Offshore West Africa. *In*: CIPM - E-Exitep 2005, Feb 20-23, 2005, Veracruz, México, pp. 1-13.

Sprague, A., Box, D., Hodgson, D. & Flint, S., 2008. A physical stratigraphic hierarchy for deep-water slope system reservoirs 2: complexes to storeys. AAPG International Conference and Exhibition, Cape Town, South Africa, Abstracts.

Sprague, A. R., 2014. Outcrop-based, integrated, core- to seismic-scale, stratigraphic and depositional models for deep water reservoirs: new concepts for stratigraphic traps. AAPG Geoscience Technology Workshop, Stratigraphic Traps and Play Concepts in Deepwater Settings, Rio de Janeiro, Brazil, May 14-15, 2014.

Spychala, Y. T., Hodgson, D. M., Prélat, A., Kane, I. A., Flint, S. S. & Mountney, N. P., 2017(a). Frontal and Lateral Submarine Lobe Fringes: Comparing Sedimentary Facies, Architecture and Flow Processes. Journal of Sedimentary Research, 87 (1), pp. 75-96.

Spychala, Y. T., Hodgson, D. M., Stevenson, C. J. & Flint, S. S., 2017(b). Aggradational lobe fringes: The influence of subtle intrabasinal seabed topography on sediment gravity flow processes and lobe stacking patterns. Sedimentology, 64 (2), pp. 582-608.

Spychala, Y. T., Hodgson, D. M. & Lee, D. R., 2017(c). Autogenic controls on hybrid bed distribution in submarine lobe complexes. Marine and Petroleum Geology, 88, pp. 1078-1093.

Stewart, J., Dunn, P., Lyttle, C., Campion, K., Oyerinde, A. & Fischer, B., 2008. Improving performance prediction in deep-water reservoirs: learning from outcrop analogues, conceptual models and flow simulation. International Petroleum Technology Conference, Malaysia, MS 12892, pp. 1–9.

Stockli, R., 2004. October, Blue marble next generation with topography and bathymetry [image]. NASA Earth Observatory. Available at: https://visibleearth.nasa.gov/view.php?id=73826. [Accessed 10 May 2018].

Stow, D. A. V., Howell, D. G. & Nelson, C. H., 1985. Sedimentary, tectonic, and sea level controls. *In*: Bouma, A. H., Normark, W. R. & Barnes, N. E. (Eds). Submarine Fans and Related Turbidite Systems, pp. 15-22.

Stow, D. A. V., Reading, H. G. & Collinson, J. D., 1996. Deep seas. *In*: Reading, H. G. (eds). Sedimentary environments; processes, facies and stratigraphy. Oxford, United Kingdom, Blackwell Science, pp. 395-453.

Stow, D.A.V. & Mayall, M., 2000. Deep-water sedimentary systems: New models for the 21st century. Marine and Petroleum Geology, 17, pp. 125-135.

Stow, D. A. V., Faugeres, J. C., Howe, J. A., Pudsey, C. J. & Viana, A. R., 2002. Bottom currents, contourites and deep-sea sediment drifts; current state-of-the-art. *In*: Deep-Water Contourite Systems: Modern Drifts and Ancient Series, Seismic and Sedimentary Characteristics. Memoirs of the Geological Society of London, Geological Society Publishing House, Bath, 22, pp. 7-20.

Stow, D. A. V., Hunter, S., Wilkinson, D. & Hernandez-Molina, F. J., 2008. The Nature of Contourite Deposition. In, Rebesco, M. and Camerlenghi, A. (Eds). Contourites. Developments in Sedimentology, Amsterdam, Elsevier Science Bv, 60, pp. 143-156.

Stow, D. A. V., Hernandez-Molina, F. J., Llave, E., Sayago-Gil, M., Diaz del Rio, V. & Branson, A., 2009. Bedform-velocity matrix: The estimation of bottom current velocity from bedform observations. Geology, 37 (4), pp. 327-330.

Straub, K. M. & Pyles, D. R., 2012. Quantifying the Hierarchical Organization of Compensation in Submarine Fans Using Surface Statistics. Journal of Sedimentary Research, 82, pp. 889-898.

Stright, L., Stewart, J., Campion, K. & Graham, S., 2014. Geologic and seismic modeling of a coarse-grained deep-water channel reservoir analog (Black's Beach, La Jolla, California). AAPG Bulletin, 98 (4), pp. 695-728.

Sugiaman, F., Cebastiant, A., Werner, K., Saller, A., Glenn, D. & May, R., 2007. Reservoir characterisation and modelling of an upper Miocene deepwater fan reservoir, Gendalo field, Kutai basin, offshore east Kalimantan. Indonesian Petroleum Association, 31st Annual Convention & Exhibition, May 2007.

Sumner, E. J., Talling, P. J. & Amy, L. A., 2009. Deposits of flows transitional between turbidity current and debris flow. Geology, 37 (11), pp. 991-994.

Sweet, M. L. & Blum, M. D., 2016. Connections Between Fluvial to Shallow Marine Environments and Submarine Canyons: Implications for Sediment Transfer to Deep Water. Journal of Sedimentary Research, 86 (10), pp. 1147-1162.

Symons, W. O., Sumner, E. J., Paull, C. K., Cartigny, M. J. B., Xu, J. P., Maier, K. L., Lorenson, T. D. & Talling, P. J., 2017. A new model for turbidity current behavior based on integration of flow monitoring and precision coring in a submarine canyon. Geology, 45 (4), pp. 367-370.

Talling, P. J., Amy, L. A., Wynn, R. B., Peakall, J. & Robinson, M., 2004. Beds comprising debrite sandwiched within co-genetic turbidite: origin and widespread occurrence in distal depositional environments. Sedimentology, 51 (1), pp. 163-194.

Talling, P. J., Masson, D. G., Sumner, E. J. & Malgesini, G., 2012. Subaqueous sediment density flows: Depositional processes and deposit types. Sedimentology, 59 (7), pp. 1937-2003.

Talling, P. J., 2014. On the triggers, resulting flow types and frequencies of subaqueous sediment density flows in different settings. Marine Geology, 352, pp. 155-182.

Terlaky, V., Rocheleau, J. & Arnott, R. W. C., 2016. Stratal composition and stratigraphic organisation of stratal elements in an ancient deep-marine basin-floor succession, Neoproterozoic Windermere Supergroup, British Columbia, Canada. Sedimentology, 63 (1), pp. 136–175.

Thorne, J., 1995. On the scale independent shape of prograding stratigraphic units. *In*: Barton, C.B., & La Pointe, P.R. (eds.), Fractals in petroleum geology and Earth processes. New York, Plenum Press, pp. 97–112.

Tőkés, L. & Patacci, M., 2018. Quantifying tabularity of turbidite beds and its relationship to the inferred degree of basin confinement. Marine and Petroleum Geology., 97, pp. 659-671.

Tripsanas, E. K., Piper, D. J. W., Jenner, K. A. & Bryant, W. R., 2008. Submarine mass-transport facies: new perspectives on flow processes from cores on the eastern North American margin. Sedimentology, 55 (1), pp. 97-136.

Tucker, M. E., 2011. Sedimentary rocks in the field: a practical guide. 4th Ed. West Sussex, Chichester: Wiley-Blackwell.

Twichell, D. C., Schwab, W. C., Nelson, C. H., Kenyon, N. H. & Lee, H. J., 1992. Characteristics of a sandy depositional lobe in the outer Mississippi fan from SeaMARCIA sidescan sonar images. Geology 20, pp.689–692.

Twichell, D. C., Schwab, W. C. & Kenyon, N. H., 1995. Geometry of sandy deposits at the distal edge of the Mississippi Fan, Gulf of Mexico. *In*: Pickering, K. T., Hiscott, R. N., Kenyon, N. H., Lucchi, F. R. & Smith, R. D. A. (Eds). Atlas of Deep Water Environments; Architectural Style in Turbidite systems. Chapman and Hall, pp. 282-286.

Twichell, D. C., Chaytor, J. D., ten Brink, U. S. & Buczkowski, B., 2009. Morphology of late Quaternary submarine landslides along the US Atlantic continental margin. Marine Geology, 264 (1-2), pp. 4-15.

Vail, P. R., Mitchum, R. M., Thompson, J. R. & Thompson, S., 1977. Seismic Stratigraphy and Global Changes of Sea Level, Part 4: Global cycles of relative changes of sea level. *In:* Payton, C. E. (ed), AAPG Memoir 26 Seismic Stratigraphy – Applications to Hydrocarbon Exploration, pp.83 – 97.

Vakarelov, B. K. &, Ainsworth, R. B., 2013. A hierarchical approach to architectural classification in marginal-marine systems: Bridging the gap between sedimentology and sequence stratigraphy. AAPG Bulletin, 97 (7) pp. 1121–1161.

van den Berg, J.H. & van Gelder, A., 1993. Prediction of suspended bed material transport in flows over silt and very fine sand. Water Resources Research, 29 (5), pp.1393-1404.

Van der Merwe, W., Flint, S. & Hodgson, D., 2010. Sequence stratigraphy of an argillaceous, deepwater basin plain succession: Vischkuil Formation (Permian), Karoo Basin, South Africa. Marine and Petroleum Geology 27, pp.321-333.

Van Wagoner, J. C., Mitchum, R. M., Posamentier, H. W. & Vail, P. R., 1987. Seismic Stratigraphy Interpretation Using Sequence Stratigraphy: Part 2: Key Definitions of Sequence Stratigraphy. Bally, A. W. (Ed.), Atlas of Seismic Stratigraphy, AAPG Special Volumes, 27 (1), pp. 11–14.

Van Wagoner, J. C., Mitchum Jr., R. M., Campion, K. M. & Rahmanian, V. D., 1990. Siliciclastic sequence stratigraphy in well logs, core and outcrop: concepts for high resolution correlation of time and facies. American Association of Petroleum Geologists, Methods in Exploration, 7, 55.

Vanneste, M., Mienert, J. & Bunz, S., 2006. The Hinlopen Slide: A giant, submarine slope failure on the northern Svalbard margin, Arctic Ocean. Earth and Planetary Science Letters, 245 (1-2), pp. 373-388.

Viana, A. R., Almeida, W., Jr., Nunes, M. C. V. & Bulhoes, E. M., 2007. The economic importance of contourites. Economic and Palaeoceanographic Significance of Contourite Deposits, 276, pp. 1-23.

Vinnels, J. S., Butler, R. W. H., McCaffrey, W. D. & Lickorish, W. H., 2010. Sediment Distribution and Architecture around a Bathymetrically Complex Basin: an Example from the Eastern Champsaur Basin, Se France. Journal of Sedimentary Research, 80 (3-4), pp. 216-235.

von Rad, U. & Tahir, M., 1997. Late Quaternary sedimentation on the outer Indus shelf and slope (Pakistan); evidence from high-resolution seismic data and coring. Marine Geology, 138 (3-4), pp. 193-236.

Waibel, A. F., 1990. Sedimentology, petrographic variability, and very-low-grade metamorphism of the Champsaur Sandstone (Paleogene, Hautes-Alpes, France). Evolution of Volcaniclastic Foreland Turbidites in the External Western Alps. Doctoral thesis, University of Geneva.

Walker, R. G., 1978. Deep-water sandstone facies and ancient submarine fans; models for exploration for stratigraphic traps. AAPG Bulletin, 62 (6), pp. 932-966.

Weimer, P., 1991. Seismic facies, characteristics, and variations in channel evolution, Mississippi Fan (Plio-Pleistocene), Gulf of Mexico. *In*: Weimer, P. & Link, M. H. (Eds). Seismic facies and sedimentary processes of submarine fans and turbidite systems, New York, NY, United States, Springer-Verlag, pp. 323-347.

Weimer, P., 2000. Interpreting Turbidite Systems with 2-D and 3-D Seismic Data: An Overview. *In*: Bouma, A. H. & Stone, C. G. (Eds). Fine-grained turbidite systems. AAPG Memoir 72/SEPM Special Publication, 68, pp. 89-92.

Weimer, P. & Slatt, R. M., 2007(a). Introduction to the Petroleum Geology of Deepwater Settings. *In*: Weimer, P. & Slatt, R. M. (Eds). Introduction to the Petroleum Geology of Deepwater Settings. AAPG Studies in Geology, 57, pp. 1-18.

Weimer, P. & Slatt, R. M., 2007(b). Deepwater Reservoir Elements: Channels and their Sedimentary Fills. *In*: Weimer, P. & Slatt, R. M. (Eds). Introduction to the Petroleum Geology of Deepwater Settings. AAPG Studies in Geology, 57, pp. 171-276.

Weimer, P. & Slatt, R. M., 2006(c). Deepwater-Reservoir Elements: Levee-Overbank Sediments and their Thin Beds. *In*: Weimer, P. & Slatt, R. M. (Eds). Introduction to the Petroleum Geology of Deepwater Settings. AAPG Studies in Geology, 57, pp. 277-342.

Weimer, P. & Slatt, R. M., 2007(d). Deepwater-Reservoir Elements: Sheet Sands and Sandstones. *In*: Weimer, P. & Slatt, R. M. (Eds). Introduction to the Petroleum Geology of Deepwater Settings. AAPG Studies in Geology, 57, pp. 343-418.

Weimer, P. & Slatt, R. M., 2006(e). Deepwater-Reservoir Elements: Mass-Transport Deposits and Slides. *In*: Weimer, P. & Slatt, R. M. (Eds). Introduction to the Petroleum Geology of Deepwater Settings. AAPG Studies in Geology, 57, pp. 419-456.

Wentworth, C. K., 1922. A scale of grade and class terms for clastic sediments. The Journal of Geology, 30 (5), pp. 377-392.

Wetzel, A., 1993. The transfer of river load to deep-sea fans; a quantitative approach. AAPG Bulletin, 77 (10), pp. 1679-1692.

Wynn, R. B., Kenyon, N. H., Masson, D. G., Stow, D. A. V. & Weaver, P. P. E., 2002. Characterization and recognition of deep-water channel-lobe transition zones. AAPG Bulletin, 86 (8), pp. 1441-1462.

Wynn, R. B., Cronin, B. T. & Peakall, J., 2007. Sinuous deep-water channels: Genesis, geometry and architecture. Marine and Petroleum Geology, 24, pp. 341-387.

Xu, J. P., 2011. Measuring currents in submarine canyons: Technological and scientific progress in the past 30 years. Geosphere, 7 (4), pp. 868-876.

Xu, J., Snedden, J. W., Galloway, W. E., Milliken, K. T. & Blum, M. D., 2017. Channel-belt scaling relationship and application to early Miocene source-to-sink systems in the Gulf of Mexico basin. Geosphere, 13 (1), pp. 179-200.

Yang, S.-Y. & Kim, J. W., 2014. Pliocene basin-floor fan sedimentation in the Bay of Bengal (offshore northwest Myanmar). Marine and Petroleum Geology, 49, pp. 45-58.

Zaragosi, S., Auffret, G. A., Voisset, M. & Garlan, T., 2003. Morphology and depositional processes of the Celtic Fan, Bay of Biscay. *In*: Mienert, J. & Weaver, P. P. E. (Eds). European Margin Sediment Dynamics: Side-Scan Sonar and Seismic Images. Berlin, Springer-Verlag, pp. 239-243.

Zhang, X., Pyrcz, M. J. & Deutsch, C. V., 2009. Stochastic surface modeling of deepwater depositional systems for improved reservoir models. Journal of Petroleum Science and Engineering, 68, pp. 118-134.

Zhang, J. J., Wu, S. H., Fan, T. E., Fan, H. J., Jiang, L., Chen, C., Wu, Q. Y. & Lin, P., 2016. Research on the architecture of submarine-fan lobes in the Niger Delta Basin, offshore West Africa. Journal of Palaeogeography-English, 5 (3), pp. 185-204.

Zhang, L. F., Pan, M. & Wang, H. L., 2017. Deepwater Turbidite Lobe Deposits: A Review of the Research Frontiers. Acta Geologica Sinica-English Edition, 91 (1), pp. 283-300.

Zhang, J. J., Wu, S. H., Hu, G. Y., Fan, T. E., Yu, B., Lin, P. & Jiang, S. N., 2018. Sea-level control on the submarine fan architecture in a deepwater sequence of the Niger Delta Basin. Marine and Petroleum Geology, 94, pp. 179-197.

Appendices

Appendix A: Summary table of DMAKS case studies

This appendix lists the deep-marine case studies entered into the DMAKS database by the author. The table lists the case studies in order of data entry, where the ID corresponds to the case study numbering used within the database. System and basin entries related to each case study are also documented. The data entered by the candidate into DMAKS includes 1632 architectural elements, 6880 facies entries and over 4000 transitional data points. This information was sourced from over 100 pieces of literature. The data was entered in accordance with the database standard discussed in Chapter 4.

ID	Case study	System	Basin	Literature
1	Late Pleistocene deposits offshore East Corsica, Golo turbidite system	Golo Turbidite System	Golo Basin	Pichevin et al ., 2003; Gervais et al., 2006(a; b); Deptuck et al., 2008; Prélat et al., 2010; Somme et al., 2011
2	Ross Sandstone, Loop Head Peninsula and Ballybunnion, Ross Formation	Ross Sandstone Submarine Fan System	Shannon Basin	Pyles 2007; MacDonald et al., 2011
3	Channel-levee system, DeSoto canyon, Joshua system, NE Gulf of Mexico	Joshua Channel System	-	Posamentier, 2003
4	Channel complex, Popo Fault Block, Brushy Canyon Formation	Brushy Canyon	Delaware Basin (during the Brushy Canyon)	O'Byrne et al., 2007(a)
5	Channel dimensions, by McHargue et al., 2011	-	-	McHargue et al., 2011a
6	Channel gradients, continental slope of the Niger Delta, by McHargue et al., 2011	-	-	McHargue et al., 2011a; McHargue et al., 2011b
7	Channel dimensions, by McHargue et al., 2011b	-	-	McHargue et al., 2011b
8	Isaac Unit 5, Castle Creek area, Isaac Formation	Isaac Formation	-	Schwarz & Arnott, 2007;
9	Turbidite sandstones in the Sierra Contreras, Tres Pasos Formation	Tres Pasos Deep-Water Slope System	Magallanes Basin (during the Cerro Toro)	Barton et al., 2007(b; c); Armitage et al., 2009; Romans et al., 2011
10	Pleistocene basin-floor offshore E Kalimantan, Kutai turbidite system	Kutai Pleistocene System	Kutai Basin (during the Pleistocene)	Saller et al., 2004; Saller et al., 2008; Sugiaman et al., 2007; Prélat et al., 2010
11	Basin-floor deposits at Willow Mountain, Bell Canyon Formation	Bell Canyon Turbidite System	Delaware Basin (during the Bell Canyon)	Barton & Dutton, 2007

12	Quaternary Amazon Fan	Amazon Turbidite System	-	Flood et al., 1991; Piper & Normark, 2001; Jegou et al., 2008; Somme et al., 2009
13	Channel-levee deposits, Lago Nordenskjold and Laguna Mellizas Sur, Cerro Toro Formation	Cerro Toro Deep-Water System	Magallanes Basin (during the Cerro Toro)	Bouma, 1982; Barton et al., 2007(b; c)
14	Turbidite lobes from the Oman margin, Al Batha turbidite system	Al Batha Turbidite System	-	Bourget et al., 2010
15	Modern deep sea fan, Zaire turbidite system	Zaire Fan	-	Babonneau et al., 2002; Droz et al., 2003; Marsset et al., 2009; Babonneau et al., 2010; Picot et al., 2016
16	Submarine canyons and fans offshore California, Santa Monica Basin	Santa Monica Basin	Santa Monica Basin	Normark et al., 1998; Piper et al., 1999; Piper & Normark, 2001; Normark et al., 2009
17	G-series turbiditic sandstones, Shwe Fan, NE Bay of Bengal	Bengal Fan	-	Barnes & Normark, 1985; Emmel & Curray, 1985; Pickering et al., 1989; Curray et al., 2003; Yang & Kim, 2014
18	Condor channel belt, Torres del Paine, Cerro Toro Formation	Cerro Toro Deep-Water System	Magallanes Basin (during the Cerro Toro)	Bouma, 1982; Barton et al., 2007(b; c)
19	Black's Beach channel system, La Jolla, California, Scripps and Ardath Formations	Black's Beach	San Diego Basin	May & Warme, 2007; Stright et al., 2014
20	San Clemente channel system, California, Capistrano Formation (studied by Li)	Capistrano Formation	Capistrano Embayment	Li et al., 2016
21	Channel complexes, Drabber Dhora, Pakistan, Pab Formation	Lower Pab Turbidite System	Pab Basin	Eschard et al., 2004; Euzen et al., 2007(a; b); Albuoy et al., 2007
22	Gendalo 1020 Fan, offshore Kalimantan, Miocene system	Gendalo Field	Kutai Basin (during the Miocene)	Sugiaman et al., 2007; Saller et al., 2008
27	Navy Fan, offshore California	Navy Fan	San Clemente Basin	Normark et al., 1979; Normark & Piper, 1985; Normark et al., 2009
28	Deep interval lobe complexes, Agbada Formation	Niger Delta System	-	Damuth, 1994; Konyuklov et al., 2008; Some et al., 2009; Prélat et al., 2010; Zhang et al., 2016
29	Active channel-mouth lobe complex, Congo-Angola margin, Zaire turbidite system	Zaire Fan	-	Dennielou et al., 2017

30	Depositional lobe 8, Mississppi Fan, Gulf of Mexico	Mississippi Fan	-	Weimer, 1991; Twichell et al., 1995; Schwab et al., 1996; Somme et al., 2009
31	Transient slope deep-sea fan, offshore NE Sicily, Villafranca Fan	Villafranca Deep-Sea Fan	Gioia intraslope Basin	Gamberi & Marani, 2006; Gamberi et al., 2014
32	Southern lobe complex, Mizala turbidite system, Almeria, SE Spain	Mizala Turbidite System	Sorbas Basin (during the Tortonian)	Postma & Kleverlaan, 2018
33	Shallow subsurface lobe complex, offshore Nigeria	Niger Delta System	-	Prélat et al., 2010

Appendix B: Database application queries

This appendix lists the queries used to interrogate the database for the example applications presented in Chapter 4. A range of queries were developed, providing output relating to architectural geometry, spatial relationships and facies proportions. A brief explanation of each query is provided. Queries are organised by application.

1. Quantification of element geometries

1.1 Channel width measurements classified by method of data acquisition

```
SELECT d13_element.element_ID, d07_subset.case_study_ID, d13_element.width,
       d13_element.width_type, d13_element.width_stype,
       d13_element.general_type,d07_subset.data_type, CASE WHEN data_type LIKE
       'outcrop%' THEN 'Outcrop' WHEN data_type like '%seismic%' THEN 'Subsurface data'
       WHEN data_type LIKE '%bathymetry%' THEN 'Subsurface data' ELSE 'Other'END AS
       Method
FROM d13_element
JOIN d07_subset ON d07_subset.subset_ID = d13_element.subset_ID
WHERE (d13_element.general_type = 'channel' OR d13_element.shape_sed_body = 'channel'
       OR d13_element.shape_geo_surface = 'channel') AND d13_element.width_type =
       'true (maximum)' AND d07_subset.el_suit like 'dimensions%'
ORDER BY  width_stype, data_type
```

Only 'true maximum' width values are returned. A channel is defined by shape or element type.

1.2 Channel width and thickness dimensions including architectural and system descriptors

```
SELECT d13_element.element_ID, d13_element.subset_ID, d13_element.thickness,
d13_element.thickness_type, d13_element.width, d13_element.width_type,
d13_element.object_type,
d13_element.general_style, d13_element.general_type, d13_element.shape_sed_body,
d13_element.shape_geo_surface,
d07_subset.basin_ID, d07_subset.system_ID, d13_element.dip_pos_within_el,
d13_element.sinuosity_index, d13_element.sinuosity,
d13_element.length_sinuous/d13_element.length_endpoints AS sinuosity_calc,
d07_subset.physiographic_setting, d07_subset.confinement, d07_subset.systems_tract,
d07_subset.gradient,d07_subset.gradient_range,
d07_subset.water_depth_modern_min, d07_subset.water_depth_modern_max,
d07_subset.water_depth_notes,
d04_system.`type`, d04_system.continental_margin_type, d04_system.tectonic_setting,
d04_system.dominant_gs, d04_system.dominant_gs_sand,
d04_system.shelf_width, d04_system.feeder_system_type, d07_subset.original_name,
d04_system.name, d13_element.unit_level, d13_element.highest_level,
d13_element.parent_el_ID, CASE WHEN data_type LIKE 'outcrop%' THEN 'Outcrop' WHEN
data_type LIKE '%seismic%' THEN 'Seismic'    ELSE 'Other' END AS Method
FROM d13_element
JOIN d07_subset ON d07_subset.subset_ID = d13_element.subset_ID
JOIN d04_system ON d04_system.system_ID = d07_subset.system_ID

WHERE  (d07_subset.el_suit LIKE 'dimensions%' OR d07_subset.largest_el_suit LIKE
'dimensions%')
AND d13_element.width_type LIKE 'true (max%' AND d13_element.thickness_type LIKE 'true
(max%'
               AND (d13_element.general_type = 'channel' OR d13_element.shape_sed_body
= 'channel' OR d13_element.shape_geo_surface = 'channel')
```

Only 'true maximum' width and thickness values are returned. A channel is defined by shape or element type.

2. Comparisons of hierarchical organisation

2.1 Architectural dimensions original source-work terminology

```
DROP TEMPORARY TABLE IF EXISTS ch_count;

CREATE TEMPORARY TABLE ch_count AS
SELECT d13_element.element_ID AS el, d13_element.subset_ID AS subset,
d13_element.parent_el_ID AS parent, d13_element.thickness,
0 AS ch_count, d13_element.original_interpretation AS interp
FROM d13_element
JOIN d07_subset ON d07_subset.subset_ID = d13_element.subset_ID
```

```
WHERE d13_element.thickness_type LIKE 'true (m%'
AND d13_element.general_type = 'channel' AND d07_subset.el_suit_proportions IS NOT NULL
AND (d13_element.highest_level = 'Y' AND d13_element.parent_el_ID IS NULL)

UNION

SELECT d13_element.element_ID AS el, d13_element.subset_ID AS subset,
d13_element.parent_el_ID AS parent, d13_element.thickness,
1 AS ch_count,d13_element.original_interpretation AS interp

FROM
(SELECT d13_element.element_ID AS el, d13_element.subset_ID AS subset,
d13_element.parent_el_ID AS parent, d13_element.thickness, 0 AS ch_count
FROM d13_element
JOIN d07_subset ON d07_subset.subset_ID = d13_element.subset_ID
WHERE d13_element.thickness_type LIKE 'true (m%'
AND d13_element.general_type LIKE 'channel' AND d07_subset.el_suit_proportions IS NOT
NULL
AND (d13_element.highest_level = 'Y' AND d13_element.parent_el_ID IS NULL))p0
LEFT JOIN d13_element ON d13_element.parent_el_ID = p0.el
WHERE d13_element.thickness_type LIKE 'true (m%' AND d13_element.general_type
LIKE'channel'

UNION

SELECT d13_element.element_ID AS el, d13_element.subset_ID AS subset,
d13_element.parent_el_ID AS parent, d13_element.thickness, 2 AS ch_count,
d13_element.original_interpretation AS interp
FROM
(SELECT d13_element.element_ID AS el, d13_element.subset_ID AS subset,
d13_element.parent_el_ID AS parent, d13_element.thickness, 1 AS ch_count
FROM
(SELECT d13_element.element_ID AS el, d13_element.subset_ID AS subset,
d13_element.parent_el_ID AS parent, d13_element.thickness, 0 AS ch_count
FROM d13_element
JOIN d07_subset ON d07_subset.subset_ID = d13_element.subset_ID
WHERE d13_element.thickness_type LIKE 'true (m%'
AND d13_element.general_type LIKE 'channel' AND d07_subset.el_suit_proportions IS NOT
NULL
AND (d13_element.highest_level = 'Y' AND d13_element.parent_el_ID IS NULL))p0
LEFT JOIN d13_element ON d13_element.parent_el_ID = p0.el
WHERE d13_element.thickness_type LIKE 'true (m%'
AND d13_element.general_type LIKE 'channel'
)p1
JOIN d13_element ON d13_element.parent_el_ID = p1.el
WHERE d13_element.thickness_type LIKE 'true (m%' AND d13_element.general_type LIKE
'channel'

UNION

SELECT d13_element.element_ID AS el, d13_element.subset_ID AS subset,
d13_element.parent_el_ID AS parent, d13_element.thickness, 3 AS ch_count,
d13_element.original_interpretation AS interp
FROM
(SELECT d13_element.element_ID AS el, d13_element.subset_ID AS subset,
d13_element.parent_el_ID AS parent, d13_element.thickness, 2 AS ch_count
FROM
(SELECT d13_element.element_ID AS el, d13_element.subset_ID AS subset,
d13_element.parent_el_ID AS parent, d13_element.thickness, 1 AS ch_count
FROM
(SELECT d13_element.element_ID AS el, d13_element.subset_ID AS subset,
d13_element.parent_el_ID AS parent, d13_element.thickness, 0 AS ch_count
FROM d13_element
JOIN d07_subset ON d07_subset.subset_ID = d13_element.subset_ID
WHERE d13_element.thickness_type LIKE 'true (m%'
AND d13_element.general_type LIKE 'channel' AND d07_subset.el_suit_proportions IS NOT
NULL
AND (d13_element.highest_level = 'Y' AND d13_element.parent_el_ID IS NULL))p0
LEFT JOIN d13_element ON d13_element.parent_el_ID = p0.el
WHERE d13_element.thickness_type LIKE 'true (m%'
AND d13_element.general_type LIKE 'channel'
)p1
JOIN d13_element ON d13_element.parent_el_ID = p1.el
WHERE d13_element.thickness_type LIKE 'true (m%'
AND d13_element.general_type LIKE 'channel'
)p2
JOIN d13_element ON d13_element.parent_el_ID = p2.el
WHERE d13_element.thickness_type LIKE'true (m%' AND d13_element.general_type LIKE
'channel';
```

```
SELECT d13_element.element_ID, d13_element.parent_el_ID, d13_element.subset_ID,
d13_element.thickness, d13_element.thickness, d13_element.unit_level,
d13_element.highest_level,
IF(ch_count.ch_count IS NULL AND highest_level = 'Y', 0, ch_count.ch_count) AS
ch_count, d13_element.original_interpretation AS interp
FROM d13_element
LEFT JOIN ch_count ON ch_count.el = d13_element.element_ID
WHERE d13_element.thickness_type LIKE'true (m%' #and thickness_type LIKE'true (m%'
AND d13_element.general_type LIKE'channel'
ORDER BY interp
```

Channel thickness classified by original terminology and parent channel element count.

2.2 Child-parent relationships

a) Channel elements

```
DROP TEMPORARY TABLE IF EXISTS HIER;

CREATE TEMPORARY TABLE HIER AS
SELECT element_ID AS child1,highest_level,parent_el_ID AS
child1p,original_interpretation,general_style,general_type,detailed_type,detailed_type_
DQI,
#d13_element.thickness AS child1thickness, thickness_type as
child1th_type,thickness_stype
d13_element.width as child1width ,width_type as child1w_type,width_stype
FROM d13_element
LEFT JOIN d07_subset ON d07_subset.subset_ID = d13_element.subset_ID
LEFT JOIN d12_2d_data ON d12_2d_data.2d_data_ID = d13_element.2d_data_ID
WHERE general_type = 'channel' AND object_type = 'sed body'
#AND d13_element.thickness IS NOT NULL AND thickness_type LIKE 'true (max%'
and d13_element.width is not null and width_type like 'true (max%'
AND parent_el_ID IS NOT NULL
AND ((d07_subset.el_suit LIKE '%dimensions%'and d07_subset.el_suit_proportions LIKE
'%2D%') OR (d12_2d_data.el_suit LIKE '%dimensions%' AND d12_2d_data.el_suit_proportions
LIKE '%2D%'));

SELECT HIER.child1, HIER.child1p, HIER.child1width, HIER.child1w_type,
HIER.original_interpretation, d13_element.element_ID AS parent1,
d13_element.parent_el_ID AS parent2,
d13_element.width AS parent1width, d13_element.width_type as
parent1w_type,d13_element.subset_ID, d13_element.original_interpretation
FROM HIER
JOIN d13_element ON d13_element.element_ID = HIER.child1p
WHERE d13_element.width IS NOT NULL AND d13_element.general_type = 'channel' AND
object_type = 'sed body' AND d13_element.width_type like 'true (max%'
```

Channel thickness dimensions for elements and their corresponding parent channel body deposits. Derives sedimentary bodies only. By using # phrases instead the query can output channel thicknesses.

b) Terminal deposits

```
DROP TEMPORARY TABLE IF EXISTS HIER;

CREATE TEMPORARY TABLE HIER AS
SELECT element_ID AS child1,highest_level,parent_el_ID AS
child1p,original_interpretation,general_style,general_type,detailed_type,detailed_type_
DQI,
d13_element.thickness AS child1thickness, thickness_type as
child1th_type,thickness_stype
#d13_element.width as child1width ,width_type,width_stype
FROM d13_element
LEFT JOIN d07_subset ON d07_subset.subset_ID = d13_element.subset_ID
LEFT JOIN d12_2d_data ON d12_2d_data.2d_data_ID = d13_element.2d_data_ID
WHERE general_type = 'terminal deposit'
AND d13_element.thickness IS NOT NULL AND thickness_type LIKE 'true (max%'
#and d13_element.width is not null and width_type like 'true (max%'
AND parent_el_ID IS NOT NULL
AND ((d07_subset.el_suit LIKE '%dimensions%'and d07_subset.el_suit_proportions LIKE
'%2D%') OR (d12_2d_data.el_suit LIKE '%dimensions%' AND d12_2d_data.el_suit_proportions
LIKE '%2D%'));
```

```
SELECT HIER.child1, HIER.child1p, HIER.child1thickness, HIER.child1th_type,
HIER.original_interpretation, d13_element.element_ID AS parent1,
d13_element.parent_el_ID AS parent2,
d13_element.thickness AS parent1thickness, d13_element.thickness_type as
parent1th_type,d13_element.subset_ID, d13_element.original_interpretation
FROM HIER
JOIN d13_element ON d13_element.element_ID = HIER.child1p
WHERE d13_element.thickness IS NOT NULL AND d13_element.general_type = 'terminal
deposit' AND d13_element.thickness_type like 'true (max%'
```

Terminal deposit thickness (and width, #) dimensions for elements and their corresponding parent terminal deposit.

3. Characterise architectural spatial arrangements

3.1 Genetically-related levee-channel width measurements

```
SELECT ch_1_w, ch_1_wt, lev_2_w, lev_2_wt, ch.original_name,
ch.original_interpretation, ch.general_style, d07_subset.original_name,
lv.element_ID AS levee, ch.element_ID AS channel, d07_subset.original_name,
d04_system.name, ch.object_type
, d07_subset.physiographic_setting, ch.dip_pos_within_el, d04_system.dominant_gs,
IF(d04_system.palaeo_lat_hemisphere IS NULL, (CASE WHEN d04_system.latitude LIKE '-%'
THEN 'S'
WHEN d04_system.latitude IS NULL THEN 'none' ELSE 'N' END),
d04_system.palaeo_lat_hemisphere) AS 'Hemisphere',
CASE WHEN ch_lv_width.locality LIKE 'left%' THEN 'left' WHEN ch_lv_width.locality LIKE
'right%' THEN 'right' ELSE NULL END AS channel_side,
CONCAT( IF(d04_system.palaeo_lat_hemisphere IS NULL, (CASE WHEN d04_system.latitude
LIKE '-%' THEN 'S'
WHEN d04_system.latitude IS NULL THEN 'none' ELSE 'N' END),
d04_system.palaeo_lat_hemisphere), ' ',
CASE WHEN ch_lv_width.locality LIKE 'left%' THEN 'left' WHEN ch_lv_width.locality LIKE
'right%' THEN 'right' ELSE NULL END) AS Lev_height,
IF(d07_subset.basin_ID IS NOT NULL, 'Basin confinement', 'No basin confinement') AS
Basin,
d04_system.`type`

FROM(
(SELECT DISTINCT d14_element_trans.element_ID_1 AS channel, el1.width AS ch_1_w,
el1.width_type AS ch_1_wt,
d14_element_trans.element_ID_2 AS levee, el2.width AS lev_2_w, el2.width_type AS
lev_2_wt, el2.locality
FROM d14_element_trans
JOIN d13_element el1 ON el1.element_ID = d14_element_trans.element_ID_1
JOIN d13_element el2 ON el2.element_ID = d14_element_trans.element_ID_2
WHERE d14_element_trans.direction = 'lateral' AND d14_element_trans.lat_pos_el_ID_2
LIKE '%crest%'
AND el1.general_type = 'channel' AND el2.general_type LIKE '%levee' #and el2.locality
LIKE 'right%'
)

UNION

(SELECT DISTINCT d14_element_trans.element_ID_2 AS channel, el11.width AS ch_1_w,
el11.width_type AS ch_1_wt,
d14_element_trans.element_ID_1 AS levee, el22.width AS lev_2_w, el22.width_type AS
lev_2_wt, el22.locality
FROM d14_element_trans
JOIN d13_element el11 ON el11.element_ID = d14_element_trans.element_ID_2
JOIN d13_element el22 ON el22.element_ID = d14_element_trans.element_ID_1
WHERE d14_element_trans.direction = 'lateral' AND d14_element_trans.lat_pos_el_ID_1
LIKE '%crest%'
AND el11.general_type = 'channel' AND el22.general_type LIKE '%levee' #and
el22.locality LIKE 'left%'
AND (el11.element_ID <> '1058' AND el22.element_ID <> '1059') #these channels are not
genetically related to the levees
)) ch_lv_width

JOIN d13_element ch ON ch.element_ID = ch_lv_width.channel
JOIN d07_subset ON d07_subset.subset_ID = ch.subset_ID
JOIN d13_element lv ON lv.element_ID = ch_lv_width.levee
JOIN d04_system ON d04_system.system_ID = d07_subset.system_ID
WHERE (ch_1_wt LIKE 'true (m%') AND (lev_2_wt LIKE 'true (m%')
```

Channel to levee genetic relationships are assured using ‘crest’ lateral transitions. Channel and levee dimensions are provided, as well as system characteristics.

3.2 Lateral transition element type probability from a known point

```
DROP TEMPORARY TABLE IF EXISTS lat_trans;
DROP TEMPORARY TABLE IF EXISTS  tab_sum;

CREATE TEMPORARY TABLE lat_trans AS
SELECT lag, target, SUM(el_count) AS el_count
FROM
(SELECT lag, target, COUNT(DISTINCT target_ID) AS el_count
FROM(
SELECT '250' as lag,
CASE    WHEN (d1>=250) THEN id1
WHEN (d2>250 AND d1<250) THEN id2
WHEN (d3>250 AND d2<250) THEN id3
WHEN (d4>250 AND d3<250) THEN id4
ELSE NULL END AS target_ID,
CASE WHEN (d1>=250) THEN 'same channel'
WHEN (d2>250 AND d1<250) THEN type2
WHEN (d3>250 AND d2<250) THEN type3
WHEN (d4>250 AND d3<250) THEN type4
ELSE NULL END AS target

FROM
(SELECT DISTINCT el1.element_ID AS id1, el2.element_ID AS id2, el3.element_ID AS id3,
el4.element_ID AS id4,
el1.general_type AS type_from, el2.general_type AS type2, el3.general_type AS
type3,el4.general_type AS type4,
el1.width/2 AS d1, el2.width AS d2, el2.width+el3.width AS
d3,el2.width+el3.width+el4.width AS d4
FROM d14_element_trans AS t1
JOIN d14_element_trans AS t2 ON t2.element_ID_2 = t1.element_ID_1  AND t2.direction =
'lateral'
JOIN d14_element_trans AS t3 ON t3.element_ID_2 = t2.element_ID_1  AND t3.direction =
'lateral'
JOIN d13_element AS el1 ON t1.element_ID_2 = el1.element_ID
JOIN d13_element AS el2 ON el2.element_ID = t1.element_ID_1  AND el2.highest_level =
'Y'
JOIN d13_element AS el3 ON el3.element_ID = t2.element_ID_1  AND el3.highest_level =
'Y' AND el1.element_ID<>el3.element_ID
JOIN d13_element AS el4 ON el4.element_ID = t3.element_ID_1 AND el4.highest_level = 'Y'
AND el2.element_ID<>el4.element_ID AND el1.element_ID<>el4.element_ID
WHERE t1.direction = 'lateral'
AND el1.object_type NOT LIKE 'geo surface' AND el1.general_type = 'channel' AND
(el1.width_type LIKE 'true%' OR el1.width_type LIKE 'app%')
AND (el1.unit_level LIKE 'unit 3' OR el1.unit_level IS NULL ) AND
(el1.original_interpretation NOT LIKE '%complex%' AND el1.original_interpretation NOT
LIKE '%canyon%')

UNION

SELECT DISTINCT el1.element_ID AS id1, el2.element_ID AS id2, el3.element_ID AS id3,
NULL AS id4,
el1.general_type AS type_from, el2.general_type AS type2, el3.general_type AS type3,
NULL AS type4,
el1.width/2 AS d1, el2.width AS d2, el2.width+el3.width AS d3, NULL AS d4
FROM d14_element_trans AS t1
JOIN d14_element_trans AS t2 ON t2.element_ID_2 = t1.element_ID_1  AND t2.direction =
'lateral'
JOIN d13_element AS el1 ON t1.element_ID_2 = el1.element_ID
JOIN d13_element AS el2 ON el2.element_ID = t1.element_ID_1  AND el2.highest_level =
'Y'
JOIN d13_element AS el3 ON el3.element_ID = t2.element_ID_1  AND el3.highest_level =
'Y' AND el1.element_ID<>el3.element_ID
WHERE t1.direction = 'lateral'
AND el1.object_type NOT LIKE 'geo surface' AND el1.general_type = 'channel' AND
(el1.width_type LIKE 'true%' OR el1.width_type LIKE 'app%')
AND (el1.unit_level LIKE 'unit 3' OR el1.unit_level IS NULL ) AND
(el1.original_interpretation NOT LIKE '%complex%' AND el1.original_interpretation NOT
LIKE '%canyon%')

UNION

SELECT DISTINCT el1.element_ID AS id1, el2.element_ID AS id2, NULL AS id3, NULL AS id4,
el1.general_type AS type_from, el2.general_type AS type2, NULL AS type3, NULL AS type4,
```

```
el1.width/2 AS d1, el2.width AS d2, NULL AS d3, NULL AS d4
FROM d14_element_trans AS t1
JOIN d13_element AS el1 ON t1.element_ID_2 = el1.element_ID
JOIN d13_element AS el2 ON el2.element_ID = t1.element_ID_1  AND el2.highest_level =
'Y'
WHERE t1.direction = 'lateral'
AND el1.object_type NOT LIKE 'geo surface' AND el1.general_type = 'channel' AND
(el1.width_type LIKE 'true%' OR el1.width_type LIKE 'app%')
AND (el1.unit_level LIKE 'unit 3' OR el1.unit_level IS NULL ) AND
(el1.original_interpretation NOT LIKE '%complex%' AND el1.original_interpretation NOT
LIKE '%canyon%')
)left_side
WHERE IF((d4>250 AND d3<250), type4, IF((d3>250 AND d2<250), type3, IF((d2>250 AND
d1<250), type2, IF((d1>=250), 'same channel', 'DISCARD')))) <> 'DISCARD'
) AS target1
GROUP BY target

UNION

SELECT lag, target, COUNT(DISTINCT target_ID) AS el_count
FROM(
SELECT '250' as lag,
CASE    WHEN (d1>=250) THEN id1
WHEN (d2>250 AND d1<250) THEN id2
WHEN (d3>250 AND d2<250) THEN id3
WHEN (d4>250 AND d3<250) THEN id4
ELSE NULL END AS target_ID,
CASE WHEN (d1>=250) THEN 'same channel'
WHEN (d2>250 AND d1<250) THEN type2
WHEN (d3>250 AND d2<250) THEN type3
WHEN (d4>250 AND d3<250) THEN type4
ELSE NULL END AS target
FROM
(SELECT DISTINCT el1.element_ID AS id1, el2.element_ID AS id2, el3.element_ID AS id3,
el4.element_ID AS id4,
el1.general_type AS type_from, el2.general_type AS type2, el3.general_type AS
type3,el4.general_type AS type4,
el1.width/2 AS d1, el2.width AS d2, el2.width+el3.width AS
d3,el2.width+el3.width+el4.width AS d4
FROM d14_element_trans AS t1
JOIN d14_element_trans AS t2 ON t2.element_ID_1 = t1.element_ID_2  AND t2.direction =
'lateral'
JOIN d14_element_trans AS t3 ON t3.element_ID_1 = t2.element_ID_2  AND t3.direction =
'lateral'
JOIN d13_element AS el1 ON t1.element_ID_1 = el1.element_ID
JOIN d13_element AS el2 ON el2.element_ID = t2.element_ID_1  AND el2.highest_level =
'Y'
JOIN d13_element AS el3 ON el3.element_ID = t3.element_ID_1  AND el3.highest_level =
'Y' AND el1.element_ID<>el3.element_ID
JOIN d13_element AS el4 ON el4.element_ID = t3.element_ID_2 AND el4.highest_level = 'Y'
AND el2.element_ID<>el4.element_ID AND el1.element_ID<>el4.element_ID
WHERE t1.direction = 'lateral'
AND el1.object_type NOT LIKE 'geo surface' AND el1.general_type = 'channel' AND
(el1.width_type LIKE 'true%' OR el1.width_type LIKE 'app%')
AND (el1.unit_level LIKE 'unit 3' OR el1.unit_level IS NULL ) AND
(el1.original_interpretation NOT LIKE '%complex%' AND el1.original_interpretation NOT
LIKE '%canyon%')

UNION

SELECT DISTINCT el1.element_ID AS id1, el2.element_ID AS id2, el3.element_ID AS id3,
NULL AS id4,
el1.general_type AS type_from, el2.general_type AS type2, el3.general_type AS type3,
NULL AS type4,
el1.width/2 AS d1, el2.width AS d2, el2.width+el3.width AS d3, NULL AS d4
FROM d14_element_trans AS t1
JOIN d14_element_trans AS t2 ON t2.element_ID_1 = t1.element_ID_2  AND t2.direction =
'lateral'
JOIN d14_element_trans AS t3 ON t3.element_ID_1 = t2.element_ID_2  AND t3.direction =
'lateral'
JOIN d13_element AS el1 ON t1.element_ID_1 = el1.element_ID
JOIN d13_element AS el2 ON el2.element_ID = t2.element_ID_1  AND el2.highest_level =
'Y'
JOIN d13_element AS el3 ON el3.element_ID = t3.element_ID_1  AND el3.highest_level =
'Y' AND el1.element_ID<>el3.element_ID
WHERE t1.direction = 'lateral'
AND el1.object_type NOT LIKE 'geo surface' AND el1.general_type = 'channel' AND
(el1.width_type LIKE 'true%' OR el1.width_type LIKE 'app%')
```

```
AND (el1.unit_level LIKE 'unit 3' OR el1.unit_level IS NULL ) AND
(el1.original_interpretation NOT LIKE '%complex%' AND el1.original_interpretation NOT
LIKE '%canyon%')

UNION

SELECT DISTINCT el1.element_ID AS id1, el2.element_ID AS id2, NULL AS id3, NULL AS id4,
el1.general_type AS type_from, el2.general_type AS type2, NULL AS type3, NULL AS type4,
el1.width/2 AS d1, el2.width AS d2, NULL AS d3, NULL AS d4
FROM d14_element_trans AS t1
JOIN d14_element_trans AS t2 ON t2.element_ID_1 = t1.element_ID_2  AND t2.direction =
'lateral'
JOIN d13_element AS el1 ON t1.element_ID_1 = el1.element_ID
JOIN d13_element AS el2 ON el2.element_ID = t2.element_ID_1  AND el2.highest_level =
'Y'
WHERE t1.direction = 'lateral'
AND el1.object_type NOT LIKE 'geo surface' AND el1.general_type = 'channel' AND
(el1.width_type LIKE 'true%' OR el1.width_type LIKE 'app%')
AND (el1.unit_level LIKE 'unit 3' OR el1.unit_level IS NULL ) AND
(el1.original_interpretation NOT LIKE '%complex%' AND el1.original_interpretation NOT
LIKE '%canyon%')
)right_side
WHERE IF((d4>250 AND d3<250), type4, IF((d3>250 AND d2<250), type3, IF((d2>250 AND
d1<250), type2, IF((d1>=250), 'same channel', 'DISCARD')))) <> 'DISCARD'
) AS target1
GROUP BY target
)left_right
WHERE target NOT LIKE 'background'
GROUP BY target;

CREATE TEMPORARY TABLE tab_sum AS
SELECT lag, SUM(el_count) AS total_count
FROM lat_trans
GROUP BY lag;

SELECT CONVERT(tab_sum.lag,UNSIGNED INTEGER) AS lag_m, target, el_count/total_count,
total_count
FROM lat_trans
JOIN tab_sum ON lat_trans.lag = tab_sum.lag
ORDER BY lag_m
```

Calculates the probability of finding a certain element type at a set distance (250m), based upon lateral transition counts, starting from a channel axis.

4. Temporal variations in architecture

4.1 Terminal deposit aspect ratio over time

```
SELECT d07_subset.original_name AS sub_name, d13_element.original_interpretation,
d13_element.original_name,
d13_element.width, d13_element.width_type,
IF(d13_element.length IS NULL, d13_element.length_endpoints, d13_element.length) AS
length, d13_element.length_type, d13_element.unit_level,
(IF(d13_element.length IS NULL, d13_element.length_endpoints,
d13_element.length)/d13_element.width) AS lw_ratio, d13_element.relative_age  AS
rel_age,
d07_subset.duration_order_of_magnitude AS duration, d13_element.age_abs
FROM d13_element
JOIN d07_subset ON d07_subset.subset_ID = d13_element.subset_ID
WHERE d13_element.relative_age IS NOT NULL AND d13_element.general_type = 'terminal
deposit' AND width_type LIKE 'true %' AND length_type LIKE 'true %'
ORDER BY sub_name, relative_age;
```

Length: width ratio of terminal deposits for subsets where relative age relationships are known.

5. Synthetic facies models

5.1 Facies general structure proportions based on element type

```
DROP TEMPORARY TABLE IF EXISTS tot_th;
DROP TEMPORARY TABLE IF EXISTS str_th;

CREATE TEMPORARY TABLE tot_th AS
SELECT ae_1 AS element_ID, el_hier.general_type, SUM(d15_facies.thickness) AS
sum_tot_th, COUNT(el_hier.facies) AS facies_n
FROM(
SELECT AE_1, GENERAL_TYPE, detailed_type, IF(ae_2 IS NULL,0,1)+ IF(ae_3 IS NULL,0,1)+
IF(ae_4 IS NULL,0,1) AS N_children, IFNULL(FACIES_4, IFNULL(FACIES_3,
IFNULL(FACIES_2,FACIES_1))) AS FACIES
```

```
FROM(
SELECT el_hier_1.element_ID AS ae_1, el_hier_2.element_ID AS ae_2, el_hier_3.element_ID
AS ae_3, el_hier_4.element_ID AS ae_4,
el_hier_4.general_type, el_hier_4.detailed_type, el_hier_4.detailed_type_DQI, NULL AS
facies_1, NULL AS facies_2, NULL AS facies_3, facies_ID AS facies_4
FROMd07_subset
JOIN d13_element AS el_hier_1 on d07_subset.subset_ID = el_hier_1.subset_ID
LEFT JOIN d13_element AS el_hier_2 ON el_hier_1.element_ID = el_hier_2.parent_el_ID
LEFT JOIN d13_element AS el_hier_3 ON el_hier_2.element_ID = el_hier_3.parent_el_ID
LEFT JOIN d13_element AS el_hier_4 ON el_hier_3.element_ID = el_hier_4.parent_el_ID
JOIN d15_facies AS facies_4 ON el_hier_4.element_ID = facies_4.parent_element_ID
JOIN d10_1d_data on d10_1d_data.1d_data_ID = facies_4.1d_data_ID

UNION

SELECT el_hier_1.element_ID AS ae_1, el_hier_2.element_ID AS ae_2, el_hier_3.element_ID
AS ae_3, NULL AS ae_4,
el_hier_3.general_type, el_hier_3.detailed_type, el_hier_3.detailed_type_DQI, NULL AS
facies_1, NULL AS facies_2, facies_ID AS facies_3, NULL AS facies_4
FROM d13_element AS el_hier_1
LEFT JOIN d13_element AS el_hier_2 ON el_hier_1.element_ID = el_hier_2.parent_el_ID
LEFT JOIN d13_element AS el_hier_3 ON el_hier_2.element_ID = el_hier_3.parent_el_ID
LEFT JOIN d13_element AS el_hier_4 ON el_hier_3.element_ID = el_hier_4.parent_el_ID
JOIN d15_facies AS facies_3 ON el_hier_3.element_ID = facies_3.parent_element_ID

UNION

SELECT el_hier_1.element_ID AS ae_1, el_hier_2.element_ID AS ae_2, NULL AS ae_3, NULL
AS ae_4,
el_hier_2.general_type, el_hier_2.detailed_type, el_hier_2.detailed_type_DQI, NULL AS
facies_1, facies_ID AS facies_2, NULL AS facies_3, NULL AS facies_4
FROM d13_element AS el_hier_1
LEFT JOIN d13_element AS el_hier_2 ON el_hier_1.element_ID = el_hier_2.parent_el_ID
LEFT JOIN d13_element AS el_hier_3 ON el_hier_2.element_ID = el_hier_3.parent_el_ID
LEFT JOIN d13_element AS el_hier_4 ON el_hier_3.element_ID = el_hier_4.parent_el_ID
JOIN d15_facies AS facies_2 ON el_hier_2.element_ID = facies_2.parent_element_ID

UNION

SELECT el_hier_1.element_ID AS ae_1, NULL AS ae_2, NULL AS ae_3, NULL AS ae_4,
el_hier_1.general_type, el_hier_1.detailed_type, el_hier_1.detailed_type_DQI, facies_ID
AS facies_1, NULL AS facies_2, NULL AS facies_3, NULL AS facies_4
FROM d13_element AS el_hier_1
LEFT JOIN d13_element AS el_hier_2 ON el_hier_1.element_ID = el_hier_2.parent_el_ID
LEFT JOIN d13_element AS el_hier_3 ON el_hier_2.element_ID = el_hier_3.parent_el_ID
LEFT JOIN d13_element AS el_hier_4 ON el_hier_3.element_ID = el_hier_4.parent_el_ID
JOIN d15_facies AS facies_1 ON el_hier_1.element_ID = facies_1.parent_element_ID
) AS 4_hierarchies
ORDER BY AE_1
) AS el_hier
JOIN d13_element ON d13_element.element_ID = el_hier.ae_1
JOIN d07_subset ON d07_subset.subset_ID = d13_element.subset_ID
JOIN d15_facies ON el_hier.facies = d15_facies.facies_ID
JOIN d10_1d_data ON d10_1d_data.1d_data_ID = d15_facies.1d_data_ID
WHERE d15_facies.facies_type LIKE '%S%'
AND ((d07_subset.facies_suit_proportions IS NOT NULL AND
d07_subset.facies_suit_proportions_type LIKE '%general structures%'
AND d07_subset.facies_suit_proportions_in LIKE '%element%')
OR (d10_1d_data.facies_suit_proportions IS NOT NULL AND
d10_1d_data.facies_suit_proportions_type LIKE '%general structures%'
AND d10_1d_data.facies_suit_proportions_in LIKE '%element%'))
GROUP BY element_ID;

CREATE TEMPORARY TABLE str_th AS
SELECT ae_1 AS element_ID, el_hier.general_type, SUM(d15_facies.thickness) AS
sum_str_th, COUNT(el_hier.facies) AS facies_n
, d15_facies.general_structure
FROM(
SELECT AE_1, GENERAL_TYPE, detailed_type, IF(ae_2 IS NULL,0,1)+ IF(ae_3 IS NULL,0,1)+
IF(ae_4 IS NULL,0,1) AS N_children, IFNULL(FACIES_4, IFNULL(FACIES_3,
IFNULL(FACIES_2,FACIES_1))) AS FACIES
FROM(
SELECT el_hier_1.element_ID AS ae_1, el_hier_2.element_ID AS ae_2, el_hier_3.element_ID
AS ae_3, el_hier_4.element_ID AS ae_4,
el_hier_4.general_type, el_hier_4.detailed_type, el_hier_4.detailed_type_DQI, NULL AS
facies_1, NULL AS facies_2, NULL AS facies_3, facies_ID AS facies_4
FROMd07_subset
JOIN d13_element AS el_hier_1 on d07_subset.subset_ID = el_hier_1.subset_ID
LEFT JOIN d13_element AS el_hier_2 ON el_hier_1.element_ID = el_hier_2.parent_el_ID
```

```
LEFT JOIN d13_element AS el_hier_3 ON el_hier_2.element_ID = el_hier_3.parent_el_ID
LEFT JOIN d13_element AS el_hier_4 ON el_hier_3.element_ID = el_hier_4.parent_el_ID
JOIN d15_facies AS facies_4 ON el_hier_4.element_ID = facies_4.parent_element_ID
JOIN d10_1d_data ON d10_1d_data.1d_data_ID = facies_4.1d_data_ID
WHERE (d07_subset.facies_suit_proportions IS NOT NULL AND
d07_subset.facies_suit_proportions_type LIKE '%general structures,laminations%'
AND d07_subset.facies_suit_proportions_in LIKE '%element%')
OR (d10_1d_data.facies_suit_proportions IS NOT NULL AND
d10_1d_data.facies_suit_proportions_type LIKE '%general structures,laminations%'
AND d10_1d_data.facies_suit_proportions_in LIKE '%elements%')

UNION

SELECT el_hier_1.element_ID AS ae_1, el_hier_2.element_ID AS ae_2, el_hier_3.element_ID
AS ae_3, NULL AS ae_4, el_hier_3.general_type, el_hier_3.detailed_type,
el_hier_3.detailed_type_DQI, NULL AS facies_1, NULL AS facies_2, facies_ID AS facies_3,
NULL AS facies_4
FROM d13_element AS el_hier_1
LEFT JOIN d13_element AS el_hier_2 ON el_hier_1.element_ID = el_hier_2.parent_el_ID
LEFT JOIN d13_element AS el_hier_3 ON el_hier_2.element_ID = el_hier_3.parent_el_ID
LEFT JOIN d13_element AS el_hier_4 ON el_hier_3.element_ID = el_hier_4.parent_el_ID
JOIN d15_facies AS facies_3 ON el_hier_3.element_ID = facies_3.parent_element_ID

UNION

SELECT el_hier_1.element_ID AS ae_1, el_hier_2.element_ID AS ae_2, NULL AS ae_3, NULL
AS ae_4,
el_hier_2.general_type, el_hier_2.detailed_type, el_hier_2.detailed_type_DQI, NULL AS
facies_1, facies_ID AS facies_2, NULL AS facies_3, NULL AS facies_4
FROM d13_element AS el_hier_1
LEFT JOIN d13_element AS el_hier_2 ON el_hier_1.element_ID = el_hier_2.parent_el_ID
LEFT JOIN d13_element AS el_hier_3 ON el_hier_2.element_ID = el_hier_3.parent_el_ID
LEFT JOIN d13_element AS el_hier_4 ON el_hier_3.element_ID = el_hier_4.parent_el_ID
JOIN d15_facies AS facies_2 ON el_hier_2.element_ID = facies_2.parent_element_ID

UNION

SELECT el_hier_1.element_ID AS ae_1, NULL AS ae_2, NULL AS ae_3, NULL AS ae_4,
el_hier_1.general_type, el_hier_1.detailed_type, el_hier_1.detailed_type_DQI, facies_ID
AS facies_1, NULL AS facies_2, NULL AS facies_3, NULL AS facies_4
FROM d13_element AS el_hier_1
LEFT JOIN d13_element AS el_hier_2 ON el_hier_1.element_ID = el_hier_2.parent_el_ID
LEFT JOIN d13_element AS el_hier_3 ON el_hier_2.element_ID = el_hier_3.parent_el_ID
LEFT JOIN d13_element AS el_hier_4 ON el_hier_3.element_ID = el_hier_4.parent_el_ID
JOIN d15_facies AS facies_1 ON el_hier_1.element_ID = facies_1.parent_element_ID
) AS 4_hierarchies
ORDER BY AE_1
) AS el_hier
JOIN d13_element ON d13_element.element_ID = el_hier.ae_1
JOIN d07_subset ON d07_subset.subset_ID = d13_element.subset_ID
JOIN d15_facies ON el_hier.facies = d15_facies.facies_ID
JOIN d10_1d_data ON d10_1d_data.1d_data_ID = d15_facies.1d_data_ID
WHERE d15_facies.facies_type LIKE '%S%'
AND ((d07_subset.facies_suit_proportions IS NOT NULL AND
d07_subset.facies_suit_proportions_type LIKE '%general structures%'
AND d07_subset.facies_suit_proportions_in LIKE '%element%')
OR (d10_1d_data.facies_suit_proportions IS NOT NULL AND
d10_1d_data.facies_suit_proportions_type LIKE '%general structures%'
AND d10_1d_data.facies_suit_proportions_in LIKE '%elements%'))
GROUP BY element_ID, general_structure;

SELECT tot_th.element_ID, tot_th.general_type,
str_th.general_structure,(str_th.sum_str_th/tot_th.sum_tot_th) AS str_prop,
tot_th.facies_N
FROM tot_th
JOIN str_th ON tot_th.element_ID = str_th.element_ID
ORDER BY general_type, element_ID, general_structure;

# element and facies counts
#SELECT general_type, COUNT(tot_th.element_ID), SUM(tot_th.facies_N)
#FROM tot_th
#GROUP BY by general_type
```

Output can be used to derive both total sum thickness proportions and average thickness proportions weighted by element thickness. Element and facies counts can be derived using additional (#) table.

5.2 Detailed element type facies types

c) Grain size

```
DROP TEMPORARY TABLE IF EXISTS tot_th;
DROP TEMPORARY TABLE IF EXISTS gs_th;
DROP TEMPORARY TABLE IF EXISTS facies;
DROP TEMPORARY TABLE IF EXISTS props;

CREATE TEMPORARY TABLE tot_th AS

SELECT ae_1 AS element_ID, el_hier.general_type, el_hier.detailed_type,
SUM(d15_facies.thickness) AS sum_tot_th, COUNT(el_hier.facies) AS facies_n
FROM (
SELECT AE_1, GENERAL_TYPE, detailed_type, IF(ae_2 IS NULL,0,1)+ IF(ae_3 IS NULL,0,1)+
IF(ae_4 IS NULL,0,1) AS N_children, IFNULL(FACIES_4, IFNULL(FACIES_3,
IFNULL(FACIES_2,FACIES_1))) AS FACIES
FROM (
SELECT el_hier_1.element_ID AS ae_1, el_hier_2.element_ID AS ae_2, el_hier_3.element_ID
AS ae_3, el_hier_4.element_ID AS ae_4,
el_hier_4.general_type, el_hier_4.detailed_type, el_hier_4.detailed_type_DQI, NULL AS
facies_1, NULL AS facies_2, NULL AS facies_3, facies_ID AS facies_4
FROM d07_subset
JOIN d13_element AS el_hier_1 on d07_subset.subset_ID = el_hier_1.subset_ID
LEFT JOIN d13_element AS el_hier_2 ON el_hier_1.element_ID = el_hier_2.parent_el_ID
LEFT JOIN d13_element AS el_hier_3 ON el_hier_2.element_ID = el_hier_3.parent_el_ID
LEFT JOIN d13_element AS el_hier_4 ON el_hier_3.element_ID = el_hier_4.parent_el_ID
JOIN d15_facies AS facies_4 ON el_hier_4.element_ID = facies_4.parent_element_ID
JOIN d10_1d_data on d10_1d_data.1d_data_ID = facies_4.1D_data_ID

UNION

SELECT el_hier_1.element_ID AS ae_1, el_hier_2.element_ID AS ae_2, el_hier_3.element_ID
AS ae_3, NULL AS ae_4,
el_hier_3.general_type, el_hier_3.detailed_type, el_hier_3.detailed_type_DQI, NULL AS
facies_1, NULL AS facies_2, facies_ID AS facies_3, NULL AS facies_4
FROM d13_element AS el_hier_1
LEFT JOIN d13_element AS el_hier_2 ON el_hier_1.element_ID = el_hier_2.parent_el_ID
LEFT JOIN d13_element AS el_hier_3 ON el_hier_2.element_ID = el_hier_3.parent_el_ID
LEFT JOIN d13_element AS el_hier_4 ON el_hier_3.element_ID = el_hier_4.parent_el_ID
JOIN d15_facies AS facies_3 ON el_hier_3.element_ID = facies_3.parent_element_ID

UNION

SELECT el_hier_1.element_ID AS ae_1, el_hier_2.element_ID AS ae_2, NULL AS ae_3, NULL
AS ae_4,
el_hier_2.general_type, el_hier_2.detailed_type, el_hier_2.detailed_type_DQI, NULL AS
facies_1, facies_ID AS facies_2, NULL AS facies_3, NULL AS facies_4
FROM d13_element AS el_hier_1
LEFT JOIN d13_element AS el_hier_2 ON el_hier_1.element_ID = el_hier_2.parent_el_ID
LEFT JOIN d13_element AS el_hier_3 ON el_hier_2.element_ID = el_hier_3.parent_el_ID
LEFT JOIN d13_element AS el_hier_4 ON el_hier_3.element_ID = el_hier_4.parent_el_ID
JOIN d15_facies AS facies_2 ON el_hier_2.element_ID = facies_2.parent_element_ID

UNION

SELECT el_hier_1.element_ID AS ae_1, NULL AS ae_2, NULL AS ae_3, NULL AS ae_4,
el_hier_1.general_type, el_hier_1.detailed_type, el_hier_1.detailed_type_DQI, facies_ID
AS facies_1, NULL AS facies_2, NULL AS facies_3, NULL AS facies_4
FROM d13_element AS el_hier_1
LEFT JOIN d13_element AS el_hier_2 ON el_hier_1.element_ID = el_hier_2.parent_el_ID
LEFT JOIN d13_element AS el_hier_3 ON el_hier_2.element_ID = el_hier_3.parent_el_ID
LEFT JOIN d13_element AS el_hier_4 ON el_hier_3.element_ID = el_hier_4.parent_el_ID
JOIN d15_facies AS facies_1 ON el_hier_1.element_ID = facies_1.parent_element_ID
) AS 4_hierarchies
WHERE (4_hierarchies.detailed_type LIKE 'lat%' OR 4_hierarchies.detailed_type LIKE
'agg%'OR 4_hierarchies.detailed_type LIKE 'master%')
AND 4_hierarchies.detailed_type_DQI NOT LIKE 'C'
ORDER BY AE_1
) as el_hier
JOIN d13_element ON d13_element.element_ID = el_hier.ae_1
JOIN d07_subset ON d07_subset.subset_ID = d13_element.subset_ID
```

```
JOIN d15_facies ON el_hier.facies = d15_facies.facies_ID
JOIN d10_1d_data ON d10_1d_data.1d_data_ID = d15_facies.1d_data_ID
WHERE ((d07_subset.facies_suit_proportions IS NOT NULL AND
d07_subset.facies_suit_proportions_type LIKE '%type%'AND
d07_subset.facies_suit_proportions_in LIKE '%element%')
OR (d10_1d_data.facies_suit_proportions IS NOT NULL AND
d10_1d_data.facies_suit_proportions_type LIKE '%type%' AND
d10_1d_data.facies_suit_proportions_in LIKE '%elements%'))
GROUP BY element_ID;

CREATE TEMPORARY TABLE gs_th AS
SELECT ae_1 AS element_ID, el_hier.general_type, el_hier.detailed_type,
SUM(d15_facies.thickness) AS sum_gs_th, COUNT(el_hier.facies) AS facies_n
, CASE WHEN facies_type like '%S%' THEN 'Sand'
WHEN facies_type like '%G%' THEN 'Gravel'
WHEN facies_type like '%Z%' THEN 'Silt'
WHEN facies_type like '%C%' THEN 'Clay'
WHEN facies_type like '%M%' THEN 'Mud'
ELSE 'Unclassified' END as grain_size
FROM(
SELECT AE_1, GENERAL_TYPE, detailed_type, IF(ae_2 IS NULL,0,1)+ IF(ae_3 IS NULL,0,1)+
IF(ae_4 IS NULL,0,1) AS N_children, IFNULL(FACIES_4, IFNULL(FACIES_3,
IFNULL(FACIES_2,FACIES_1))) AS FACIES
FROM(
SELECT el_hier_1.element_ID AS ae_1, el_hier_2.element_ID AS ae_2, el_hier_3.element_ID
AS ae_3, el_hier_4.element_ID AS ae_4,
el_hier_4.general_type, el_hier_4.detailed_type, el_hier_4.detailed_type_DQI, NULL AS
facies_1, NULL AS facies_2, NULL AS facies_3, facies_ID AS facies_4
FROM d07_subset
JOIN
d13_element AS el_hier_1 on d07_subset.subset_ID = el_hier_1.subset_ID
LEFT JOIN d13_element AS el_hier_2 ON el_hier_1.element_ID = el_hier_2.parent_el_ID
LEFT JOIN d13_element AS el_hier_3 ON el_hier_2.element_ID = el_hier_3.parent_el_ID
LEFT JOIN d13_element AS el_hier_4 ON el_hier_3.element_ID = el_hier_4.parent_el_ID
JOIN d15_facies AS facies_4 ON el_hier_4.element_ID = facies_4.parent_element_ID
JOIN d10_1d_data on d10_1d_data.1d_data_ID = facies_4.1D_data_ID

UNION

SELECT el_hier_1.element_ID AS ae_1, el_hier_2.element_ID AS ae_2, el_hier_3.element_ID
AS ae_3, NULL AS ae_4,
el_hier_3.general_type, el_hier_3.detailed_type, el_hier_3.detailed_type_DQI, NULL AS
facies_1, NULL AS facies_2, facies_ID AS facies_3, NULL AS facies_4
FROM d13_element AS el_hier_1
LEFT JOIN d13_element AS el_hier_2 ON el_hier_1.element_ID = el_hier_2.parent_el_ID
LEFT JOIN d13_element AS el_hier_3 ON el_hier_2.element_ID = el_hier_3.parent_el_ID
LEFT JOIN d13_element AS el_hier_4 ON el_hier_3.element_ID = el_hier_4.parent_el_ID
JOIN d15_facies AS facies_3 ON el_hier_3.element_ID = facies_3.parent_element_ID

UNION

SELECT el_hier_1.element_ID AS ae_1, el_hier_2.element_ID AS ae_2, NULL AS ae_3, NULL
AS ae_4,
el_hier_2.general_type, el_hier_2.detailed_type, el_hier_2.detailed_type_DQI, NULL AS
facies_1, facies_ID AS facies_2, NULL AS facies_3, NULL AS facies_4
FROM d13_element AS el_hier_1
LEFT JOIN d13_element AS el_hier_2 ON el_hier_1.element_ID = el_hier_2.parent_el_ID
LEFT JOIN d13_element AS el_hier_3 ON el_hier_2.element_ID = el_hier_3.parent_el_ID
LEFT JOIN d13_element AS el_hier_4 ON el_hier_3.element_ID = el_hier_4.parent_el_ID
JOIN d15_facies AS facies_2 ON el_hier_2.element_ID = facies_2.parent_element_ID

UNION

SELECT el_hier_1.element_ID AS ae_1, NULL AS ae_2, NULL AS ae_3, NULL AS ae_4,
el_hier_1.general_type, el_hier_1.detailed_type, el_hier_1.detailed_type_DQI, facies_ID
AS facies_1, NULL AS facies_2, NULL AS facies_3, NULL AS facies_4
FROM d13_element AS el_hier_1
LEFT JOIN d13_element AS el_hier_2 ON el_hier_1.element_ID = el_hier_2.parent_el_ID
LEFT JOIN d13_element AS el_hier_3 ON el_hier_2.element_ID = el_hier_3.parent_el_ID
LEFT JOIN d13_element AS el_hier_4 ON el_hier_3.element_ID = el_hier_4.parent_el_ID
JOIN d15_facies AS facies_1 ON el_hier_1.element_ID = facies_1.parent_element_ID
) AS 4_hierarchies
WHERE (4_hierarchies.detailed_type LIKE 'lat%' or 4_hierarchies.detailed_type LIKE
'agg%'or 4_hierarchies.detailed_type LIKE 'master%')
AND 4_hierarchies.detailed_type_DQI NOT LIKE 'C'
ORDER BY AE_1
) AS el_hier
JOIN d13_element ON d13_element.element_ID = el_hier.ae_1
JOIN d07_subset ON d07_subset.subset_ID = d13_element.subset_ID
```

```
JOIN d15_facies ON el_hier.facies = d15_facies.facies_ID
JOIN d10_1d_data ON d10_1d_data.1d_data_ID = d15_facies.1d_data_ID
WHERE ((d07_subset.facies_suit_proportions IS NOT NULL AND
d07_subset.facies_suit_proportions_type LIKE '%type%'AND
d07_subset.facies_suit_proportions_in LIKE '%element%')
OR (d10_1d_data.facies_suit_proportions IS NOT NULL AND
d10_1d_data.facies_suit_proportions_type LIKE '%type%' AND
d10_1d_data.facies_suit_proportions_in LIKE '%elements%'))


GROUP BY element_ID, grain_size;

#CREATE TEMPORARY TABLE props AS
SELECT tot_th.element_ID, tot_th.general_type, tot_th.detailed_type,
CASE WHEN(gs_th.grain_size = 'Clay' OR gs_th.grain_size = 'Mud') THEN 'Mud' ELSE
gs_th.grain_size END AS grain_size_m,
(gs_th.sum_gs_th/tot_th.sum_tot_th) AS gs_prop, tot_th.facies_N
FROM tot_th
JOIN gs_th ON tot_th.element_ID = gs_th.element_ID

ORDER BY detailed_type, element_ID, grain_size;

# grain size sum thicknesses, remember clay has been joined to the 'mud' class
#SELECT props.detailed_type, props.grain_size_m, AVG(props.gs_prop) AS mean_gs_prop
#FROM props
#JOIN tot_th ON tot_th.element_ID = props.element_ID
#GROUP BY detailed_type, grain_size_m

# element and facies counts
#SELECT detailed_type, COUNT(element_ID), SUM(facies_N)
#FROM tot_th
#GROUP BY detailed_type
```

Either average, weighted by element thicknesses, or sum facies thicknesses (as in case of # grain size sum thicknesses table) can be calculated from this output. Facies and element counts can be derived from final (#) table.

d) Sedimentary structure, including lamination type

```
DROP TEMPORARY TABLE IF EXISTS tot_th;
DROP TEMPORARY TABLE IF EXISTS str_th;
DROP TEMPORARY TABLE IF EXISTS facies;
DROP TEMPORARY TABLE IF EXISTS props;

CREATE TEMPORARY TABLE tot_th AS
SELECT ae_1 AS element_ID, el_hier.general_type, el_hier.detailed_type,
SUM(d15_facies.thickness) AS sum_tot_th, COUNT(el_hier.facies) AS facies_n
FROM(
SELECT AE_1, GENERAL_TYPE, detailed_type, IF(ae_2 IS NULL,0,1)+ IF(ae_3 IS NULL,0,1)+
IF(ae_4 IS NULL,0,1) AS N_children, IFNULL(FACIES_4, IFNULL(FACIES_3,
IFNULL(FACIES_2,FACIES_1))) AS FACIES
FROM(
SELECT el_hier_1.element_ID AS ae_1, el_hier_2.element_ID AS ae_2, el_hier_3.element_ID
AS ae_3, el_hier_4.element_ID AS ae_4,
el_hier_4.general_type, el_hier_4.detailed_type, el_hier_4.detailed_type_DQI, NULL AS
facies_1, NULL AS facies_2, NULL AS facies_3, facies_ID AS facies_4
FROM d07_subset
JOIN d13_element AS el_hier_1 on d07_subset.subset_ID = el_hier_1.subset_ID
LEFT JOIN d13_element AS el_hier_2 ON el_hier_1.element_ID = el_hier_2.parent_el_ID
LEFT JOIN d13_element AS el_hier_3 ON el_hier_2.element_ID = el_hier_3.parent_el_ID
LEFT JOIN d13_element AS el_hier_4 ON el_hier_3.element_ID = el_hier_4.parent_el_ID
JOIN d15_facies AS facies_4 ON el_hier_4.element_ID = facies_4.parent_element_ID
JOIN d10_1d_data on d10_1d_data.1d_data_ID = facies_4.1d_data_ID

UNION

SELECT el_hier_1.element_ID AS ae_1, el_hier_2.element_ID AS ae_2, el_hier_3.element_ID
AS ae_3, NULL AS ae_4,
el_hier_3.general_type, el_hier_3.detailed_type, el_hier_3.detailed_type_DQI, NULL AS
facies_1, NULL AS facies_2, facies_ID AS facies_3, NULL AS facies_4
FROM d13_element AS el_hier_1
LEFT JOIN d13_element AS el_hier_2 ON el_hier_1.element_ID = el_hier_2.parent_el_ID
LEFT JOIN d13_element AS el_hier_3 ON el_hier_2.element_ID = el_hier_3.parent_el_ID
LEFT JOIN d13_element AS el_hier_4 ON el_hier_3.element_ID = el_hier_4.parent_el_ID
JOIN d15_facies AS facies_3 ON el_hier_3.element_ID = facies_3.parent_element_ID
```

```
UNION

SELECT el_hier_1.element_ID AS ae_1, el_hier_2.element_ID AS ae_2, NULL AS ae_3, NULL
AS ae_4,
el_hier_2.general_type, el_hier_2.detailed_type, el_hier_2.detailed_type_DQI, NULL AS
facies_1, facies_ID AS facies_2, NULL AS facies_3, NULL AS facies_4
FROM d13_element AS el_hier_1
LEFT JOIN d13_element AS el_hier_2 ON el_hier_1.element_ID = el_hier_2.parent_el_ID
LEFT JOIN d13_element AS el_hier_3 ON el_hier_2.element_ID = el_hier_3.parent_el_ID
LEFT JOIN d13_element AS el_hier_4 ON el_hier_3.element_ID = el_hier_4.parent_el_ID
JOIN d15_facies AS facies_2 ON el_hier_2.element_ID = facies_2.parent_element_ID

UNION

SELECT el_hier_1.element_ID AS ae_1, NULL AS ae_2, NULL AS ae_3, NULL AS ae_4,
el_hier_1.general_type, el_hier_1.detailed_type, el_hier_1.detailed_type_DQI, facies_ID
AS facies_1, NULL AS facies_2, NULL AS facies_3, NULL AS facies_4
FROM d13_element AS el_hier_1
LEFT JOIN d13_element AS el_hier_2 ON el_hier_1.element_ID = el_hier_2.parent_el_ID
LEFT JOIN d13_element AS el_hier_3 ON el_hier_2.element_ID = el_hier_3.parent_el_ID
LEFT JOIN d13_element AS el_hier_4 ON el_hier_3.element_ID = el_hier_4.parent_el_ID
JOIN d15_facies AS facies_1 ON el_hier_1.element_ID = facies_1.parent_element_ID
) AS 4_hierarchies
WHERE (4_hierarchies.detailed_type LIKE 'lat%' OR 4_hierarchies.detailed_type LIKE
'agg%' OR 4_hierarchies.detailed_type LIKE 'master%')
AND 4_hierarchies.detailed_type_DQI NOT LIKE 'C'
ORDER BY AE_1
) AS el_hier
JOIN d13_element ON d13_element.element_ID = el_hier.ae_1
JOIN d07_subset ON d07_subset.subset_ID = d13_element.subset_ID
JOIN d15_facies ON el_hier.facies = d15_facies.facies_ID
JOIN d10_1d_data ON d10_1d_data.1d_data_ID = d15_facies.1d_data_ID
WHERE d15_facies.facies_type LIKE '%S%'
AND ((d07_subset.facies_suit_proportions IS NOT NULL AND
d07_subset.facies_suit_proportions_type LIKE '%general structures,laminations%'AND
d07_subset.facies_suit_proportions_in LIKE '%element%')
or (d10_1d_data.facies_suit_proportions IS NOT NULL AND
d10_1d_data.facies_suit_proportions_type LIKE '%general structures,laminations%' AND
d10_1d_data.facies_suit_proportions_in LIKE '%elements%'))
GROUP BY element_ID;

CREATE TEMPORARY TABLE str_th AS
SELECT ae_1 as element_ID, el_hier.general_type, el_hier.detailed_type,
SUM(d15_facies.thickness) AS sum_str_th, COUNT(el_hier.facies) AS facies_n
, CASE WHEN d15_facies.general_structure = 'laminated' THEN
IF(d15_facies.lamination_type IS NULL, 'laminated (type not specified)',
d15_facies.lamination_type)
ELSE d15_facies.general_structure END AS structure_type
FROM(
SELECT AE_1, GENERAL_TYPE, detailed_type, IF(ae_2 IS NULL,0,1)+ IF(ae_3 IS NULL,0,1)+
IF(ae_4 IS NULL,0,1) AS N_children, IFNULL(FACIES_4, IFNULL(FACIES_3,
IFNULL(FACIES_2,FACIES_1))) AS FACIES
FROM(
SELECT el_hier_1.element_ID AS ae_1, el_hier_2.element_ID AS ae_2, el_hier_3.element_ID
AS ae_3, el_hier_4.element_ID AS ae_4,
el_hier_4.general_type, el_hier_4.detailed_type, el_hier_4.detailed_type_DQI, NULL AS
facies_1, NULL AS facies_2, NULL AS facies_3, facies_ID AS facies_4
FROM d07_subset
JOIN d13_element AS el_hier_1 on d07_subset.subset_ID = el_hier_1.subset_ID
LEFT JOIN d13_element AS el_hier_2 ON el_hier_1.element_ID = el_hier_2.parent_el_ID
LEFT JOIN d13_element AS el_hier_3 ON el_hier_2.element_ID = el_hier_3.parent_el_ID
LEFT JOIN d13_element AS el_hier_4 ON el_hier_3.element_ID = el_hier_4.parent_el_ID
JOIN d15_facies AS facies_4 ON el_hier_4.element_ID = facies_4.parent_element_ID
JOIN d10_1d_data ON d10_1d_data.1d_data_ID = facies_4.1d_data_ID
where (d07_subset.facies_suit_proportions is not null and
d07_subset.facies_suit_proportions_type like '%general structures,laminations%'
and d07_subset.facies_suit_proportions_in like '%element%')
or (d10_1d_data.facies_suit_proportions is not null and
d10_1d_data.facies_suit_proportions_type like '%general structures,laminations%'
and d10_1d_data.facies_suit_proportions_in like '%elements%')

UNION

SELECT el_hier_1.element_ID AS ae_1, el_hier_2.element_ID AS ae_2, el_hier_3.element_ID
AS ae_3, NULL AS ae_4,
el_hier_3.general_type, el_hier_3.detailed_type, el_hier_3.detailed_type_DQI, NULL AS
facies_1, NULL AS facies_2, facies_ID AS facies_3, NULL AS facies_4
FROM d13_element AS el_hier_1
LEFT JOIN d13_element AS el_hier_2 ON el_hier_1.element_ID = el_hier_2.parent_el_ID
```

```
LEFT JOIN d13_element AS el_hier_3 ON el_hier_2.element_ID = el_hier_3.parent_el_ID
LEFT JOIN d13_element AS el_hier_4 ON el_hier_3.element_ID = el_hier_4.parent_el_ID
JOIN d15_facies AS facies_3 ON el_hier_3.element_ID = facies_3.parent_element_ID

UNION

SELECT el_hier_1.element_ID AS ae_1, el_hier_2.element_ID AS ae_2, NULL AS ae_3, NULL
AS ae_4,
el_hier_2.general_type, el_hier_2.detailed_type, el_hier_2.detailed_type_DQI, NULL AS
facies_1, facies_ID AS facies_2, NULL AS facies_3, NULL AS facies_4
FROM d13_element AS el_hier_1
LEFT JOIN d13_element AS el_hier_2 ON el_hier_1.element_ID = el_hier_2.parent_el_ID
LEFT JOIN d13_element AS el_hier_3 ON el_hier_2.element_ID = el_hier_3.parent_el_ID
LEFT JOIN d13_element AS el_hier_4 ON el_hier_3.element_ID = el_hier_4.parent_el_ID
JOIN d15_facies AS facies_2 ON el_hier_2.element_ID = facies_2.parent_element_ID

UNION

SELECT el_hier_1.element_ID AS ae_1, NULL AS ae_2, NULL AS ae_3, NULL AS ae_4,
el_hier_1.general_type, el_hier_1.detailed_type, el_hier_1.detailed_type_DQI, facies_ID
AS facies_1, NULL AS facies_2, NULL AS facies_3, NULL AS facies_4
FROM d13_element AS el_hier_1
LEFT JOIN d13_element AS el_hier_2 ON el_hier_1.element_ID = el_hier_2.parent_el_ID
LEFT JOIN d13_element AS el_hier_3 ON el_hier_2.element_ID = el_hier_3.parent_el_ID
LEFT JOIN d13_element AS el_hier_4 ON el_hier_3.element_ID = el_hier_4.parent_el_ID
JOIN d15_facies AS facies_1 ON el_hier_1.element_ID = facies_1.parent_element_ID
) AS 4_hierarchies
WHERE (4_hierarchies.detailed_type LIKE 'lat%' OR 4_hierarchies.detailed_type LIKE
'agg%' OR 4_hierarchies.detailed_type LIKE 'master%')
AND 4_hierarchies.detailed_type_DQI NOT LIKE 'C'
ORDER BY AE_1
) AS el_hier
JOIN d13_element ON d13_element.element_ID = el_hier.ae_1
JOIN d07_subset ON d07_subset.subset_ID = d13_element.subset_ID
JOIN d15_facies ON el_hier.facies = d15_facies.facies_ID
JOIN d10_1d_data ON d10_1d_data.1d_data_ID = d15_facies.1d_data_ID
WHERE d15_facies.facies_type LIKE '%S%'
AND ((d07_subset.facies_suit_proportions IS NOT NULL AND
d07_subset.facies_suit_proportions_type LIKE '%general structures,laminations%'AND
d07_subset.facies_suit_proportions_in LIKE '%element%')
OR (d10_1d_data.facies_suit_proportions IS NOT NULL AND
d10_1d_data.facies_suit_proportions_type LIKE '%general structures,laminations%' AND
d10_1d_data.facies_suit_proportions_in LIKE '%elements%'))
GROUP BY element_ID, structure_type;

#CREATE TEMPORARY TABLE props AS
SELECT tot_th.element_ID, tot_th.general_type, tot_th.detailed_type,
str_th.structure_type,
(str_th.sum_str_th/tot_th.sum_tot_th) AS str_prop, tot_th.facies_N
FROM tot_th
JOIN str_th ON tot_th.element_ID = str_th.element_ID
ORDER BY detailed_type, element_ID, structure_type;

# structure averages
#SELECT props.detailed_type, props.structure_type, AVG(props.str_prop) AS mean_str_prop
#FROM props
#JOIN tot_th ON tot_th.element_ID = props.element_ID
#GROUP BY detailed_type, structure_type

# element and facies counts
#SELECT detailed_type, COUNT(tot_th.element_ID), SUM(tot_th.facies_N)
#FROM tot_th
#GROUP BY detailed_type
```

Either average, weighted by element thicknesses, or sum facies thicknesses (as in case of # structure average table) can be calculated from this output. Facies and element counts can be derived from final (#) table.

6. Vertical organization of facies

6.1 Vertical transition grain size probability

```
DROP TEMPORARY TABLE IF EXISTS el;
DROP TEMPORARY TABLE IF EXISTS start_f;
DROP TEMPORARY TABLE IF EXISTS vert_f;
DROP TEMPORARY TABLE IF EXISTS tot;
```

```
CREATE TEMPORARY TABLE el AS
SELECT d13_element.element_ID, d13_element.parent_el_ID AS parent,
d13_element.subset_ID, d13_element.original_name, d13_element.original_interpretation,
d13_element.shape_sed_body,
d13_element.shape_geo_surface, d13_element.general_type, d13_element.detailed_type
FROM d13_element
WHERE d13_element.general_type = 'channel' OR d13_element.shape_sed_body = 'channel'

UNION

SELECT d13_element.element_ID, p_el.element_ID AS parent, p_el.subset_ID,
p_el.original_name, p_el.original_interpretation, p_el.shape_sed_body,
p_el.shape_geo_surface, p_el.general_type, p_el.detailed_type
FROM d13_element
JOIN d13_element p_el ON d13_element.parent_el_ID = p_el.element_ID
WHERE d13_element.shape_sed_body IS NULL AND d13_element.general_type IS NULL AND
d13_element.detailed_type IS NULL AND p_el.general_type = 'channel';

CREATE TEMPORARY TABLE start_f AS
SELECT d15_facies.1d_data_ID, d15_facies.facies_ID AS start_ID, el.element_ID,
d15_facies.thickness, d15_facies.facies_type AS f_ft, d15_facies.grain_size_sand AS
f_gs, d15_facies.general_structure,
d15_facies.1d_data_order AS log_order, d15_facies.parent_element_ID AS el
FROM d15_facies
JOIN el ON el.element_ID = d15_facies.parent_element_ID
JOIN d07_subset on d07_subset.subset_ID = el.subset_ID
JOIN d04_system on d04_system.system_ID = d07_subset.system_ID
JOIN d10_1d_data ON d10_1d_data.1d_data_ID = d15_facies.1d_data_ID
WHERE d10_1d_data.facies_suit_proportions_type LIKE 'type,grain size%' AND
d10_1d_data.facies_suit_transitions LIKE '1D vertical%'
AND d10_1d_data.facies_description_DQI NOT LIKE 'C' AND d04_system.dominant_gs NOT LIKE
'mud rich'
ORDER BY el.subset_ID, el, log_order;

CREATE TEMPORARY TABLE vert_f AS
SELECT el, start_ID, f_ft, f_gs,
(CASE WHEN f_ft like '%G%' THEN 'Gravel'
WHEN f_ft like '%S%' THEN  IF (f_gs IS NULL, 'DISCARD', CONCAT('Sand ',f_gs))
WHEN f_ft like '%Z%' THEN 'Silt'
WHEN f_ft like '%C%' OR f_ft LIKE '%M%' THEN 'Mud'
ELSE NULL END
)AS start_facies
,log_order, d15_facies.1d_data_order, d15_facies.facies_ID AS vert_ID,
d15_facies.facies_type, d15_facies.grain_size_sand,
(CASE WHEN d15_facies.facies_type like '%G%' THEN 'Gravel'
WHEN d15_facies.facies_type LIKE '%S%' THEN  IF (d15_facies.grain_size_sand IS NULL,
'DISCARD', CONCAT('Sand ', d15_facies.grain_size_sand))
WHEN d15_facies.facies_type LIKE '%Z%' THEN 'Silt'
WHEN d15_facies.facies_type LIKE '%C%' OR d15_facies.facies_type LIKE '%M%' THEN 'Mud'
ELSE NULL END
)AS vert_facies
FROM start_f
JOIN d15_facies ON (start_f.1d_data_ID = d15_facies.1d_data_ID AND start_f.el =
d15_facies.parent_element_ID AND start_f.log_order = d15_facies.1d_data_order-1)
WHERE facies_type NOT LIKE 'unknown' and f_ft NOT LIKE 'unknown'
ORDER BY  el, log_order;

CREATE TEMPORARY TABLE tot AS
SELECT start_facies, COUNT(vert_ID) AS total_f, COUNT(DISTINCT el) AS el_n, el
FROM vert_f
WHERE start_facies <> vert_facies AND start_facies NOT LIKE 'DISCARD' AND vert_facies
NOT LIKE 'DISCARD'
GROUP BY start_facies;

SELECT vert_f.start_facies, vert_f.vert_facies, COUNT(vert_f.vert_ID)/tot.total_f AS
f_prob, tot.total_f AS facies_n, tot.el_n
FROM vert_f
JOIN tot on tot.start_facies = vert_f.start_facies
WHERE vert_f.start_facies <> vert_f.vert_facies AND vert_f.start_facies NOT LIKE
'DISCARD' AND vert_f.vert_facies NOT LIKE 'DISCARD'
GROUP BY vert_facies, start_facies
ORDER BY start_facies, vert_facies
```

Starting facies and vertical transitioning facies are derived from 1D data order data. Mud includes clay portion. Query restricted to channels in sandy systems

6.2 Facies proportions for a specific subset's channel architecture

a) Proportion of vertical facies transitions

```
DROP TEMPORARY TABLE IF EXISTS clem;
DROP TEMPORARY TABLE IF EXISTS start_f;
DROP TEMPORARY TABLE IF EXISTS vert_f;
DROP TEMPORARY TABLE IF EXISTS cat_f;
DROP TEMPORARY TABLE IF EXISTS tot;
DROP TEMPORARY TABLE IF EXISTS facies_n;
DROP TEMPORARY TABLE IF EXISTS prob;

CREATE TEMPORARY TABLE clem AS
SELECT d15_facies.1d_data_ID, d15_facies.facies_ID AS start_ID, d15_facies.thickness,
d15_facies.facies_type AS f_ft, d15_facies.general_structure AS f_struc
, d15_facies.lamination_type AS f_lam, d15_facies.1d_data_order AS log_order,
d15_facies.parent_element_ID AS el, d15_facies.trans_from_below_bed_boundary AS
start_co
FROM d15_facies
JOIN d10_1d_data ON d10_1d_data.1d_data_ID = d15_facies.1d_data_ID
JOIN d13_element ON d13_element.element_ID = d15_facies.parent_element_ID
JOIN d07_subset ON d07_subset.subset_ID = d13_element.subset_ID
WHERE d15_facies.local_bed_ID IS NOT NULL AND d10_1d_data.facies_suit_proportions_type
LIKE 'type,%general structures,laminations' AND d10_1d_data.facies_suit_transitions
LIKE '1D vertical%'
AND d10_1d_data.facies_description_DQI NOT LIKE 'C'
AND d07_subset.subset_ID = '43'
ORDER BY el, log_order;

CREATE TEMPORARY TABLE vert_f AS
SELECT el, start_ID,
(CASE WHEN f_ft LIKE '%G%' THEN 'Gravel'
WHEN f_ft LIKE '%S%' THEN  'Sand'
WHEN f_ft LIKE '%C%' OR f_ft like '%M%' OR f_ft LIKE '%Z%' THEN 'Mud'
ELSE NULL END
) AS start_facies,
IF(((f_ft LIKE '%S%' OR f_ft LIKE '%G%') AND f_struc IS NOT NULL), IF(f_lam IS NOT
NULL, CONCAT('laminated ', f_lam), f_struc), NULL) AS f_slam,
start_co ,log_order, d15_facies.1d_data_order, d15_facies.trans_from_below_bed_boundary
as vert_co, d15_facies.facies_ID as vert_ID, d15_facies.facies_type,
d15_facies.grain_size_sand,
(CASE WHEN d15_facies.facies_type LIKE '%G%' THEN 'Gravel'
WHEN d15_facies.facies_type LIKE '%S%' THEN  'Sand'
WHEN d15_facies.facies_type LIKE '%C%' OR d15_facies.facies_type LIKE '%M%' or
d15_facies.facies_type LIKE '%Z%' THEN 'Mud'
ELSE NULL END
)AS vert_facies,
IF(((d15_facies.facies_type LIKE '%S%' OR d15_facies.facies_type LIKE '%G%')AND
d15_facies.general_structure IS NOT NULL),IF(d15_facies.lamination_type IS NOT NULL,
CONCAT('laminated ', d15_facies.lamination_type), d15_facies.general_structure), NULL)
AS vert_slam
FROM clem
JOIN d15_facies ON (clem.1d_data_ID = d15_facies.1d_data_ID AND clem.el =
d15_facies.parent_element_ID AND clem.log_order = d15_facies.1d_data_order-1)
WHERE facies_type NOT LIKE 'unknown' AND f_ft NOT LIKE 'unknown' AND
d15_facies.trans_from_below_bed_boundary LIKE 'N'
ORDER BY  el, log_order;

CREATE TEMPORARY TABLE cat_f AS
SELECT el, start_ID, IF(f_slam IS NULL, start_facies, CONCAT(start_facies, ' ',
f_slam)) AS start_facies, vert_ID,
IF(vert_slam IS NULL, vert_facies, CONCAT (vert_facies,' ', vert_slam))AS vert_facies
FROM vert_f;

CREATE TEMPORARY TABLE tot AS
SELECT start_facies, COUNT(vert_ID) AS total_f, COUNT(DISTINCT el) AS el_n, el, 1 as ky
FROM cat_f
WHERE start_facies <> vert_facies AND start_facies NOT LIKE '%DISCARD' AND vert_facies
NOT LIKE '%DISCARD'
AND start_facies NOT LIKE 'Sand' AND vert_facies NOT LIKE 'Sand' AND start_facies NOT
LIKE 'Sand laminated' AND vert_facies NOT LIKE 'Sand laminated'
GROUP BY start_facies;

CREATE TEMPORARY TABLE facies_n AS
SELECT SUM(total_f) AS n, 1 as ky
FROM tot;
```

```
SELECT cat_f.start_facies, cat_f.vert_facies, COUNT(cat_f.vert_ID)/tot.total_f AS
f_prob, tot.total_f AS facies_n, tot.el_n, COUNT(cat_f.vert_ID)/(facies_n.n) AS
total_prop
FROM cat_f
JOIN tot ON tot.start_facies = cat_f.start_facies
JOIN facies_n ON tot.ky = facies_n.ky
WHERE cat_f.start_facies <> cat_f.vert_facies AND cat_f.start_facies NOT LIKE
'%DISCARD' AND cat_f.vert_facies NOT LIKE '%DISCARD'
AND cat_f.start_facies NOT LIKE 'Sand' AND cat_f.vert_facies NOT LIKE 'Sand' AND
cat_f.start_facies NOT LIKE 'Sand laminated' AND cat_f.vert_facies NOT LIKE 'Sand
laminated'
GROUP BY vert_facies, start_facies
ORDER BY start_facies, vert_facies;
```

Vertical transitions, derived from 1D data order, between different facies grain size and sedimentary structure types.

b) Basal facies type within a bed

```
DROP TEMPORARY TABLE IF EXISTS el;
DROP TEMPORARY TABLE IF EXISTS facies;

CREATE TEMPORARY TABLE el AS
SELECT d13_element.element_ID, d13_element.parent_el_ID AS parent,
d13_element.subset_ID, d13_element.original_name, d13_element.original_interpretation,
d13_element.shape_sed_body,
d13_element.shape_geo_surface, d13_element.general_type, d13_element.detailed_type
FROM d13_element
WHERE d13_element.general_type = 'channel' OR d13_element.shape_sed_body = 'channel'

UNION

SELECT d13_element.element_ID, p_el.element_ID AS parent, p_el.subset_ID,
p_el.original_name, p_el.original_interpretation, p_el.shape_sed_body,
p_el.shape_geo_surface, p_el.general_type, p_el.detailed_type
FROM d13_element
JOIN d13_element p_el ON d13_element.parent_el_ID = p_el.element_ID
WHERE d13_element.shape_sed_body IS NULL AND d13_element.general_type IS NULL AND
d13_element.detailed_type IS NULL AND p_el.general_type = 'channel';

CREATE TEMPORARY TABLE facies AS
SELECT d15_facies.1d_data_ID, d15_facies.facies_ID AS start_ID, el.element_ID,
d15_facies.thickness, d15_facies.facies_type AS f_ft, d15_facies.general_structure AS
f_struc, d15_facies.lamination_type AS f_lam,
d15_facies.1d_data_order AS log_order, d15_facies.trans_FROM_below_bed_boundary AS
base, d15_facies.parent_element_ID AS el
FROM d15_facies
JOIN el on el.element_ID = d15_facies.parent_element_ID
JOIN d10_1d_data ON d10_1d_data.1d_data_ID = d15_facies.1d_data_ID
WHERE d10_1d_data.facies_suit_proportions_type LIKE 'type,%general
structures,laminations' AND d10_1d_data.facies_suit_transitions LIKE '1D vertical%'
AND d10_1d_data.facies_description_DQI NOT LIKE 'C' AND el.subset_ID = '43' AND
d15_facies.trans_FROM_below_bed_boundary = 'Y'
ORDER BY el.subset_ID, el, log_order;


SELECT IF(f_lam IS NULL, CONCAT(f_ft, ' ', f_struc), CONCAT(f_ft, ' ', f_struc, ' ',
f_lam)) AS facies_type, SUM(thickness), COUNT(start_ID)
FROM facies
WHERE f_struc IS NOT NULL
GROUP BY facies_type
```

Provides facies output, specific to a single case-study.

7. Net-to-gross ratios

7.1 Mud fraction in element types

```
DROP TEMPORARY TABLE IF EXISTS mud_frac;
#CREATE TEMPORARY TABLE mud_frac AS


SELECT tot_facies_t.element_id, tot_facies_t.general_type,
IF(sum_mud_t IS NOT NULL, (sum_mud_t/sum_tot_t), '0') AS mud_fraction, facies_n
FROM
```

```
(SELECT ae_1 AS element_id, general_type, SUM(d15_facies.thickness) AS sum_tot_t,
COUNT(facies) AS facies_n
FROM
(SELECT AE_1, GENERAL_TYPE, IF(ae_2 IS NULL,0,1)+ IF(ae_3 IS NULL,0,1)+ IF(ae_4 IS
NULL,0,1) AS N_children, IFNULL(FACIES_4, IFNULL(FACIES_3, IFNULL(FACIES_2,FACIES_1)))
AS FACIES
FROM
(SELECT el_hier_1.element_id AS ae_1, el_hier_2.element_id AS ae_2,
el_hier_3.element_id AS ae_3, el_hier_4.element_id AS ae_4,
el_hier_4.general_type, NULL AS facies_1, NULL AS facies_2, NULL AS facies_3, facies_id
AS facies_4
FROM d07_subset
JOIN d13_element AS el_hier_1 on d07_subset.subset_ID = el_hier_1.subset_ID
LEFT JOIN d13_element AS el_hier_2 ON el_hier_1.element_id = el_hier_2.parent_el_id
LEFT JOIN d13_element AS el_hier_3 ON el_hier_2.element_id = el_hier_3.parent_el_id
LEFT JOIN d13_element AS el_hier_4 ON el_hier_3.element_id = el_hier_4.parent_el_id
JOIN d15_facies AS facies_4 ON el_hier_4.element_id = facies_4.parent_element_ID
JOIN d10_1d_data ON d10_1d_data.1d_data_ID = facies_4.1d_data_ID
WHERE ((d07_subset.facies_suit_proportions is not null and
d07_subset.facies_suit_proportions_in like '%element%')
OR (d10_1d_data.facies_suit_proportions is not null and
(d10_1d_data.facies_suit_proportions_in like '%element%' or
d10_1d_data.facies_suit_proportions_in like '%1D%')))

UNION

SELECT el_hier_1.element_id AS ae_1, el_hier_2.element_id AS ae_2, el_hier_3.element_id
AS ae_3, NULL AS ae_4,
el_hier_3.general_type, NULL AS facies_1, NULL AS facies_2, facies_id AS facies_3, NULL
AS facies_4
FROM d13_element AS el_hier_1
LEFT JOIN d13_element AS el_hier_2 ON el_hier_1.element_id = el_hier_2.parent_el_id
LEFT JOIN d13_element AS el_hier_3 ON el_hier_2.element_id = el_hier_3.parent_el_id
LEFT JOIN d13_element AS el_hier_4 ON el_hier_3.element_id = el_hier_4.parent_el_id
JOIN d15_facies AS facies_3 ON el_hier_3.element_id = facies_3.parent_element_ID

UNION

SELECT el_hier_1.element_id AS ae_1, el_hier_2.element_id AS ae_2, NULL AS ae_3, NULL
AS ae_4,
el_hier_2.general_type, NULL AS facies_1, facies_id AS facies_2, NULL AS facies_3, NULL
AS facies_4
FROM d13_element AS el_hier_1
LEFT JOIN d13_element AS el_hier_2 ON el_hier_1.element_id = el_hier_2.parent_el_id
LEFT JOIN d13_element AS el_hier_3 ON el_hier_2.element_id = el_hier_3.parent_el_id
LEFT JOIN d13_element AS el_hier_4 ON el_hier_3.element_id = el_hier_4.parent_el_id
JOIN d15_facies AS facies_2 ON el_hier_2.element_id = facies_2.parent_element_ID

UNION

SELECT el_hier_1.element_id AS ae_1, NULL AS ae_2, NULL AS ae_3, NULL AS ae_4,
el_hier_1.general_type,
facies_id AS facies_1, NULL AS facies_2, NULL AS facies_3, NULL AS facies_4
FROM d13_element AS el_hier_1
LEFT JOIN d13_element AS el_hier_2 ON el_hier_1.element_id = el_hier_2.parent_el_id
LEFT JOIN d13_element AS el_hier_3 ON el_hier_2.element_id = el_hier_3.parent_el_id
LEFT JOIN d13_element AS el_hier_4 ON el_hier_3.element_id = el_hier_4.parent_el_id
JOIN d15_facies AS facies_1 ON el_hier_1.element_id = facies_1.parent_element_ID
) AS 4_hierarchies
ORDER BY AE_1
) AS el_hier
JOIN d15_facies ON el_hier.facies = d15_facies.facies_ID
GROUP BY element_id
) AS tot_facies_t
LEFT JOIN
(SELECT ae_1 AS element_id, general_type, SUM(d15_facies.thickness) AS sum_mud_t
FROM
(SELECT AE_1, GENERAL_TYPE, IF(ae_2 IS NULL,0,1)+ IF(ae_3 IS NULL,0,1)+ IF(ae_4 IS
NULL,0,1) AS N_children, IFNULL(FACIES_4, IFNULL(FACIES_3, IFNULL(FACIES_2,FACIES_1)))
AS FACIES
FROM
(SELECT el_hier_1.element_id AS ae_1, el_hier_2.element_id AS ae_2,
el_hier_3.element_id AS ae_3, el_hier_4.element_id AS ae_4,
el_hier_4.general_type, NULL AS facies_1, NULL AS facies_2, NULL AS facies_3, facies_id
AS facies_4
FROM
d07_subset JOIN
d13_element AS el_hier_1 on d07_subset.subset_ID = el_hier_1.subset_ID
LEFT JOIN d13_element AS el_hier_2 ON el_hier_1.element_id = el_hier_2.parent_el_id
```

```
LEFT JOIN d13_element AS el_hier_3 ON el_hier_2.element_id = el_hier_3.parent_el_id
LEFT JOIN d13_element AS el_hier_4 ON el_hier_3.element_id = el_hier_4.parent_el_id
JOIN d15_facies AS facies_4 ON el_hier_4.element_id = facies_4.parent_element_ID
JOIN d10_1d_data ON d10_1d_data.1d_data_ID = facies_4.1d_data_ID
WHERE ((d07_subset.facies_suit_proportions is not null and
d07_subset.facies_suit_proportions_in like '%element%')
OR (d10_1d_data.facies_suit_proportions is not null and
(d10_1d_data.facies_suit_proportions_in like '%element%' or
d10_1d_data.facies_suit_proportions_in like '%1D%')))

UNION

SELECT el_hier_1.element_id AS ae_1, el_hier_2.element_id AS ae_2, el_hier_3.element_id
AS ae_3, NULL AS ae_4,
el_hier_3.general_type, NULL AS facies_1, NULL AS facies_2, facies_id AS facies_3, NULL
AS facies_4
FROM d13_element AS el_hier_1
LEFT JOIN d13_element AS el_hier_2 ON el_hier_1.element_id = el_hier_2.parent_el_id
LEFT JOIN d13_element AS el_hier_3 ON el_hier_2.element_id = el_hier_3.parent_el_id
LEFT JOIN d13_element AS el_hier_4 ON el_hier_3.element_id = el_hier_4.parent_el_id
JOIN d15_facies AS facies_3 ON el_hier_3.element_id = facies_3.parent_element_ID UNION
SELECT el_hier_1.element_id AS ae_1, el_hier_2.element_id AS ae_2, NULL AS ae_3, NULL
AS ae_4,
el_hier_2.general_type, NULL AS facies_1, facies_id AS facies_2, NULL AS facies_3, NULL
AS facies_4
FROM d13_element AS el_hier_1
LEFT JOIN d13_element AS el_hier_2 ON el_hier_1.element_id = el_hier_2.parent_el_id
LEFT JOIN d13_element AS el_hier_3 ON el_hier_2.element_id = el_hier_3.parent_el_id
LEFT JOIN d13_element AS el_hier_4 ON el_hier_3.element_id = el_hier_4.parent_el_id
JOIN d15_facies AS facies_2 ON el_hier_2.element_id = facies_2.parent_element_ID UNION
SELECT el_hier_1.element_id AS ae_1, NULL AS ae_2, NULL AS ae_3, NULL AS ae_4,
el_hier_1.general_type,
facies_id AS facies_1, NULL AS facies_2, NULL AS facies_3, NULL AS facies_4
FROM d13_element AS el_hier_1
LEFT JOIN d13_element AS el_hier_2 ON el_hier_1.element_id = el_hier_2.parent_el_id
LEFT JOIN d13_element AS el_hier_3 ON el_hier_2.element_id = el_hier_3.parent_el_id
LEFT JOIN d13_element AS el_hier_4 ON el_hier_3.element_id = el_hier_4.parent_el_id
JOIN d15_facies AS facies_1 ON el_hier_1.element_id = facies_1.parent_element_ID
) AS 4_hierarchies
ORDER BY AE_1
) AS el_hier
JOIN d15_facies ON el_hier.facies = d15_facies.facies_ID
WHERE facies_type LIKE '%S%' OR facies_type LIKE '%G%' #OR facies_type LIKE '%M%'
GROUP BY element_id
) AS mud_facies_t
ON tot_facies_t.element_id = mud_facies_t.element_id
JOIN d13_element ON d13_element.element_ID = tot_facies_t.element_id
ORDER BY general_type;

#SELECT general_type, AVG(mud_fraction), SUM(facies_n) AS facies_n, COUNT(element_ID)
AS el_n
#FROM mud_frac
#GROUP BY general_type
```

Calculates proportion of sand and gravel thickness in all elements, whether they include any of these facies or not. Average proportion and count statistics for each element type can be derived using table (#).

7.2 Channel grain size proportions specified by lateral position

```
DROP TEMPORARY TABLE IF EXISTS tot_t;
DROP TEMPORARY TABLE IF EXISTS part_t;
DROP TEMPORARY TABLE IF EXISTS props;
DROP TEMPORARY TABLE IF EXISTS facies;
DROP TEMPORARY TABLE IF EXISTS facies_tot;
DROP TEMPORARY TABLE IF EXISTS fin;

CREATE TEMPORARY TABLE tot_t AS
SELECT IFNULL(d13_element.element_ID, p.element_ID) AS el_ID, d15_facies.position_lat,
SUM(d15_facies.thickness) AS thickness, d07_subset.physiographic_setting,
IF(position_lat='axis/core',IFNULL(d13_element.element_ID,
p.element_ID),IF(position_lat='off-axis',CONCAT(999,IFNULL(d13_element.element_ID,
p.element_ID)),IF(position_lat='margin/fringe',CONCAT(999999,IFNULL(d13_element.element
_ID, p.element_ID)),'none'))) AS pos_el_id
FROM d15_facies
INNER JOIN d13_element ON d13_element.element_ID = d15_facies.parent_element_ID
RIGHT OUTER JOIN d10_1d_data ON d10_1d_data.1d_data_ID = d15_facies.1d_data_ID
```

```
RIGHT OUTER JOIN d07_subset ON d07_subset.subset_ID = d13_element.subset_ID
RIGHT OUTER JOIN d04_system ON d04_system.system_ID = d07_subset.system_ID
LEFT OUTER JOIN d13_element p ON d13_element.parent_el_ID = p.element_ID
WHERE d15_facies.position_lat IS NOT NULL
AND d13_element.general_type = 'channel'
AND (d10_1d_data.facies_suit_proportions_type LIKE 'type%' OR
d07_subset.facies_suit_proportions_type LIKE 'type%')
AND d07_subset.physiographic_setting = 'slope'
AND IFNULL(d04_system.dominant_gs, d07_subset.sy_dominant_gs) NOT LIKE 'mud rich'
GROUP BY el_ID, position_lat;

CREATE TEMPORARY TABLE part_t AS
SELECT IFNULL(d13_element.element_ID, p.element_ID) AS el_ID,
COUNT(d15_facies.facies_ID) AS N, d15_facies.position_lat, SUM(d15_facies.thickness) AS
thickness, d07_subset.physiographic_setting,
IF(position_lat='axis/core',IFNULL(d13_element.element_ID,
p.element_ID),IF(position_lat='off-axis',CONCAT(999,IFNULL(d13_element.element_ID,
p.element_ID)),IF(position_lat='margin/fringe',CONCAT(999999,IFNULL(d13_element.element
_ID, p.element_ID)),'none'))) AS pos_el_id,
(CASE WHEN facies_type LIKE '%S%' THEN 'Sand'
WHEN facies_type LIKE '%G%' THEN 'Gravel'
WHEN facies_type LIKE '%Z%' THEN 'Silt'
WHEN facies_type LIKE '%C%' THEN 'Clay'
WHEN facies_type LIKE '%M%' THEN 'Mud'
ELSE 'Unclassified' END) AS grain_size
FROM d15_facies
INNER JOIN d13_element ON d13_element.element_ID = d15_facies.parent_element_ID
RIGHT OUTER JOIN d10_1d_data ON d10_1d_data.1d_data_ID = d15_facies.1d_data_ID
RIGHT OUTER JOIN d07_subset ON d07_subset.subset_ID = d13_element.subset_ID
RIGHT OUTER JOIN d04_system ON d04_system.system_ID = d07_subset.system_ID
LEFT OUTER JOIN d13_element p ON d13_element.parent_el_ID = p.element_ID
WHERE d15_facies.position_lat IS NOT NULL
AND d13_element.general_type = 'channel'
AND (d10_1d_data.facies_suit_proportions_type LIKE 'type%' OR
d07_subset.facies_suit_proportions_type LIKE 'type%')
AND d07_subset.physiographic_setting = 'slope'
AND IFNULL(d04_system.dominant_gs, d07_subset.sy_dominant_gs) NOT LIKE 'mud rich'
GROUP BY el_ID, position_lat, grain_size;

CREATE TEMPORARY TABLE props AS
SELECT tot_t.el_ID, tot_t.position_lat, grain_size, part_t.thickness/tot_t.thickness AS
proportion, N
FROM tot_t
JOIN part_t ON tot_t.pos_el_id = part_t.pos_el_id;

CREATE TEMPORARY TABLE facies_tot AS
SELECT el_ID, SUM(N)
FROM props
WHERE N > '5'
GROUP BY el_ID;

CREATE TEMPORARY TABLE facies (facies VARCHAR(8));
INSERT INTO facies (facies) VALUES ('Sand');
INSERT INTO facies (facies) VALUES ('Gravel');
INSERT INTO facies (facies) VALUES ('Silt');
INSERT INTO facies (facies) VALUES ('Clay');
INSERT INTO facies (facies) VALUES ('Mud');

#CREATE TEMPORARY TABLE fin AS
SELECT facies_tot.el_ID, position_lat, facies,
CASE WHEN facies = 'Sand' OR facies = 'Gravel' THEN 'S' ELSE 'M' END AS S_M,
MAX(IF(props.grain_size = facies.facies,proportion,0)) AS proportion,
MAX(IF(props.grain_size = facies.facies, N, 0)) AS N
FROM props
JOIN facies
INNER JOIN facies_tot ON facies_tot.el_ID = props.el_ID

GROUP BY el_ID, position_lat, facies;

#SELECT position_lat, CASE WHEN facies = 'Clay' OR facies = 'Silt' OR facies = 'Mud'
THEN 'Mud' ELSE 'Sand' END AS facies_m_s, AVG(proportion), SUM(N), COUNT(DISTINCT
el_ID)
#FROM fin
#GROUP BY position_lat, facies_m_s
```

Grain size proportions, for slope channel lateral positions are derived, weighted by individual element. (#) table works out proportion of mud and sand in each channel position. Can change net requirements, or facies groupings through last two tables.

Appendix C: Bespoke hierarchical classification used in DMAKS

Presented in this appendix is the current classification scheme utilised by DMAKS established based upon the findings of Chapter 3. Architectural units can be assigned a 'unit level' class. These hierarchical classes are based upon common observations of architectural depositional scales, as well as the current process interpretations, derived from the literature (see synthesis in Cullis et al., 2018; Chapter 3). This classification is mainly applicable to 'channel' and 'terminal deposit' element types due to their extensive coverage within the literature. More levels of hierarchical nesting may be observed within a system, and equally some architecture may not present all unit levels described below. Each unit level is assigned on a case by case process from the bottom-up, whereby the source-work descriptions are matched to an applicable unit level. If a hierarchical order cannot be translated with certainty this attribute is left null. This system is numeric to help avoid any terminological bias, as a vast array of hierarchical nomenclature exists in the literature. This classification can be modified as the understanding of deep-marine environments and processes develop, therefore it is preferred that unit levels are assigned based upon architectural observations, not by process interpretation alone.

Unit Level	Description and Interpretation
Unit 1	A 'bed' is described as a layer of sedimentary rock bound below and above by accretionary or erosional bounding surfaces (Campbell, 1967), this unit can be single- or multi-pulsed. These units are limited in their areal extent and represent a relatively short time-span, geologically speaking (0 – 1000 years; cf. Fig. 23, Cullis et al., 2018). These time-stratigraphic intervals are often interpreted as a single depositional event. In DMAKS, these units are exclusively stored in the Facies table.
Unit 2	Multiple genetically-related 'bed' (unit 1) elements stack to define a unit 2 architecture. The internal unit 1 elements superimpose upon one another, thus limited lateral offset is seen within a unit 2 elements stacking as subsequent bodies predominantly overlap. Distinct lateral (axis to fringe) and vertical (initiation, growth and retreat) facies associations are found within these elements which are bound by either erosive or accretionary contacts. This unit scale is often not resolvable by conventional seismic surveys. These units are often described as 'sub-elements' of their larger parent architecture (Mutti & Normark, 1987; Sprague et al., 2005; Campion et al., 2007, 2011) as their geometrical extent is constrained by their parent element and they typically mimic their parent body's geometry. These units are interpreted to be the result of local environmental changes caused by autogenic controls (Prélat et al., 2009; Groenenberg et al., 2010; Terlaky et al., 2016).
Unit 3	This mesoscale unit is the most universally recognised scale due to its discernible geometry in outcrop and (conventional or high-resolution) seismic. These distinct geometries are used to discern specific element types (e.g., channel, terminal deposit, levee etc.) based upon variability in the environmental setting. These units are 'semi-regional' in scale, 100-1000's metres wide and 10's metres thick. They are composed of genetically-related lower unit levels which are bound by erosive or accretionary contacts. Internal stacking is typically vertical within channelized architecture but compensational organisation is most commonly observed in distributary lobate geometries. No significant breaks (unconformities) in sedimentation are seen within these unit bodies, reflecting a relatively contiguous cycle of deposition – again reflecting a vertical transition through phases of initiation, growth and retreat. The unit's upper bounding surface typically accommodates a thin mud-prone, background sedimentation interval, marking a temporary (semi-regional) cessation in deposition (Mayall et al., 2006; Prélat et al., 2009). These units are seen to suggest a transition towards allogenic-dominant

	controls at this scale within the system (Mutti & Normark, 1987; Prélat et al., 2009; Terlaky et al., 2016).
Unit 4	A unit 4 element contains genetically-related unit 3 architecture, bound in a regional-scale erosive or accretionary surface. Internal vertical stacking no longer dominates within channelised environments; internal unit 3 channel bodies are seen to typically transition from low aggrading to highly aggrading bodies (McHargue et al., 2011; Jobe et al., 2016). The stacking within unit 4 channelised bodies are typically interjected with additional quantities of background deposition, allowing non-amalgamated unit relationships to form at this scale. Lobate geometries display compensational stacking of their unit 3 child elements. The internal lobate child units are seen to be delineated by background sedimentation marking upstream channel-avulsion episodes. Unlike lower level units, a unit 4 architecture can contain multiple different element types, e.g., a unit 4 channel can bound internal levee, channel and background components. A unit 4 body is capped by a relatively thicker background deposit, resulting from a period of widespread basin starvation. These deposits are again seen to reflect a cycle of initiation-growth-retreat for both channelised and lobate architectures (Gardner et al., 2003; Hadler-Jacobsen et al., 2005; Hodgson et al., 2006; Prélat et al., 2009; McHargue et al., 2011). These units are derived from the same feeder system and are interpreted in the existent literature to be the product of allogenic controls.

Appendix D: Additional system case studies used in Chapter 5

This table lists the additional deep-marine systems and their regional characteristics of the May 2019 version of DMAKS used in Chapter 5. These 11 systems are all derived from bathymetric and 2D seismic investigations. Like Table 5.1, the 'shelf width' and 'slope gradient' are averages for each system, while the 'maximum water depth' corresponds to the maximum bathymetric water depth observed.

ID	System name and locality	Length (km)	Width (km)	Margin type (tectonic regime)	Shelf width (m)	Slope gradient (m/m)	Maximum water depth (m)	References
A1	**Almeria turbidite system**, Almeria margin, Alboran Sea, SW Mediterranean	99000	30000	active margin (convergent)	67000	0.0208	1850	Alonso & Ercilla, 2003; Garcia et al., 2015
A2	**Bering Sea basin**, North of the Aleutian Islands, Bering Sea	364000	868000	passive margin	-	0.06	3750	Kenyon & Millington, 1995
A3	**Brazos-Trinity turbidite system**, Offshore Texas, Western Gulf of Mexico	70500	20500	passive margin	173000	0.017	1500	Beaubouef & Friedmann, 2000; Beaubouef et al., 2003
A4	**Celtic deep-sea fan**, Offshore Ireland, Bay of Biscay	315000	197000	passive margin	-	0.0699	4900	Bourillet et al., 2003; Zaragosi et al., 2003
A5	**Ebro turbidite system**, Offshore Spain, NW Mediterranean	50000	111000	passive margin	70000	0.052	1700	Nelson et al., 1984; Garcia et al., 2015
A6	**Guadiaro turbidite system**, Marbella margin, Alboran Sea, SW Mediterranean	30000	16000	active margin (convergent)	42000	0.0333	850	Alonso & Ercilla, 2003; Garcia et al., 2015
A7	**Gulf of Cadiz**, Offshore Spain and Portugal, NE Atlantic	166800	368300	passive margin	28000	0.02	1222	Habgood et al., 2003; Hernandez-Molina et al., 2003; Hanquiez et al., 2010; Marches et al., 2010
A8	**Nile deep-sea turbidite system**, Offshore Nile delta, E Mediterranean	260000	590000	passive margin	50000	0.017	3200	Ducassou et al., 2009; Migeon et al., 2010
A9	**Ogoue deep sea turbidite system**, Offshore Gabon, S Atlantic	450000	220000	passive margin	30000	0.025	850	Biscara et al., 2011; Mignard et al., 2017
A10	**Sacratif turbidite system**, Motril margin, Alboran Sea, SW Mediterranean	30000	14000	active margin (convergent)	24000	0.0585	900	Alonso & Ercilla, 2003; Garcia et al., 2015
A11	**Cap Ferret**, Bay of Biscay, NE Atlantic	415000	162000	passive margin	125000	0.031	5000	Barnes & Normark, 1985; Cremer et al., 1985; Ercilla et al., 2008; Somme et al., 2011; Brocheray et al., 2014; Garcia et al., 2015

Appendix E: Statistical methods used in Chapter 5

1. System-scale analysis

Spearman's rank (r_s) was used to analyse the strength of the relationships found between the system-scale parameters in Section 5.3.1. This non-parametric test was used due to the non-linear relationships found in the datasets, hence the plots are shown on log-log scales. The level of significance (p-value) used in this study was 0.05.

The regression analysis values (r^2) were calculated related to the power-law regression lines.

2. Highest-order terminal deposit dimensions

The bi-modal characteristics (i.e., the two peaks) in the global distribution of width and length highest-order terminal deposit datasets (Fig. 5.4A and B) show non-normal distributions. This non-normality is still observed within log transformed width and length datasets, Fig. D1, most notably for width.

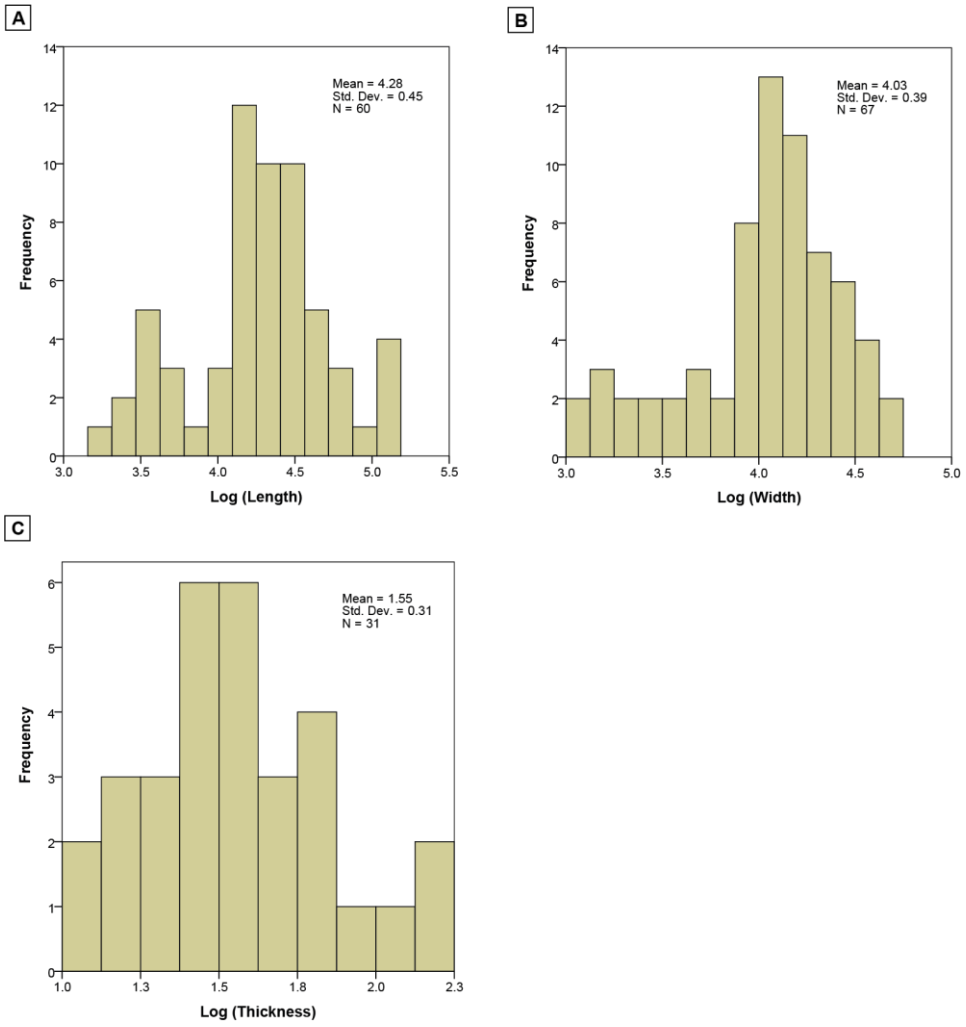

Fig. D1. Log transformed length (A), width (B) and thickness (C) histograms, showing the global distributions of the highest-order terminal deposit dataset considered in Chapter 5.

Statistical summaries for each parameter and its end-member classes are shown in Tables D1, D2 and D3 for the highest-order terminal deposit length, width and thickness data

respectively. Non-normal distributions are observed for each end-member class, indicated by statistical outliers and significantly different median and mean values; variability is also seen between each parameters end-member shapes, as indicated by statistical skewness. Therefore, the non-parametric Mann-Whitney U test was used to compare the mean ranks between the highest-order deposit end-member classes. The difference in mean ranks (U) is shown alongside a 2-tailed p-value, where significance is observed <0.05.

Table D1, D2 and D3. Summary of length (D1), width (D2) and thickness (D3) statistics for the highest-order terminal deposits, categorised by parameters examined in Fig. 5.4.

D1.

Fig. 5.4	LENGTH		n=	Mean	Median	Standard deviation	Skew-ness	Mann-Whitney U test	p-value
D	Local gradient (m/m)	>0.01	16	8147.38	4993.50	6952.26	1.06	37	<0.001
		<0.01	39	40583.38	29500.00	32680.96	1.73		
G	Local water depth (km)	>2.5	35	42540.86	30108.43	33652.87	1.63	44	<0.001
		<2.5	18	9842.50	7000.00	7589.76	0.49		
J	Slope gradient (m/m)	>0.03	17	9367.94	6000.00	7302.08	0.77	61	<0.001
		<0.03	39	39479.64	27971.25	33158.15	1.72		
M	Shelf width (km)	>30	35	41306.74	29500.00	33785.52	1.71	59	<0.001
		<30	20	11561.25	7000.00	13030.45	2.93		
P	Margin type	passive	39	39479.64	27971.25	33158.15	1.72	119	<0.001
		other	20	12741.70	9072.50	11715.50	1.52		
S	System length (km)	>100	41	39494.75	29500.00	32352.52	1.78	65	<0.001
		<100	19	9356.84	6000.00	7241.60	0.69		

D2.

Fig. 5.4	WIDTH		n=	Mean	Median	Standard deviation	Skew-ness	Mann-Whitney U test	p-value
E	Local gradient (m/m)	>0.01	18	5729.11	3325.00	4894.39	1.02	61	<0.001
		<0.01	41	18980.32	15072.74	10203.46	1.16		
H	Local water depth (km)	>2.5	37	19525.14	15731.17	10487.90	1.07	86	<0.001
		<2.5	18	6875.67	3325.00	6367.58	1.04		
K	Slope gradient (m/m)	>0.03	19	7279.84	5435.00	6088.19	0.95	139	<0.001
		<0.03	43	17768.84	13690.00	10712.87	1.1		
N	Shelf width (km)	>30	42	17215.72	13663.82	10202.36	1.18	138	<0.001
		<30	18	8184.28	4492.50	9596.05	2.57		
Q	Margin type	passive	44	17592.28	13663.82	10652.15	1.13	248	0.001
		other	22	10175.18	8274.50	10121.45	1.61		
T	System width (km)	>100	42	17215.72	13663.82	10202.36	1.18	279	0.002
		<100	24	11088.50	8274.50	11722.83	1.53		

D3.

Fig. 5.4	THICKNESS		n=	Mean	Median	Standard deviation	Skew-ness	Mann-Whitney U test	p-value
F	Local gradient (m/m)	>0.01	9	52.40	35.30	49.72	0.63	19	0.37
		<0.01	6	64.17	47.50	55.63	1.79		
I	Local confinement	unconfined	17	36.65	30.00	20.14	0.52	84	0.69
		confined	11	60.56	35.00	57.91	1.15		
L	Data type	modern	10	31.11	25.00	19.19	1.36	-	-
		sub-surface	6	93.33	87.50	61.13	0.19		
		outcrop	15	38.63	36.00	22.72	0.73		
O	Basin topography	no	11	41.65	30.00	30.53	1.98	104	0.83
		yes	20	49.62	38.00	43.47	1.8		
R	Margin type	passive	8	48.75	46.11	32.92	1.76	71	0.45
		other	22	46.37	34.65	42.55	1.92		
U	System length (km)	>100	12	48.83	37.50	29.00	1.42	83	0.22
		<100	19	45.51	34.00	44.94	2		

Appendix F: Queries used to characterise terminal deposits

Listed below are the SQL queries developed for the characterisation of deep-marine terminal deposits, from multiple datasets. The outputs of these queries were presented in Chapter 5. A brief description of the output derived from each query is also shown.

1. Summary table for deep-marine systems containing terminal deposit dimensions

```
SELECT  IF(d07_subset.basin_ID IS NOT NULL, 'Y', 'N') AS basin, d04_system.name AS
sys_name,
d04_system.length, d04_system.length_type, d04_system.width, d04_system.width_type,
d04_system.fan_area,
IF(d04_system.length_type LIKE 'true%' AND d04_system.width_type LIKE 'true%',
pi()*(0.5*d04_system.length)*(0.5*d04_system.width)/1000000, NULL) AS system_area,
IF(d07_subset.water_depth_modern_max IS NOT NULL, d07_subset.water_depth_modern_max,
d07_subset.water_depth_notes) AS water_depth,
d04_system.dominant_gs AS sys_gs, d04_system.slope_gradient AS sys_slope_grad,
d04_system.shelf_width AS sys_shelf_width, d04_system.feeder_system_type,
IFNULL(d04_system.continental_margin_type, d04_system.tectonic_setting) AS
tectonic_setting
FROM d13_element
JOIN d07_subset ON d07_subset.subset_ID = d13_element.subset_ID
JOIN d04_system ON d04_system.system_ID = d07_subset.system_ID
WHERE d13_element.general_type = 'terminal deposit' AND d13_element.highest_level IS
NOT NULL
AND (d13_element.width_type LIKE '%true%' OR d13_element.length_type LIKE '%true%' OR
d13_element.thickness_type LIKE '%true%' OR d13_element.dimensions_notes LIKE
'%calculated %')

GROUP BY d04_system.name
```

For each deep-marine system it lists the systems width, length, fan-area, dominant grain-size, maximum water depth (related to subsets), slope gradient, shelf width, tectonic setting (or continental margin type) and feeder system. The system area is also calculated using the area of an ellipse, if 'true' system length and width values are known.

2. Source metadata table

```
DROP TEMPORARY TABLE IF EXISTS lobe;
CREATE TEMPORARY TABLE lobe AS
SELECT d04_system.name AS sys_name, d04_system.system_ID, d07_subset.basin_ID,
d07_subset.case_study_ID
FROM d13_element
JOIN d07_subset ON d07_subset.subset_ID = d13_element.subset_ID
JOIN d04_system ON d04_system.system_ID = d07_subset.system_ID
WHERE d13_element.general_type = 'terminal deposit' AND d13_element.highest_level IS
NOT NULL
AND (d13_element.width_type LIKE '%true%' OR d13_element.length_type LIKE '%true%' OR
d13_element.thickness_type LIKE '%true%' OR d13_element.dimensions_notes LIKE
'%calculated %')

GROUP BY d04_system.name;

SELECT distinct lobe.sys_name, d03_source.db_literature_ID,
d03_source.source_unpublished_ID, d03_source.notes, db_literature.author,
db_literature.year, db_literature.title, db_literature.journal
FROM d03_source
JOIN db_literature on db_literature.id = d03_source.db_literature_ID
JOIN lobe on lobe.system_ID = d03_source.system_ID OR lobe.basin_ID =
d03_source.basin_ID OR lobe.case_study_ID = d03_source.case_study_ID
ORDER BY sys_name ASC, db_literature.year, db_literature.author
```

Query returns a list of literature references (author, year, title, and journal) related to the data stored in the primary table ('lobe' in this example).

3. Highest-order terminal deposit dimensions, including system metadata

```
SELECT d13_element.element_ID, d13_element.subset_ID, d07_subset.basin_ID,
IF(d07_subset.basin_ID IS NULL, 'N', 'Y') AS basin, d04_system.name AS
sys_name,d07_subset.original_name AS sub_name, d13_element.original_name,
d13_element.original_interpretation, d13_element.highest_level,
d13_element.unit_level,d13_element.length, d13_element.length_type,
d13_element.length_stype, d13_element.dimensions_notes,
d07_subset.duration_order_of_magnitude AS sub_duration, d07_subset.confinement AS
confinement_txt, IF(d07_subset.confinement LIKE '%unconfined%', 'unconfined',
IF(d07_subset.confinement IS NULL, NULL, 'confined')) AS
confinement,d07_subset.physiographic_setting, IFNULL(d07_subset.gradient,
d07_subset.gradient_range) AS grad, d07_subset.distance_from_shelf,
IF(d07_subset.water_depth_modern_max IS NOT NULL, d07_subset.water_depth_modern_max,
d07_subset.water_depth_notes) AS water_depth,d04_system.fan_area,
IF(d04_system.length_type LIKE 'true%', d04_system.length, NULL) AS sys_length,
IF(d04_system.width_type LIKE 'true%', d04_system.width, NULL) AS sys_width,
IF((d04_system.length_type LIKE 'true%' AND d04_system.length > '1000000'), '1000+',
IF((d04_system.length_type LIKE 'true%' AND d04_system.length > '100000'),
'100',IF((d04_system.length_type LIKE 'true%' AND d04_system.length > '10000'), '10',
IF(d04_system.length_type LIKE 'true%' AND d04_system.length > '1000', '1', NULL)))) AS
sys_length_mag,
IF((d04_system.length_type LIKE 'true%' AND d04_system.width_type like 'true%' AND
(d04_system.length*d04_system.width) > '1000000000000'), 'more than
1000',IF((d04_system.length_type LIKE 'true%' AND d04_system.width_type like 'true%'
AND (d04_system.length*d04_system.width) > '10000000000'), 'between 100 and 1000',
IF((d04_system.length_type LIKE 'true%' AND d04_system.width_type like 'true%' AND
d04_system.length*d04_system.width) < '10000000000'), 'less than 100', NULL))) AS
sys_area_mag, d04_system.dominant_gs AS sys_gs, d04_system.slope_gradient AS
sys_slope_grad, d04_system.shelf_width AS sys_shelf_width,
d04_system.feeder_system_type, CASE WHEN d04_system.continental_margin_type LIKE
'passive%' THEN 'passive'
WHEN d04_system.continental_margin_type IS NOT NULL THEN 'other'
WHEN d04_system.tectonic_setting IS NOT NULL THEN 'other' ELSE NULL end as tectonic
FROM d13_element
JOIN d07_subset ON d07_subset.subset_ID = d13_element.subset_ID
JOIN d04_system ON d04_system.system_ID = d07_subset.system_ID
WHERE d13_element.general_type = 'terminal deposit' AND d13_element.highest_level IS
NOT NULL AND (d13_element.length_type LIKE '%true%' OR d13_element.dimensions_notes
LIKE '%calculated % L% m%')
ORDER BY d13_element.unit_level
```

Returns terminal deposits ‘true’ or ‘calculated’ length dimensions for elements classified as the ‘highest-order’. System characteristics for each element entry are also shown. This query can be amended to extract width and thickness data.

4. Terminal deposit width and length data

```
SELECT d13_element.element_ID, d13_element.subset_ID, d04_system.name AS sys_name,
d07_subset.original_name AS sub_name, d13_element.original_name,
d13_element.original_interpretation,d13_element.highest_level,
d13_element.unit_level,d13_element.length, d13_element.length_type, d13_element.width,
d13_element.width_type, d13_element.dimensions_notes, d07_subset.confinement AS
confinement_txt, IF(d07_subset.confinement LIKE '%unconfined%', 'unconfined',
IF(d07_subset.confinement IS NULL, NULL, 'confined')) AS
confinement,d07_subset.physiographic_setting, IFNULL(d07_subset.gradient,
d07_subset.gradient_range) AS grad,
d07_subset.distance_from_shelf,IF(d07_subset.water_depth_modern_max IS NOT NULL,
d07_subset.water_depth_modern_max, d07_subset.water_depth_notes) AS
water_depth,d04_system.fan_area, IF(d04_system.length_type like 'true%',
d04_system.length, NULL) AS sys_length, IF(d04_system.width_type LIKE 'true%',
d04_system.width, NULL) AS sys_width, IF((d04_system.length_type LIKE 'true%' AND
d04_system.width_type like 'true%' AND (d04_system.length*d04_system.width) >
'10000000000'), 'more than 100',
IF((d04_system.length_type LIKE 'true%' AND d04_system.width_type like 'true%' AND
(d04_system.length*d04_system.width) < '10000000000'), 'less than 100', NULL)) AS
sys_area_mag, d04_system.dominant_gs AS sys_gs, d04_system.slope_gradient AS
sys_slope_grad, IF(d04_system.slope_gradient > '0.03', 'steep',
IF(d04_system.slope_gradient < '0.03', 'gentle', NULL)) AS slope_type,
d04_system.shelf_width AS sys_shelf_width, IF(d04_system.shelf_width > '30000', 'long',
IF(d04_system.shelf_width <'30000', 'short', NULL)) AS shelf_type,
IF(d07_subset.basin_ID IS NOT NULL, 'Y', 'N') as basin, d04_system.feeder_system_type
AS sys_feeder_type, IFNULL(d04_system.continental_margin_type,
```

```
d04_system.tectonic_setting) AS sys_tectonic, IF(d04_system.continental_margin_type
LIKE 'passive%', 'passive', IF((d04_system.continental_margin_type IS NULL AND
d04_system.tectonic_setting IS NULL), NULL, 'other')) AS tectonic
FROM d13_element
JOIN d07_subset ON d07_subset.subset_ID = d13_element.subset_ID
JOIN d04_system ON d04_system.system_ID = d07_subset.system_ID
WHERE d13_element.general_type = 'terminal deposit' #AND d13_element.unit_level IS NOT
NULL
AND (d13_element.length_type LIKE 'true%' OR d13_element.dimensions_notes LIKE
'%calculated% L % m%') AND
(d13_element.width_type LIKE 'true%' OR d13_element.dimensions_notes LIKE '%calculated%
W % m%')
ORDER BY d04_system.name, d13_element.unit_level DESC
```

'True' width and length dimensions are extracted for all terminal deposits. System characteristics are shown alongside each entry. 'Calculated' dimensions are also extracted, data is stored in 'dimension notes'.

5. Planform area and thickness data for all terminal deposits

```
SELECT d13_element.element_ID, d13_element.subset_ID, d04_system.name AS sys_name,
d07_subset.original_name AS sub_name, d13_element.highest_level,
d13_element.unit_level,d13_element.length, d13_element.length_type, d13_element.width,
d13_element.width_type,d13_element.planform_area,
((pi()*(0.5*d13_element.length)*(0.5*d13_element.width))/1000000) as
plan_calc,d13_element.thickness, d13_element.thickness_stype,
d13_element.dimensions_notes, d07_subset.confinement AS confinement_txt,
d07_subset.distance_from_shelf,IF(d07_subset.confinement LIKE '%unconfined%',
'unconfined', IF(d07_subset.confinement IS NULL, NULL, 'confined')) AS
confinement,d07_subset.physiographic_setting, IFNULL(d07_subset.gradient,
d07_subset.gradient_range) AS grad, d04_system.shelf_width AS sys_shelf_width,
IF(d04_system.shelf_width > '30000', 'long', IF(d04_system.shelf_width <'30000',
'short', NULL)) AS shelf_type, d04_system.slope_gradient AS sys_slope_grad,
IF(d04_system.slope_gradient > '0.03', 'steep', IF(d04_system.slope_gradient < '0.03',
'gentle', NULL)) AS slope_type,
IF(d07_subset.water_depth_modern_max IS NOT NULL, d07_subset.water_depth_modern_max,
d07_subset.water_depth_notes) AS water_depth,d04_system.dominant_gs,
IF(d04_system.continental_margin_type LIKE 'passive%',
'passive',IF(d04_system.continental_margin_type NOT LIKE 'passive%' OR
d04_system.tectonic_setting IS NOT NULL, 'other', NULL)) AS
tectonic,IF(d04_system.length_type like 'true%', d04_system.length, NULL) AS
sys_length, IF(d04_system.width_type like 'true%', d04_system.width, NULL) AS sys_width
FROM d13_element
JOIN d07_subset ON d07_subset.subset_ID = d13_element.subset_ID
JOIN d04_system ON d04_system.system_ID = d07_subset.system_ID
WHERE d13_element.general_type = 'terminal deposit'
AND d13_element.thickness_type LIKE 'true (maximum)'
AND ((d13_element.length_type LIKE 'true%' AND d13_element.width_type LIKE 'true%')
OR(d13_element.dimensions_notes LIKE '%calculated% pl% km%' OR
d13_element.dimensions_notes LIKE '%calculated% L % w% m%' OR
d13_element.dimensions_notes LIKE '%calculated% W% L% m%' OR d13_element.planform_area
IS NOT NULL))
ORDER BY sys_name
```

For each terminal deposit it returns the 'true (maximum)' thickness, the stored planform area, as well as a calculated area (based upon the area of an ellipse using true width and length data), along with a suite of system characteristics, including the local water depth and depositional gradient (from associated subset).